The Met.Office

Forecasters' reference book

Met.O.1012

First published 1970
Second edition 1993

ISBN 0 86180 306 X

Published by the Meteorological Office
London Road
Bracknell
Berkshire
RG12 2SZ

PREFACE

This pocket book draws together a set of rules and techniques for day-to-day use by an operational weather forecaster. Much of the content has been extracted from the original *Forecasters' Reference Book* but additional material has been added from a variety of sources. Each rule has been stated as concisely as possible and the text provides full instructions on any computations or the use of tables and diagrams. It should be noted that the forecasting techniques and rules contained in the book apply mainly to the British Isles and the north-west region of Europe and will not **necessarily** be applicable in other areas.

Each section deals with a specific subject and the chapter heading and contents listing at the front of the book facilitate rapid reference to each topic. Cross references have also been included where appropriate within the text. The terminology and symbols used in the text follow standard meteorological notation although some abbreviations have been included where the meanings of these are quite obvious.

Meteorological Office College
Shinfield Park

CONTENTS

CHAPTER 1 — WIND

CHAPTER 2 — TEMPERATURE

CHAPTER 5 — LAYER CLOUDS AND PRECIPITATION

CHAPTER 6 — TURBULENCE, ICING, CONTRAILS AND SEA WAVES

CHAPTER 7 — ANALYSIS OF METEOROLOGICAL DATA

CHAPTER 8 — SUBJECTIVE FORECASTING AIDS AND TECHNIQUES

APPENDIX III — PHYSICAL TABLES AND CONSTANTS

CHAPTER 1 — WIND

1.1 Geostrophic wind (V_g)

This is defined as the steady (unaccelerating), horizontal wind which results from the balance of two forces only — namely the pressure gradient force and the Coriolis force.

It follows that geostrophic flow only occurs with isobars (or contours) which are straight, parallel and not changing with time. There is no vertical motion, and no other forces, such as friction, are acting on the air.

On MSL charts, or any other chart at a constant height level

$$V_g = 1/\rho f \, \text{grad} \, p,$$

and on charts at a constant pressure level

$$V_g = g/f \, \text{grad} \, z$$

where grad p is the horizontal pressure gradient (in Pa m^{-1}) and grad z is the height gradient along a constant pressure surface (in m m^{-1}) and V_g is expressed in m s^{-1}.

1.1.1 *Tables for geostrophic winds*

For charts on which no geostrophic wind scale is provided, the following table gives the wind speed (kn) corresponding to the pressure, or contour height, change over a distance of 300 n mile (or 5° latitude).

Latitude	Pressure/height change over 300 n mile	
	Isobars (hPa) multipliers	Contours (dam)
70	2.1	2.5
60	2.3	2.7
55	2.4	2.9
50	2.6	3.1
45	2.8	3.3
40	3.1	3.7
35	3.4	4.1
30	3.9	4.7

Examples:

(a) A gradient of 5 hPa per 300 n mile at 55° N corresponds to $V_g = 5 \times 2.4 = 12$ kn (approx), and

(b) A gradient of 12 dam per 300 n mile at 50° N corresponds to $V_g = 12 \times 3.1 = 37$ kn (approx.).

If gradients are measured over shorter distances, the factors should be altered in proportion, i.e. for 150 n mile (2½° latitude span) the factors are doubled.

Correction factors for density variations may be applied to geostrophic wind values measured by scales based on the Standard Atmosphere (1013.2 hPa, 15 °C) as follows:

Pressure	Temperature (°C)								
(hPa)	+40	+30	+20	+10	0	−10	−20	−30	−40
920	120	116	112	108	104	101	97	93	89
940	117	113	110	106	102	98	95	91	87
960	115	111	107	104	100	96	93	89	85
980	112	109	105	102	98	94	91	87	84
1000	110	107	103	100	96	93	89	85	82
1020	108	104	101	98	94	91	87	84	80
1040	106	102	99	96	92	89	86	82	79
1060	104	101	97	94	91	87	84	81	77

Percentage corrections to geostrophic wind

Example:

If the measured $V_g = 25$ kn at a location where the pressure is 1030 hPa and the temperature is −10 °C, then the true $V_g = 25 \times 90\% = 22.5$ kn.

1.2 Ageostrophic wind

The vector difference between the actual and geostrophic winds is termed the ageostrophic wind. It can be represented as the sum of five effects, of which only three can be assessed even qualitatively in practice. The effects are due to friction, time changes in the pressure field (isallobars) and spatial changes in the pressure field (isobars not straight and parallel). Consideration of the first two is mainly relevant to surface pressure charts and the last one to upper-air contour charts.

1.2.1 *Friction*

The gradient of the frictional stress near the ground decreases the wind speed and hence the Coriolis force, but leaves the pressure force unchanged. A cross-isobar wind component towards low pressure develops. Statistical relationships between the wind above the friction layer and the surface wind are given in section 1.4.

1.2.2 *Isallobaric wind*

When the pressure field is changing, the balance of forces required for geostrophic flow is upset. An isallobaric wind component may be measured by using a geostrophic scale on the spacing of 1 hPa isallobars of the 3-hour pressure change and then correcting this measured value using the following Table.

Latitude (°)	30	35	40	45	50	55	60	65	70
Factor	1.27	1.11	0.99	0.90	0.83	0.78	0.73	0.70	0.68

Example:

If the isallobaric spacing gives a geostrophic scale reading of 10 kn at latitude 52½° N, the correction factor of 0.8 gives an isallobaric wind component = 0.8 × 10 = 8 kn.

This ageostrophic wind component is directed perpendicularly across the isallobars from positive values (pressure rises) to negative values (pressure falls). Air should remain in the area of the isallobaric forcing for about 4 hours for the effect to become noticeable.

1.2.3 *Downwind changes in the contour field*

Air moving through the slow-moving patterns of an upper-level contour field experiences accelerations as its motion adjusts to changes in the gradient which it encounters downstream. Where the contours are curved, there is a centripetal acceleration (see section 1.3). Where the contour gradient gradually changes, without significant curvature of the flow, there is an acceleration due to the downwind change in V_g. This generates a cross-contour component of ageostrophic motion (V_d) as illustrated in Fig. 1.1.

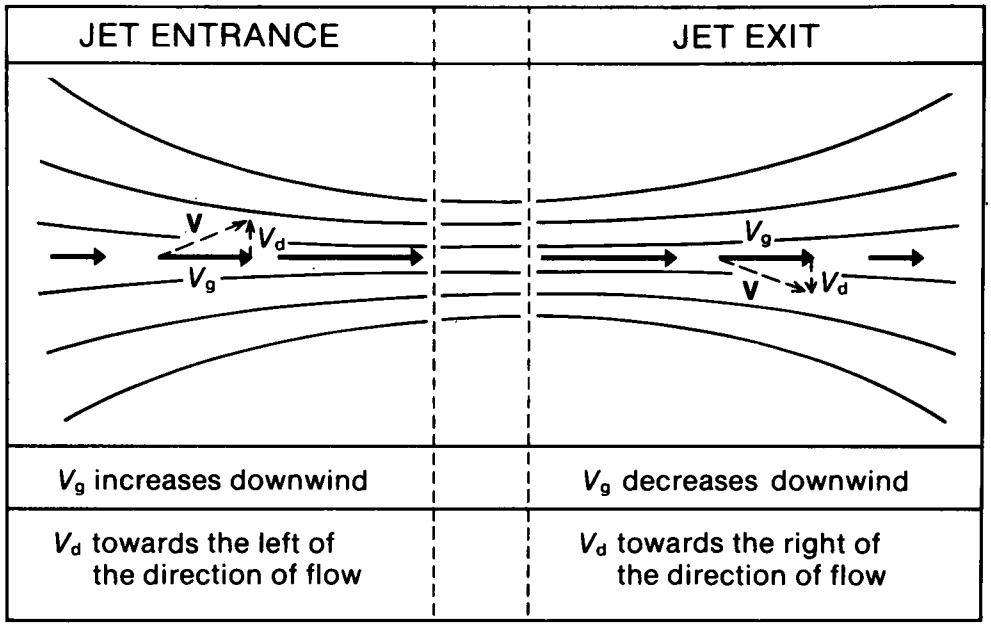

Figure 1.1. Illustrating the geostrophic departure (V_d) due to the change of V_g along contour lines.

At a jet entrance, where V_g increases downwind, V_d is directed towards the low contour side.

At a jet exit, where V_g decreases downwind, V_d is directed towards the high contour side.

The value of the angle between the true wind (V) and the geostrophic wind (V_g), when V_g changes downwind, can be assessed from the magnitude of the acceleration. This is given by the distance between successive 40 kn isotachs measured along a contour line, as follows:

Latitude (°)	Distance (n mile) along a contour between isotachs at 40 kn intervals								
	60	90	120	150	180	210	240	300	360
	Angle between V and V_g (degrees)								
70	53	42	34	28	24	21	19	15	13
60	56	44	36	30	26	23	20	16	14
50	59	48	40	34	29	25	23	18	15
40	63	53	45	38	33	29	26	22	18
30	69	59	52	45	40	36	32	27	23
25	72	63	56	50	45	41	37	31	27

Example:

At latitude 40°, a distance of 150 n mile between the isotachs 80 kn and 120 kn gives a cross-contour angle of flow of 38 °. This would be towards the left of the flow at a jet entrance, and towards the right at a jet exit.

1.3 Gradient wind

When its trajectory is curved, air is subjected to a local centrifugal force, V^2/r, where V is the gradient wind velocity and r is the radius of curvature of the trajectory.

The gradient wind equations are:

For cyclonic curvature

$$V_{gr} = \tfrac{1}{2}[-rf + \sqrt{(r^2f^2 + 4rfV_g)}]$$

and for anticyclonic curvature

$$V_{gr} = \tfrac{1}{2}[-rf - \sqrt{(r^2f^2 - 4rfV_g)}].$$

1.3.1 *Estimation of gradient wind (table method)*

Corrections to be applied to the geostrophic wind to obtain the gradient wind are given in Table 1.1. The top section of the table shows how changes in the Coriolis parameter affect the results. Thus a radius of 600 n mile at latitude 50° is equivalent to a radius of 490 n mile at latitude 70° or 920 n mile at latitude 30°.

Table 1.1 Gradient wind corrections

Latitude (°)	Radius of curvature of isobar or contour (n mile)											
70	98	147	196	245	367	489	737	978	1467	1957	2446	3261
60	106	159	212	265	398	531	796	1061	1592	2123	2654	3538
50	120	180	240	300	450	600	900	1200	1800	2400	3000	4000
40	143	215	286	358	536	715	1073	1430	2145	2860	3575	4767
30	184	276	368	460	689	919	1379	1839	2758	3677	4596	6128

Continued overleaf

Geostrophic speed (knots)	Cyclonic curvature correction (knots)											
10	−1	−1	−1	−1	0	0	0	0	0	0	0	0
20	−5	−4	−3	−3	−2	−1	−1	−1	−1	0	0	0
30	−9	−7	−6	−5	−4	−3	−2	−2	−1	−1	−1	−1
40	−14	−11	−10	−8	−6	−5	−4	−3	−2	−2	−1	−1
60	−25	−21	−18	−16	−12	−10	−8	−6	−4	−3	−3	−2
80	−37	−32	−28	−25	−20	−17	−13	−10	−7	−6	−5	−4
100	−51	−44	−39	−35	−28	−24	−18	−15	−11	−9	−7	−6
120	−64	−56	−50	−46	−38	−32	−25	−21	−15	−12	−10	−8
140	−78	−69	−62	−57	−47	−41	−32	−27	−20	−16	−13	−10
160	−93	−83	−75	−69	−58	−50	−40	−33	−25	−20	−17	−13
180	−108	−96	−88	−81	−69	−60	−48	−40	−31	−25	−21	−16
200	−123	−111	−101	−94	−80	−70	−57	−48	−37	−30	−25	−20
220	−138	−125	−115	−107	−91	−81	−66	−56	−43	−35	−30	−24
240	−154	−140	−129	−120	−103	−91	−75	−64	−50	−41	−35	−28
260	−170	−154	−143	−133	−115	−103	−85	−73	−57	−47	−40	−32
280	−185	−169	−157	−147	−128	−114	−95	−82	−64	−53	−46	−37

Geostrophic speed (knots)	Anticyclonic curvature correction (to be added) (knots)											
10	4	2	1	1	1	0	0	0	0	0	0	0
20	—	—	8	5	3	2	1	1	1	0	0	0
30	—	—	—	26	8	5	3	2	1	1	1	1
40	—	—	—	—	20	11	6	4	2	2	1	1
60	—	—	—	—	—	52	16	10	6	4	3	2
80	—	—	—	—	—	—	39	21	12	8	6	4
100	—	—	—	—	—	—	—	41	20	13	10	7
120	—	—	—	—	—	—	—	104	32	20	15	11
140	—	—	—	—	—	—	—	—	50	30	22	15
160	—	—	—	—	—	—	—	—	79	42	30	20
180	—	—	—	—	—	—	—	—	156	59	40	26
200	—	—	—	—	—	—	—	—	—	83	53	34

These corrections are to be applied to the geostrophic wind to obtain the gradient wind when the system of isobars or contours is stationary. The theoretical maximum gradient wind for anticyclonic curvature is equal to twice the geostrophic wind.

Differences between the curvature of trajectories and the curvature of isobars or contours occur when the systems are in motion are illustrated in Fig. 1.2. Where the flow is at right angles to the direction of motion of the system the difference in curvature is least. Where the flow is almost parallel to the movement of the system the difference is greatest.

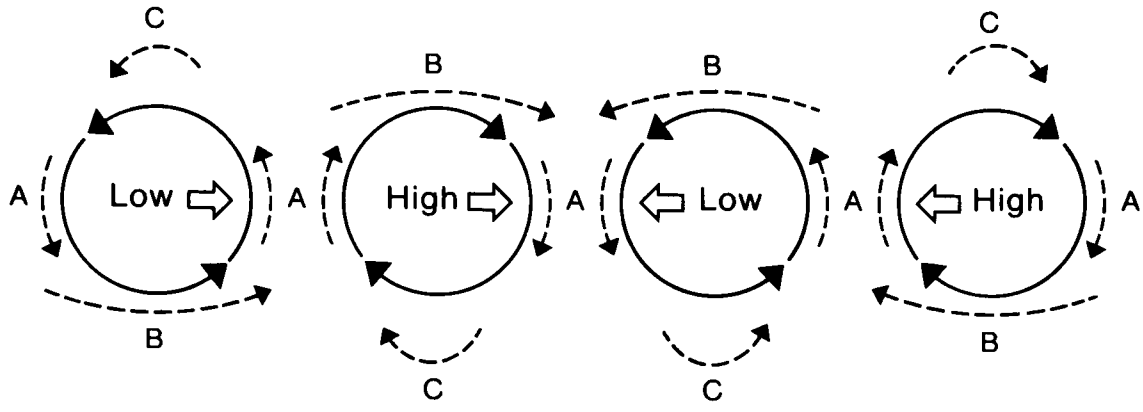

Figure 1.2. Comparison of trajectories and contours when the contour pattern is moving. Full lines represent contours, and dashed lines show the shapes of typical air trajectories on each side of a moving high or low. At points marked 'A', the values in Table 1.1 need no adjustment. At 'B', the Table overestimates the correction and at 'C', the Table underestimates it.

1.3.2 *Estimation of gradient wind (graphical method)*

Fig. 1.3 is a graph for obtaining the gradient wind speed from the speed of the geostrophic wind and the radius of curvature. The graph is drawn for use at latitude 50°. For use at other latitudes the radius of curvature must be multiplied by a correction factor to obtain the equivalent value at latitude 50°.

To use the graph:

(a) Use the right-hand inset to find the equivalent radius of curvature for latitudes other than 50°. Divide the actual radius by the percentage factor shown against the value for latitude. If, for example, the radius at latitude 39.5° N is 1200 n mile, the correction factor is 120% and the equivalent radius at latitude 50° is 1000 n.mile.

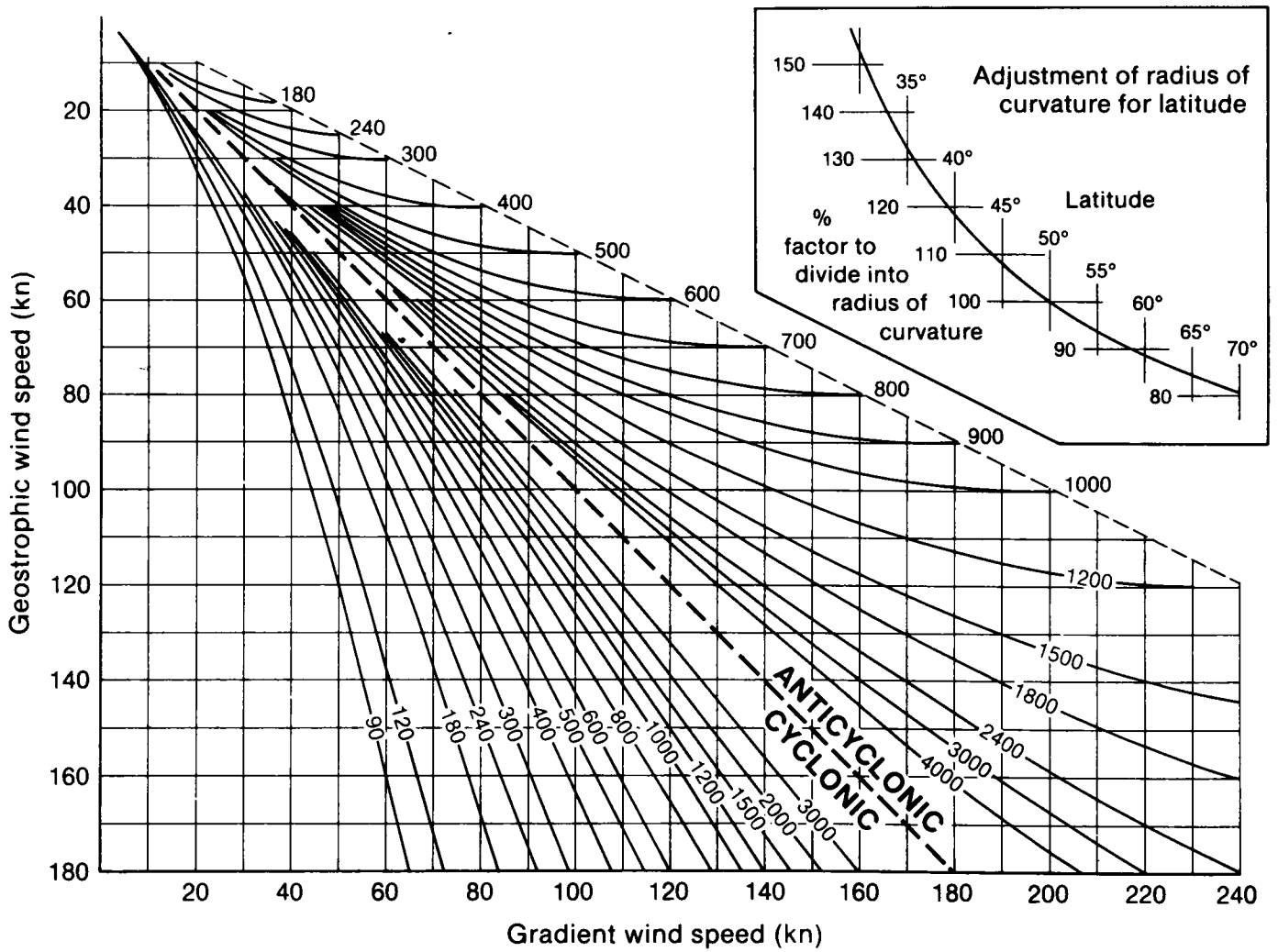

Figure 1.3. A graph to obtain the gradient wind speed from the speed of the geostrophic wind and the radius of curvature.

(b) Find the point of intersection of the geostrophic wind speed (shown along the left-hand axis) with the curve showing the radius of curvature. The cyclonic curves lie to the left and the anticyclonic curves lie to the right of the straight line denoting infinite radius. The gradient wind speed is shown along the top of the diagram. Thus with a radius of curvature of 1000 n mile and V_g = 90 kn, the gradient wind is 76 kn for cyclonic curvature and 136 kn for anticyclonic curvature.

The theoretical maximum gradient wind speed for anticyclonic curvature is twice the geostrophic wind. The graphs show that as the gradient wind approaches this value, small increases in the geostrophic wind can produce very large increases in the gradient wind.

1.4 Vertical wind shear in the lowest layers

1.4.1 *Surface wind and gradient wind*

The surface wind is usually decreased in speed and backed in direction from the gradient wind. The magnitude of the change depends on the stability of the air and the roughness of the surface. Rough surfaces increase the frictional effect; greater stability reduces the turbulent exchange of energy between the flow aloft and that at the surface.

1.4.2 *Surface wind and 900 m wind (statistical relations)*

The following tables show some observed relationships between the speed of the surface wind (V_0) and the 900 m wind (V_9), together with the angle (α) between them.

Lapse-rates are classified as:

1. Superadiabatic
2. Conditionally unstable
3. Conditionally stable
4. Stable
5. Isothermal/Inversion

(a) Over the sea: at 59° N, 19° W and 52° N, 20° W

Lapse class	900 m wind speed (kn) 10–19		20–29		30–39		40–49		⩾50	
	V_0/V_9	α	V_0/V_9	α	V_0/V_9	α	V_0/V_9	α	V_0/V_9	α
1	0.95	0	0.90	0	0.85	0	0.80	0	0.90	0
2	0.90	5	0.85	5	0.80	5	0.75	5	0.75	5
3	0.85	10	0.75	10	0.70	15	0.65	10	0.65	10
4	0.80	15	0.70	20	0.65	20	0.60	20	0.60	20
5	0.75	15	0.70	20	0.65	20	0.60	20	0.55	25

(b) Over land: at London (Heathrow) Airport

Lapse class	900 m wind speed (kn) 10–19		20–29		30–39		40–49		⩾50	
	V_0/V_9	α	V_0/V_9	α	V_0/V_9	α	V_0/V_9	α	V_0/V_9	α
Daytime										
1,2	0.65	5	0.55	5	0.50	10	0.50	10	0.35*	15*
3	0.50	20	0.45	20	0.45	20	0.45	20	0.45	15
4	0.45	35	0.45	30	0.40	25	0.30	20	0.40*	25*
5	0.35	45	0.40	35	0.35	35	0.40*	30*	0.40*	30*
Night-time										
1,2	0.25*	20*	0.35	25	0.30*	35*	0.40*	15*	0.40*	25*
3	0.35	25	0.35	30	0.35	25	0.35	20	0.35	15
4	0.30	35	0.30	35	0.30	30	0.35	30	0.35*	15*
5	0.30	45	0.25	40	0.25	35	0.30*	30*	No obs	

*Results based on less than 10 observations

1.4.3 *Vertical wind shear over surfaces with different roughness*

For neutral stability the variation of wind speed (V) with height (h) may be expressed by $V = Kh^p$ where K is a constant and p depends on the roughness of the terrain. Fig. 1.4 shows the calculated ratio V_h/V_{10} (the winds at 10 m and h m) for different surfaces.

The curves show that over wooded country if the 600 m wind is 23 kn the 300 m wind should be just under 20 kn and the 10 m wind should be 10 kn.

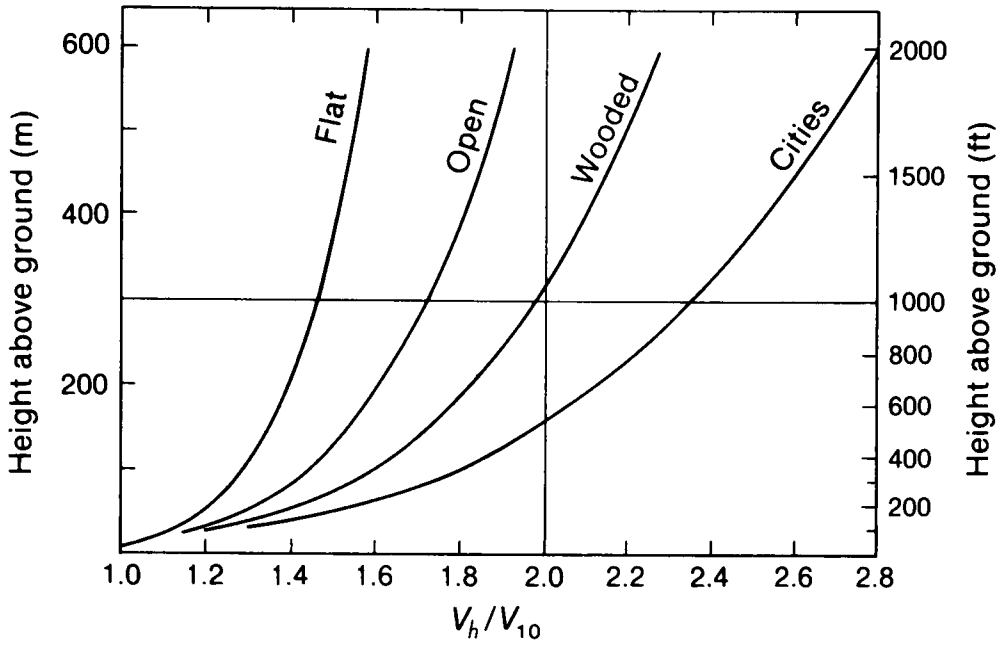

Figure 1.4. Calculated ratio of V_h/V_{10} over different surfaces in neutral stability conditions.

1.4.4 *Vertical wind shear in different stability conditions*

Fig. 1.5 shows how the ratio V_h/V_{10} alters with changes of stability. It is based on observations at Cardington of wind changes between the surface and 400 ft with lapse rates ranging from +2 °C to −6 °C through that layer.

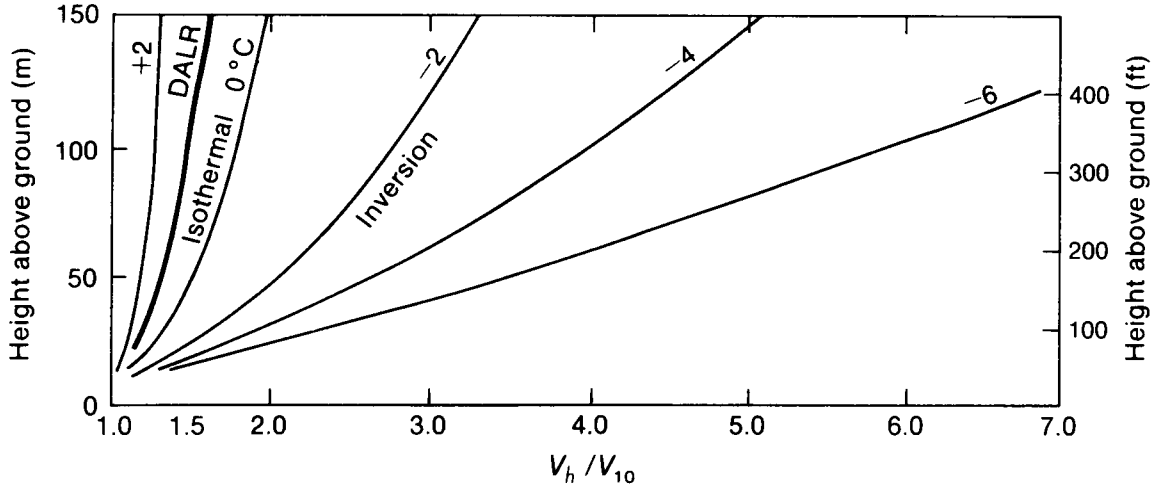

Figure 1.5. Observed ratio of V_h/V_{10} for different lapse-rates, measured at Cardington.

1.4.5 *Diurnal variations of vertical wind shear*

In anticyclonic conditions large differences in the vertical wind structure may occur between day and night. Fig. 1.6 illustrates the occurrence of a nocturnal 'jet' with its associated shear, which dissipates during the day.

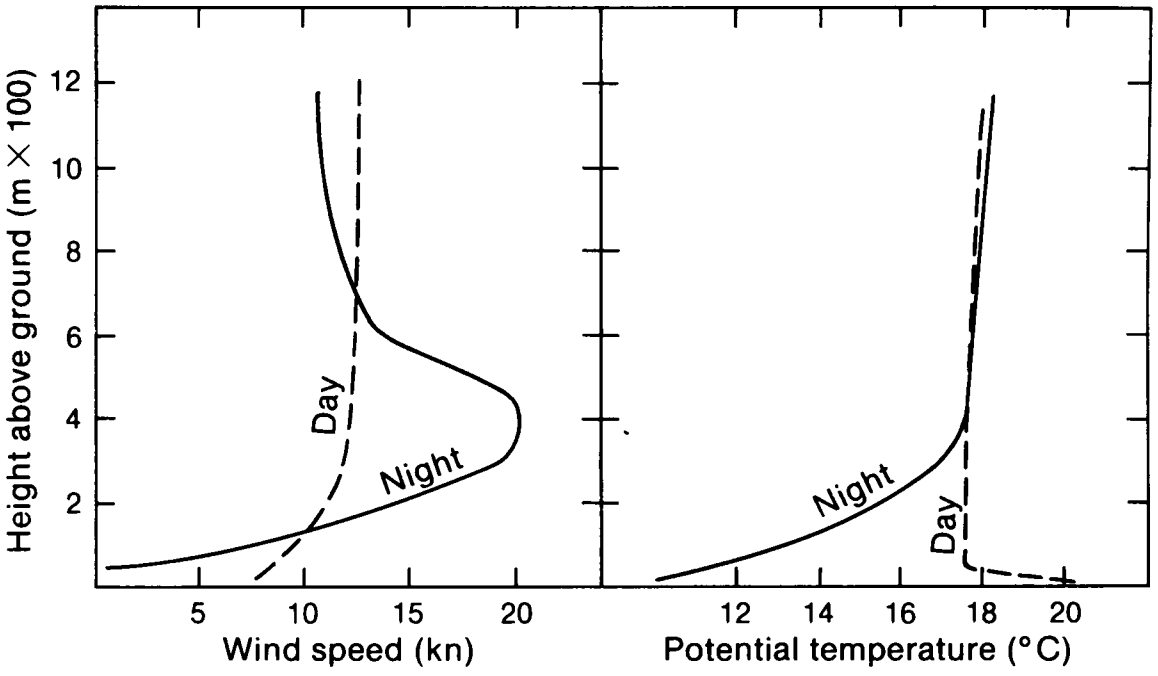

Figure 1.6. Vertical profiles of wind speed and potential temperature by night and day under typical fair-weather conditions with little or no low cloud

1.4.6 *Frequency of vertical wind shears*

Estimates of the overall frequency of different wind shears across the layer 10–40 m for a conglomerate of worldwide airports are shown below. The figures are based on two-minute averages.

Vertical wind shear	Percentage of time exceeded
3 kn per 30 m	50
5 kn per 30 m	17
8 kn per 30 m	2
10 kn per 30 m	0.4

1.4.7 *Examples of strong wind shears*

(a) At the passage of a cold front. At an airport in the USA in August 1973, the following wind structure was observed:

Surface	308°	5 kn
300 ft	211°	14 kn
500 ft	194°	29 kn
700 ft	195°	33 kn

(b) Associated with a nocturnal 'jet', observed at Cardington on a radiation night:

Wind-speed shear of 15 kn between 9 m and 45 m (approx 30–150 ft) = 0.42 kn m^{-1}.

(c) Associated with a thunderstorm downburst, or microburst (see section 1.6.2). Gust fronts from these systems may travel 15 n mile from the originating storm and produce shears of 25 kn per km.

1.5 Gusts and squalls

1.5.1 *Ratio of maximum gust to mean hourly speed*

Location	Range of ratios	Estimated average
Open sea	1.3	1.3
Isolated hill tops	1.4–1.5	1.4
Flat open country	1.4–1.8	1.6
Rolling country (few wind-breaks)	1.5–2.0	1.7
Rolling country (numerous wind-breaks), forest areas, towns, outskirts of large cities	1.7–2.1	1.9
Centres of large cities	1.9–2.3	2.1

1.5.2 *Squalls*

(a) Associated with thunderstorms: the downdraughts and subsequent outflow from severe thunderstorms may produce a squall line which moves outward from the storm for up to 15 n mile.

Peak wind speeds depend largely on the temperature difference between the downdraught air and the surrounding warmer air at the surface.

Downdraught temperature may be estimated from an upper-air sounding by drawing a saturated adiabat from the level where the wet-bulb curve cuts the 0 °C isotherm to the surface pressure. Fig. 1.7 illustrates the construction on a tephigram.

Fig. 1.8 shows the relationship between the temperature difference and the peak wind speed. A correlation of 0.86 was found in the USA.

(b) Associated with cold fronts: active fronts with rearward-sloping warm conveyor belt, line convection, marked wind shift and sharp pressure changes indicate the likelihood of a squall.

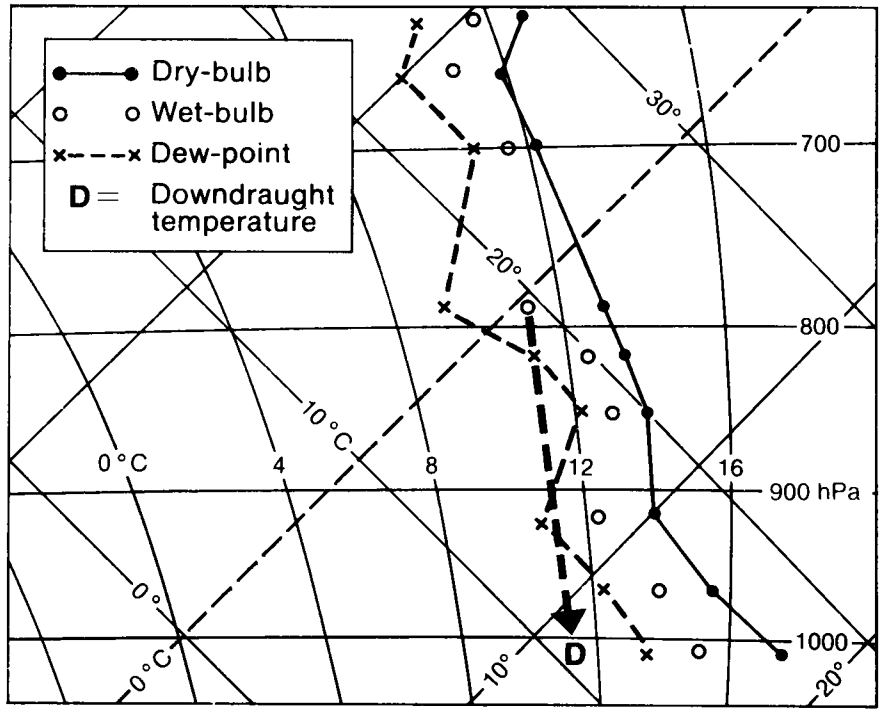

Figure 1.7. Example of a tephigram, illustrating the computation of the downdraught temperature in non-frontal thunderstorms in the USA (after Fawbush and Miller).

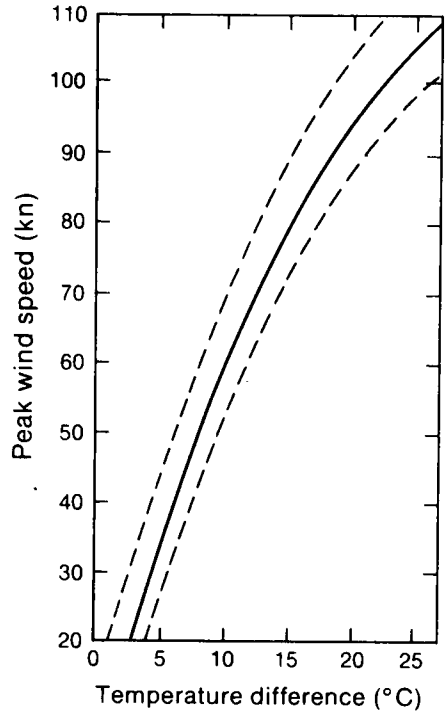

Figure 1.8. Peak wind speed at the surface related to the temperature difference between cold downdraught air and the warm surface air, during non-frontal thunderstorms in the USA.

The severity of the squall probably depends on:

i. Wind speed in the low-level jet ahead of the cold front.
ii. Wind speeds in the medium-level layers near the frontal surface.

1.6 Tornadoes and microbursts

1.6.1 *Tornadoes*

These are usually associated with severe convective storms. They normally require:

(a) Great depth of convective instability
(b) High values of θ_w in the lowest layers (18–23 °C).
(c) Marked potential instability (θ_w falling 5 °C or more up to 500 hPa).
(d) Marked vertical wind shear with winds increasing and veering with height.

The very strong updraughts within the storm cloud are associated with strong low-level convergence and intensification of the vorticity which existed before the storm. The rotating air is concentrated within a narrow funnel where pressure falls greatly and wind speeds rise to exceptional levels.

In the United Kingdom tornadoes occur mainly in association with vigorous cold fronts or during heavy showers or thunderstorms with convective PVA features.

1.6.2 *Microbursts (or downbursts)*

These are strong downdraughts from very deep and vigorous cumulonimbus clouds, producing a violent outflow spreading out at the ground and causing tornado-like damage. Doppler radars show that microbursts may rotate. In the USA characteristic features are:

(a) Size usually less than 4 km.
(b) Calculated vertical velocities 50–70 kn.
(c) Observed horizontal velocities up to 60 kn.
(d) Tremendous low-level wind-shear.

Wet microbursts are associated with shafts of intense thunderstorm precipitation. Dry microbursts also occur, having virga visible but no precipitation reaching the surface. Cooling of the air by evaporation may intensify the downdraught, so that dry microbursts may produce stronger wind-shears and more dangerous conditions than wet microbursts.

Radar often shows a spearhead-shaped echo which may contain more than one downburst cell, as shown in Fig. 1.9.

1.7 Local winds

1.7.1 *Sea-breezes*

(a) *Seasonal variation*: In the United Kingdom sea-breezes occur from March to late September. The majority occur from May to August with the peak in June.

(b) *Penetration inland*: Movement inland starts around 10 UTC from the coast and may extend as much as 50 n mile by 22 UTC over the south and east of England. In tropical regions the penetration starts earlier and may extend up to 180 n mile.

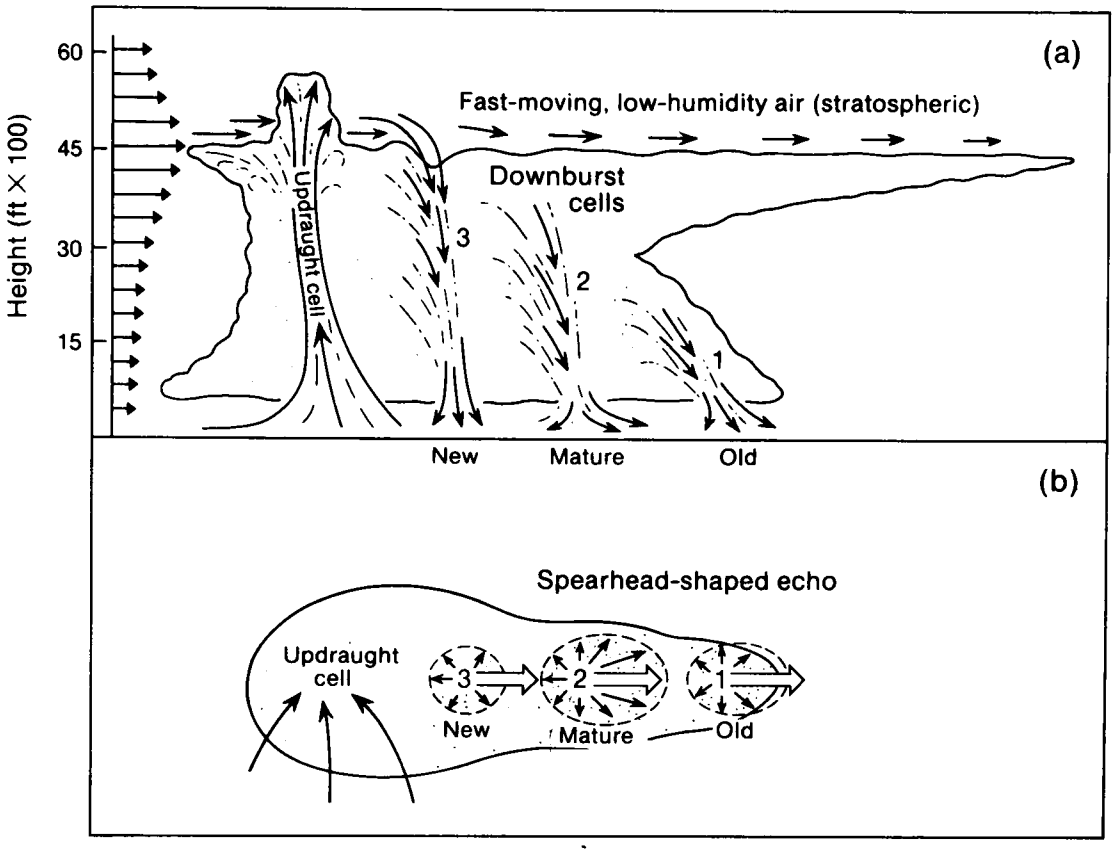

Figure 1.9. Multicell storms and radar 'spearhead' echo. (a) Vertical cross-section, and (b) radar plan view of a multicell cumulonimbus with a new updraught on the left and three downburst cells.

The distance depends on the offshore component of the geostrophic wind, the land–sea temperature contrast, the depth of convection and the topography. High ground delays or deflects the flow of sea air which tends to move up wide valleys rather than climb over hills see Fig. 1.10.

(c) *Sea-breeze front*: The convergence line where incoming sea air meets the land air is often termed the sea-breeze front. A small offshore component to the geostrophic wind is generally needed for the development of a well-defined front. A narrow line of rising air occurs along the front producing enhanced convection.

(d) *Speed of movement*: The average in the United Kingdom is 4–8 km h^{-1}.. The rate of advance is not constant. The front moves inland in a series of surges with a speed less than that of the incoming sea air.

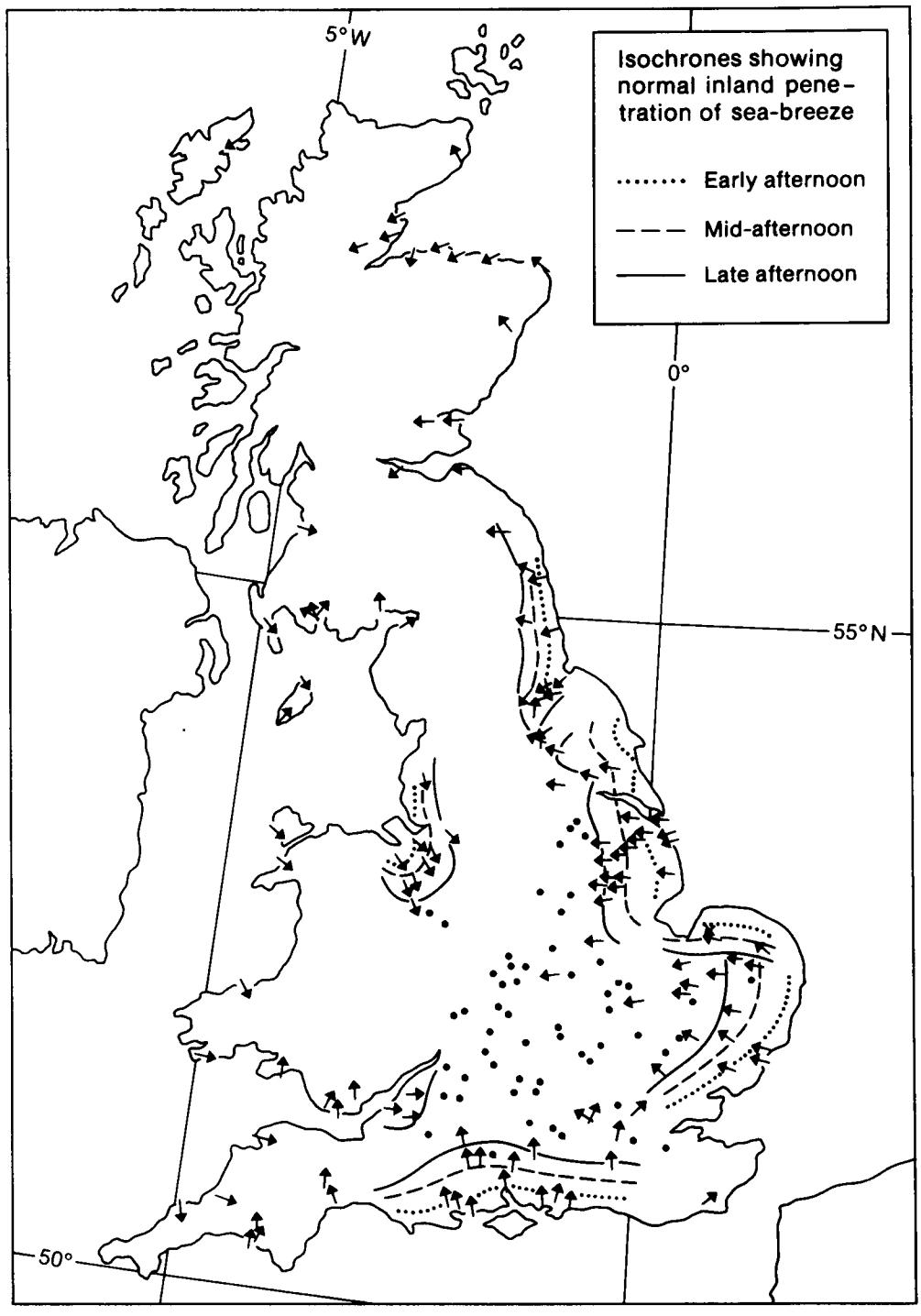

Figure 1.10. The normal direction and penetration of sea-breezes during summer months. Each arrow or dot represents an individual airfield. Arrows show the late afternoon direction of the sea-breeze (a few places having two preferred directions). Dots show airfields where sea-breezes have not been specially recorded in the local weather notes. The isochrones show the normal rate of progress inland of the sea-breeze on a summer afternoon.

(e) *Depth of sea air*: The incoming sea air often extends to a height of 2 000 ft, occasionally 3 000 ft at the front where the depth is greatest but the top descends to about half the maximum after the front has passed.

(f) *Criteria for sea-breezes*: Higher temperatures over land than sea, and a weak offshore wind component initially, as typified by the following observations for:

i. Lake-breezes in USA.
ii. The coast of Lincolnshire, England.

Offshore component (kn)		2	4	6	8	10	12	14	16
Temperature contrast (°C)	(i)	1.5	3.6	7.2	12	18	—	—	—
	(ii)	3.5	5.0	6.0	7.3	9.0	11	14	—

Convective instability inland should extend up to above 4500 ft.

If the air is so stable that the convection is confined to a very shallow layer there will be little or no penetration of the sea-breeze regardless of the temperature difference between land and sea. A moderate depth of convection favours deep penetration. Deep convection leading to shower or thundery activity tends to halt the sea-breeze.

1.7.2 *Slope and valley winds*

(a) *Anabatic winds*: flow up slopes warmed by solar heating. The flow is generally shallow. Maximum speeds occur within a few metres of the slope surface.

(b) *Katabatic winds*: flow down slopes and along valleys cooled by nocturnal radiation. The flow is usually shallow. Winds may be strong in arctic or antarctic regions where there are long ice-covered slopes.

(c) Valley wind systems on any occasion may have anabatic or katabatic components, but complicated by the presence of a gradient wind flow above the level of the surrounding ridge tops and varying through the day as the sun's orientation changes and different slopes are in the sun or in shadow. Fig. 1.11 illustrates the general pattern, in which there are three main layers with different airflows:

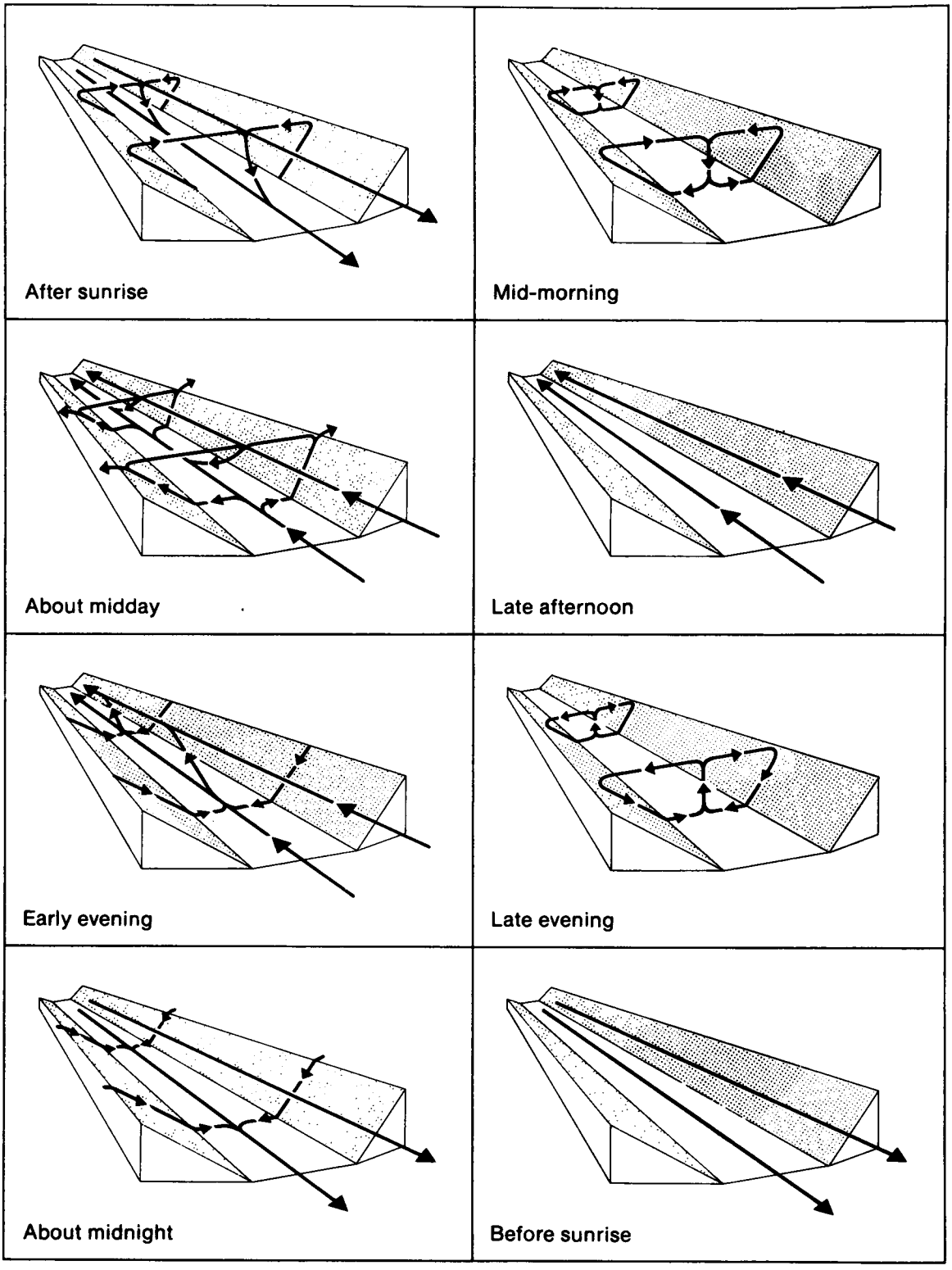

Figure 1.11. Valley wind systems. A schematic display of the diurnal variation of upslope and downslope winds forced by the changing effects of solar heating at the surface.

i. The lowest layer in contact with the slopes flows upwards while the slope is heated and descends towards the valley floor when radiation cools the slopes.
ii. An intermediate layer where the flow is often reversed. This has been termed the "anti-" wind which tends to balance the lowest-level flow.
iii. At the top is the gradient wind, controlled by large-scale synoptic systems.

The depth of the whole system is roughly that of the valley–ridge height. The anabatic and katabatic components are only a few metres deep, the remainder of the valley depth being taken up with the returning anti-wind. Gradient wind speeds over 12 kn will distort the valley wind circulation.

When marked inversions develop in winter, with weak solar heating, the surface flow is often cut off from that at ridge level and is usually from high pressure to low along the valley.

1.7.3 *Downslope winds*

Differing from shallow katabatic winds are downslope winds produced by the large-scale flow extending far above the level of high ground.

(a) Föhn winds occur on the lee side of mountain ranges when the winds aloft blow across the axis of the main ridges. Two examples are shown in Fig. 1.12. In (a) the low-level flow is blocked upstream and only the higher-level flow crosses the ridge to plunge down the lee side as a very dry adiabatically warmed current.
In Fig. 1.12 (b) all the upstream air crosses the ridge. Orographic lifting produces cloud; precipitation over the mountains then depletes the moisture content; the drier air then descends the lee side, warming adiabatically.

(b) Lee waves may give rise to severe downslope winds when the waves reach a critical amplitude and wavelength. The streamlines of flow are concentrated down the lee slope to produce an exceptionally strong wind. These extreme winds may extend for some distance across the plain before the flow leaves the surface to form the upstream face of a large-amplitude wave above a rotor (see Fig. 1.13). Surface charts may show a marked lee trough. Structural damage and uprooting of trees has been caused by such winds in the United Kingdom.

Indications: Strong gales over the mountain tops
Inversion or stable layer above mountains
Increasing winds aloft (usually near jet streams).

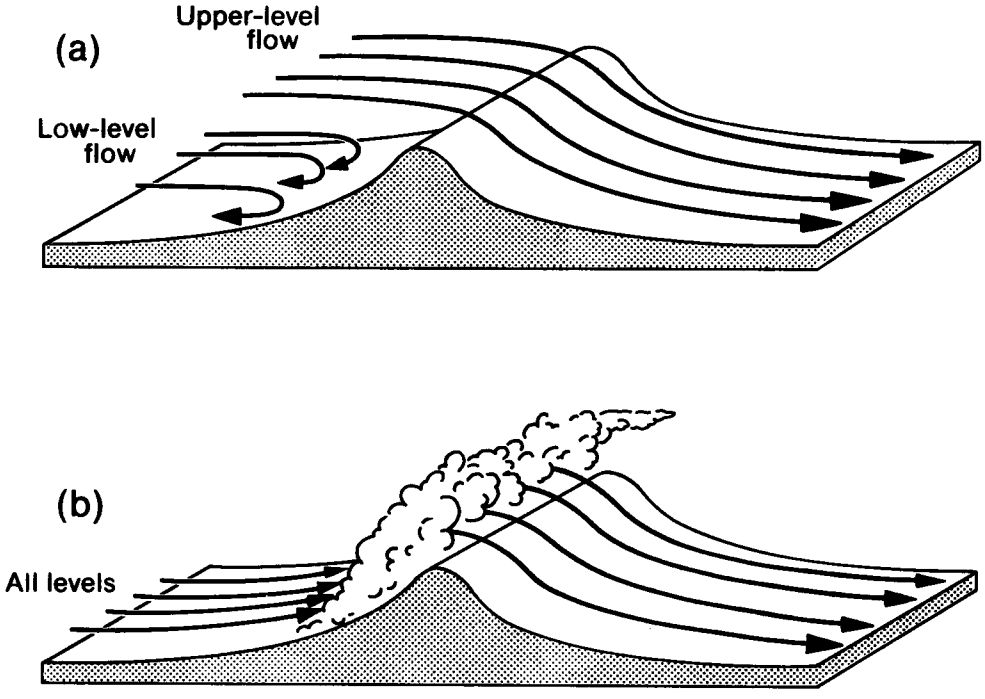

Figure 1.12. Föhn winds. (a) The low-level flow is blocked upstream of the hill barrier and only the higher-level air flows across the ridge, and (b) all the upstream air crosses the ridge.

1.8 Jet streams

A jet stream is a narrow ribbon of fast-moving air whose length (several hundred kilometres) is often ten times its width, while the depth is only one or two kilometres. The vertical wind shear is often in the range 3 to 6 kn per 1000 ft; the horizontal shear may be of the order of 20 kn per 100 n mile. An arbitrary lower limit of 60 kn maximum wind-speed defines jets at high level. Low-level 'jets' have no such restriction.

1.8.1 *The polar-front jet*

This is so named for its links with the polar front but the term is applied to any jet formed where the baroclinic zone extends down through the troposphere. This jet is found over a wide range of latitudes between 35° and 70°. The mean position

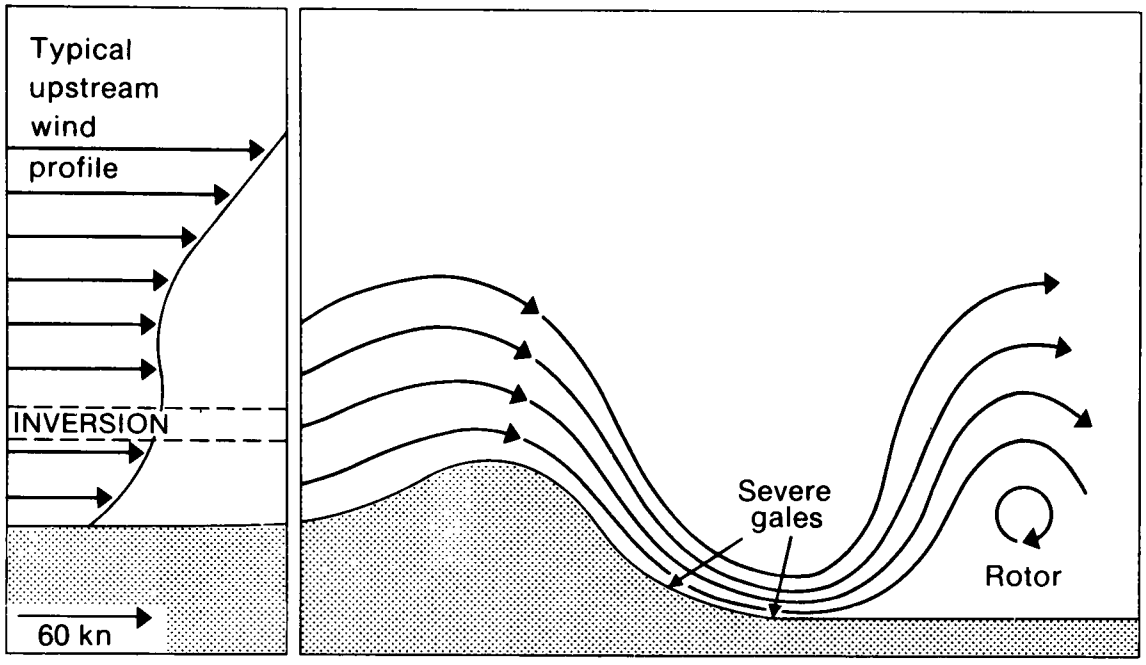

Figure 1.13. Severe downslope winds. The vertical profile shows the typical wind structure upstream. The concentration of streamlines down the lee slope of the ridge indicates the region of abnormally high wind speeds. Further downwind the flow separates and a rotor forms.

is nearer the equator in winter than in summer. A cross-section through a typical example of a polar-front jet is shown in Fig. 1.14, and the relationship between the location of surface fronts and jet core in a mature system in Fig. 1.15.

Height: The jet core is located in the warm air about 3000 ft below the tropopause, usually between 300 and 250 hPa, and vertically above the position of the frontal zone at 500 hPa. The level varies along the length of the jet, being higher round ridges and lower near troughs.

Direction: The majority of jets have a component from the west and blow from between 190° and 350°. Northerly or north-easterly jets occur at times in the winter months. South-easterly jets are rare.

Speeds: Jet speeds are normally higher in winter than in summer. Winter jets can often reach 150 kn and may sometimes exceed 200 kn. The 300 hPa wind speed is approximately twice the maximum thermal wind in the 500 to 1000 hPa layer, but displaced some 60 n mile to the cold side of the thermal wind maximum. The core of a jet at any level crosses the contour pattern on the entrance and exit regions of a jet, due to the ageostrophic effects described in Section 1.2.3. See Fig. 1.16.

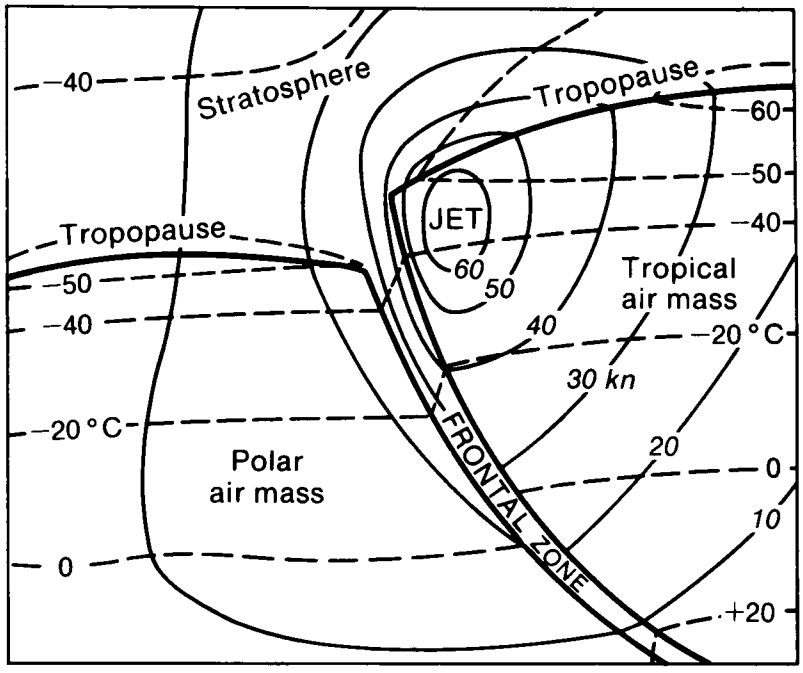

Figure 1.14. Vertical cross-section through a polar-front jet, showing wind speed (into the paper) and temperature structure.

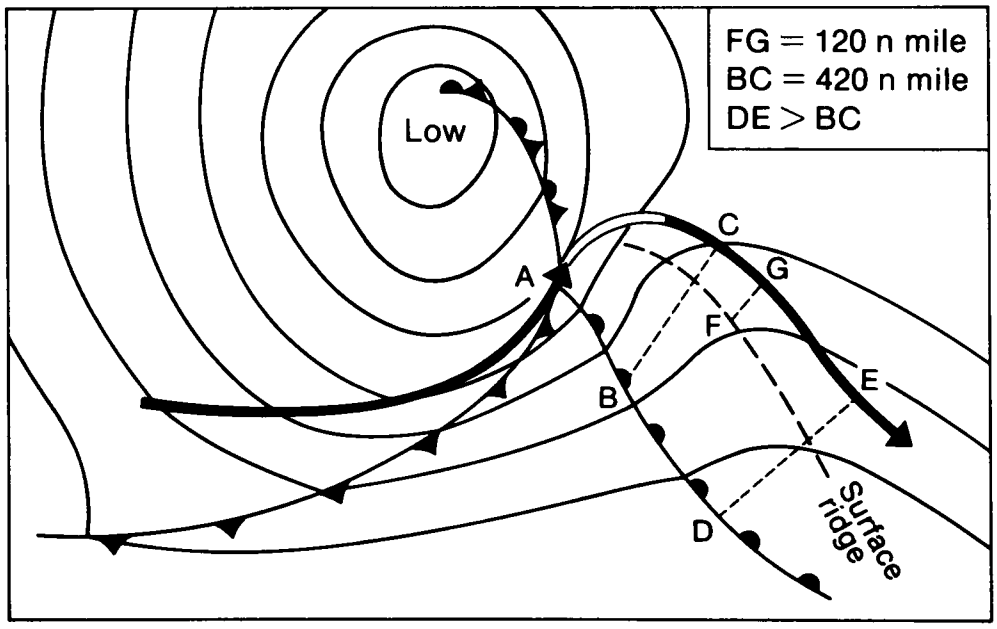

Figure 1.15. Polar-front jet in relation to surface fronts. The broad arrow represents the core of the jet at 300 hPa, which is weak or broken in the unshaded section. A is the tip of the warm sector.

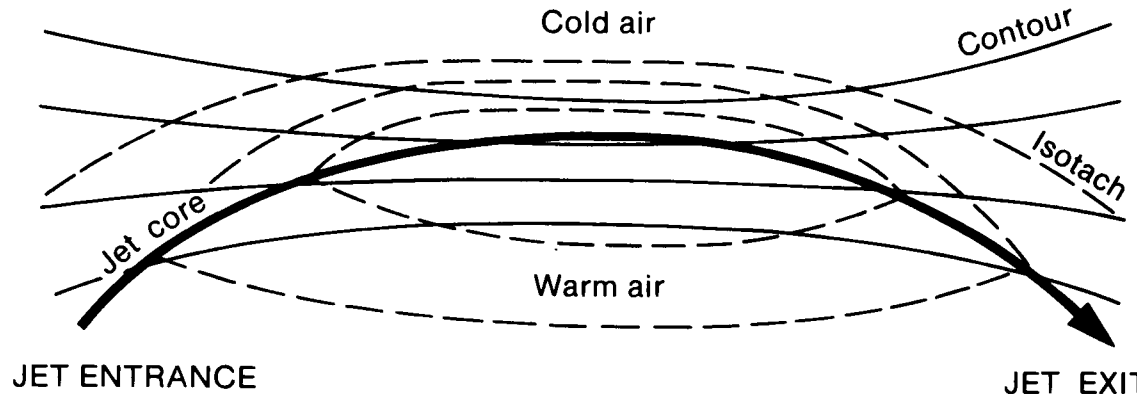

Figure 1.16. Position of the jet core on an upper-level chart, in relation to the contour lines. In the entrance and exit regions, ageostrophic effects produce cross-contour flows. In the steady part of the jet the core is displaced towards the cold side of the contour pattern.

Vertical shear: This varies in relation to the strength of the jet.

Typical values are:

Normal	3–6 kn per 1000 ft
Large	10–15 kn per 1000 ft
Extreme	more than 20 kn per 1000 ft.

Horizontal shear: The maximum horizontal shear is generally on the cold side of the jet at about the core level, or slightly below. On the warm side of the jet the maximum anticyclonic shear is slightly above the core level. Theoretically the anticyclonic shear cannot exceed the Coriolis parameter which has values as follows:

Latitude	30	35	40	45	50	55	60	65	70
Coriolis parameter (kn/100 n mile)	26	30	34	37	40	43	45	47	49

When the warm-side maximum shear values are attained, or exceeded, the flow becomes turbulent.

Surface developments: Ageostrophic motion in jet entrance and exit regions lead to consequential developments in the surface pressure pattern. Fig. 1.17 shows the association of C (cyclonic) and A (anticyclonic) surface developments with the 'left entrance', 'right entrance', 'left exit' and 'right exit' regions of the jet. In the

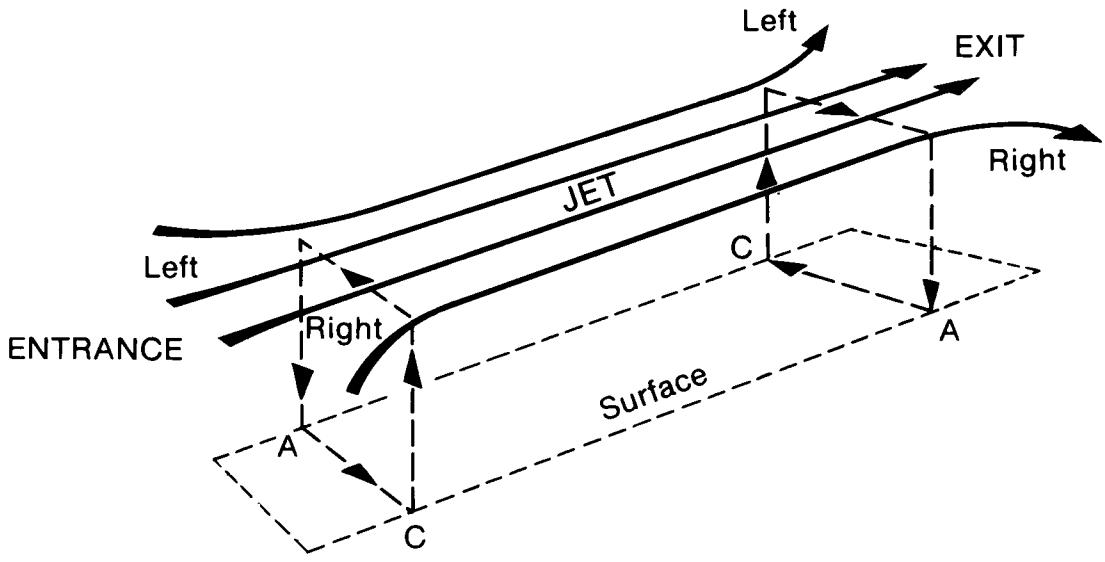

Figure 1.17. The association of jet-stream regions with surface pressure developments. C = Cyclonic development area. A = Anticyclonic development area.

exit region for example, the upper-level ageostrophic component of the flow (see Fig. 1.1) depletes the mass of air above C, where the surface pressure consequently falls and ascent of air is favoured. Similarly, air accumulates above A where the surface pressure rises and subsidence predominates. The vertical circulation is completed by the cross-isobar frictional effect at the surface, from high to low pressure.

1.8.2 *The subtropical jet*

The subtropical jet generally occurs between latitudes 20° to 30° and is most marked during the winter months. The basic differences between it and the polar front jet are:

(a) The level of maximum wind is about 200 hPa and may rise to 150 hPa when the axis is nearer the equator.

(b) The associated baroclinic zone is restricted to the upper part of the troposphere. Below 500 hPa the atmosphere may be quasi-barotropic.

(c) There is little direct connection between the subtropical jet and surface developments.

Seasonal variations

The mean position of the subtropical jet moves towards the equator in winter and polewards in summer. Over India, the jet splits during the summer months to produce one axis north of the Himalayas and another to the south.

Overlapping of jets

Satellite pictures show that a cyclonically curved polar-front jet may cross underneath the anticyclonically curved subtropical jet. There are then two velocity maxima, one near 200 hPa and the other near 300 hPa. Very sharp changes of wind direction can occur in the relatively shallow layer between the two jet cores, resulting in severe CAT.

1.8.3 *Equatorial easterly jet*

This is a band of very strong easterly winds which occur between the equator and latitude 20° N. The winds reach jet strength between the Philippines and the Sudan and also over West Africa.

The level of maximum wind ranges between 100 hPa near latitude 20° to 200 hPa at the equator. Maximum speeds exceed 120 kn.

1.8.4 *Polar-night jet*

This jet occurs in the winter hemisphere between latitudes 60° and 70° at a height of about 1 hPa (between 45 and 50 km) during the winter months when the polar regions are in perpetual darkness to great altitudes. Radiational cooling results in a large cold pool in the polar stratosphere. The polar-night jet is located along the strong temperature gradient on the edge of this cold pool. From 60° N to 70° N the temperature may fall from −50 °C to −80 °C. A maximum wind of 364 kn at a height of 47 km was recorded above South Uist in the Hebrides on 13 December 1967.

1.8.5 *Low-level jets*

These are bands of strong winds in the lower troposphere. Unlike high-level jets there is no specified minimum speed and many do not exceed 60 kn. These jets are often associated with large vertical and horizontal wind shears.

(a) *Low-level jets ahead of cold fronts*

These jets occur in the warm conveyor belt just ahead of a surface cold front. There may be more than one core, each about 100 km wide. Maximum speeds

are in the range 50–60 kn and at a height of about 1 km. A cross-section through one example of a low-level jet associated with a front is at Fig. 1.18.

(b) *The nocturnal jet*

This jet occurs at night overland when radiation cooling produces a temperature inversion near the surface. The frictional force is greatly reduced in the upper part of the boundary layer where speeds become super-geostrophic. Near the top of the inversion the wind speed may be more than 1.5 times the geostrophic value.

Over England speeds of 40 kn have been measured at a height of 400 ft above the ground at the end of a radiation night. The speed decreases rapidly after sunrise.

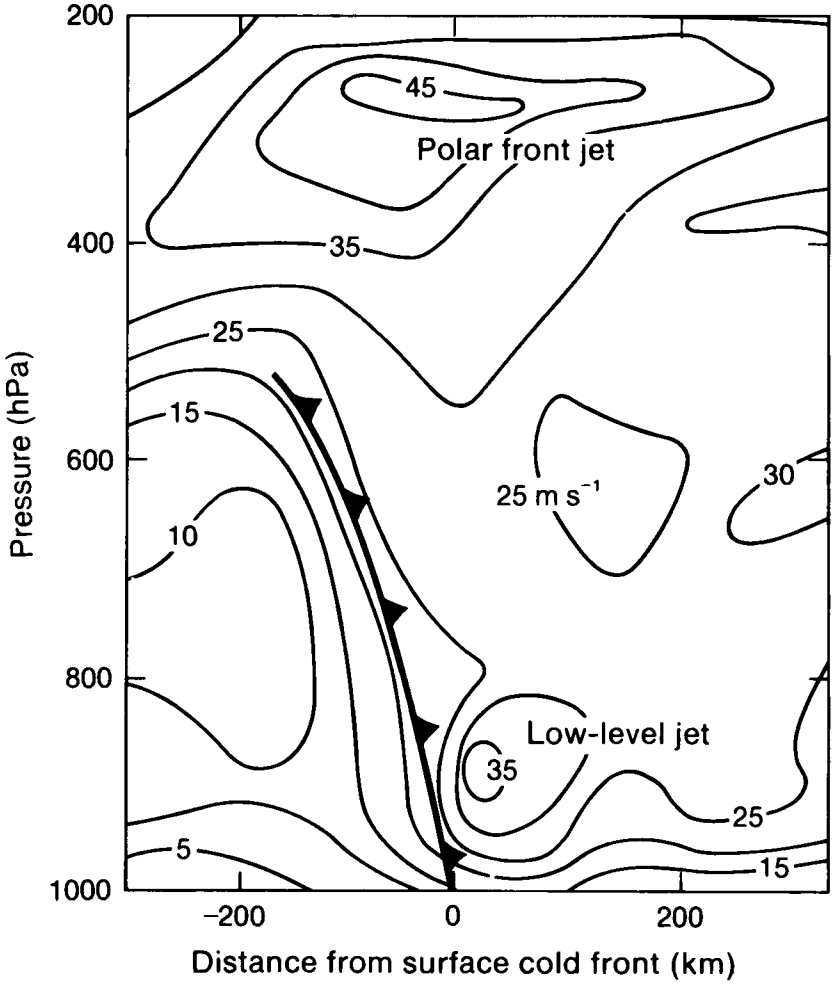

Figure 1.18. Low-level 'jet' associated with a front. Isotachs at intervals of 5 m s^{-1} show the wind flow into the paper.

On the eastern side of Arabia wind speeds of 50 kn have been observed at heights of 1300 to 1600 ft during the summer months. When a strong inversion develops the wind maximum may occur as low as 600 ft.

In Kansas and Nebraska speeds of 70 kn have been observed at a height of 1600 ft above the ground.

With such winds there is a very strong low-level shear which presents a hazard to aircraft on the final stages of an approach to landing. Descending aircraft experience a sudden decrease of air speed which may cause a stall just short of the runway.

(c) *East African cross-equatorial jet*

Another low-level jet is found in an arc from Madagascar to eastern Kenya and Somalia during the northern hemisphere summer. Speeds frequently exceed 40 kn and may reach 100 kn within the height band from 2000 to 7500 ft. The wind speed is strongest just before dawn.

1.9 Use of the hodograph

1.9.1 *Plotting*

Wind vectors are plotted on a hodograph so that they end at the centre of the diagram. Fig. 1.19 shows a 900 hPa wind of 240° 20 kn and an 800 hPa wind of

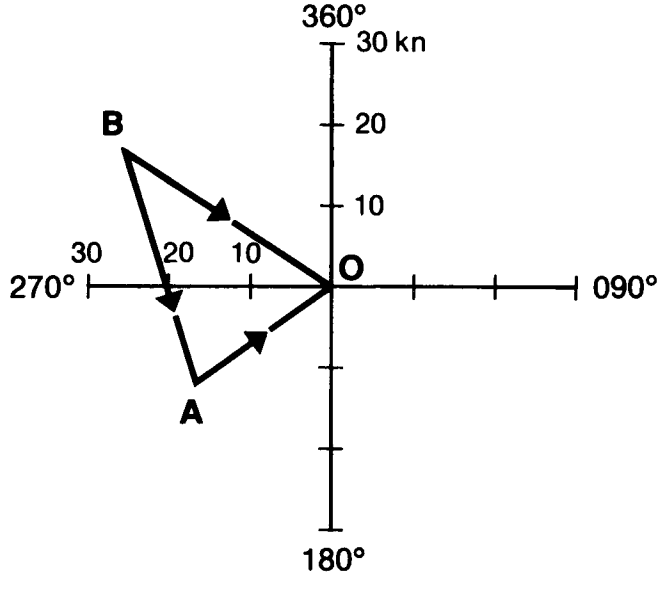

Figure 1.19. Plotting wind vectors on a hodograph. AO is the lower-level wind vector (say, 900 hPa). BO is the upper-level wind vector (say, 800 hPa). BA is the thermal wind vector (directed from the upper to the lower wind vectors).

300° 30 kn. The thermal wind in this layer is the vector from 8 to 9. A normal hodograph plot only shows the points at each pressure level, joined to show the thermal winds in each layer (see Fig. 1.20).

1.9.2 *Identifying the direction of warm and cold air*

In Fig. 1.20 the colder air is shown by light stippling and the warmer air by heavy stippling. Arrows show the direction of the thermal winds in the different layers.

Thus between 850 and 500 hPa the thermal wind direction is 240° which shows that the colder air lies towards the north-west. Between 500 and 400 hPa the thermal wind direction is 005° indicating that in that layer the colder air is towards the east.

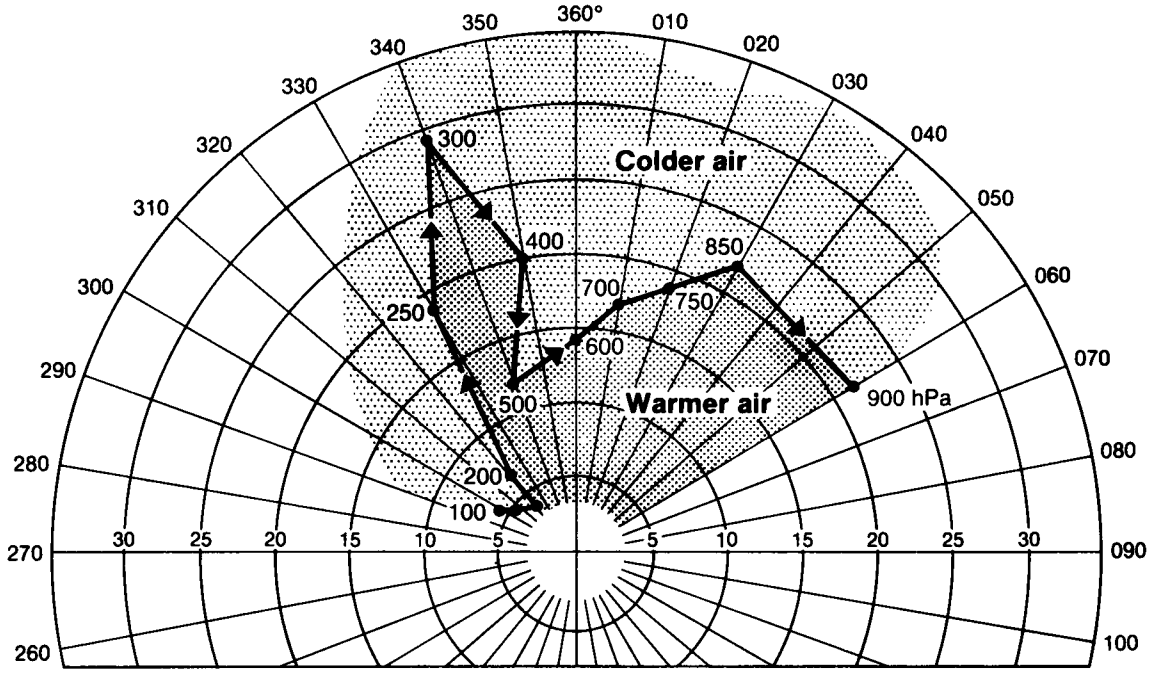

hPa	deg	kn
900	060	22
650	030	22
750	020	19
700	010	17

hPa	deg	kn
600	360	14
500	340	12
400	350	20
300	340	29

hPa	deg	kn
250	330	18
200	320	7
150	320	4
100	300	6

Figure 1.20. Hodograph example: Stornoway, 0600 UTC, 9 June 1961.

1.9.3 *Warm and cold advection*

Between 900 and 850 hPa in Fig. 1.20 the thermal wind direction is 315°, indicating colder air to the north-east. Since the mean wind direction between these levels is from the north-east colder air is being advected towards the station. This cold advection is in fact taking place at all levels up to 500 hPa.

Between 500 and 400 hPa the thermal wind is from 005° while the mean wind is about 345° indicating weak warm advection.

1.9.4 *Fronts and vertical motion*

Fig. 1.21 shows a construction which can be useful when a frontal surface lies over the station at some level.

(a) Mark the surface front through the centre of the hodograph, at its orientation as shown on a surface chart.

(b) Determine the upper and lower levels of the frontal zone from a tephigram, and mark them on the hodograph. The thermal wind direction in the frontal zone is roughly parallel to the front.

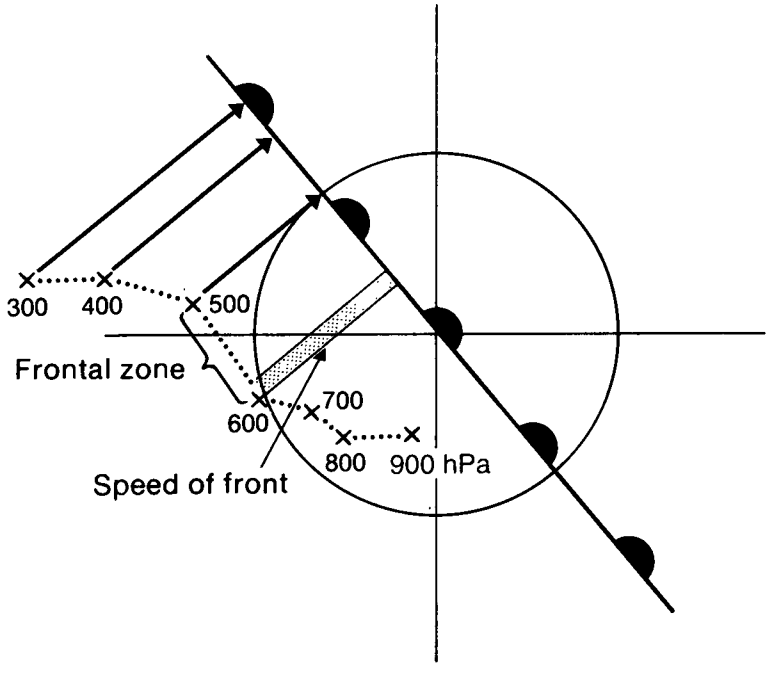

Figure 1.21. Assessment of ana- and kata-frontal characteristics from a hodograph.

(c) Measure the wind component normal to the front at each level in the frontal zone and in the warm air mass above.

(d) The frontal speed at the surface approximates to the speed of the cold air normal to the front at the base of the frontal zone.

(e) If the wind component normal to the front increases with height in the warm air, then:

i. A warm front is an anafront, and
ii. A cold front is a katafront.

(f) If the wind component normal to the front decreases with height in the warm air, then:

i. A warm front is a katafront, and
ii. A cold front is an anafront.

1.9.5 *Waves on quasi-stationary fronts*

When a quasi-stationary front is inactive the thermal wind direction is parallel to the front over a considerable depth. The first indication of the development of a wave upstream may be the backing of winds at high levels. This suggests the start of upslope flow caused by the approach of an upper trough whose axis is much further upstream. The new wave is likely to form ahead of this trough axis.

CHAPTER 2 — TEMPERATURE

2.1 Extremes of surface temperature

Table 2.1 Absolute maxima and minima recorded in the United Kingdom

Month	Max (°C)	Place	Min (°C)	Place
Jan.	18.3	Aber	−27.2	Braemar
Feb.	19.4	Barnstaple	−27.2	Braemar
Mar.	25.0	Wakefield	−22.8	Logie Coldstone
		Santon Downham		
		Cromer		
Apr.	29.4	Camden Square	−15.0	Newton Rigg
May	32.8	Camden Square	−10.0	Ben Nevis
		Greenwich		
		Tunbridge Wells		
		Horsham		
		Long Sutton		
June	35.6	Camden Square	−5.6	Dalwhinnie
		Southampton (Mayflower Park)		Santon Downham
July	35.9	Cheltenham	−4.5	Lagganlia
Aug.	37.1	Cheltenham	−5.0	Carnwath
Sept.	35.6	Bawtry	−7.8	Ben Nevis
Oct.	29.4	March*	−11.7	Dalwhinnie, Braemar
Nov.	21.7	Prestatyn	−23.3	Braemar
Dec.	18.3	Achnashellach	−26.7	Kelso

Note: Higher maximum temperatures have been recorded in July and August in non-standard screens or exposures.

* A maximum of 29.5 °C was recorded at Waddon on the same day as the maximum at March but this value is regarded as suspect.

2.2 Daytime rise of surface temperature

2.2.1 *Forecasting T_{max} (Inglis' method, using 1000–850 hPa thickness)*

This method assumes that the lapse rate before dawn in the 1000–850 hPa layer is approximately three-quarters of the saturated adiabatic lapse rate; the relative humidity of the layer is 75% and the surface pressure is 1020 hPa. Table 2.2 gives monthly values for the maximum temperature from April to September based on the 1000–850 hPa thickness. It is not valid for days with extensive cloud cover.

Table 2.2 Prediction of maximum temperatures (°C) from 1000–850 hPa thickness

Thickness (gpm)	Month					
	Apr.	May	June	July	Aug.	Sept.
1280	6.4	7.5	8.0	7.8	7.3	6.3
1290	8.3	9.4	9.9	9.7	9.2	8.2
1300	10.2	11.3	11.8	11.6	11.1	10.1
1310	12.1	13.2	13.7	13.5	13.0	12.0
1320	14.0	15.1	15.6	15.4	14.9	13.9
1330	15.9	17.0	17.5	17.3	16.8	15.8
1340	17.8	18.9	19.4	19.2	18.7	17.7
1350	19.6	20.7	21.2	21.0	20.5	19.5
1360	21.4	22.5	23.0	22.8	22.3	21.3
1370	23.2	24.3	24.8	24.6	24.1	23.1
1380	25.1	26.2	26.7	26.5	26.0	25.0
1390	26.9	28.0	28.5	28.3	27.8	26.8
1400	28.8	29.9	30.5	30.2	29.7	28.7
1410	30.7	31.8	32.3	32.1	31.6	30.6
1420	32.6	33.7	34.2	34.0	33.5	32.5

2.2.2 *Forecasting T_{max} (Callen and Prescott's method, using 1000–850 hPa thickness)*

This is an empirical method based on the maximum temperatures observed at Gatwick and the 1000–850 hPa thickness values at midday at Crawley. There are three steps:

(a) Classify the cloud cover or presence of fog between dawn and 1200 UTC on a scale from 0 to 3, as follows:

Class 0 $C_L + C_M \leq 3/8$, $C_H \leq 5/8$; or any fog confined to dawn period
Class 1 $C_L + C_M + C_H = 4/8–6/8$; or any fog clearing slowly during morning
Class 2 $C_L + C_M \geq 6/8$; or any fog clearing before noon
Class 3 Predominantly overcast with precipitation (not including very slight drizzle) or persistent fog.

(b) Using Fig. 2.1, obtain the temperature adjustment for the month for the appropriate cloud class.

(c) Apply this adjustment to the values given in Table 2.3 to find the predicted maximum temperature.

The relationship between 1000–850 thickness (h) and the unadjusted maximum temperature (T_u) is given by

$$T_u = -192.65 + 0.156h.$$

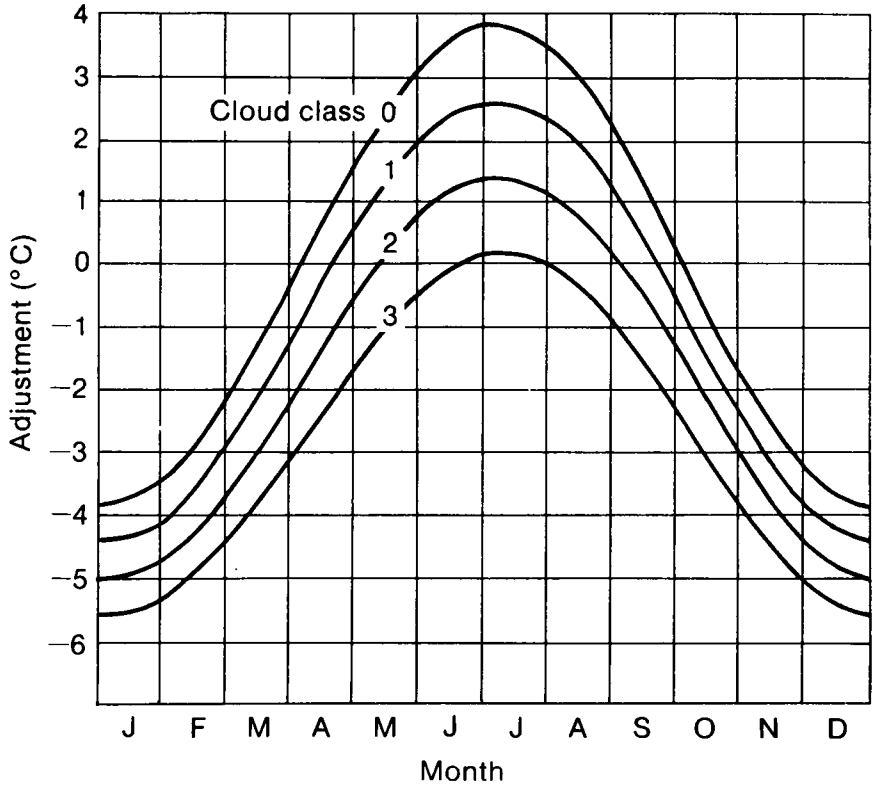

Figure 2.1 Adjustments to be applied to the values in Table 2.3 to allow for cloud classification and time of year.

Table 2.3 Unadjusted maximum temperature (°C) in terms of 1000–850 hPa thickness

Thickness (gpm)	Maximum temperature									
	0	1	2	3	4	5	6	7	8	9
1230	−0.8	−0.6	−0.5	−0.3	−0.1	0.0	0.2	0.3	0.5	0.6
1240	0.8	0.9	1.1	1.3	1.4	1.6	1.7	1.9	2.0	2.2
1250	2.3	2.5	2.7	2.8	3.0	3.1	3.3	3.4	3.6	3.8
1260	3.9	4.1	4.2	4.4	4.5	4.7	4.8	5.0	5.2	5.3
1270	5.5	5.6	5.8	5.9	6.1	6.2	6.4	6.6	6.7	6.9
1280	7.0	7.2	7.3	7.5	7.7	7.8	8.0	8.1	8.3	8.4
1290	8.6	8.7	8.9	9.1	9.2	9.4	9.5	9.7	9.8	10.0
1300	10.1	10.3	10.5	10.6	10.8	10.9	11.1	11.2	11.4	11.6
1310	11.7	11.9	12.0	12.2	12.3	12.5	12.6	12.8	13.0	13.1
1320	13.3	13.4	13.6	13.7	13.9	14.0	14.2	14.4	14.5	14.7
1330	14.8	15.0	15.1	15.3	15.5	15.6	15.8	15.9	16.1	16.2
1340	16.4	16.5	16.7	16.9	17.0	17.2	17.3	17.5	17.6	17.8
1350	17.9	18.1	18.3	18.4	18.6	18.7	18.9	19.0	19.2	19.4
1360	19.5	19.7	19.8	20.0	20.1	20.3	20.4	20.6	20.8	20.9
1370	21.1	21.2	21.4	21.5	21.7	21.8	22.0	22.2	22.3	22.5
1380	22.6	22.8	22.9	23.1	23.3	23.4	23.6	23.7	23.9	24.0
1390	24.2	24.3	24.5	24.7	24.8	25.0	25.1	25.3	25.4	25.6
1400	25.7	25.9	26.1	26.2	26.4	26.5	26.7	26.8	27.0	27.2
1410	27.3	27.5	27.6	27.8	27.9	28.1	28.2	28.4	28.6	28.7
1420	28.9	29.0	29.2	29.3	29.5	29.6	29.8	30.0	30.1	30.3
1430	30.4	30.6	30.7	30.9	31.1	31.2	31.4	31.5	31.7	31.8
1440	32.0	32.1	32.3	32.5	32.6	32.8	32.9	33.1	33.2	33.4

2.2.3 *Forecasting the hourly rise of temperature on sunny days, using a tephigram*

This method relates the amount of solar energy available for heating the lower layers of the atmosphere to an equivalent area on a tephigram. The area is a triangle with sides formed by the surface isobar, an isothermal and a dry adiabat.

It is assumed that the lapse rate at dawn can be adjusted to the equivalent isothermal (see Fig. 2.2). During the day, solar heating will change this isothermal state to a dry adiabatic. The area between the surface isobar, isotherm and dry adiabat can be defined by the difference in pressure (Δp) between the surface (p_0) and the intersection between the isothermal (IH) and the dry adiabat (IF). GHF is the surface isobar (p_0) and GADBE is the observed or estimated vertical temperature structure at dawn — the environment curve.

Use a transparent scale having two lines (IH and IF) on it at right angles (these are shown as dashed lines on the diagram. Point I is placed on the isobar ($p_0 - \Delta p$) with IF along a dry adiabat and IH along an isotherm in such a way that it intersects the environment curve to form equal areas on either side, i.e. in this case area BAD equals area GH A plus area BIE. The point F then gives the value of the forecast surface temperature.

Table 2.4 gives the values of Δp for each hour from dawn, to the time of day maximum temperature, for the middle of each month. No allowance is made for any superadiabatic lapse rate which may occur close to the surface. This table is a modified version of the original table attributed to Johnston. Small corrections have been made to remove some discrepancies in the early part of the day.

Note: The temperatures predicted by this method are critically dependent on the accuracy of the temperature sounding, particularly if there is an inversion within the layer which is to be heated. It is necessary to modify midnight radiosonde soundings to allow for cooling up to dawn.

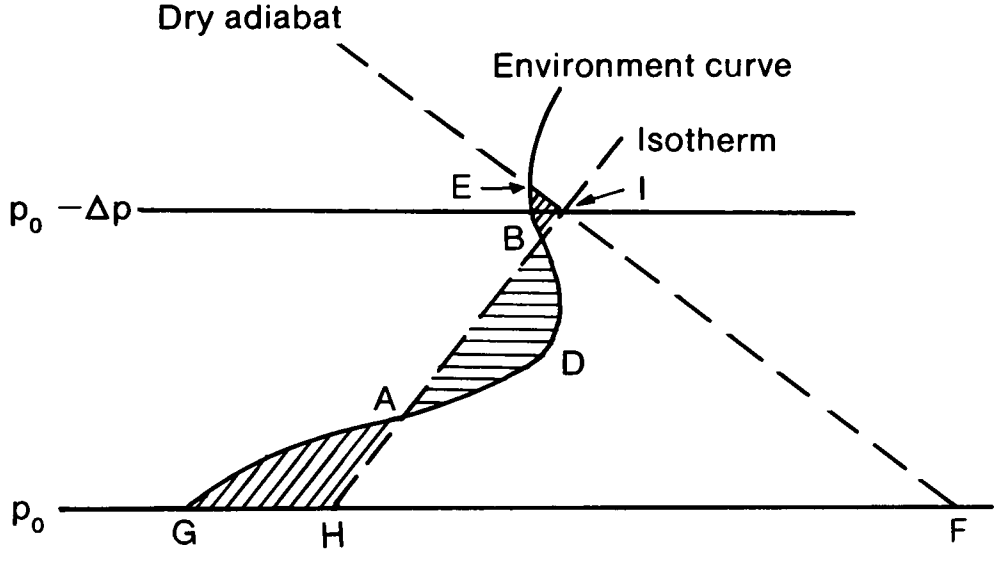

Figure 2.2 Estimating the rise of temperature on a sunny day by a tephigram construction. Δp is the thickness of the layer (hPa) and F is the forecast surface temperature. See text for details of construction.

Table 2.4 The thickness of the layer (Δp in hectopascals) which is changed from an isothermal to an adiabatic state by insolation at 52° N, 00° W .

Month	Time UTC											
	05	06	07	08	09	10	11	12	13	14	15	MAX
Jan.	—	—	—	—	03	18	35	48	58	61		61
Feb.	—	—	—	01	15	33	50	65	75	80		81
Mar.	—	—	02	17	35	53	68	81	90	95		97
Apr.	—	04	19	37	54	71	86	98	107	112	115	115
May	04	19	36	54	70	86	100	110	119	124	127	127
June	08	23	40	58	74	89	102	113	122	127	130	131
July	04	19	36	53	69	84	98	109	118	123	126	126
Aug.	—	08	24	41	59	75	89	101	110	116	119	119
Sept.	—	—	10	27	44	60	76	88	96	102	104	104
Oct.	—	—	01	13	29	45	60	72	80	85		86
Nov.	—	—	—	—	11	25	38	49	57	61		61
Dec.	—	—	—	—	02	15	30	42	50	53		53

Notes:

(a) These values do not take into account any superadiabatic close to the surface. Add 2 °C to the resulting forecast temperature with clear skies and light winds in summer, to allow for superadiabats.

(b) Approximate corrections to be applied to allow for cloud cover:

8/8 Ci	use	90% of depth (Δp in hectopascals)
8/8 As	use	60%
8/8 Sc	use	50%
8/8 Ns	use	35%

(c) The value of Δp may be reduced if the ground is wet and/or the lowest layers of the atmosphere are very humid.

(d) In summer, if the ground is very dry and humidity in the bottom layers is low, the value of Δp may be increased. These changes are generally only significant in the first 3 or 4 hours of heating.

2.2.4 *Forecasting the temperature rise on days with fog or low cloud (Jefferson's method)*

(a) Use the method in section 2.2.3 to draw a curve showing the rise of temperature to be expected if the sky was clear.

(b) Evaluate a constant 'delay factor' f. This may be done from the observation of temperature at least 3 hours after sunrise. If h_0 is the time of sunrise, h_2 is the time at which the temperature is observed and h_1 is the time at which that temperature would have been observed on a sunny day, then

$$f = (h_1 - h_0)/(h_2 - h_0).$$

(c) Plot points C, F, etc., as shown in Fig. 2.3, such that

$$AB/AC = DE/DF = \ldots f.$$

(As a first estimate, take f=0.25 for deep fog or thick stratus and f=0.35 for shallow fog or thin stratus.) Points C, F, etc. provide a forecast temperature curve for a foggy day.

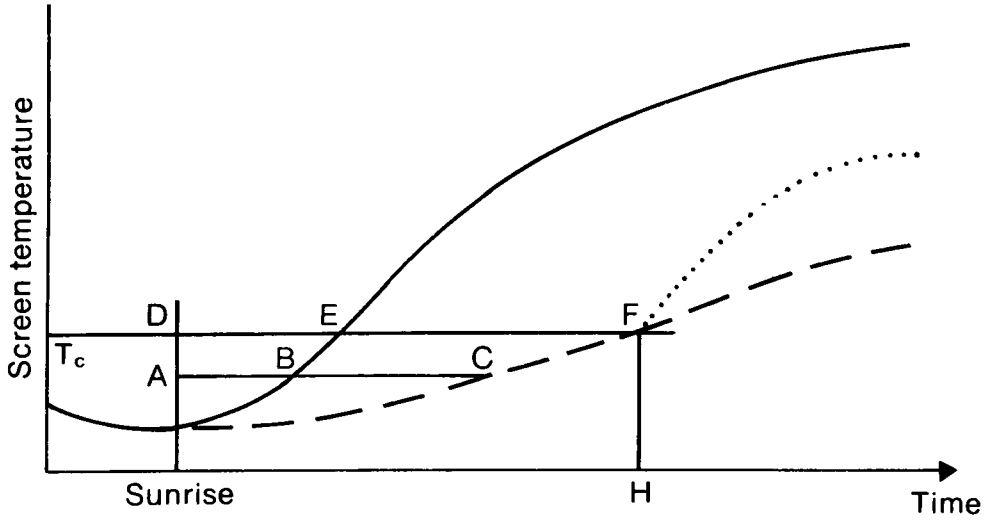

Figure 2.3 Constructing a forecast temperature curve on a foggy morning. The solid line is the forecast temperature curve for a clear day. The dashed line is the forecast for a foggy day, based on a delay factor of 0.35. The dotted line is the forecast for the later part of the day if the fog clears when the temperature reaches the critical value (T_c), at time H. See text for details of construction.

(d) If this curve reaches the temperature (T_C) at which the fog can be expected to disperse, the subsequent temperature rise will be steeper and more in line with conditions for a clear day (dotted line in Fig. 2.3).

2.3 Nocturnal fall of surface temperature

2.3.1 *Forecasting T_{min} (McKenzie's method)*

The night-time minimum air temperature (T_{min}) can be forecast as follows:

$$T_{min} = \tfrac{1}{2}(T_{max} + T_d) - K$$

where T_{max} = maximum temperature, T_d = air-mass dew-point at time of T_{max}, and K = local constant (depending on forecast surface wind and cloud amount).

Values of K have been calculated for most airports in the United Kingdom. Many inland low-level airports have values similar to those for Birmingham (see Table 2.5).

2.3.2 *Forecasting T_{min} (Craddock and Pritchard's method)*

The following regression equation was obtained from a statistical investigation of 16 stations in eastern England not close to the sea:

$$\begin{aligned} T_{min} &= 0.316\,T_{12} + 0.548\,T_{d12} - 1.24 + K \\ &= X + K \end{aligned}$$

where T_{12} = screen temperature at 1200 UTC and T_{d12} = dew-point temperature at 1200 UTC

For ease of use, the value for X may be obtained from Table 2.6 while the values for K, which depend on forecast values of the mean geostrophic wind and mean cloud amount, are given in Table 2.7 The means are forecast values for 1800, 0000 and 0600 UTC.

2.3.3 *Forecasting the hourly fall of temperature during the night (Barthram's method)*

The following steps are used in conjunction with the Night Cooling Nomogram, see Fig. 2.4(a) and (b), to obtain a cooling curve:

(a) Use a representative upper-air sounding to determine whether there is an inversion with its base below 900 hPa at the time of maximum temperature.

(b) Decide if nocturnal cloud cover will be best described as cloudless or 8/8.

(c) From steps (a) and (b), select one of the four rows marked 'Dew-point at time of maximum temp'. A series of vertical lines descends from these dew-point values.

(d) Follow a horizontal line from the value for the maximum temperature (marked on the left-hand side) until it cuts the vertical line descending from the dew-point value selected in step (c). From this point, follow one of the diagonal lines to the line marked 'Saunders discontinuity temperature T_R'.

(e) The time of this discontinuity depends on the date. Use the small graph at the bottom of the nomogram where the months are marked. Find the time of T_R for the required date from the curve marked 'time of discontinuity'.

(f) Follow the vertical line upwards from the time of T_R and extend it to the main graph to meet the value of T_R established in step (d).

(g) The next stage brings in a correction for the forecast gradient wind overnight. Select one of the diagonal lines on the right-hand side of the nomogram marked 'gradient wind speed'.

(h) Follow the horizontal line from T_R until it cuts the selected diagonal line marked 'gradient wind speed'. From this point of intersection, descend along a vertical line to the diagonal marked 'Minimum temp. under clear skies'. The preliminary value for T_{min} can be read off here.

(i) The preliminary value for T_{min} needs corrections for cloud amount and wind speed. The two small graphs (lower left) show amounts to be added to the preliminary T_{min} value to allow for the effect of nocturnal cloud cover and wind.

(j) In summer a further correction is needed because the short nights give a reduced period for cooling. Use the small graph (lower right) to find this value.

(k) After raising the preliminary T_{min} by adding the corrections in steps (i) and (j) the final value of T_{min} is plotted on the main graph above the time for sunrise shown on the lower graph.

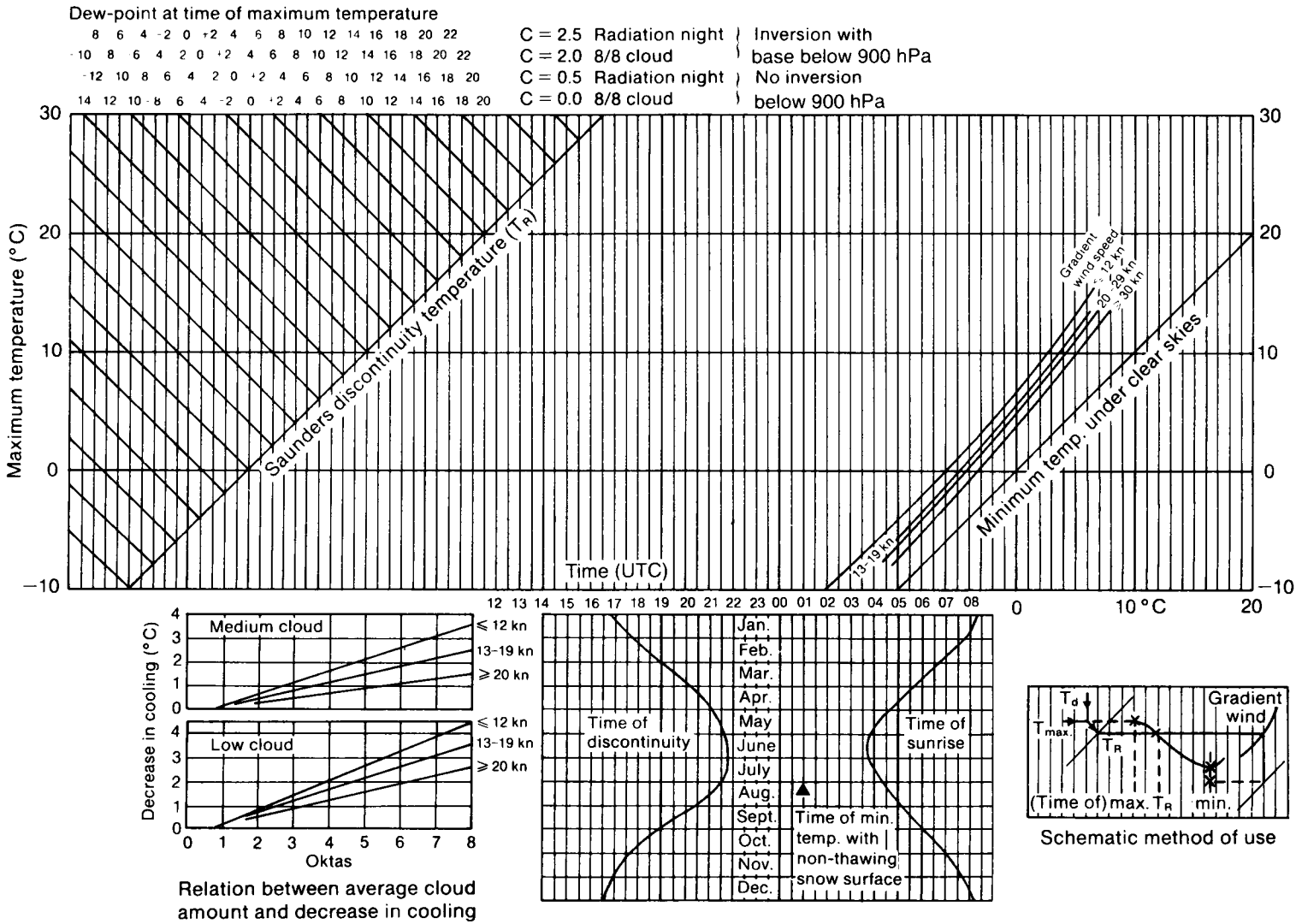

Figure 2.4(a) Night Cooling Nomogram for winter (October–March). See text for method of use.

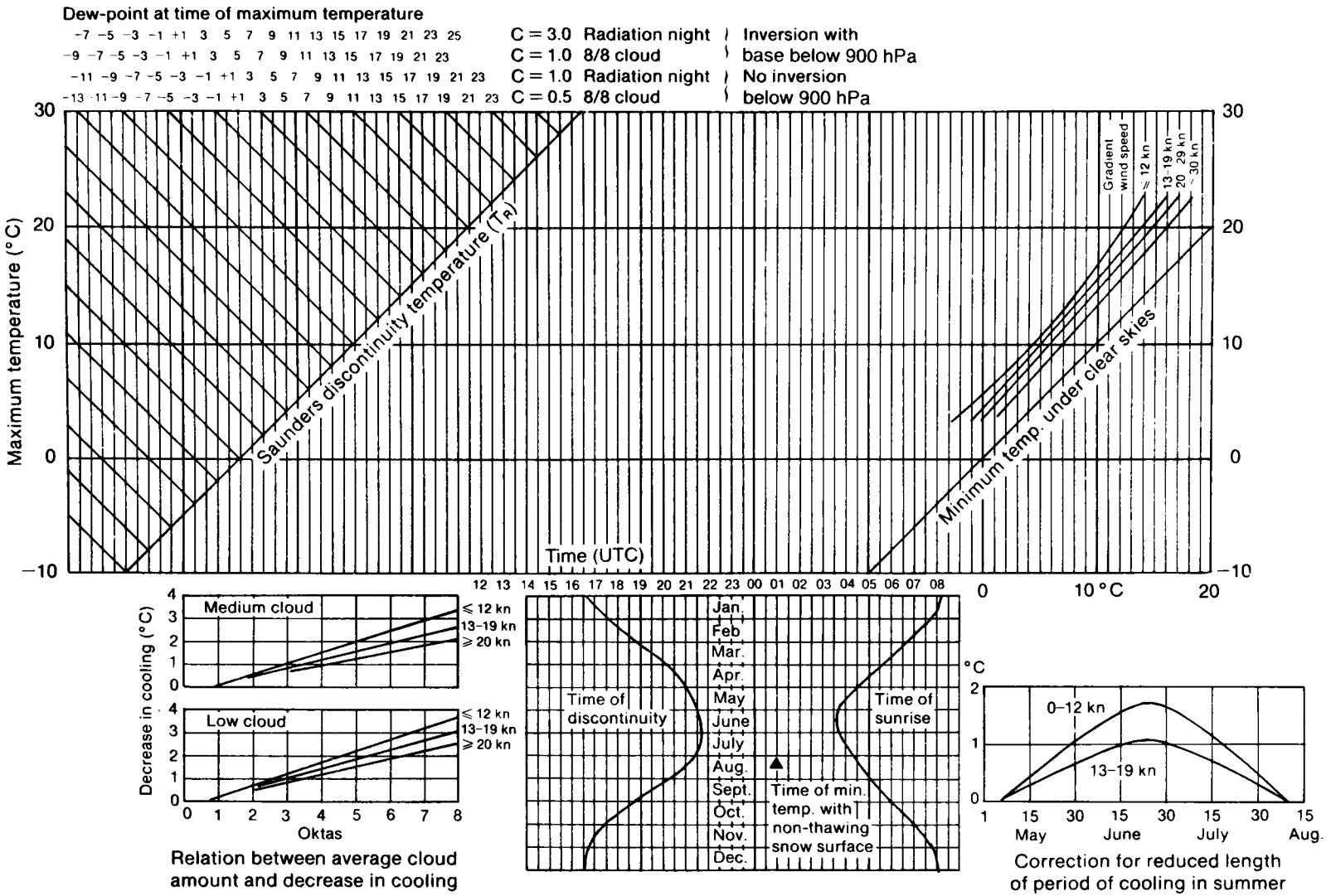

Figure 2.4(b) Night Cooling Nomogram for summer (April–September). See text for method of use.

(l) This fixes three points on the cooling curve: T_{max} at approximately mid afternoon, T_R and T_{min}. The cooling curve can be drawn through these three points.

There are small differences between cooling for summer and winter and separate diagrams are provided for summer (April to September) (Fig. 2.4(b)) and for winter (October to March) (Fig. 2.4(a)).

Table 2.5. Values of local constant (K) for Birmingham Airport

Mean overnight surface wind (kn)	Average cloud amount overnight (oktas)				
	0	1–2	3–4	5–6	7–8
Calm	8.8	8.0	7.3	6.7	3.2
1–3	8.2	7.7	6.7	5.1	2.8
4–6	6.5	5.8	5.2	4.0	2.3
7–10	4.7	4.3	3.9	3.1	1.8
11–16	2.3	2.8	2.5	2.1	1.4
17–21	0.5	0.8	2.0	1.1	0.8

Monthly variations have been found which apply at all stations. The value of K may usefully be corrected by the following amounts:

	Jan.	Feb.	Mar.	Apr.	May	June	July	Aug.	Sept.	Oct.	Nov.	Dec.
A	−1.0	−0.5	+0.5	0.0	0.0	0.0	0.0	0.0	+0.5	+1.0	0.0	−1.0
B	−0.5	−0.5	0.0	0.0	+0.5	+0.5	+0.5	+0.5	0.0	0.0	−0.5	−0.5

A = Good radiation nights B = Poor radiation nights

Note: Exceptionally low minimum temperatures may occur if:

(a) the ground is covered by fresh snow,
(b) there is a large catchment area for katabatic drainage, and
(c) the lowest layers (950–850 hPa) are very dry (e.g. dew-point depression 20–40 °C).

Table 2.6 Computation of the value of X (°C)

Air temperature at 1200	Dew-point at 1200 UTC																			
	−3	−2	−1	0	1	2	3	4	5	6	7	8	9	10	11	12	13	14	15	16
27	5.7	6.2	6.7	7.3	7.8	8.4	8.9	9.5	10.0	10.6	11.1	11.7	12.2	12.8	13.3	13.9	14.4	15.0	15.5	16.1
26	5.4	5.9	6.4	7.0	7.5	8.1	8.6	9.2	9.7	10.3	10.8	11.4	11.9	12.5	13.0	13.6	14.1	14.6	15.2	15.7
25	5.1	5.6	6.1	6.7	7.2	7.8	8.3	8.9	9.4	9.9	10.5	11.0	11.6	12.1	12.7	13.2	13.8	14.3	14.9	15.4
24	4.8	5.2	5.8	6.3	6.9	7.4	8.0	8.5	9.1	9.6	10.2	10.7	11.3	11.8	12.4	12.9	13.5	14.0	14.6	15.1
23	4.5	4.9	5.5	6.0	6.6	7.1	7.7	8.2	8.8	9.3	9.9	10.4	11.0	11.5	12.1	12.6	13.2	13.7	14.2	14.8
22	4.1	4.6	5.2	5.7	6.3	6.8	7.4	7.9	8.5	9.0	9.5	10.1	10.6	11.2	11.7	12.3	12.8	13.4	13.9	14.5
21	3.8	4.3	4.8	5.4	5.9	6.5	7.0	7.6	8.1	8.7	9.2	9.8	10.3	10.9	11.4	12.0	12.5	13.1	13.6	14.2
20	3.5	4.0	4.5	5.1	5.6	6.2	6.7	7.3	7.8	8.4	8.9	9.5	10.0	10.6	11.1	11.7	12.2	12.8	13.3	13.8
19	3.2	3.7	4.2	4.8	5.3	5.9	6.4	7.0	7.5	8.1	8.6	9.1	9.7	10.2	10.8	11.3	11.9	12.4	13.0	13.5
18	2.9	3.4	3.9	4.4	5.0	5.5	6.1	6.6	7.2	7.7	8.2	8.8	9.4	9.9	10.5	11.0	11.6	12.1	12.7	13.3
17	2.6	3.0	3.6	4.1	4.7	5.2	5.8	6.3	6.9	7.4	8.0	8.5	9.1	9.6	10.2	10.7	11.3	11.8	12.4	12.9
16	2.3	2.7	3.3	3.8	4.4	4.9	5.5	6.0	6.6	7.1	7.7	8.2	8.7	9.3	9.8	10.4	10.9	11.5	12.0	12.6
15	1.9	2.4	3.0	3.5	4.0	4.6	5.1	5.7	6.2	6.8	7.3	7.9	8.4	9.0	9.5	10.1	10.6	11.2	11.7	
14	1.6	2.1	2.6	3.2	3.7	4.3	4.8	5.4	5.9	6.5	7.0	7.6	8.1	8.7	9.2	9.8	10.3	10.9		
13	1.3	1.8	2.3	2.9	3.4	4.0	4.5	5.1	5.6	6.2	6.7	7.3	7.8	8.3	8.9	9.4	10.0			
12	1.0	1.5	2.0	2.6	3.1	3.6	4.2	4.7	5.3	5.8	6.4	6.9	7.5	8.0	8.6	9.1				
11	+0.7	1.1	1.7	2.2	2.8	3.3	3.9	4.4	5.0	5.5	6.1	6.6	7.2	7.7	8.3					
10	+0.4	+0.8	1.4	1.9	2.5	3.0	3.6	4.1	4.7	5.2	5.8	6.3	6.9	7.4						
9	−0.0	+0.5	1.1	1.6	2.2	2.7	3.2	3.8	4.3	4.9	5.4	6.0	6.5							
8	−0.4	+0.2	+0.7	1.3	1.8	2.4	2.9	3.5	4.0	4.6	5.1	5.7								
7	−0.7	−0.1	+0.4	1.0	1.5	2.1	2.6	3.2	3.7	4.3	4.8									
6	−1.0	−0.4	+0.1	+0.7	1.2	1.8	2.3	2.8	3.4											
5	−1.3	−0.8	−0.2	+0.3	+0.9	1.4	2.0	2.5	3.1											
4	−1.6	−1.1	−0.5	+0.0	+0.6	1.1	1.7	2.2												
3	−1.9	−1.4	−0.8	-0.3	+0.3	+0.8	1.4													

Table 2.7 Values of K (°C) based on mean forecast values of wind speed and cloud amount for 1800, 0000 and 0600 UTC

Mean geostrophic wind speed (kn)	Mean cloud amount (oktas) 0–2	2–4	4–6	6–8
0–12	−2.2	−1.7	−0.6	0
13–25	−1.1	0	+0.6	+1.1
26–38	−0.6	0	+0.6	+1.1
39–51	+1.1	+1.7	+2.8	—

Notes:

(a) The method applies to nights without fog.

(b) If the ground is snow covered the actual minimum is likely to be lower than that forecast by this method.

2.3.4 *Description of the severity of air frost*

When actual or forecast air temperatures fall below 0 °C, the severity of the frost is described by the terms 'Slight', 'Moderate', 'Severe' or 'Very severe' according to the temperature and the surface wind speed at the time, as illustrated in Fig. 2.5.

2.4 Grass and concrete minimum temperatures

2.4.1 *Forecasting the grass minimum temperature, using the geostrophic wind speed and cloud amount*

$$T_g = T_n - K$$

where T_g is the grass minimum temperature, T_n is the air minimum temperature, and K is a constant which depends on forecast values of geostrophic wind speed and cloud amount.

Values of K (°C)

V_g (kn)	N (oktas) 0–2	2–4	4–6	6–8
0–12	5.0	5.0	4.0	4.0
13–25	4.0	4.0	3.0	2.0
26–38	3.5	3.0	2.5	2.5
39–52	2.5	2.5	2.5	3.0

Values of V_g and N are means of the 18, 00 and 06 UTC values.

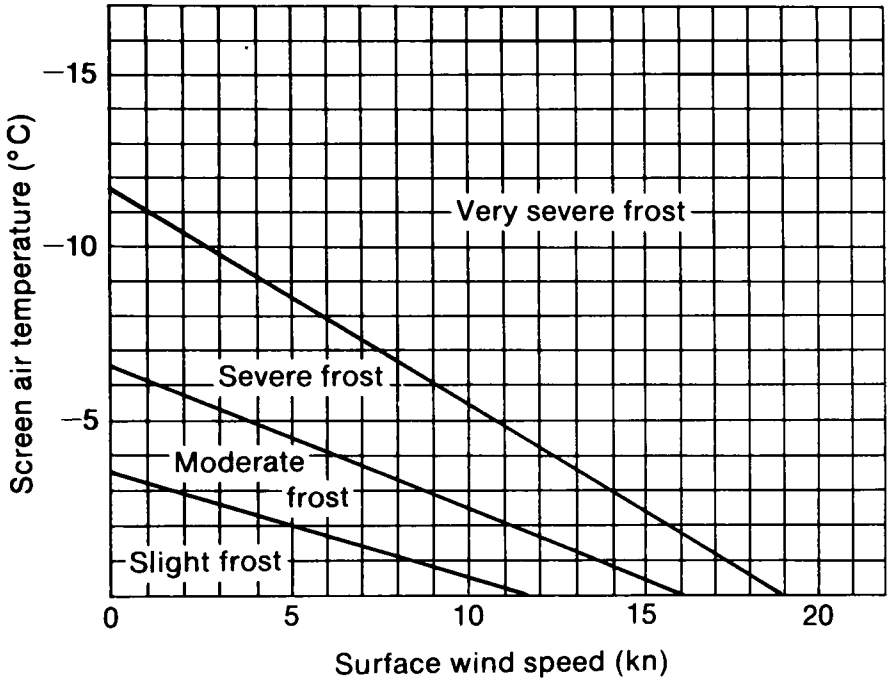

Figure 2.5 Diagram for determining the severity of air frost for actual or forecast wind speeds and air temperatures.

2.4.2 *Forecasting the grass minimum temperature from the geostrophic wind speed (graphical method)*

Fig. 2.6 shows isopleths of the depression of the grass minimum temperature below the air minimum temperature at Cottesmore in central England. Only low-cloud cover is considered, and 'sky obscured' is taken to be the same as 8 oktas.

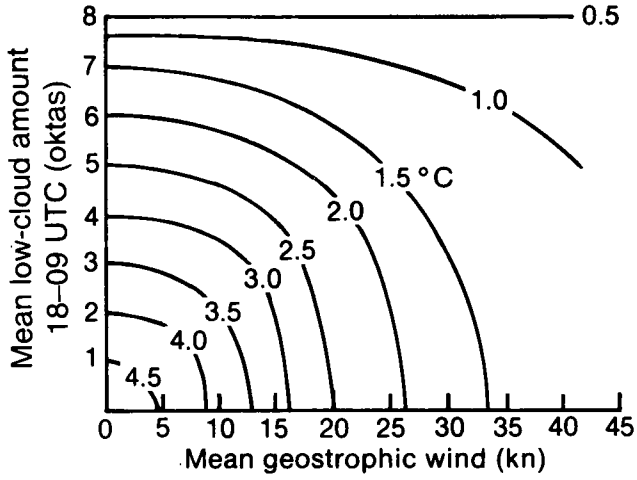

Figure 2.6 Depression (°C) of the grass minimum temperature below the air minimum temperature at Cottesmore.

2.4.3 *Forecasting the grass minimum temperature from the surface wind speed*

Use the same formula as in section 2.4.1 but with values of K as follows:

Values of K (°C)

Surface wind (kn)	Clear sky (up to 2/8)		Cloudy (8/8 cloud)
	Mean	(Max)	Mean
1–5	5.0	(8.0)	1.0
6–10	3.5	(8.6)	1.0
11–15	2.5	(3.5)	1.0
>15	1.5	(2.8)	1.0

Cloud cover is C_L, C_M or $C_L + C_M$

The mean values have been rounded to 0.5 °C. They are averaged for six stations in England.

2.4.4 *Minimum temperatures on a concrete slab*

The following values are taken from curves produced from investigations at Wyton in central England. The values show the depression of the concrete temperature (T_c) below the air minimum (T_{min}).

Depression of concrete temperature below air minimum (°C)

	Jan.	Feb.	Mar.	Apr.	May	June	July	Aug.	Sept.	Oct.	Nov.	Dec.
$T_{min} - T_c$	1.6	1.4	1.0	0.2	−0.6	−1.0	−1.0	−0.6	0.3	1.0	1.5	1.7

Negative values mean that the concrete temperature was above T_{min}.

The points through which the curve was drawn showed a scatter of ±2.5 °C in winter and ±3.5 °C in summer.

2.4.5 *Minimum temperature on roads*

At Watnall (near Nottingham) it was found that the difference between screen minimum and road minimum temperature varied with the length of night. The following regression equation was obtained:

$$T_{min} - T_r = 0.28t - 2.9$$

where T_r = minimum temperature on the road, t is the length of night (in hours).

Minimum temperature on roads (°C)

	Jan.	Feb.	Mar.	Apr.	May	June	July	Aug.	Sept.	Oct.	Nov.	Dec.
$T_{min} - T_r$ (observed)	2.0	1.5	1.0	0.0	—	—	—	—	—	0.5	1.5	2.0
from the formula for latitude 52° N	1.5	1.1	0.5	0.0	−0.6	−1.1	−0.7	−0.3	0.3	0.8	1.4	1.6

Forecasting the temperature of road surfaces is specially important in winter when icy conditions may occur. It is not straightforward, because of the wide variations which are found over short distances on the same night. Amongst the relevant factors are:

(a) Small-scale meteorological effects, such as urban heat islands and local winds. Katabatic drainage of cold air and variations in exposure of a road to the sun are particularly significant.

(b) Variations in the thermal capacity and conductivity of different types of road. These may be very marked, especially between motorways, major roads and minor roads. The latter are shallower in construction and generally cool more quickly than deeply constructed major roads and motorways. The wetness of the surface is also relevant, since evaporation from the surface will cool it.

2.5 Modification of surface air temperature over the sea

2.5.1 *Advection of cold air over warm sea (Frost's method)*

If T_o (°C) and r_o (g kg^{-1}) are the temperature and humidity mixing ratio of the air before crossing the sea, T and r the values after crossing at least 60 miles of sea; T_s and r_s are the sea temperature and humidity mixing ratio of saturated air at temperature T_s, then:

$$T = T_o + 0.6\,(T_s - T_o)$$
$$r = r_o + 0.6\,(r_s - r_o).$$

Notes:

(a) These formulae apply to all cold air streams crossing a warmer sea surface, e.g. a cold northerly outbreak reaching north Scotland or a cold westerly current reaching Norway.

(b) In applying these formulae, make the best estimate of the sea surface temperature along the trajectory. Determine r_o and r_s by using a tephigram.

(c) Although this method is simple to use it has been criticized because:

(i). The factor of 0.6 only applies to sea crossings of over 300 n mile (550 km).
(ii). The presence of any inversion is ignored.
(iii). The values of r can exceed the saturated humidity mixing ratio at the temperature T_s.

Blackall put forward a more empirically based method to overcome these objections, see 2.5.2.

2.5.2 *Advection of cold air over a warm sea (Blackall's method)*

This is an empirically based method which takes into account both the duration of the sea crossing and the depth of convection. The method uses the equation

$$T = T_s - (T_s - T_0) \exp(-12t/d)$$

where T_s = sea temperature (°C), t is the duration of the sea crossing (hours), d is the depth of convection in hectopascals, and T is the final and T_0 the original air temperature.

The procedure is as follows:

(a) On a sounding in the air upwind of the sea crossing, draw in the MSL isobar and, if necessary, extend the ascent downwards to meet this isobar at the coastal temperature.

(b) Draw a dry adiabatic through the sea temperature T_s (Fig. 2.7). The pressure at which this line meets the environment curve is subtracted from the surface pressure to give the depth of convection d in hectopascals.

(c) Establish the expected lapse rate; if the air already has a lapse rate implying convection through the layer d, the environment curve should not be changed. If a lapse rate needs to be forecast modify the environment curve as follows: draw a line through the layer d with an appropriate lapse (use Table 2.8) such that the environment curve encloses equal areas (A and B in Fig. 2.7(b)) on each side of the line. Where this line meets the surface isobar is T_0. This step represents complete mixing without the addition of heat.

(d) Determine the time t that the air will spend over the sea from the wind in the layer d and the fetch. Using gradient winds from the isobars and 850 hPa contours should be sufficiently accurate in most cases.

(e) From Table 2.8 look up the value of $\exp(-12t/d)$ using the appropriate values of t (hours) and d (hectopascals). Then find T from the equation, above.

(f) From temperature T on the surface isobar, draw a line parallel to the environment curve produced in step (c); this is the predicted environment curve when the air finishes its crossing.

(g) A mean value of the sea temperature will often give good answers; however if changes in T_s alter the value of d and thus $\exp(-12t/d)$ it will be necessary to proceed by steps. This will also be necessary when the sea passage is expected to take more than 24 hours.

Note:

The procedure above does not allow for fronts and other dynamic means of heating and cooling.

The increase in surface humidity mixing ratio is taken to be

$$r - r_0 = 0.18\,(T - T_0)$$

with the dew-point remaining constant with height.

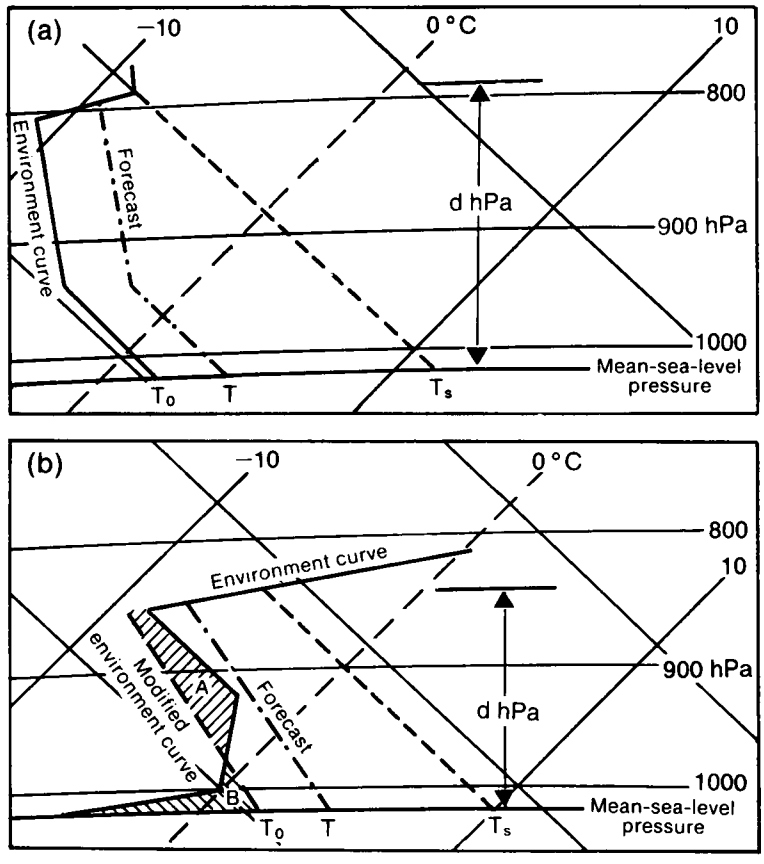

Figure 2.7 Forecasting the warming of cold air moving over a warm sea (Blackall's method) when (a) the upstream environment curve already indicates convective mixing is occurring, and (b) the environment curve is initially stable and needs modification. See text for details of construction.

Table 2.8 Values of exp $(-12t/d)$

Temp. lapse in the layer with depth d (°C)	d (hPa)	Duration of crossing t (hours)													
		1	2	3	4	5	6	7	8	9	12	15	18	21	24
	700	0.98	0.97	0.95	0.93	0.92	0.90	0.89	0.87	0.86	0.81	0.77	0.73	0.70	0.66
	600	0.98	0.96	0.94	0.92	0.90	0.89	0.87	0.85	0.84	0.79	0.74	0.70	0.66	0.62
40	500	0.98	0.95	0.93	0.91	0.89	0.86	0.84	0.82	0.81	0.75	0.70	0.65	0.60	0.56
31	400	0.97	0.94	0.91	0.89	0.86	0.84	0.81	0.79	0.76	0.70	0.64	0.58	0.53	0.49
26	350	0.97	0.93	0.90	0.87	0.84	0.81	0.79	0.76	0.73	0.64	0.60	0.54	0.49	0.44
22	300	0.96	0.92	0.89	0.85	0.82	0.79	0.76	0.73	0.70	0.62	0.55	0.49	0.43	0.38
17	250	0.95	0.91	0.86	0.83	0.79	0.75	0.71	0.68	0.65	0.57	0.49	0.42	0.36	0.32
14	200	0.94	0.89	0.84	0.79	0.74	0.70	0.66	0.62	0.58	0.49	0.41	0.34	0.28	0.24
13	180	0.94	0.88	0.82	0.77	0.72	0.67	0.63	0.59	0.55	0.45	0.37	0.30	0.25	0.20
12	160	0.93	0.86	0.80	0.74	0.69	0.64	0.59	0.55	0.51	0.41	0.33	0.26	0.21	0.17
10	140	0.92	0.84	0.77	0.71	0.65	0.60	0.55	0.50	0.46	0.36	0.28	0.21	0.17	0.13
9	120	0.90	0.82	0.74	0.67	0.61	0.55	0.50	0.45	0.41	0.30	0.22	0.17	0.12	0.09
8	100	0.89	0.79	0.70	0.62	0.55	0.49	0.43	0.38	0.34	0.24	0.17	0.12	0.08	0.06
6	80	0.86	0.74	0.64	0.55	0.47	0.41	0.35	0.30	0.26	0.17	0.11	0.07	0.04	0.03
5	60	0.82	0.67	0.55	0.45	0.37	0.30	0.25	0.20	0.17	0.09	0.05	0.03	0.01	
4	50	0.79	0.62	0.49	0.38	0.30	0.24	0.19	0.15	0.12	0.06	0.03	0.01		
4	40	0.74	0.55	0.41	0.30	0.22	0.17	0.12	0.09	0.07	0.03	0.01			
1	30	0.67	0.45	0.30	0.20	0.14	0.09	0.06	0.04	0.03	0.01				

2.5.3 *Advection of cold air over a warm sea (Grant's method)*

(a) Use air trajectory and wind speed to find length of fetch(es).

(b) Use sea temperature charts to find the mean sea temperature (T_s) and from a tephigram, determine the saturated humidity mixing ratio (r_s) at this temperature.

(c) On a representative upstream sounding:

i. Draw in the MSL isobar (p_s).
ii. Draw a dry adiabat from T_s to meet the environment curve.
iii. Draw the isobar through this meeting point and note the depth of convection (d) in hectopascals.

(d) Modify the initial air temperature (T_o) by

i. Drawing the expected condensation level (CL) at end of sea crossing. Use $p_s - 60$ hPa as a first guess.
ii. If the sounding is well inland, modify the lower part to fit the reported temperatures at the upwind coast.
iii. Draw the path followed by a parcel of air condensing at the expected CL so that equal areas (A=B) are enclosed between the path curve, the environment curve and the isobar $p_s - d$ (see Fig. 2.8).
iv Note value of modified initial temperature (T_o).
v. Note value of $T_s - T_o$. This is used in (f)(ii.) below.

(e) Modify the initial mixing ratio (r_o)

i. Draw a constant-mixing-ratio line up to the CL and a saturated adiabat above, so that the total water-vapour content between the isobars p_s and $p_s - d$ is unchanged. Since water content is not proportional to area this construction is not an 'equal area' one, but the lower area where water content is large must be less than the upper one where water contents are smaller, i.e. area C < area D.
ii. Note the modified value of r_o.

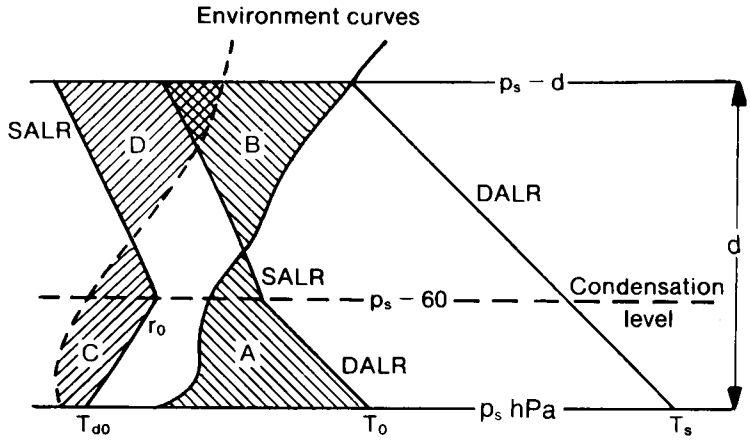

Figure 2.8 Forecasting the warming of cold air moving over a warm sea (Grant's method) — the modification of an initially stable temperature and moisture structure where T_s is the sea temperature at mean-sea-level pressure (p_s), ($p_s - 60$) is a first estimate of condensation level and ($p_s - d$) is the expected top of the convective layer. See text for method of construction.

(f) Use the nomogram in Fig. 2.9

i. Starting from the scale for 'fetch', move horizontally to 'd' the depth of convection and from this point draw a line downward to the lower part of the nomogram.
ii. Enter left-hand scale for ($T_s - T_0$) and draw a horizontal line to meet the vertical. The meeting point is marked by a small circle on the example plotted on Fig. 2.9
iii. Read off the value ΔT from the family of full curves. The downwind temperature is then $T_0 + \Delta T$.
iv. Read off Z to the nearest 0.01 from the family of pecked curves.
The final mixing ratio is given by

$$r = r_0 + Z(r_s - r_0).$$

v. Use a tephigram to convert 'r' to the corresponding dew-point T_d.
vi. The final CL is given approximately by 120 ($T - T_d$) m
or 400 ($T - T_d$) ft.

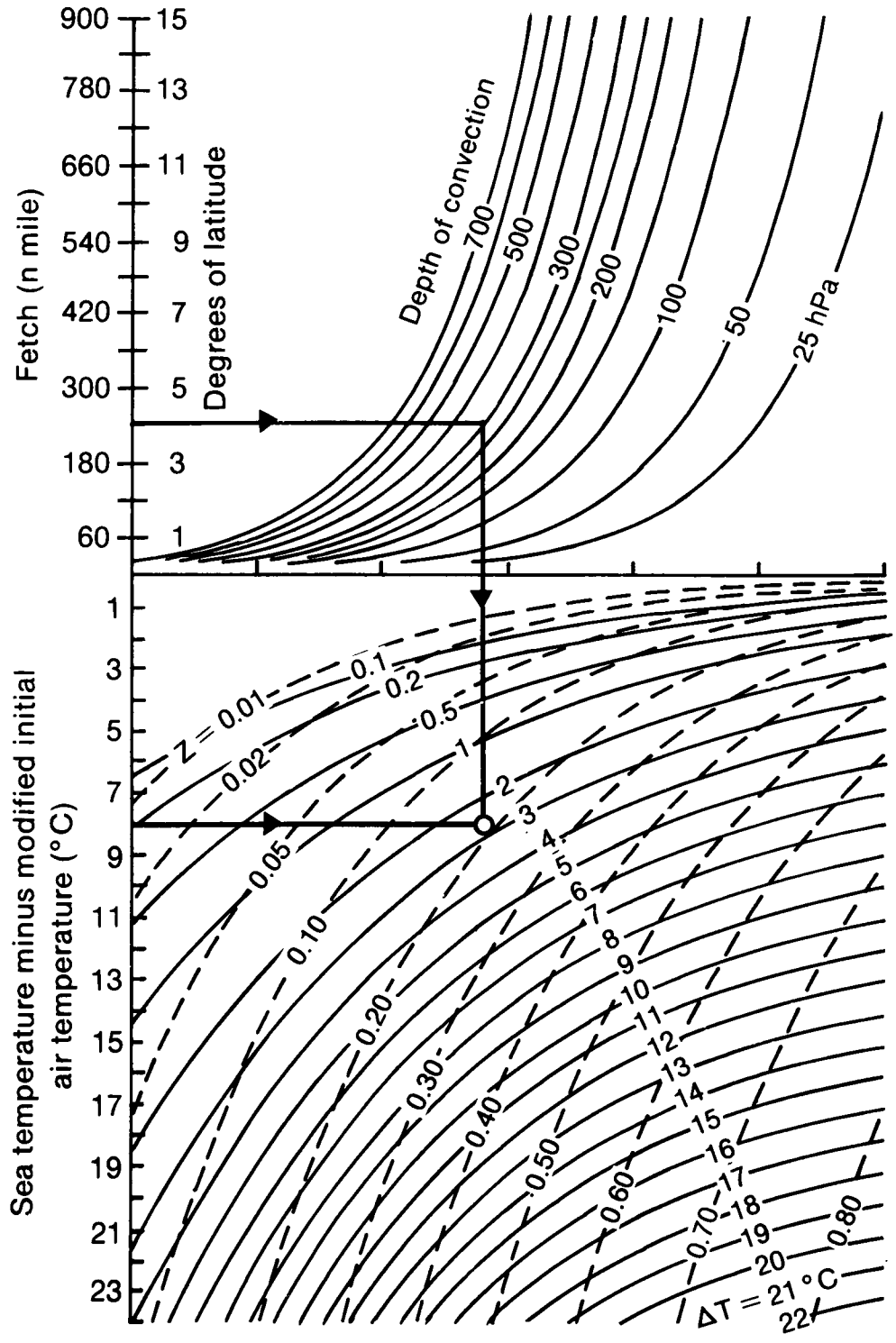

Figure 2.9 Nomogram for determining the surface temperature increase (ΔT) from the fetch(es), the depth of convection and the sea–air temperature difference. The pecked lines show isopleths of the moisture lines, Z. See text for method of use.

2.5.4 *Advection of warm air over a cold sea (Lamb and Frost's method)*

For surface winds less than 20 kn

$$T - T_s = (T_s - T_o)\, f(d)$$
$$r - r_s = (r_s - r_o)\, f(d)$$

where d is the fetch (km) over the sea and other symbols are as in 2.5.1.

Values of f(d)

d (km)	100	200	300	400	500	600	700	800	900	1000
f (d)	0.175	0.152	0.141	0.133	0.127	0.123	0.119	0.116	0.113	0.110

Note:

A cool sea surface exerts a powerful and rapid control on the temperature at screen height.

2.6 Cooling of air by precipitation

2.6.1 *Cooling of air by rain*

The lowest temperature to which the air can be cooled by evaporation of water is the wet-bulb temperature. A dry-bulb temperature close to the wet-bulb value is reached after about ½ hour of very heavy rain or about 1 to 2 hours of rain of lesser intensity.

2.6.2 *Downdraught temperatures in non-frontal thunderstorms*

The temperatures of strong downdraughts reaching the ground are very close to the surface temperature of the saturated adiabatic through the intersection of the wet-bulb curve and the 0 °C isotherm (see 1.6.2).

2.6.3 *Cooling of air by snow*

Falling snow gradually lowers the 0 °C level. However, the reduction of the surface temperature to 0 °C is unlikely if:

(a) the wet-bulb temperature at the surface is higher than 2.5 °C in prolonged frontal precipitation.

(b) the wet-bulb at the surface is higher than 3.5 °C within extensive areas of moderate or heavy instability precipitation.

Note:

The relation between wet-bulb temperature and the form of precipitation is given in 5.4.4

2.7 Thermodynamics and the tephigram

The tephigram is an aerological diagram with rectangular co-ordinates T (temperature) and ϕ (entropy).

2.7.1 *Definitions*

Adiabatic: describes a thermodynamic process in which heat neither enters nor leaves the system.

Density: (ρ) the mass of unit volume of a substance at specified temperature and pressure.

The density of dry air at 1000 hPa and 290 K is 1.201 kg m^{-3}.

Dry adiabatic lapse rate (DALR): $\Lambda_d = g/c_p = 9.8$ °C/km = 5.4 °F/1000 ft.

Enthalpy: or sensible heat (H): represents the total heat content per unit mass, in units of J kg^{-1}.

$$dH = c_p\, dT.$$

A change in enthalpy (dH) is the heat gained or lost in an isobaric process.

Entropy: (ϕ), or in some text-books (S), is a function of pressure, volume and temperature. On a tephigram, entropy is constant along a dry ADIABAT. It is related to POTENTIAL TEMPERATURE (θ) by

$$\phi = c_p \ln \theta + \text{constant}.$$

Equivalent temperature (T_e): the temperature obtained if all the water in a mass of air were condensed and the latent heat of condensation used to raise the air temperature. (No change of pressure takes place.)

Equivalent potential temperature (θ_e): can be found on a tephigram by following a dry adiabat from T_e at a given pressure level to the 1000 hPa level.

$$T_e = T + Lr/c_p.$$

If r is in g kg^{-1} $T_e = T + 2.5\,r$.

Humidity mixing ratio (r): is the ratio of the mass (m_v) of water vapour to the mass (m_a) of dry air

$$r = m_v/m_a.$$

It is usually expressed in g kg^{-1}.

Isentropic: constant ENTROPY, or constant POTENTIAL TEMPERATURE (θ). (For dry air, isentropic is equivalent to ADIABATIC.)

Normand's theorem: on an aerological diagram, the dry ADIABATIC through the dry-bulb temperature, the saturated adiabatic through the wet-bulb temperature and the HUMIDITY MIXING RATIO line through the dew-point temperature of an air sample, all meet at one point.

Potential temperature (θ): the temperature which a given sample of air would attain if transferred at the DALR to the standard pressure 1000 hPa

$$\theta = T(1000/p)^{\kappa}$$

where $\kappa = R/c_p = 0.286$.

It is related to ENTROPY (see definition above).

Vapour pressure (e): that part of the total atmospheric pressure exerted by water vapour.

Saturation vapour pressure (SVP) with respect to water (e_w) is greater than SVP with respect to ice (e_i). The excess of e_w over e_i is a maximum (0.27 hPa) at about -12 °C.

Virtual temperature (T_v): the virtual temperature of moist air is that temperature at which completely dry air (of the same total pressure) would have the same density as the moist air.

For a practical approximation $T_v = T + r/6$ where r is in g kg^{-1}.

Table 2.9. Difference between virtual temperature and actual temperature for saturated air.

Temperature °C	Pressure (hPa)							
	1000	900	800	700	600	500	400	300
				($T_v - T$)				
40	8.8	9.9						
35	6.6	7.3						
30	4.8	5.4	6.1					
25	3.6	4.0	4.5					
20	2.6	2.9	3.2	3.7				
15	1.8	2.0	2.3	2.6				
10	1.3	1.5	1.6	1.9				
5	0.8	0.9	1.1	1.2	1.4			
0	0.6	0.7	0.8	0.9	1.0	1.3		
−5	0.3	0.3	0.3	0.4	0.4	0.5	0.6	
−10	0.2	0.2	0.2	0.2	0.3	0.3	0.4	
−20	0.1	0.1	0.1	0.1	0.2	0.2	0.2	0.3

The values above show corrections needed when the relative humidity is 100%. Use a proportion of the figures appropriate to the actual humidity.

Wet-bulb temperature (T_w): the temperature at which pure water must be evaporated into a given sample of air adiabatically, and at constant pressure, in order to saturate the air at the temperature (T_w) under steady state conditions.

Wet-bulb potential temperature (θ_w): the wet-bulb temperature which a sample of saturated air would have if transferred at the SALR to the standard pressure level of 1000 hPa.

2.7.2 *Constructions using a tephigram*

(a) The following are illustrated in Fig. 2.10, using temperatures specified for a parcel of air at 850 hPa:

Normand's theorem. The dry adiabat through the dry-bulb temperature (T), the saturated adiabat through the wet-bulb temperature (T_w) and the humidity mixing ratio line through the dew-point temperature (T_d) meet at N, the condensation level.

Potential temperature. A dry adiabat through the dry-bulb temperature (T) intersects the 1000 hPa isobar at the potential temperature (θ).

Wet-bulb potential temperature. A saturated adiabat through the wet-bulb temperature (T_w) intersects the 1000 hPa isobar at the wet-bulb potential temperature (θ_w).

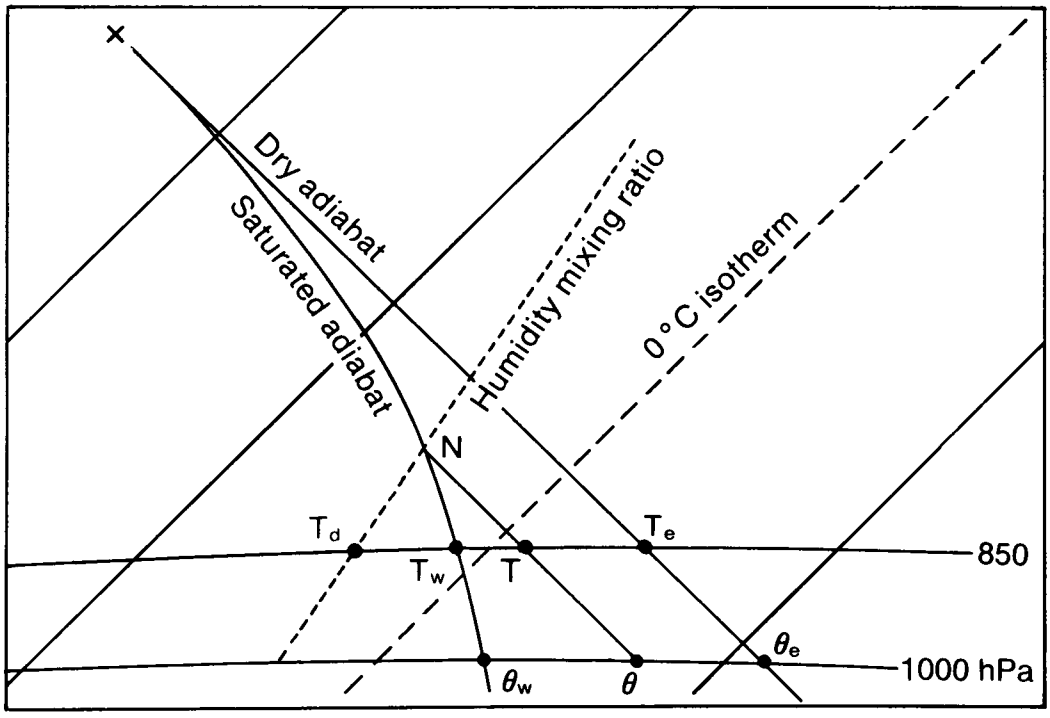

Figure 2.10 Constructions on a tephigram to illustrate Normand's theorem, and to obtain potential temperatures (θ, θ_w) and equivalent temperatures (T_e, θ_e. The constructions are based on a parcel of air at 850 hPa, with temperature (T), wet-bulb temperature (T_w) and and dew-point (T_d). See text for method of construction.

Equivalent temperature. Follow a saturated adiabat through T_w up to the level at which the saturated and dry adiabats are parallel. For practical purposes this occurs at −50 °C. From this point (X), a dry adiabat down to the original pressure level gives the 'equivalent temperature' (T_e).

Potential equivalent temperature. From T_e, a dry adiabat intersects the 1000 hPa isobar at the potential equivalent temperature θ_e.

Relative humidity. The values of the humidity mixing ratio lines passing through the dry-bulb temperature (T) and the dew-point temperature (T_d), give

$$RH = (\text{HMR for } T_d)/(\text{HMR for } T) \times 100\%.$$

(b) The following are illustrated in Fig. 2.11.

Vapour pressure (e). Follow the isotherm through the dew-point (T_d) up to the 622 hPa isobar. From this point follow a humidity mixing ratio line to the base of the diagram where values are printed in g kg^{-1}. This value is then relabelled as the vapour pressure in hectopascals. In this case e is 5 hPa.

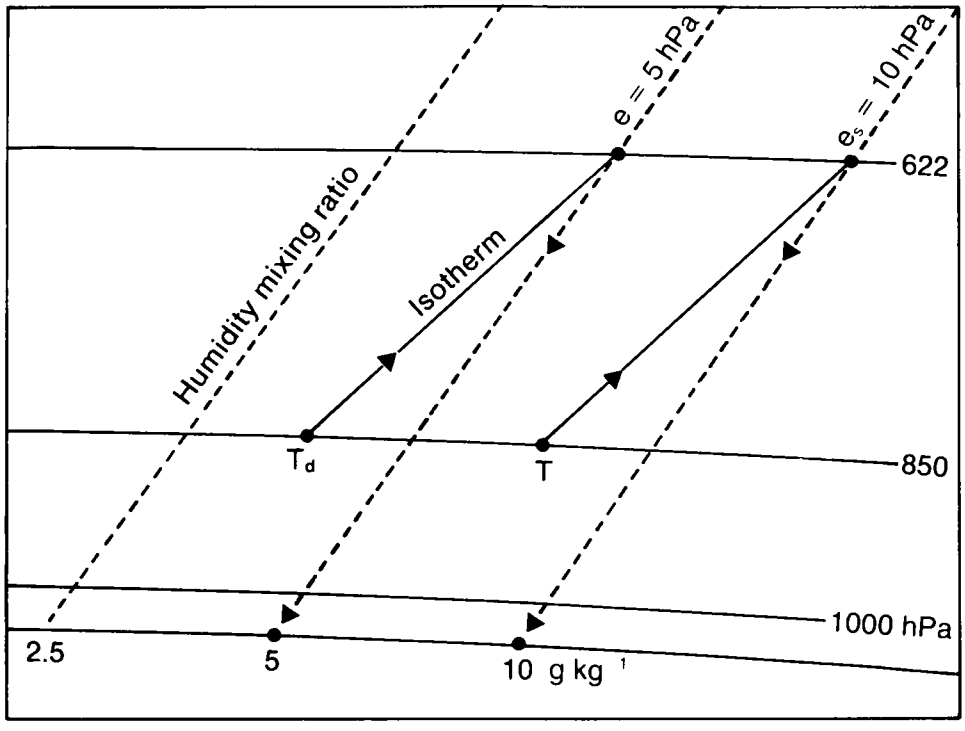

Figure 2.11 Constructions on a tephigram to obtain vapour pressure (e) and saturation vapour pressure (e_s) based on the air temperature (T) and dew-point (T_d) of a parcel of air at 850 hPa. See text for method of construction.

Saturated vapour pressure (e_s). Repeat the construction for obtaining e, but follow the isotherm through the dry-bulb temperature (T) up to the 622 hPa isobar. In this case e_s is 10 hPa.

2.7.3 *Calculation of heights on a tephigram*

This is illustrated in Fig. 2.12. Divide the temperature profile into a series of layers, 100 hPa deep up to the 300 hPa isobar, and then 50 hPa deep between 300 and 100 hPa. Use a transparent scale marked with a straight line. Lay this over the temperature profile in each of the layers, parallel to the isotherms so as to create equal positive and negative areas either side of the mean isotherm.

Read off the layer thicknesses, in decametres, as marked along the intermediate isobars at 950, 850, 750 hPa, etc. The height of a standard pressure level is the sum of all the partial thicknesses below that level, plus the height of the 1000 hPa level. The height of the 1000 hPa surface may be read off from the nomogram printed on standard tephigrams. When the MSL pressure is less than 1000 hPa, the 1000 hPa heights are negative.

The formula for height calculations involving layers which are not at standard levels is:

$$H = 67.442\, T_v \ln(p_0/p_1)$$

where H is in metres and T_v is the mean virtual temperature (K) of the layer $p_0 - p_1$.

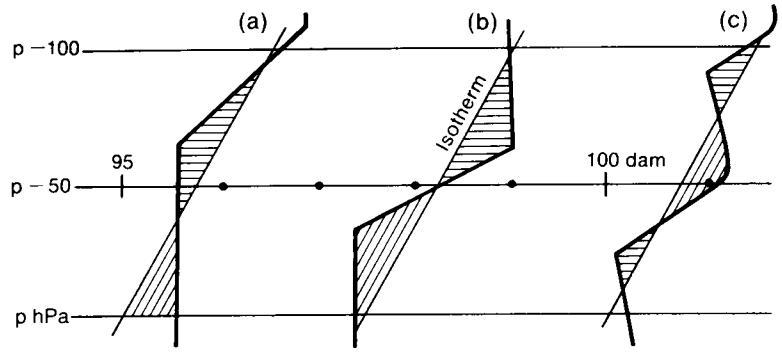

Figure 2.12 Calculating the thickness of a 100 hPa layer (base pressure $=p$). Shaded areas show equal positive and negative areas either side of a mean isotherm for three different shapes of environment curve. Thickness values are read off the scale on intermediate isobars. The examples show thickness values of (a) 95.7 dam, (b) 98.2 dam, and (c) 100.7 dam. See text for method of calculation.

CHAPTER 3 — VISIBILITY

3.1 Fog

3.1.1 *Types of fog*

Fog forms when the air near the surface is cooled below its dew-point.

(a) Radiation fog is caused by loss of heat from the air, to ground cooled by nocturnal radiation.

(b) Advection fog is caused by passage of air over a surface whose temperature is below the dew-point of the air.

(c) Upslope fog is caused by adiabatic cooling of air during upslope motion.

On many occasions the development of fog is due to more than one of these factors.

3.1.2 *Synoptic-scale conditions for fog*

(a) *Radiation fog requirements*

i. Almost clear skies.
ii. Slack pressure gradient, allowing the surface wind (measured at 10 m) to decrease to near calm.

The frequency of geostrophic wind speeds (V_g) at Cardington during periods of fog were found to be as follows:

Percentage of frequency V_g in various speed ranges
kn

	0–2	3–5	6–8	9–11	12–14	15–17	18–20	21–23	24–26	27–29	30+
A	7.1	16.7	23.8	23.0	18.3	10.3	0.8	—			
B	6.7	16.0	18.0	20.0	16.3	11.3	6.7	2.5	1.5	0.5	0.7

A = when fog first formed, B = while fog persisted

The wind speed at 10 m during the same fogs had the following frequency distribution:

Percentage frequencies of surface wind in various speed ranges

kn

0–2	3–5	6–8	9–11	12–14	15–17
58.5	28.6	10.5	2.1	0.3	—

The stronger winds occurred when North Sea stratus spread inland replacing local radiation fog with widespread advection fog.

Recent studies have shown that the wind speed at 1–2 m was more important that the 10 m wind. Fog forms when the 2 m wind falls below 2 kn. The wind at 10 m may be significantly stronger than the 2 m wind on radiation nights.

Synoptic studies demonstrate the preferred occurrence of radiation fog with anticyclonic pressure patterns (highs, ridges and cols). Only about one fog in seven occurs in a cyclonic situation. Within these pressure patterns there is a greater tendency for fog to form in those sectors where there is a southerly component to the geostrophic wind (by a factor of about 3 to 1).

(b) *Advection fog requirements*

(i) Passage of air over a surface colder than the dew-point of the air.
(ii) A stable lapse rate in the lowest layers.

Typical examples are sea fog and fog over very cold land. Thawing snow is commonly associated with advection fog over land.

The advection of moist air also renders radiation fogs more frequent. Radiation fog is likely to be more widespread and persistent when advection brings an increase in vapour content just above the surface. Low-lying stations in eastern England experience an increased frequency of radiation fogs when there is a weak flow from the North Sea.

(c) *Upslope fog requirements*

(i) Flow of moist air over gently rising ground.
(ii) A stable lapse rate in the lowest layers.

Very stable air may be deflected around the edge of steeply rising ground if there are gaps in the escarpment.

On radiation nights, weak moist advection may be combined with gentle upslope motion producing multiple conditions favourable for fog.

3.2 Radiation fog — physics of formation

3.2.1 *The formative stage*

(a) The ground cools by radiation to space. Initially there is a rapid fall of ground-surface temperature. Later in the night the cooling rate of the ground surface is gradually reduced by the heat flux generated up through the soil.

(b) Air near the ground cools by radiating to the ground, and the air in contact with the ground cools by conduction. Turbulent mixing spreads the intense cooling near the ground through a greater depth.

(c) When the temperature of the air in contact with the ground falls below its dew-point, dew is deposited. This dries out the air and releases latent heat, both of which inhibit fog formation for a while.

(d) Further cooling leads to the wind in the lowest 2 m slowing to less than 2 kn and becoming non-turbulent. Mixing no longer occurs and the radiative cooling has its full effect in this layer. Wispy layers of fog form just above the ground, at a time when the 10 m wind does not show the same decrease.

(e) Continued cooling deepens the foggy layer and leads to the mature stage.

3.2.2 *The mature stage*

(a) When the fog depth is 20–50 m, the upper part of the fog becomes the effective radiating region to space. Near the ground, upward radiation from the surface is increasingly balanced by downward radiation from fog droplets. The temperature inversion rises from the surface and the 'present weather' reports a change from 'sky visible' to 'sky obscured'.

(b) The ground temperature stops falling and, with the soil heat flux continuing, it may even rise in a mature fog.

(c) The fog-top temperature also remains remarkably constant (to within 0.5 °C of the surface temperature at the time the inversion lifted off the ground and the sky became 'obscured'). Through the depth of the fog a SALR is established.

(d) The base of the inversion is in the upper part of the fog, just below the fog top. At the fog top there is a marked wind shear.

Figs 3.1 and 3.2 show the conditions observed in a fog at Cardington in November 1983, which passed from its formative to its mature stage at about 01 UTC.

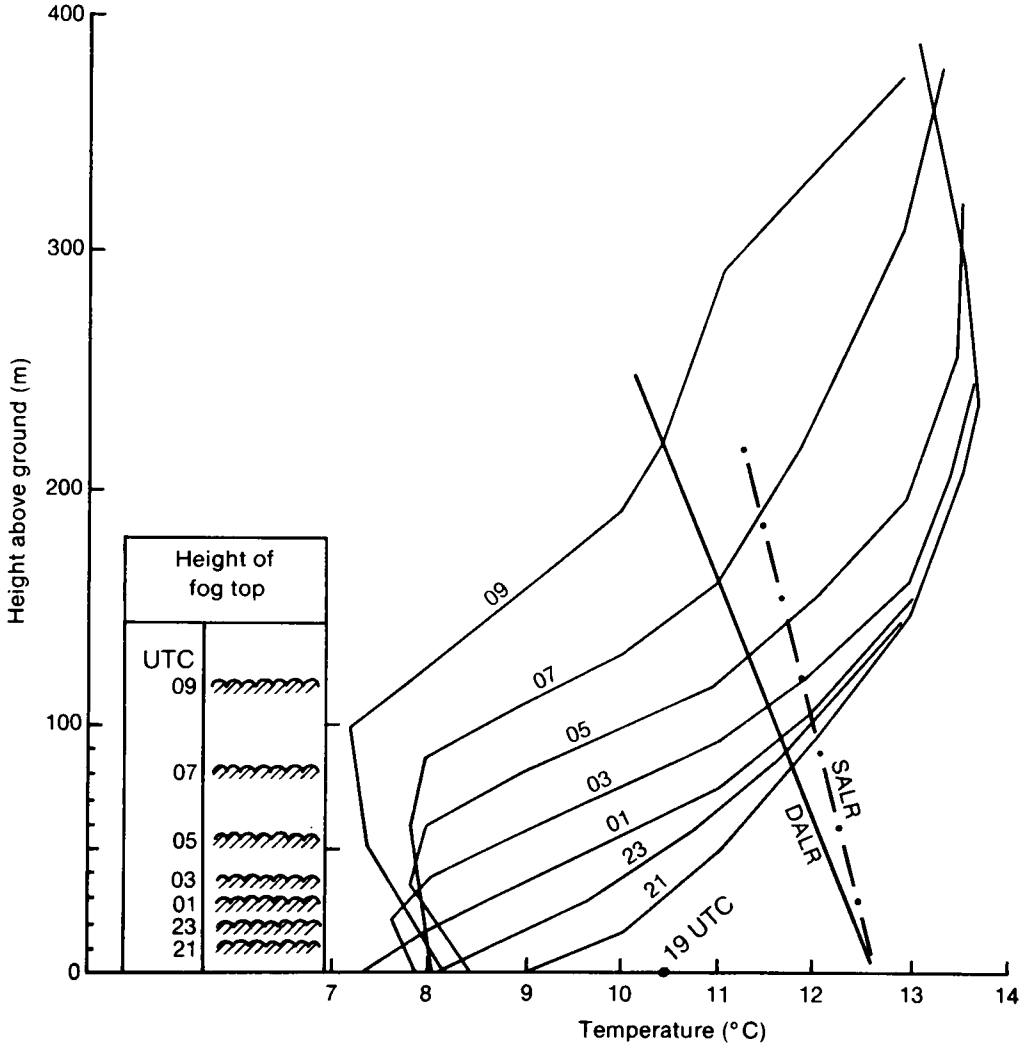

Figure 3.1 Temperature–height diagram showing the temperature structure and fog top at Cardington at various times during the night of 9/10 November 1983.

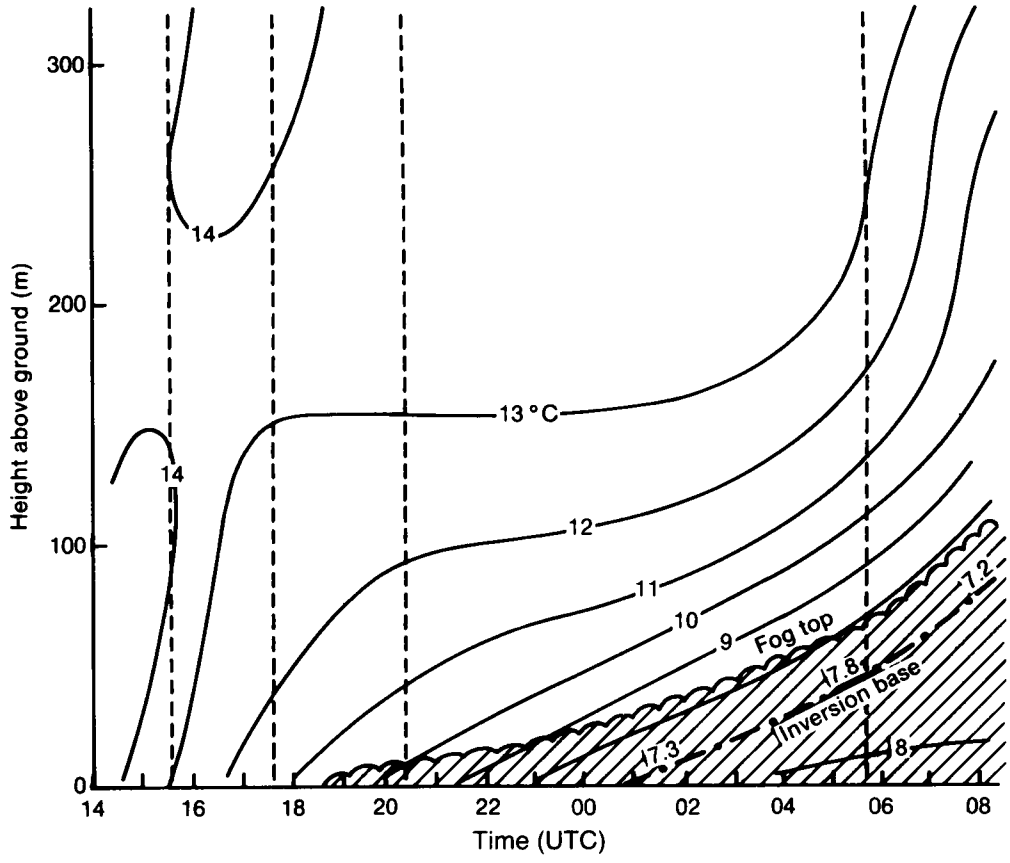

Figure 3.2 Time-section of the vertical temperature profile and fog depth at Cardington on the night of 9/10 November 1983. Fog formed at about 1830 UTC. The change from 'sky visible' to 'sky obscured' occurred just before 0100 UTC, which was also the time of the minimum surface temperature.The fog-top temperature from this time on remained steady, with the coldest temperature just below the fog top.

3.3 Radiation fog — forecasting its formation

3.3.1 *Calculation of fog-point (Saunders's method)*

(a) Select a representative upper-air sounding and find the condensation level from the maximum temperature and the dew-point at that time, using Normand's theorem (section 2.7.2).

(b) Find the humidity mixing ratio at the condensation level and read off the temperature where the humidity mixing ratio line cuts the surface isobar. This is the expected fog-point temperature.

This process needs modification to allow for different types of sounding (see Fig. 3.3).

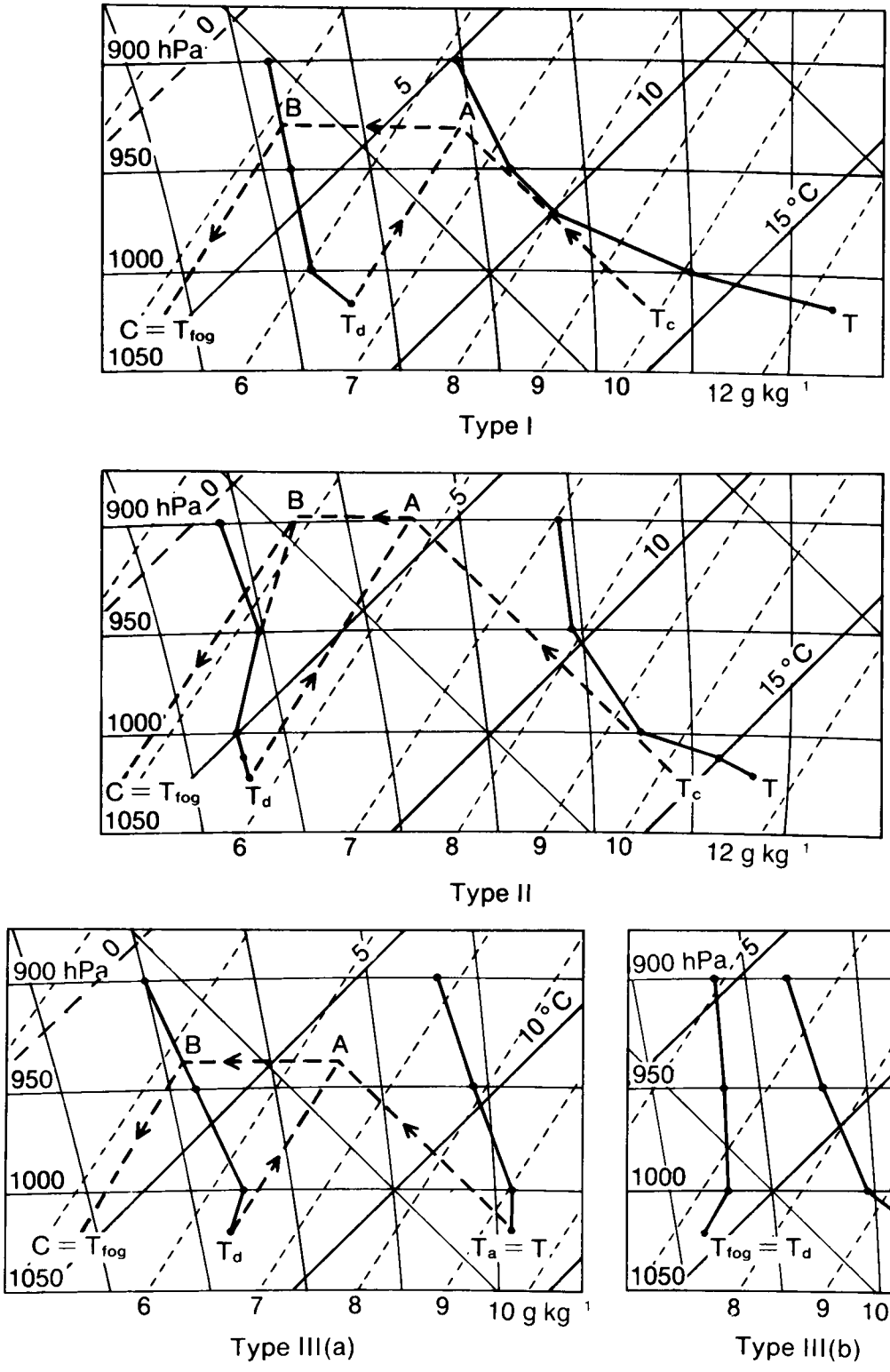

Figure 3.3 Estimation of fog-point (Saunders's method) with adjustments to midday soundings under various conditions. See text for explanation of the types.

Type I has a constant dew-point lapse rate except near the ground where the surface dew-point lies on, or to the right of, a downward extension of the upper dew-point curve.

T is the maximum temperature and T_d is the surface dew-point. If there is a superadiabatic, use the value T_c instead of T to eliminate the superadiabatic section.

The pecked lines through T_c and the dew-point T_d meet at the condensation level A. The humidity mixing ratio at this level is at B and the fog-point is at C.

In **Type II** the dew-point lapse rate increases aloft. Point B is found by extrapolating the lower part of the dew-point curve above the point at which the lapse rate increases.

In **Type III** the surface dew-point lies to the left of the downward extension of the upper dew-point curve, two possibilities are illustrated:

(a) If the temperature lapse in the lowest layers is less than a dry adiabatic, the construction follows the basic principles as for **Type I.**

(b) If the temperature lapse rate in the lowest layer is equal to or greater than a dry adiabat, then no Normand construction is drawn and the fog-point is taken to equal the dew-point.

Notes:

(a) If a subsidence inversion has brought dry air down to within 30 hPa of the ground, use the dew-point (T_d) as the fog-point.

(b) If rain falls during the afternoon leaving the ground wet, the actual fog-point may be higher than the calculated value.

(c) If a sea-breeze reaches the area later in the day, the fog-point may be much higher than calculated.

3.3.2 *Calculation of fog-point (Craddock and Pritchard's method)*

If T_f is the fog-point, T_{12} is the screen temperature at 1200 UTC, and T_{d12} is the dew-point at 1200 UTC, then

$$T_f = 0.044\,(T_{12}) + 0.844\,(T_{d12}) - 0.55 + A = Y + A.$$

Values of A and Y can be obtained from Table 3.1.

Table 3.1 Values of Y (°C) corresponding to the observed values of T_{12} and T_{d12}

	T_{12}								
T_{d12}	30	25	20	15	10	5	0	5	−10
20	17.7	17.4	17.2						
18	16.0	15.7	15.5						
16	14.3	14.1	13.8						
14	12.6	12.4	12.1	11.9					
12	10.9	10.7	10.5	10.2					
10	9.2	9.0	8.8	8.6	8.3				
8	7.5	7.3	7.1	6.9	6.6				
6	5.8	5.6	5.4	5.2	5.0				
4	4.1	3.9	3.7	3.5	3.3	3.0			
2	2.5	2.2	2.0	1.8	1.6	1.4			
0	0.8	0.6	0.3	0.1	−0.1	−0.3	−0.6		
−2	−0.9	−1.1	−1.4	−1.6	−1.8	−2.0	−2.2		
−4	−2.6	−2.8	−3.0	−3.3	−3.5	−3.7	−3.9		
−6	−4.3	−4.5	−4.7	−5.0	−5.2	−5.4	−5.6	−5.8	
−8	−6.0	−6.2	−6.4	−6.6	−6.9	−7.1	−7.3	−7.5	
−10	−7.7	−7.9	−8.1	−8.3	−8.6	−8.8	−9.0	−9.2	−9.4

The number A (°C) is an adjustment which depends upon the forecast cloud amount and geostrophic wind speed, as tabulated overleaf.

Mean* cloud amount (oktas)	Mean* geostrophic wind speed (kn)	
	0–12	13–25
0–2	0.0	−1.5
2–4	0.0	0.0
4–6	+1.0	+0.5
6–8	+1.5	+0.5

*Mean of forecast values for 1800, 0000, and 0600 UTC.

Notes:

(a) The equation for T_f was derived from the combined data for 13 widely separated stations in England. There was considerable variation from station to station in their proximity to major smoke sources.

(b) Account was not taken of variations in atmospheric pollution so that, in effect, an average degree of pollution is assumed in using this technique (in contrast to Saunders's method which refers mainly to fog in clean air).

(c) If the minimum temperature is predicted using Craddock and Pritchard's method it is suggested that:

If T_f is 1 °C or more above T_{min}, forecast fog.

If T_f is 0.5 °C above to 1.5 °C below T_{min}, forecast a risk of fog.

If T_f is 2 °C or more below T_{min}, do not forecast fog.

3.3.3 *The fog-point in relation to the 850 hPa wet-bulb potential temperature*

The 850 hPa wet-bulb potential temperature is useful as a means of identifying air masses. The probability of fog occurring increases as the temperature difference (T_D) of the surface temperature below the 850 hPa WBPT increases, see Fig. 3.4.

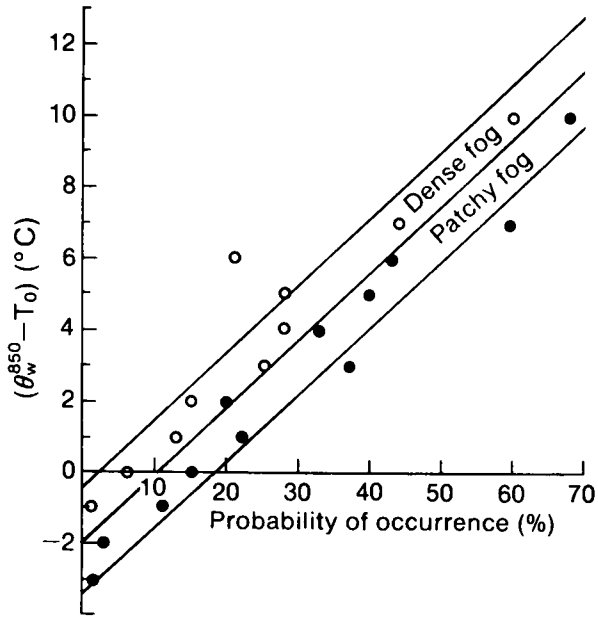

Figure 3.4 The probability of fog corresponding to a given depression of the surface temperature (T_0) below the 850 hPa wet-bulb potential temperature (θ_w^{850}).

3.4 Radiation fog — forecasting its clearance

3.4.1 *Fog clearance by insolation*

The time of clearance depends on the thickness of the fog and the insolation available at a particular latitude and time of year. The fog depth must be known or estimated, together with a fog clearance temperature.

(a) *Estimation of fog top*

(i) Visual estimation: if the sky is visible, the fog depth is probably about 5 hPa in dense fog, and 10 hPa in thin fog.
(ii) If the sky is obscured at dawn, and no local mini-sonde ascent is available, the most representative midnight sounding should be modified to allow for changes between midnight and the time of minimum temperature.

(b) *Modifying the temperature profile on a tephigram*

When the sky is visible, the temperature profile at dawn may be constructed by drawing a line from the surface night minimum temperature to a point 10 hPa up a saturated adiabat and then along an isobar to the environment curve.

When the sky is obscured and the midnight temperature profile has an inversion, the top of which is well-defined (point A on Fig. 3.5), make the following adjustments:

(i) Subtract an amount Δp from the pressure at A and mark a point B at this level on the environment curve:
In summer, take $\Delta p = 6$ hPa,
In spring and autumn, $\Delta p = 12$ hPa, and
In winter, $\Delta p = 18$ hPa.

(ii) On the surface isobar, mark the night minimum temperature (D).

(iii) If hourly synoptic observations are available throughout the night, use the physical model from 3.2 to estimate the fog-top temperature. Identify the time at which the fog was observed to change from 'sky visible' to 'sky obscured' and use the screen temperature at that time as the fog-top temperature. Draw a SALR from D to F on Fig. 3.5 (the level where the temperature equals the assumed fog-top temperature).

(iv) If hourly observations are not available, an alternative procedure is to join DB, and extend the dew-point curve downwards to cut DB at a point E. This defines the assumed fog-top level. Draw a SALR from D to F, where F and E are at the same level.

(v) The modified temperature profile at dawn is DFB.

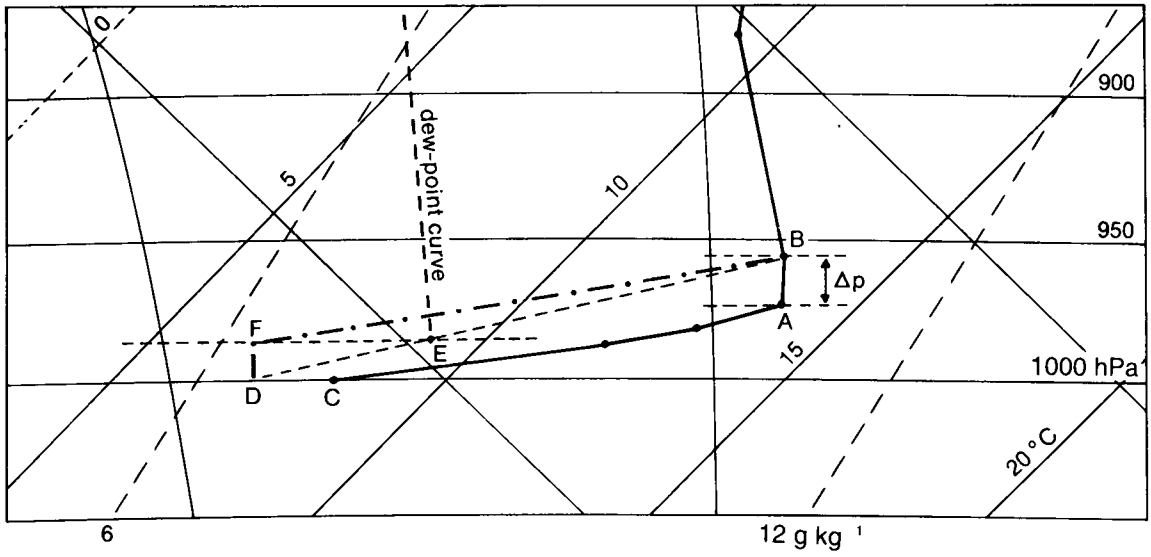

Figure 3.5 Fog clearance — adjustment of midnight soundings to represent the temperature structure at dawn. See text for method of construction.

If there is no clear-cut inversion on the midnight temperature profile, mark the point B as follows:

In summer (May–July), 30 hPa above the surface pressure.
In spring and autumn (Aug.–Oct., Feb.–Apr.), 35 hPa above the surface pressure.
In winter (Nov.–Jan.), 40 hPa above the surface pressure.

Then continue as from (b) above.

Although this procedure gives a guide to the likely changes in the temperature profile between midnight and dawn under nearly calm conditions, much greater changes may occur if there is any advection in progress. In such circumstances, a sounding from a local mini-sonde will be invaluable.

(c) *Estimation of fog-clearance temperature (see Fig. 3.6)*

Use the modified temperature profile (DFB in Figs 3.5 and 3.6). Extend the dew-point curve down from E to the surface at G and follow the SALR from E down to the surface isobar.

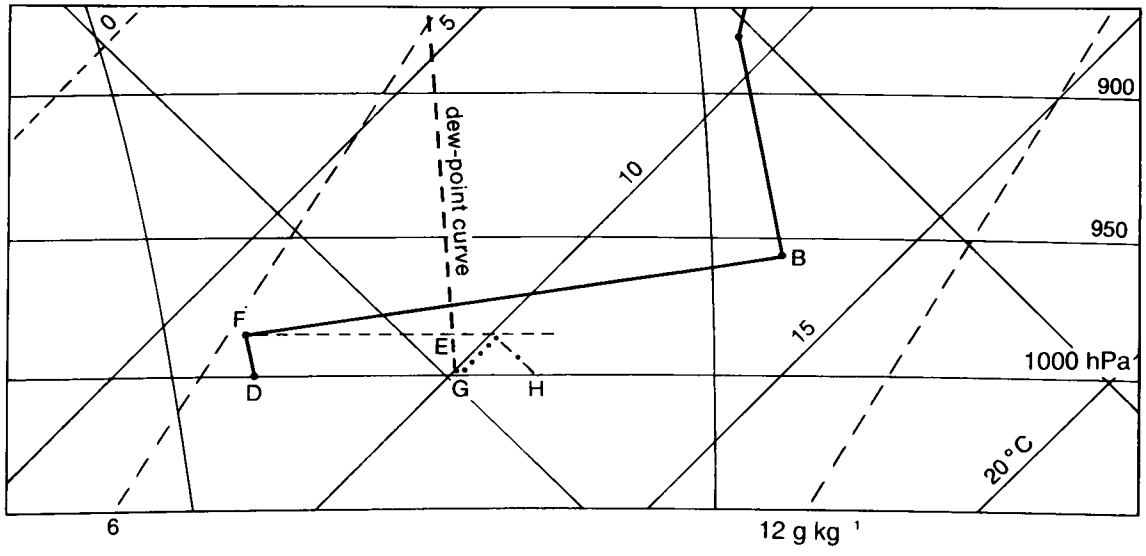

Figure 3.6 Estimating the fog clearance temperature. DFB is the estimated temperature profile at dawn and E is defined as in Fig. 3.5. EG is extended dew-point curve and EH is a dry adiabat. The fog lifts to stratus when the surface temperature exceeds that at G, and the stratus disperses when the surface temperature exceeds that at H.

The surface temperature thus obtained represents the probable value above which the fog will lift to very low stratus.

The fog or low stratus should disperse entirely when the condensation level reaches the level of the inversion base (fog top will rise as fog lifts into stratus).

Caution: During winter when the sun is at a very low angle, the fog top will continue to radiate after sunrise. The fog will increase in depth for some time before the absorption of insolation is effective in starting the clearance process.

(d) *A nomogram for forecasting clearance of fog by insolation*

Fig. 3.7 is a nomogram (Barthram 1964) for predicting the time of fog clearance due to insolation.

T_1 = surface temperature at dawn
T_2 = fog-clearance temperature
d = depth of fog at dawn in hectopascals

To use the nomogram:

(a) Enter the fog-depth on the left-hand diagram and move to the right to meet the vertical from the value (T_2-T_1). From this point move downwards and to the right following the curved lines representing Q to the right-hand edge of the diagram.

(b) Move horizontally across to the middle diagram and then as far as the vertical from the value T_2+T_1. Then follow the curves for fQ to the right-hand edge of the diagram.

(c) From this point move horizontally across to the right-hand diagram to meet one of the curves marked with dates. From this curve go down to the baseline where the time of clearance is marked.

If the fog is thin (visibility more than 600 m or depth $<$ 20 hPa) the insolation needed is reduced by one third. Take the value on the left-hand margin and follow one of the diagonal pecked lines down to the inner (thin fog) scale and continue as before.

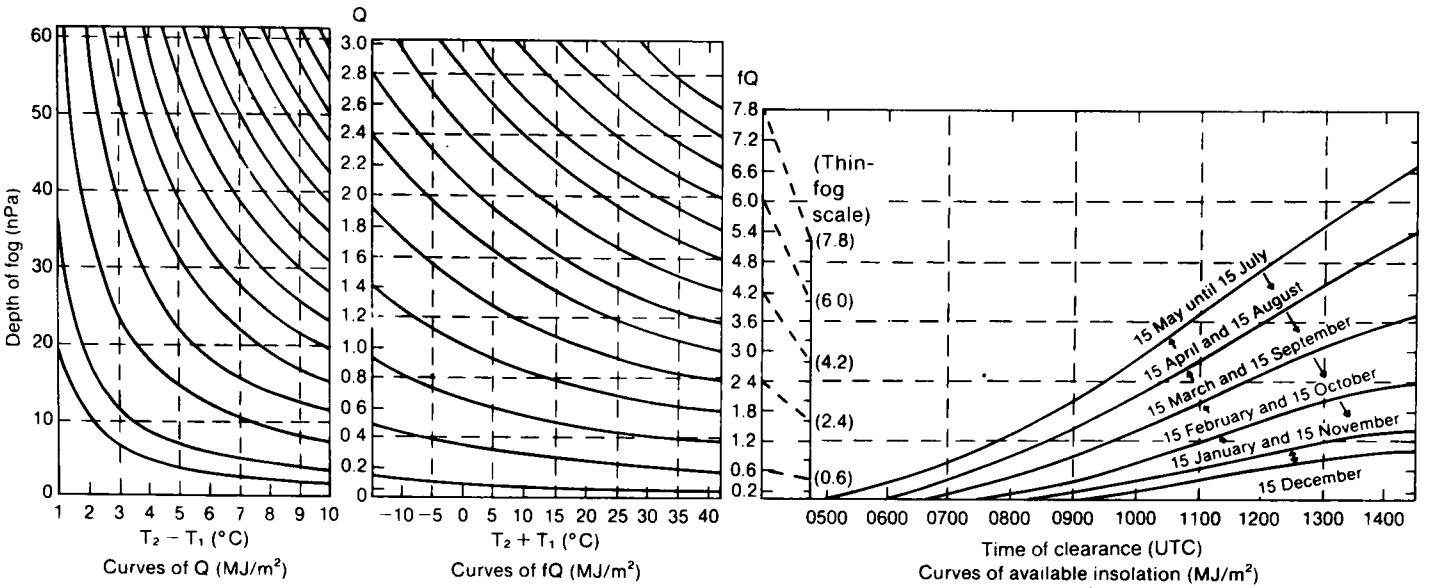

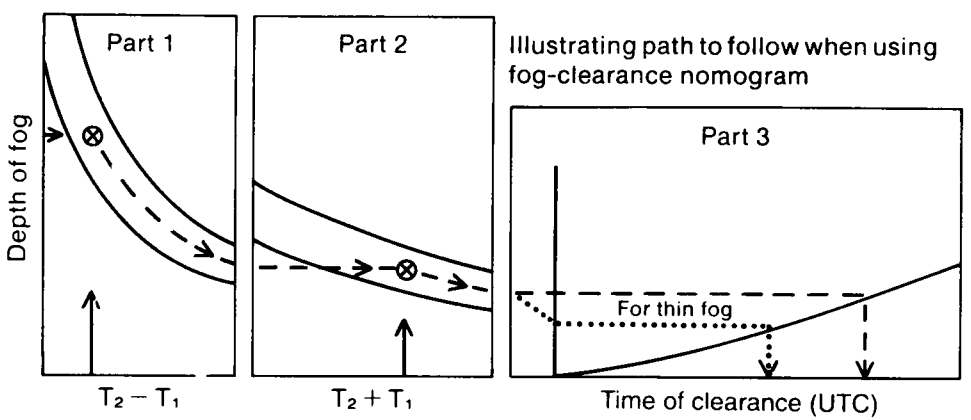

Figure 3.7 Nomogram for forecasting the clearance of radiation fog by insolation.

3.4.2 *Fog clearance without insolation*

(a) *Fog clearance following the spread of cloud*

The arrival of a cloud sheet over water fog often leads to the clearance of the fog because it stops, or reverses, the continual radiative cooling of the fog. The lower the cloud sheet the more effective it is in clearing the fog. Provided the ground is not frozen, heat flux from the soil lifts the fog into low stratus before its complete dispersal. The time taken for fog to clear decreases with higher temperatures, as is shown by the following observations made at Exeter Airport in south-west England.

Initial grass temp. (°C)	< 0	0–2	3–5	6–8	9–10	11–13
Average time (hours) for fog to clear after arrival of cloud sheet	3.1	2.2	1.1	1.5	0.9	0.5
Number of cases	10	10	5	10	5	3

(b) *Fog clearance due to increase of wind*

Although fog does not normally form unless the wind falls very light, its dispersal may be delayed until the winds aloft are quite strong. Mature fog, with a well developed inversion capping it, is shielded from the turbulent mixing associated with strong winds aloft. The more intense the inversion, the greater must be the wind above in order to produce turbulent mixing and dispersal of fog.

As a guide, the geostrophic wind speed required for fog to be dispersed by the increasing wind is 15–20 kn over flat coastlands, 20–25 kn inland and 30–40 kn in deep valleys lying across the wind flow. Even at Cardington a peak geostrophic wind of 37 kn was estimated on one occasion before the fog cleared.

While increasing winds may lift fog into a layer of low stratus, localities downstream, especially where the ground has a gradual slope upwards, are liable to experience a delay in clearance, or the arrival of stratus if there was no fog initially.

(c) *Fog clearance due to dry-air advection*

Local variations in surface characteristics and moisture content can create mesoscale patches of drier air which cannot be detected on synoptic-scale charts. Unexpected nocturnal clearance of fog may occur when advection brings in drier air.

3.4.3 *Persistent fogs*

If a persistent fog is defined as one which forms one night and lasts all through the following day, not clearing till after dusk; this occurs most commonly in England in winter in eastern districts.

In December and January, one third of all fogs are persistent (according to this definition). In November and February the proportion is about one sixth. Great care should therefore be exercised in predicting that overnight fogs between late November to early February will clear during the morning.

On the other hand most of these fogs are found to clear during the second night (44% by midnight and 80% by 0900 UTC on the next morning). Only 5–10% persist beyond midday on the second day.

Most of the clearances are associated with the strengthening of winds aloft and/or an increase in low cloudiness, often (but not always) associated with a front within 200 km.

3.5 Advection fog

The general conditions favourable for advection fog are listed in section 3.1.2(b).

3.5.1 *Sea fog*

There are two main sources of warm moist air giving sea fog over coasts and waters around the British Isles:

(a) A south-westerly flow from the Atlantic west of Spain. This air is often associated with the warm sector of a frontal depression. With a ridge over Scotland, the flow may turn southwards to affect eastern coasts of Scotland and England down to the Tyne as a 'haar' on a north to north-east wind.

(b) A south-easterly flow from the Mediterranean across Europe which reaches east coast areas of the United Kingdom with surface winds between north-east and south-east.

Wind speed in sea fog is most commonly 10–15 kn, but it is not unusual to find winds of 25 kn. In some cases the wind speed may reach gale force, though such observations are usually confined to Ocean Weather Ships in mid Atlantic.

3.5.2 *Prediction of sea fog*

Satellite imagery is invaluable for locating the boundaries of existing areas of sea fog. The shape of the foggy areas may correspond to areas of particularly low sea temperature (for example along the coast of north-east England) but other patterns are due to the incursion of tongues of much drier air, usually of continental origin.

For prediction, a detailed and up-to-date chart of sea surface temperatures is essential, combined with an analysis of the dew-point distribution over the sea and a prediction of the low-level air flow.

3.5.3 *Advection of fog from land to sea*

Radiation fog carried out to sea by a light offshore wind may drift considerable distances over a slightly warmer sea before being dispersed. Radiation from the fog top may effectively disperse heat supplied to the lower layers of the fog by warmer waters. This results in a mature fog type of profile (see 3.2.2). Occasionally such fogs may be carried back to land by a sea-breeze.

3.5.4 *Advection of fog from sea to land*

Sea fog is frequently carried inland over coastal districts by winds off the sea. Nocturnal penetration may be extensive over low-lying ground where the liability to fog will be increased by radiational cooling. By day sea fog usually lifts to low stratus overland and 'burns off' with adequate insolation. Such clearances start off well inland and gradually spread upwind towards the coast.

During the summer months sea-breezes carry fog a little way inland by day. However, the circulation set up by a heat low overland may halt the sea breeze in some areas and even reverse its flow, carrying a tongue of fog-free air out over the sea. This effect has been studied in the Moray Firth, off north-east Scotland.

3.5.5 *Advection fog over land*

(a) For advection fog over land to be at all widespread or persistent it is generally necessary for the ground to be very cold, either frozen or snow covered. Particularly widespread and persistent fog may occur when warm air starts snow cover thawing.

(b) During the coldest months, when insolation is too weak to disperse mature fogs, any change in wind speed or direction needs to be watched for signs that persistent fog patches may be advected into previously clear zones. Such movements can occur even in the middle of the day when a deterioration is least expected.

3.6 Convective activity above fog

3.6.1 *Convection over land fog*

Although fog is normally associated with a stable air mass the top of the inversion may be below the level of adjacent hills. During the day fog-free high ground may become warm enough to set off cumulus clouds. Points to watch for are:

(a) The development of thermally induced circulations in the low-level air flow; these may start the fog bank moving.

(b) Where large areas of low-lying fog persist throughout the day the heating of fog-free areas may result in the development of a pseudo sea-breeze effect during the afternoon. In winter, foggy air may be advected for many miles to produce sudden deteriorations in previously clear localities. In south and east England, wind speeds in excess of 15 kn have been observed as the fog front advanced.

3.6.2 *Convection over sea fog*

Around the coasts of southern England, fog formed in warm moist air advected over the sea may be capped by a potentially unstable layer at higher levels. Convergence in the layers above the fog may set off vigorous convective activity and thunderstorms. In the early stages these may not affect the fog but the downrush of air associated with heavy storms will lead to localized clearances.

The following features may be used as a guide:

(a) Upper-level convective developments occur chiefly over the Channel with a south-easterly flow at low levels and relatively high dew-points near the surface.

(b) Wet-bulb potential temperatures show a decrease with height in the middle levels.

(c) The potential instability is realized if an upper low or trough in the contours at 500 and 300 hPa moves across the area.

(d) This development will become apparent on infrared satellite imagery where the cold tops of instability cloud appear white above the grey of the sea fog. It will also be evident on the radar-network pictures once precipitation has started to form.

3.7 Haze

3.7.1 *General points*

Haze is a problem for aircraft in flight at low levels. During the day it tends to be thickest just beneath the base of a main stable layer. Visibilities reported at the surface do not give an accurate indication of the slant visibilities observed from aircraft under these conditions, particularly when looking towards the sun.

Haze particles may be produced by:

(a) Industrial pollution.

(b) Dust and fine sand raised by the wind, which can reach much of England from as far away as north Africa.

(c) Salt spray produced by rough seas and carried inland by strong winds.

Haze boundaries are often sharply defined, and may be associated with convergence lines (e.g. sea-breeze fronts). The position of weak synoptic-scale fronts may also be located at times by haze boundaries. These boundaries can be seen on high-quality satellite pictures, but low-resolution imagery is usually too coarse to show up haze adequately.

3.7.2 *Depth of haze*

With a well-marked stable layer near the ground, the haze top is often very clear-cut. The tops of shallow cumulus generally extend just above the haze layer, see Fig. 3.8. If the air above is conditionally unstable, large cumulus or cumulonimbus may rise many thousands of feet above the haze top, which is usually at, or below, the level where the environment lapse rate decreases to less than the SALR.

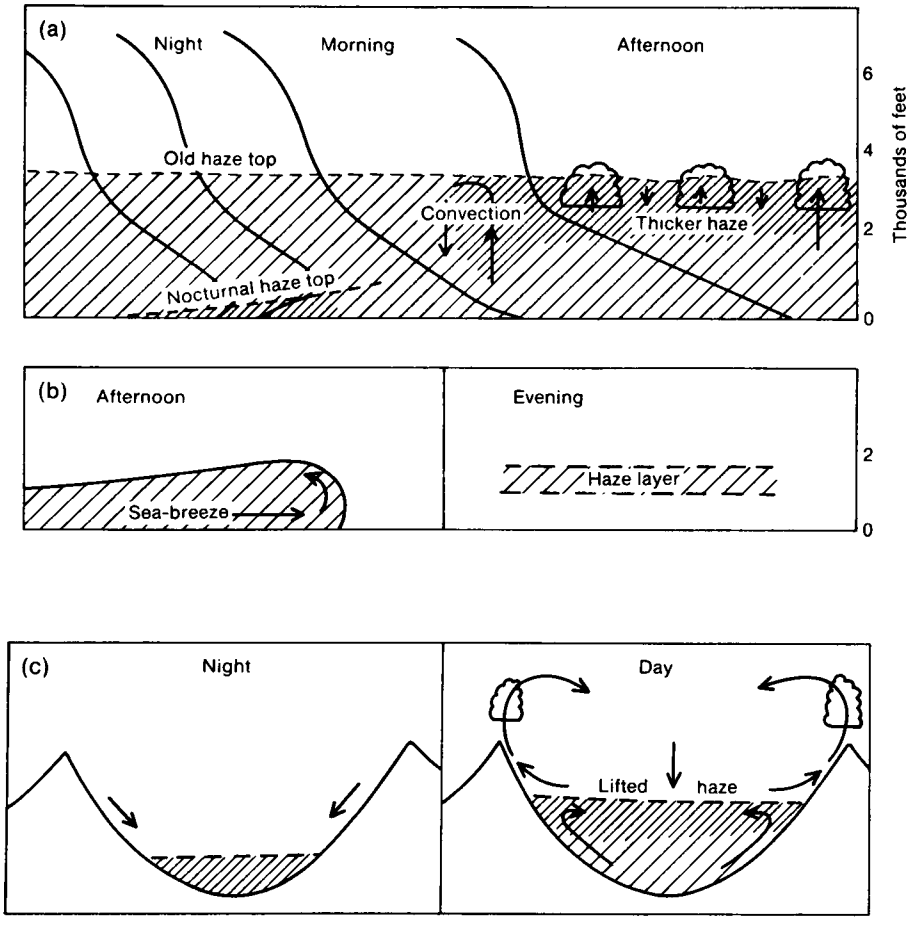

Figure 3.8 Idealized patterns of the diurnal variation of haze. (a) Under calm conditions with a stable layer at 3000–4000 ft. Curved full lines give an impression of the temperature profiles. (b) Association of haze with sea-breezes, which degenerate in the evening leaving an elevated haze layer. (c) Valley haze. Daytime convection over surrounding high ground generates subsidence over the valley which keeps the haze trapped in a restricted depth.

Haze appears thicker when the humidity is high. Ahead of a warm front, when the clouds are increasing, the visibility from the air often deteriorates in the layer extending about 300 ft below the cloud base.

Dispersing layer clouds may leave thin layers of elevated haze. These are rarely apparent from the ground but can be seen from aircraft when viewed horizontally during climb or descent.

3.7.3 *Diurnal variation of haze*

At the surface, haze thickens during the night as a nocturnal low-level inversion intensifies. It thins out during the day when this inversion is destroyed by solar heating.

Daytime convective mixing increases the haze depth and improves the horizontal visibility reported at the surface, but during the day the haze thickens at the inversion level. This effect is particularly marked when the inversion is low and the haze is being channelled into the valleys intersecting areas of high ground.

Mesoscale weather systems exert important controls on the distribution of haze. The sea-breeze circulation, for example, with its diurnal rhythm, often very clearly distinguishes the well mixed, convective air inland from the much hazier, stable, sea air (see Fig. 3.8).

3.7.4 *Dispersal of haze*

Continuous rain is effective in washing out most of the haze particles from the air. Showers, and even heavy thunderstorms, are much less effective.

Frontal convergence may initially concentrate the haze, but the subsequent large-scale vertical motion thins it out.

3.7.5 *Synoptic situations favourable for haze*

(a) Haze is usually thickest in anticyclonic conditions when low-level winds are light. An increase in surface wind often leads to improved visibility, and a decrease in wind to poorer visibility at the surface.

(b) In the United Kingdom a high proportion of haze days are associated with winds from Europe (see Fig. 3.9). Surface wind directions from 060°–120° commonly bring the worst haze.

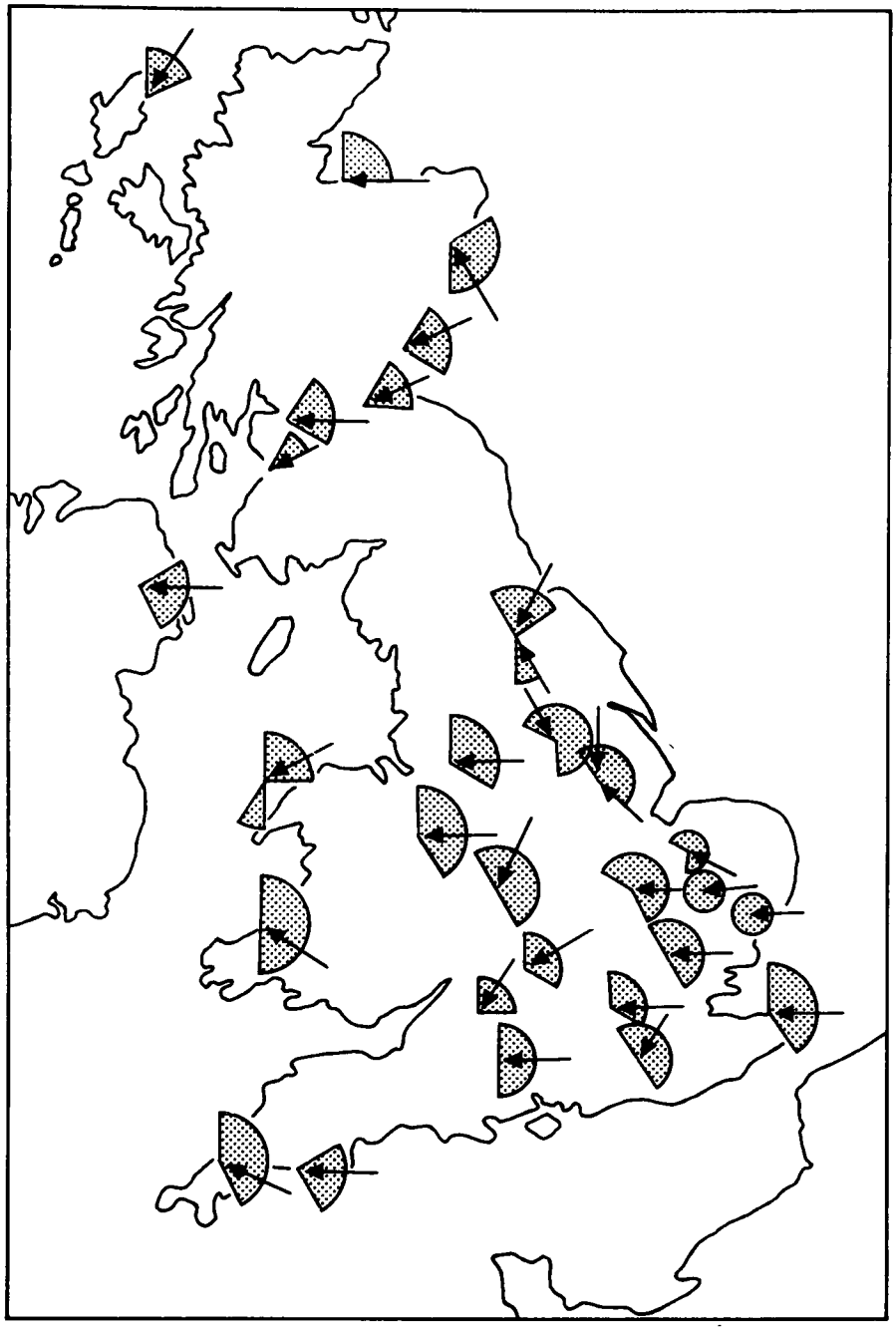

Figure 3.9 Surface wind direction and summer haze. Shaded sectors show the range of directions most often associated with visibilities in the range 1.8 to 9.9 km. Where variations are small the area shown is circular, and the arrows denote the worst directions. The radius of the sector arcs has no significance.

Fig. 3.10 has been produced as a forecasting aid in easterly situations over southern England. The afternoon and late evening visibilities at the surface are related to the relative humidity and surface wind speed.

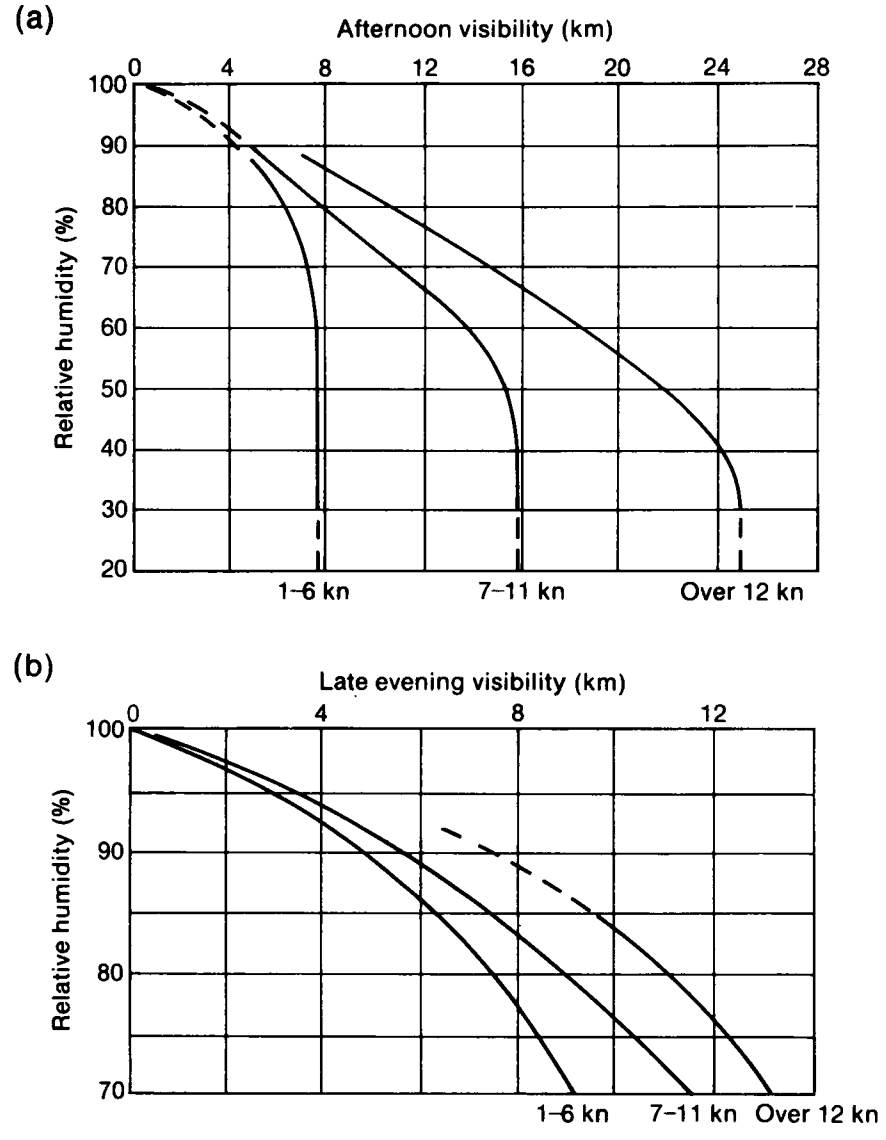

Figure 3.10 Visibility over southern England in hazy easterly situations, related to the relative humidity and wind speed. (a) In the afternoon (1200–1600 UTC), and (b) in the late evening (2100–2300 UTC). Median values of visibility are shown, for three ranges of surface wind speed (1–6 kn, 7–11 kn and over 12 kn). Pecked lines indicate provisional values where data is sparse.

CHAPTER 4 — CONVECTION AND SHOWERS

4.1 Definitions

Conditional instability — describes a temperature sounding in a layer where the actual lapse rate lies between the SALR and the DALR.

Latent instability — describes a temperature sounding which is stable near the ground and unstable above, typically at night. Even though no convection is occurring at the time of the sounding, it may be released later in the day as a result of solar heating.

Potential instability — is shown by the decrease of wet-bulb potential temperature with height through a layer. This form of instability is released when the air is lifted bodily (e.g. over a hill, or in a rising frontal air current).

4.2 Forecasting convective cloud — general principles

4.2.1 *Constructions on a tephigram*

Fig. 4.1 illustrates the general method, using a temperature sounding made before dawn (usually midnight) to forecast cumulus cloud during the day. ABCD is the environment curve. T and T_d are the surface temperature and dew-point expected as a result of daytime heating. BU is the condensation level, CV is the level where the lapse-rate of the environment decreases to less than the SALR.

(a) The parcel method

This method assumes that a small parcel of air, of negligible mass, is warmed at the surface and becomes buoyant, rising up through the environment without disturbing it or mixing with it until it reaches a level where it is no longer warmer than its surroundings.

In Fig. 4.1 the path curve of the rising parcel is shown by TUVWX. At T the parcel is warmer than the environment at that level (A) and it rises. From T to U its temperature falls at the DALR. U is the condensation level and cloud base, at which point it is still buoyant and continues to rise, but at the SALR. At W the rising parcel has a temperature equal to that of the environment and it is no longer buoyant. Most convective cloud tops will be around the level W. It is possible that the ascent of the rising parcel will give it the momentum to carry it

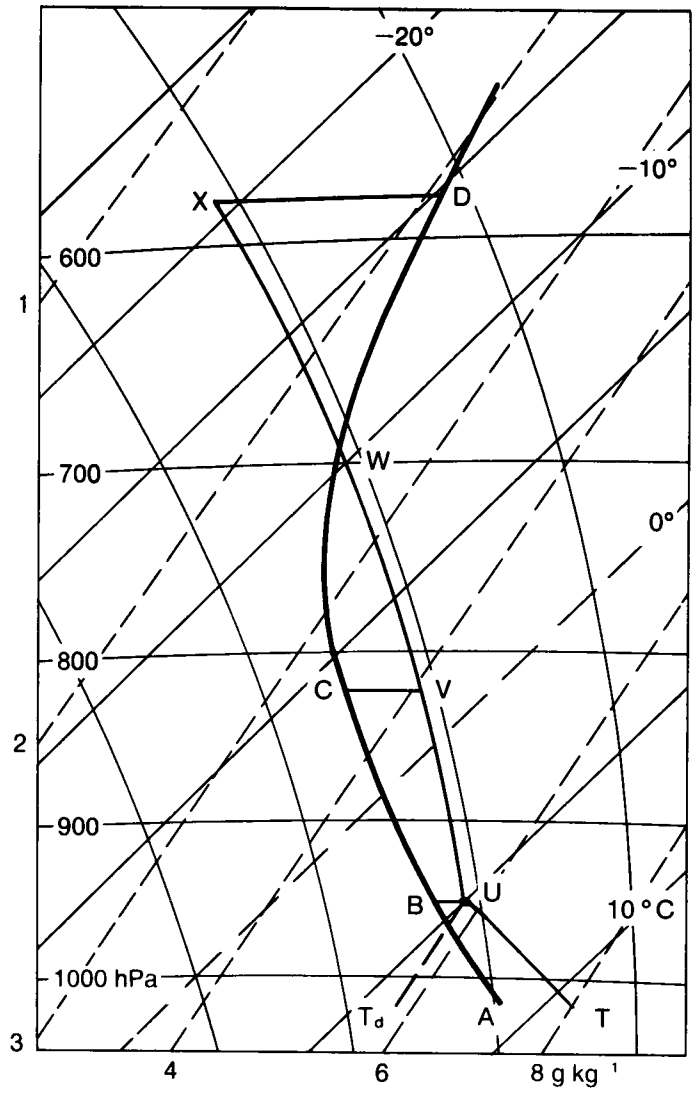

Figure 4.1 Tephigram construction for estimating the base and tops of convection cloud. See text for method of use.

above W before it sinks back again to that level. In extreme cases, vigorous convection cloud may penetrate to X, which is defined as the level which is such that the 'negative area' XDWX equals the 'positive area' WVTACW.

(b) *The slice method*

This method assumes that a rising convective current is compensated by downward motion in the surrounding air. This causes adiabatic warming of the environment, reducing the excess temperature of the rising air. As a result the ascent ceases at a lower level than that predicted by the parcel method. The

level C in Fig. 4.1, where the lapse-rate of the environment becomes less than the SALR, is the cloud-top level for most of the cumulus.

4.2.2 *Choosing a representative ascent*

The identification of a temperature sounding which will be representative of the air affecting an area later in the day is not always easy. At the time a forecast is being prepared, the appropriate sounding will be upwind of the area and in the correct air mass. Even if no fronts are expected to cross the area bringing major air-mass changes, there may be significant variations in the convective activity within the same air mass. Enhanced convection may be associated with the occurrence of synoptic-scale features such as upper troughs or lows. Similarly, suppressed convection may accompany an upper ridge. Mesoscale variations are also common, and may be associated with regions of low-level convergence/ divergence or variations in low-level moisture content.

4.2.3 *Prediction of surface dew-points*

Fig. 4.2 shows a tephigram construction for finding a representative daytime dew-point from a night-time sounding.

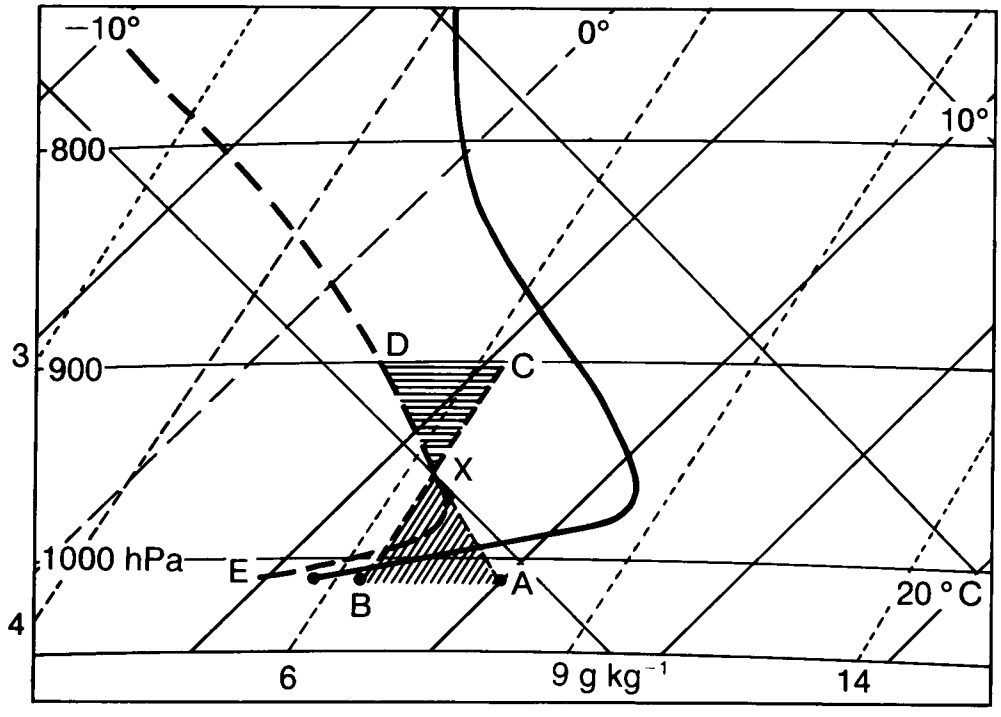

Figure 4.2 Tephigram construction for estimating a representative daytime value of the surface dew-point. See text for method of use.

(a) The full line is the dry-bulb curve and the pecked line is the dew-point curve at dawn. The maximum surface dew-point may be found by extrapolating down to the surface that part of the dew-point curve (DX) which has been unaffected by nocturnal cooling in the boundary layer. The dew-point so obtained, A, is the maximum daytime value of the dew-point. This will occur in the late morning when cumulus cloud first forms.

(b) With the onset of vigorous convection, at midday or soon after, the boundary layer develops an almost constant HMR. The afternoon value of the dew-point (B) may be found by drawing a line of constant HMR (CXB) such that the total moisture content represented by the values along DX equals that represented by the values along XA. Since the HMR scale is not linear, DX should be slightly longer than XA. In practice it may be assumed that DX equals XA to a first approximation.

(c) In this example it has been assumed that the mixed layer extends up to 900 hPa. In midsummer it may be necessary to raise this level to a point 150 hPa above the surface.

(d) On days with strong heating the reported dew-points may show wide differences between adjacent inland stations by mid afternoon, especially if winds are light. Stations on or near the coast report much higher dew-points when there is an influx of air from the sea.

4.3 Forecasting the cloud base of cumulus

4.3.1 *Estimating the condensation level*

The surface temperature (T) and dew-point (T_d) may be used to estimate the condensation level (H).

(a) As a rough approximation:

$$H = 4\,(T - T_d)$$

where T, T_d are in degrees Celsius and H in hundreds of feet.

(b) On a tephigram, Normand's theorem (see section 2.7.2) gives the condensation level at the intersection of a dry adiabat through T and a HMR line through T_d. This is the level BU in Fig. 4.1

4.3.2 *Relationship between condensation level and cloud base*

(a) While surface temperatures are rising quickly during the morning, the base of cumulus cloud is close to the calculated condensation level.

(b) During the afternoon when convective upcurrents are strongest the base of cumulus may be 700 ft above the condensation level.

Note: These relationships are based on data from gliding sites where light aircraft and sailplanes provided frequent reports of cloud base. Aircraft observations from Bircham Newton and Aldergrove, made during the months from April to September showed an average cloud base 25 hPa above the condensation level.

(c) After the time of maximum temperature the cloud base remains almost constant although the falling surface temperatures imply a lowering of the condensation level.

(d) Even in an apparently homogeneous air mass there may be significant variations in the cumulus cloud base over short distances. The difference is usually greatest during the morning when the air is not well mixed. Different rates of heating over dry hilly areas and moist low lying areas can lead to temporary variations of the cloud base of as much as 2000 ft within a distance of 1 km.

4.4 Forecasting the tops of convective cloud

4.4.1 *First estimates — using a tephigram*

An initial estimate of the cumulus/cumulonimbus cloud tops may be made following the method illustrated in Fig. 4.1. This may lead to a wide range of values, depending on whether the 'Parcel' or the 'Slice' method is used. However, observations often confirm the irregular level of actual cumulus tops.

It is suggested that, as a first estimate, using Fig. 4.1:

V is taken as the tops of most of the clouds
W is forecast for the tops of occasional large clouds
X is forecast only when conditions seem favourable for exceptionally vigorous and deep convection

4.4.2 *Synoptic-scale indicators of enhanced or suppressed convection*

The forecast height of convective cloud tops suggested in section 4.4.1 should be modified according to the synoptic-scale and mesoscale developments expected during the day. For example:

(a) *Factors indicating an increased depth of convection*

Approach of a trough, or low, in the 500, 300 or 200 hPa contour pattern.

Advection of warm, moist air at low levels.

A trough, or increased cyclonic curvature, on the surface chart.

A southerly low-level jet approaching an upper jet with winds from the south-west or west.

A convergence line (e.g. sea-breeze front).

Over mountains in summer when the winds are light.

Airflow over the sea across the isotherms towards warmer water.

(b) *Factors indicating a decreased depth of convection*

Approach of a ridge in the 500, 300 or 200 hPa contour pattern.

Advection of dry air at low levels.

Increasing anticyclonic curvature, or the approach of a ridge, on the surface chart.

At the left entrance or right exit of a jet stream.

Over valleys or lower ground surrounded by mountains when upper winds are light in summer.

Airflow over the sea across the isotherms towards cooler water.

4.5 The spreading out of cumulus into a layer of stratocumulus

4.5.1 *Cloud cover beneath an inversion*

When the depth of convection is limited by an inversion, cumulus tops may spread out to form an almost unbroken sheet which covers large areas and persists for long periods. This is common in subsided polar maritime air masses, particularly on the eastern flanks of anticyclones. Fig. 4.3 illustrates an empirical method for estimating the cloud cover beneath an inversion. B is the condensation level, derived from the expected surface temperature T and dew-point T_d. BC is a saturated adiabat from cloud base to cloud top. DE is a dry adiabat from the base of the capping inversion, cutting BC at E. The expected cloud amount equals CE divided by CB, where the depths are conveniently measured in hectopascals and the answer is a fraction which can be expressed in terms of oktas.

4.5.2 *Criteria for development of stratocumulus spread-out*

(a) An inversion or well-marked stable layer strong enough to halt all convective upcurrents even at the time of maximum insolation.

(b) A lapse-rate close to the DALR from the surface to near the base of the inversion when convection starts.

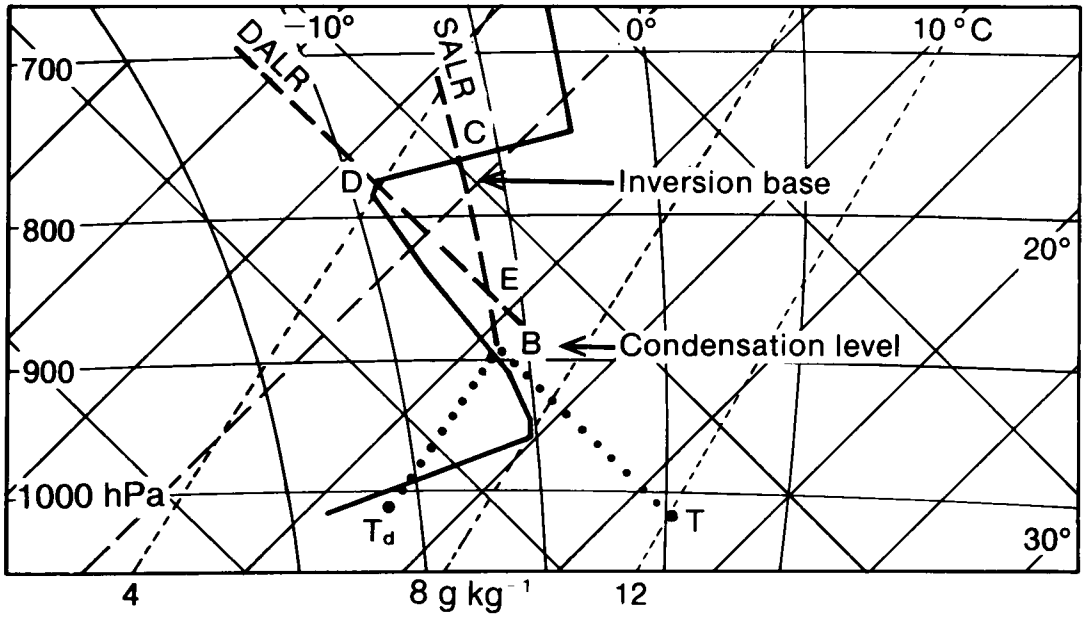

Figure 4.3 Estimating the spread out of cumulus cover beneath an inversion. See text for method of construction.

(c) Condensation level at least 2000 ft below the level of the inversion.

(d) A dew-point depression of 5 °C or less in the layer between the condensation level and the base of the inversion.

4.5.3 *Criteria for break-up of cloud sheet*

(a) Decreasing surface dew-points, lifting the condensation level to within 30 hPa of the inversion.

(b) Increasing surface temperatures, sufficient to lift the condensation level to within 30 hPa of the inversion.

(c) Continued subsidence, bringing the inversion down to within 30 hPa of the condensation level.

(d) A weakening of the inversion, allowing cumulus tops to break through to a higher level.

(e) If the cloud layer is formed due to diurnal heating over land, nocturnal cooling usually results in the dispersal of the layer. Cloud formed by convection over the sea shows no such diurnal variation.

4.6 Forecasting showers

4.6.1 *Intensities of showery precipitation*

Rain showers —	Slight	less than 2.0 mm h^{-1}
	Moderate	2.0 to 10.0 mm h^{-1}
	Heavy	10.0 to 50.0 mm h^{-1}
	Violent	more than 50 mm h^{-1}

4.6.2 *Depth of cloud needed for showers*

The diagram at Fig. 5.1 may be used as a rough guide for both convective and non-convective precipitation. Showers are likely to be heavier in intensity than layer-cloud precipitation for the same thickness of cloud. The diagram only applies if the difference in water content at the base and top of a shower cloud exceeds 2 g kg^{-1}.

See also section 4.7.4 for guidance on the probability of thunderstorms related to the height of cumulonimbus tops.

4.6.3 *Forecasting hail*

Deep and vigorous convection is required. The following criteria are a guide:

(a) Cumulonimbus tops are colder than −20 °C.

(b) The 'parcel' path curve is warmer than the environment curve by 4 °C at some level (CV in Fig. 4.1).

(c) Vertical wind shear exists between the base and top of cumulonimbus (see section 4.7.2).

4.7 Forecasting cumulonimbus and thunderstorms

4.7.1 *The main factors*

(a) Large quantities of Convectively Available Potential Energy (CAPE) are needed, which can be released through convection. On a tephigram this energy is represented by the area between the environment curve and the path curve of a rising parcel (ATVWCB in Fig. 4.1).

(b) Vertical wind shear through the depth of the convective layer (see section 4.7.2).

The severity of the storms depends on whether the CAPE is released by many small cumulonimbus clouds or by a few giant ones.

4.7.2 *Effect of vertical wind shear*

(a) With no shear, the updraught and downdraught in a cumulonimbus are coincident. Initially, the cloud grows and its updraught strengthens; then precipitation forms in the upper parts of the cloud. The precipitation falls through the updraught. Hence the updraught is weakened by the drag of the falling precipitation, and the cloud quickly decays.

(b) With wind speeds varying with height but no directional shear, the updraught is tilted and the precipitation falls down beside the updraught. With

up and down currents coexisting side by side, the cloud persists longer than in a no-shear situation. Eventually the updraught may be cut off at the surface by the spreading out of the cold down draught beneath the storm.

(c) With directional and speed shear, some complex mesoscale storm systems may result (see 7.4.5). These may develop into self-generating steady-state systems which can persist for many hours, quite independently of any surface heating.

4.7.3 *Movement of thunderstorms: the steering level*

With a cumulonimbus extending through a deep layer in which there is marked wind-shear, the storm cloud is steered by the wind at the level approximately one third of its depth, measured from the base of the cloud, i.e. $H_{base} + \frac{1}{3}(H_{top} - H_{base})$.

Often in the United Kingdom, the steering level is around 700 hPa.

4.7.4 *Forecasting thunderstorms — depth of cumulonimbus*

If cumulonimbus tops are at:

less than 13 000 ft	thunder unlikely
14 000–18 000 ft	thunder probable
greater than 18 000 ft	thunder highly probable

4.7.5 *Forecasting thunderstorms — instability indices*

(a) *Boyden Index*

$$I = (Z\text{–}200) - T$$

where Z = 1000–700 hPa thickness (dam)
T = 700 hPa temperature (°C)

Thunder is probable if $I \geqslant 94/95$, in the United Kingdom.

This index should not be used in Mediterranean or tropical areas, or where the ground level is high.

(b) *Rackliff Index*

$$T = \theta_{w900} - T_{500}$$

where θ_{w900} is the 900 hPa wet-bulb potential temperature (°C)
T_{500} is the 500 hPa temperature (°C).

Thunder is probable if $T \geqslant 29/30$, in the United Kingdom.

(c) *Modified Jefferson Index*

$$T_{mj} = 1.6\,\theta_{w900} - T_{500} - \tfrac{1}{2}\,D_{700} - 8$$

where D_{700} = dew-point depression (°C) at 700 hPa.

Thunder is probable if $T_{mj} \geqslant 29$, in the United Kingdom.

The formula can be reduced to $T_{mj} = \Delta T + X$ and computed more easily by using Fig. 4.4, where the value of $(-\tfrac{1}{2}\,D_{700} - 8)$ is replaced by the constant -11.

(i) From the values of 500 hPa temperature (x-axis) and 900 hPa θ_w (y-axis), obtain a value of ΔT given by the sloping lines.
(ii) Correct this value of ΔT, according to the actual 700 hPa dew-point depression, using the small graph (top right) to obtain the correction X.

(d) *Potential instability index*

$$P = \theta_{w500} - \theta_{w850}$$

Thunder is possible if P is negative.

4.7.6 *Forecasting thunderstorms — synoptic features*

The objective forecasting techniques given in sections 4.7.4 and 4.7.5 should not be used in isolation. Their value is greatly enhanced when they are used in conjunction with features which can be analysed on synoptic charts.

Upper-air soundings alone do not always reveal the extent of the thunder risk. Often the soundings available before a thundery outbreak fail to show exceptional

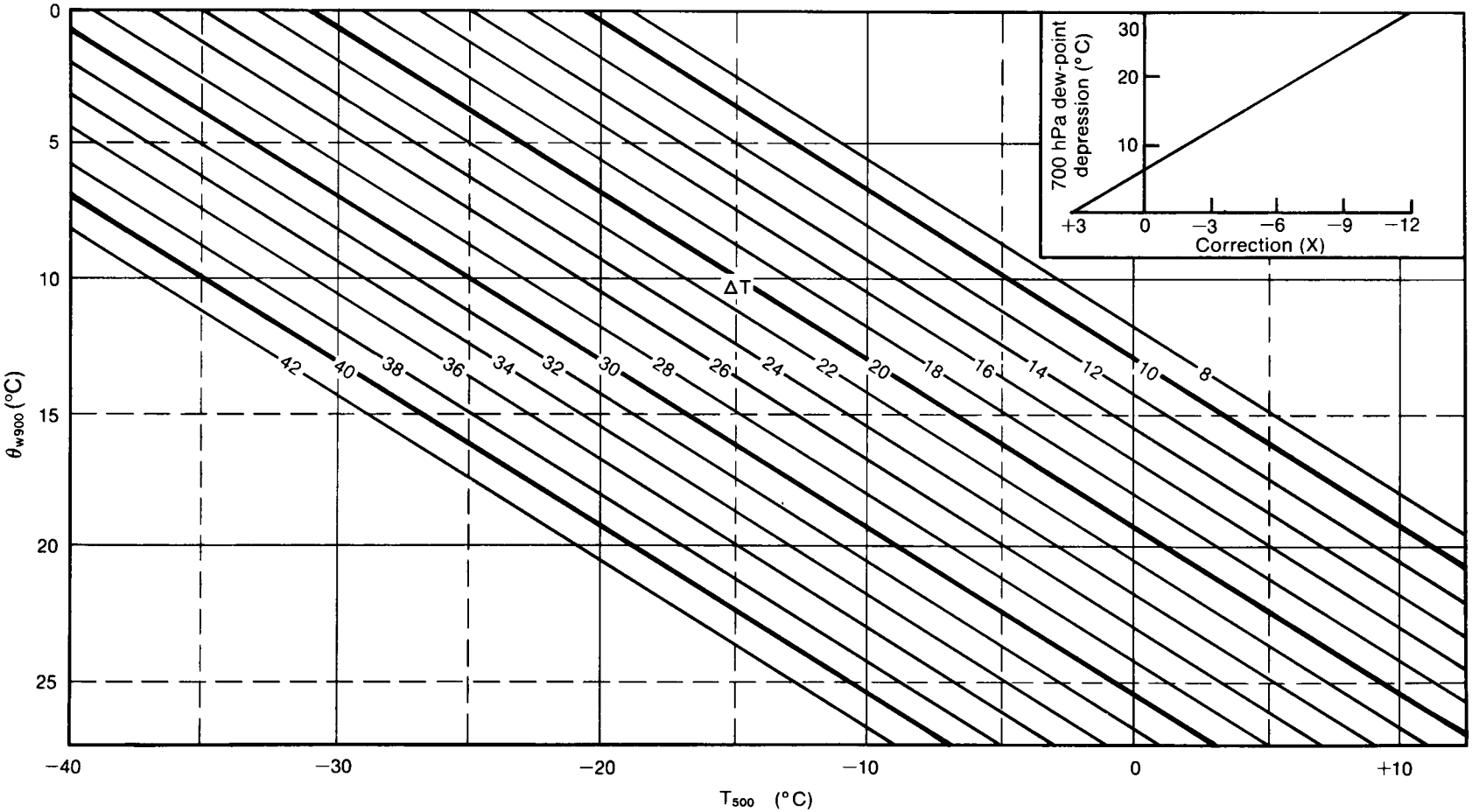

Figure 4.4 Computing the modified Jefferson Instability Index. See text for method of use.

instability. Instability indices are only a guide to the degree of instability at the time of a sounding. Consideration should be given to factors likely to release the energy available for convection, such as:

(a) The position and movement of upper-level troughs or lows.

Thunderstorms are much more likely to break out along or ahead of an upper trough, or near an upper low.

(b) The existence and movement of low-level convergence lines, such as surface fronts, or sea-breeze fronts.

(c) Areas of high ground which may become very warm by day in the summer months.

Other useful synoptic tools are:

(d) Dew-point analysis:

The movement of a tongue of air with high dew-points may help to define a thunder-threatened area.

(e) Charts of θ_w at 850 hPa:

These serve a similar purpose as surface dew-point analyses.

(f) Charts of the difference between θ_w at 500 and 850 hPa

These show where θ_w decreases with height over a significant depth of the atmosphere, and potential instability exists.

(g) Cyclonic curvature of surface isobars

Minor troughs are associated with convergence and enhanced convection.

4.7.7 *Conditions favouring severe thunderstorms*

Severe storms are mesoscale weather systems and are briefly described in Chapter 7. This section is concerned only with the synoptic-scale setting in which the storms occur. Relevant points for southern England, are:

(a) *Upper-air soundings*

Some of the most severe and widespread outbreaks of thunder have occurred some 12–18 hours after a sounding showed a layer of warm air capping a shallow convective layer. This cap can prevent the early release of the convective energy, allowing it to build up with continued surface heating and be released explosively in one big storm later.

(b) *Advection of low-level moisture*

Surface dew-points should exceed 13 °C; but often reach 18 °C or more in severe storms over southern England.

At 850 hPa, similar values of θ_w are experienced.

The winds at this level are usually in the sector SE–SSW, with a speed of 20–30 kn, often in a narrow tongue.

(c) *Medium-level advection of dry air*

With potential instability present, θ_w values at 500 hPa may be 2–5 °C lower than at 850 hPa. Winds at 500 hPa should be 20–40° veered from those at 850 hPa, with speeds of 35–50 kn.

(d) *Upper-level strong winds*

Further veering above 500 hPa, with 300 hPa winds in the sector SSW–W and speeds 50–85 kn, are good conditions for positioning the downdraughts in the favoured position for generating severe storms.

Fig. 4.5 summarizes the points described in (b), (c) and (d).

(e) *Positive vorticity advection (PVA) at 500 and 300 hPa*

This usually occurs in the region in advance of an upper trough or upper low. Isopleths of vorticity cross the contour lines at an angle of 30° or more.

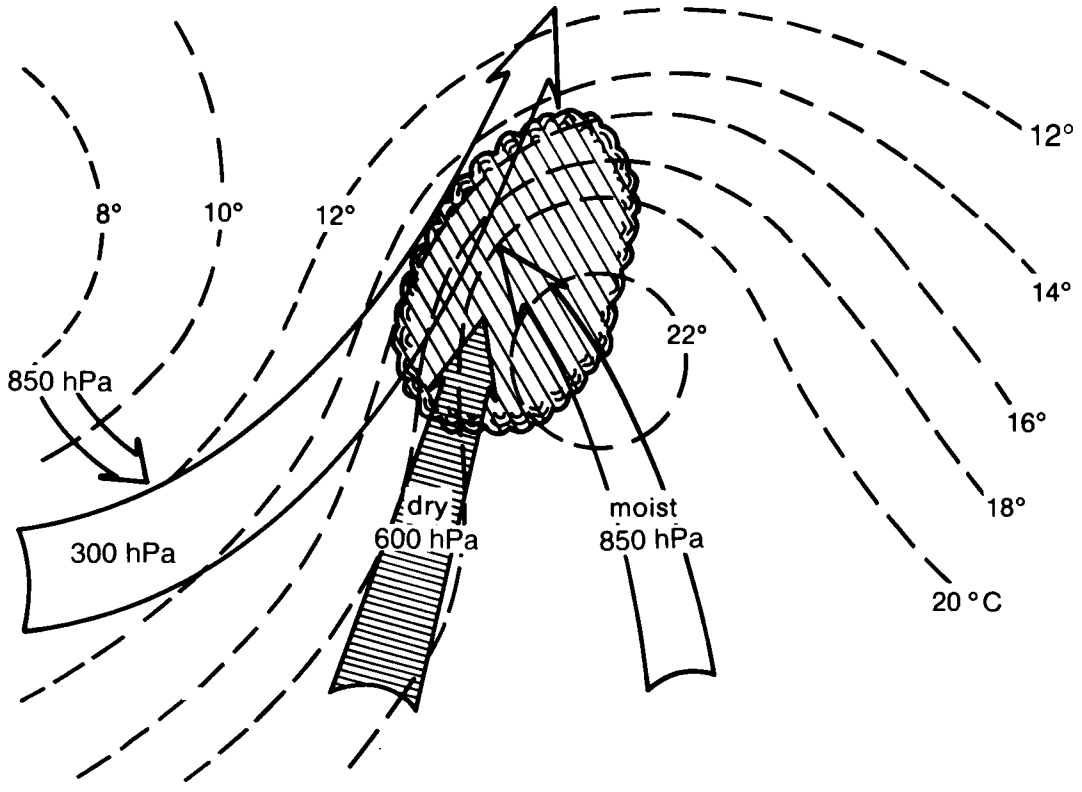

Figure 4.5 A schematic diagram of the three main synoptic-scale currents associated with the development of severe thunderstorms over southern England, together with typical isopleths of θ_w at 850 hPa. The hatched area indicates the the location of the storms.

CHAPTER 5 — LAYER CLOUDS AND PRECIPITATION

5.1 Stratus and drizzle

5.1.1 *Formation of low Stratus*

(a) Low stratus forms when air with a lapse rate less than the SALR is either (i) cooled below its dew-point or (ii) has extra moisture added by the evaporation of falling precipitation. The cooling of the air may be due to advection over a colder surface and/or upslope motion. Extra moisture may be added by evaporation from wet surfaces, especially when snow or heavy frost begins to thaw.

(b) To predict the formation of stratus, the following data are needed:

(i) vertical temperature and dew-point profiles of the air mass expected
(ii) sea temperature (if flow is from over the sea)
(iii) predicted wind field
(iv) predicted amount and depth of nocturnal cooling overland
(v) knowledge of the topography.

5.1.2 *Forecasting the temperature of stratus formation over land*

To forecast the temperature at which stratus will form as a result of nocturnal cooling over land:

(a) Obtain the fog-point by Saunders' method (see section 3.3.1).

(b) Assess the height of the top of the nocturnal surface turbulent layer.

(c) On a tephigram draw the constant mixing ratio line through the fog-point temperature (plotted on the surface isobar).

(d) From the intersection of this line with the isobar corresponding to the top of the surface turbulent layer, draw a dry adiabatic. The intersection of this adiabatic with the surface isobar indicates the temperature at which stratus will form.

5.1.3 *Forecasting the advection of stratus from the sea*

(a) If there has been little change in the synoptic situation during the day, the temperature at which stratus cleared in the morning is a good estimate of the temperature at the coast when the stratus will start to move inland.

(b) The movement of stratus inland can be forecast from the direction and speed of the 10 m wind at the time when convection and turbulence are still operative in the lowest layers, and before the surface temperature begins to fall towards evening.

(c) If there is upslope motion, stratus may form over higher ground before the main cloud sheet spreads in from the coast.

The level at which stratus will form can be determined from a representative vertical profile of temperature and dew-point. Use a Normand construction (section 2.7.1) to determine the condensation levels of air lifted from several levels. The lowest condensation level represents the pressure at the base of any orographic stratus.

5.1.4 *The formation of stratus in continuous precipitation*

Evaporation of precipitation can cool the air to its wet-bulb temperature. A temperature close to the wet-bulb value is reached after about half an hour of very heavy rain or 1–2 hours of moderate rain. Prolonged drizzle and light winds frequently lead to the formation of very low stratus even when upslope motion is apparently negligible.

Advection of warm air across thawing snow often results in stratus forming at or very near the surface.

5.1.5 *Forecasting drizzle*

For drizzle to reach the ground it must fall from stratus cloud with its base less than 1000 ft. The dew-point depression in the air below cloud should be less than 2 °C, otherwise the very small drizzle droplets (0.2–0.5 mm diameter) will evaporate.

Heavy drizzle mostly occurs within clouds that are covering high ground.

5.2 Stratocumulus

5.2.1 *Stratocumulus formed from spreading out of cumulus* (see section 4.5)

5.2.2 *Nocturnal dissipation of stratocumulus over land* (James' rule)

The cloud will break if

$$D_m > D_c$$

where:

D_m is the max dew-point depression (°C) in the 50 hPa layer **above** cloud
D_c is the value given in the Table 5.1 below, in which
- b is the difference (g kg^{-1}) between HMR at top and bottom of the 50 hPa layer **below** cloud
- z is the cloud thickness (hPa).

Table 5.1. Values of D_c (°C) for use with James' rule

	b (g kg^{-1})					
	0.25	0.50	0.75	1.00	1.25	1.50
z (hPa)						
10	—	—	1	3	6	8.5
20	0	2.5	5	8	10	13
30	4	7	9	12	14.5	17
40	9	11	14	16	19	21
50	13	15	18	20.5	23	26
60	17	20	22	25	27	30
70	21	24	26.5	29	32	34

Note: a linear hydrolapse in the layer is assumed.

Only use this technique if the stratocumulus sheet is bounded by a dry inversion, there is no surface front within 400 miles and the cloud sheet is extensive giving almost complete cloud cover (>6/8 for 2 or more hours).

5.2.3 *Dissipation of stratocumulus by convection* (Kraus' rule)

A cloud layer will not disperse by convective mixing with the air above if the pressure (hPa) at the cloud top is less than P_c, as given below. (If the pressure at cloud top is greater than P_c the cloud may or may not disperse.)

$$P_c = P + a\,(P_0 - 1000)$$

where P_0 is the surface pressure (hPa) and P and 'a' are given in Table 5.2 below.

Table 5.2. Values of P and 'a' (for use with Kraus' rule) for given cloud-top temperatures (water or ice cloud) and strength of inversion.

		Magnitude of inversion containing the cloud layer (°C)									
		10		8		6		4		2	
	Temp. at cloud top (°C)	P	a	P	a	P	a	P	a	P	a
Water cloud	20	833	0.80	861	0.83	891	0.87	924	0.90	960	0.95
	10	803	0.75	834	0.79	869	0.82	906	087	951	0.93
	0	755	0.67	789	0.71	830	0.76	877	0.82	932	0.90
	−10	680	0.56	719	0.60	765	0.66	823	0.73	898	0.84
Ice cloud	0	779	0.71	812	0.75	850	0.79	891	0.85	941	0.91
	−10	702	0.59	739	0.63	786	0.69	839	0.76	908	0.85
	−20	586	0.45	628	0.49	679	0.54	747	0.62	841	0.74
	−30	451	0.30	489	0.34	540	0.38	613	0.45	728	0.58

5.3 Seeder and feeder clouds

When a very moist low-level air flow is forced to rise over high ground, thick stratus/stratocumulus layers form. By itself this cloud may produce rather little precipitation, especially if the wind speed is strong and there is insufficient time for precipitation to form before the air flows down the lee side of the hills.

If, however, rain is already falling from upper-level cloud layers (seeder clouds) above the stratus/stratocumulus, it will fall through the low-level (feeder) cloud,

scouring out the droplets within, considerably enhancing the rainfall rate at the surface. The effect is additive, not multiplicative.

This is a common mechanism for producing heavy rain over high ground in warm sectors approaching the United Kingdom from the south-west quadrant and is illustrated in Fig. 7.17.

The effect is increased if there is any release of potential instability, and when the low-level flow is strong and prolonged, replenishing the supply of moist air continuously.

5.4 Precipitation from layered clouds

5.4.1 *Definition of intensities of (non-showery) precipitation*

(a) *Rain*

Slight	less than 0.5 mm h^{-1}
Moderate	0.5 to 4.0 mm h^{-1}
Heavy	more than 4.0 mm h^{-1}

(b) *Snow*

Slight	less than 0.5 cm h^{-1}
Moderate	about 0.5 to 4.0 cm h^{-1}
Heavy	more than 4.0 cm h^{-1}

Note: 1.25 cm of fresh snow $\approx$ 1 mm water.

5.4.2 *Precipitation in frontal depressions*

The amount and intensity of the precipitation depends on:

(a) large-scale ascent of air,

(b) the continued availability of moist air, originating at low levels,

(c) the release of potential instability aloft, and

(d) orographic enhancement over high ground.

Frontal precipitation often occurs in bands, usually but not always parallel to one of the surface fronts, see Fig. 7.1. Bands of rain ahead of a cold front may penetrate well into the warm sector or even ahead of the warm front. These bands are mesoscale phenomena, and are described in Chapter 7.

5.4.3 *Depth of cloud for precipitation*

Fig. 5.1 gives a guide to the intensity of precipitation at ground level, over flat terrain, associated with different thicknesses of cloud. It is constructed for layer clouds in which the difference in water content between the base and the top is over 1.5 g kg^{-1}.

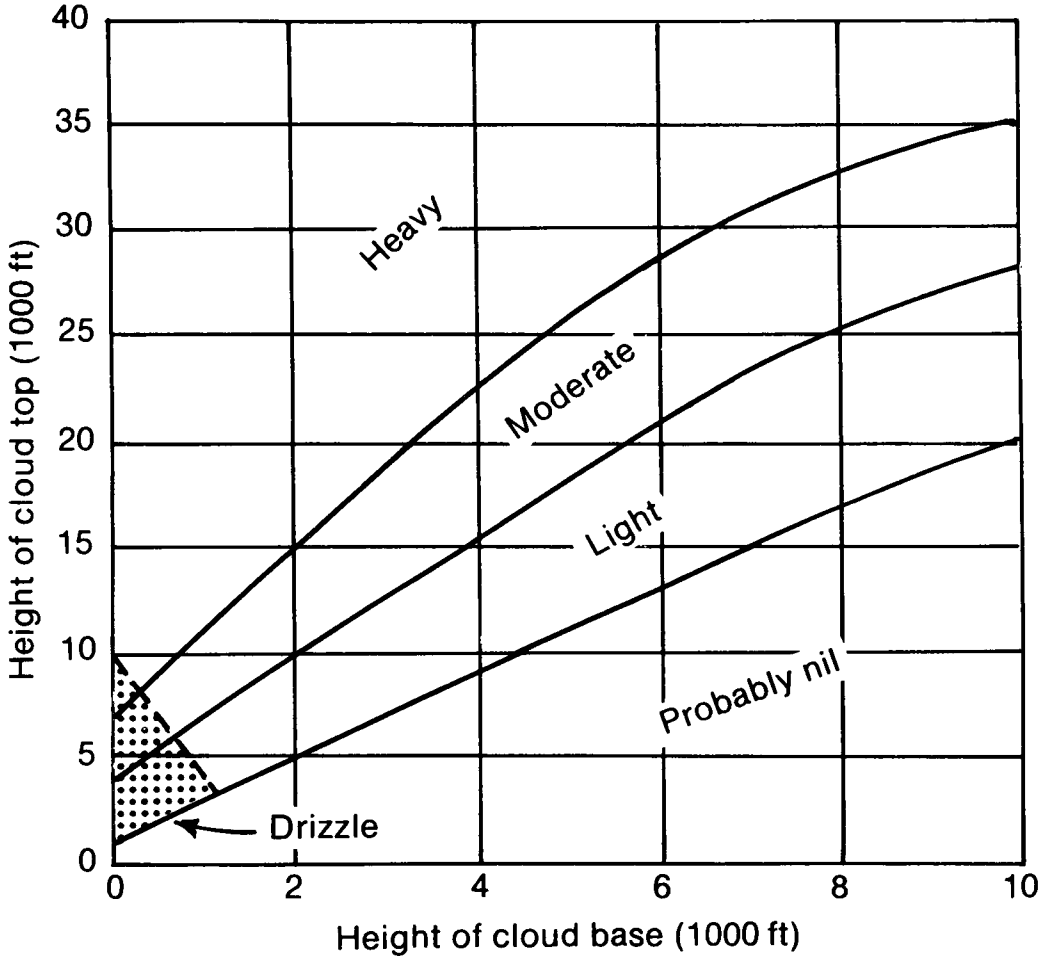

Figure 5.1 The depth of cloud related to intensity of precipitation. The stippled area indicates the conditions for the precipitation to be mainly drizzle.

5.4.4 *Criteria for forecasting snow*

Various criteria have been derived for estimating the probability of precipitation in the United Kingdom falling as snow rather than rain. The following summary lists them in a rough order of merit:

		Percentage probability of snow				
		90%	70%	50%	30%	10%
Adjusted value of 1000–850 hPa thickness (see Note 1)	(gpm)	1281	1290	1293	1298	1303
Height of 0 °C isotherm (see Note 2)	(hPa)	12	25	35	45	61
Surface temperature	(°C)	−0.3	1.2	1.6	2.3	3.9
1000–500 hPa thickness	(gpm)	5180	5238	5258	5292	5334

Notes

1. The 1000–850 hPa thickness needs adjustment for the 1000 hPa height (H_{1000}) and the height of the ground above sea level (H_{GR}). The adjustment (m) is given by $(H_{1000} - H_{GR})/30$ and this quantity may be conveniently read off from Fig. 5.2.

2. The height of the 0 °C wet-bulb temperature is an equally good criterion:

Height of 0 °C wet-bulb temperature	Form of precipitation
3000 ft or over	Almost always rain; snow rare
2000–3000 ft	Mostly rain; snow unlikely
1000–2000 ft	Rain readily turns to snow
Below 1000 ft	Mostly snow; only light or occasional precipitation falls as rain. Near windward coasts, moderate or heavy precipitation persists as rain.

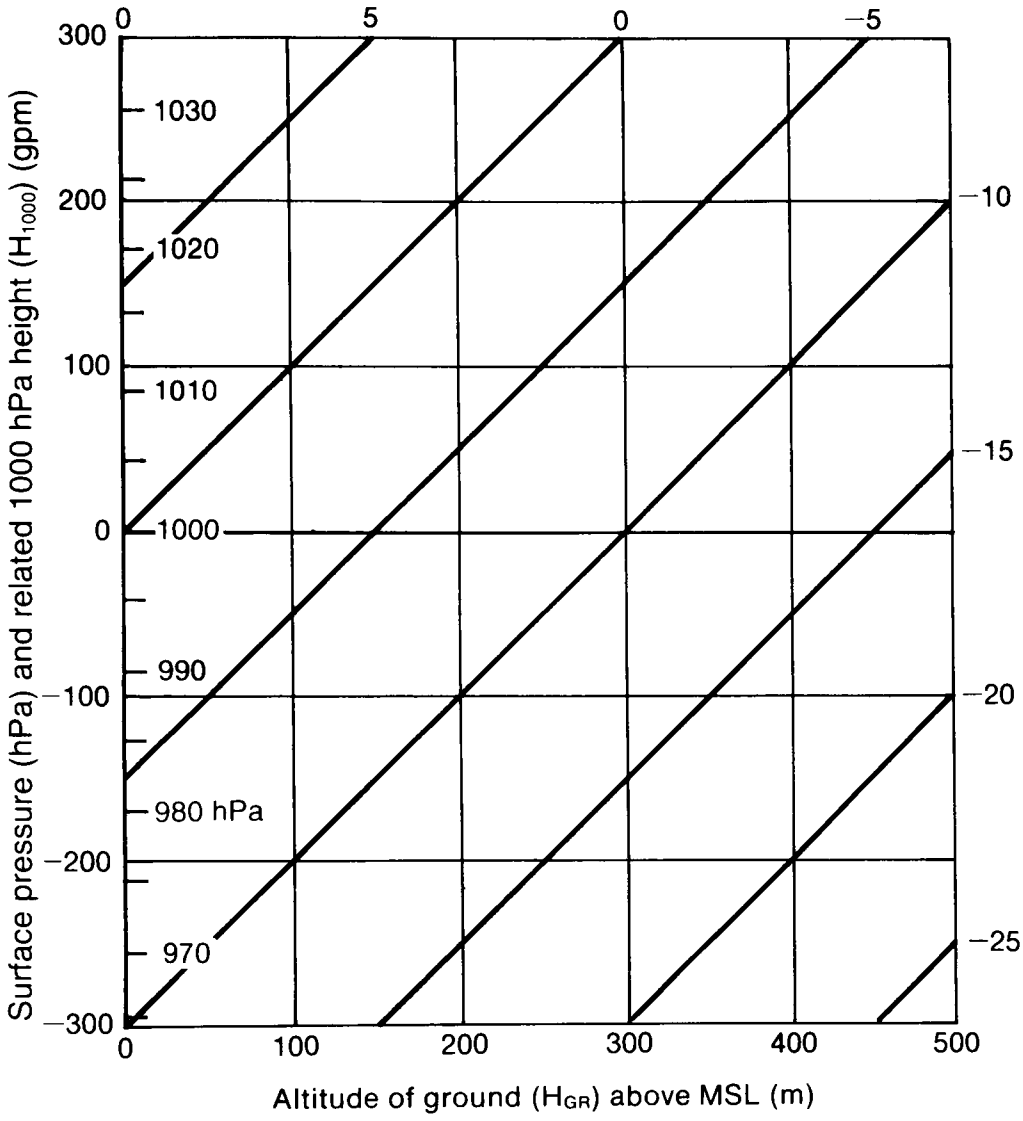

Figure 5.2 Forecasting the probability of precipitation as snow. The nomogram indicates the adjustment to be made to the 1000–850 hPa thickness to allow for the 1000 hPa height (or surface pressure) and altitude of ground above sea-level

5.4.5 *Snow over high ground*

If the forecast probability of precipitation falling as snow at MSL is known, from the grid-point output of a numerical model, the increased probability at higher levels can be read off from Fig. 5.3

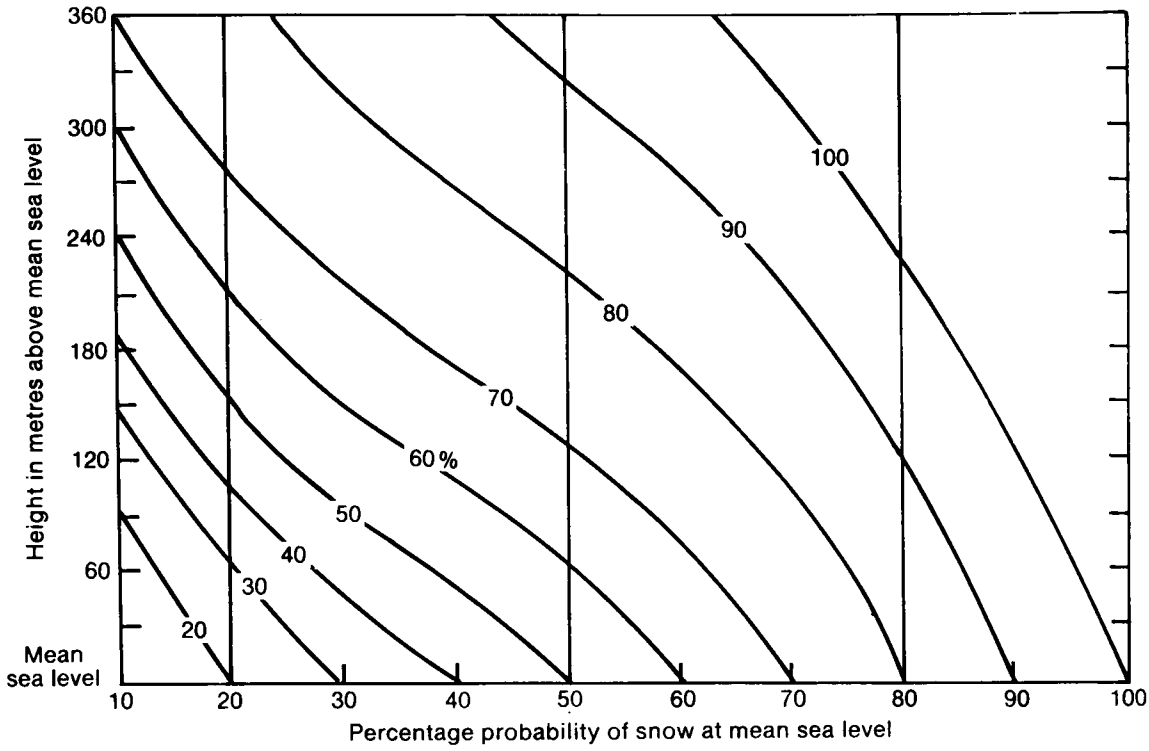

Figure 5.3 Snowfall over high ground. The increased probability of precipitation falling as snow over high ground, given its probability of occurrence at mean sea level.

Notes

1. The 80%, 50% and 20% snow probability lines on the fine-mesh forecast charts are based on forecast 1000–850 hPa thickness values and refer to mean sea level.

2. The nomogram (Fig. 5.3) has been prepared to help forecasters to adjust these values in order to estimate the probability of snow at higher levels. Thus a snow probability forecast of 20% at mean sea level becomes 50% at 150 m (e.g. most of the Marlborough Downs and the Cotswolds) and over 70% at 300 m.

5.4.6 *Drifting of snow*

With the temperature below 0 °C, drifting of loose snow starts when the wind speed exceeds 12 kn. Serious drifting occurs with winds above 17 kn.

A blizzard is defined by the UKMO as 'the simultaneous occurrence of moderate or heavy snowfall with winds of at least force 7, causing drifting snow and reduction of visibility to 200 m or less'.

5.4.7 *Synoptic situations for snow in the United Kingdom*

(a) Over England, substantial falls of snow are mainly associated with a warm front or warm occlusion approaching from between south and west. In such situations a large supply of moisture is available. Frontal progress is very slow as the warm air rises over a much colder continental easterly flow at low levels, so that snowfall is prolonged.

(b) Polar lows in a northerly airstream can produce substantial snowfalls but more frequently in Scotland than further south.

(c) Easterly winds bring snow showers, intensified by the passage of troughs, and give substantial falls of snow in eastern Scotland and England. Less frequently, exposed north-facing coasts of England, as far south as Norfolk and Kent, can be seriously affected when there is an unstable northerly airflow in winter.

5.4.8 *Climatology of snow*

In the United Kingdom, January and February are the snowiest months. Over low ground the main high-risk season is from mid-December to mid-March, though severe falls can occur throughout the spring. Over high ground the high risk season is several weeks longer at each end.

Fig. 5.4 illustrates the annual incidence of days with snowfall.

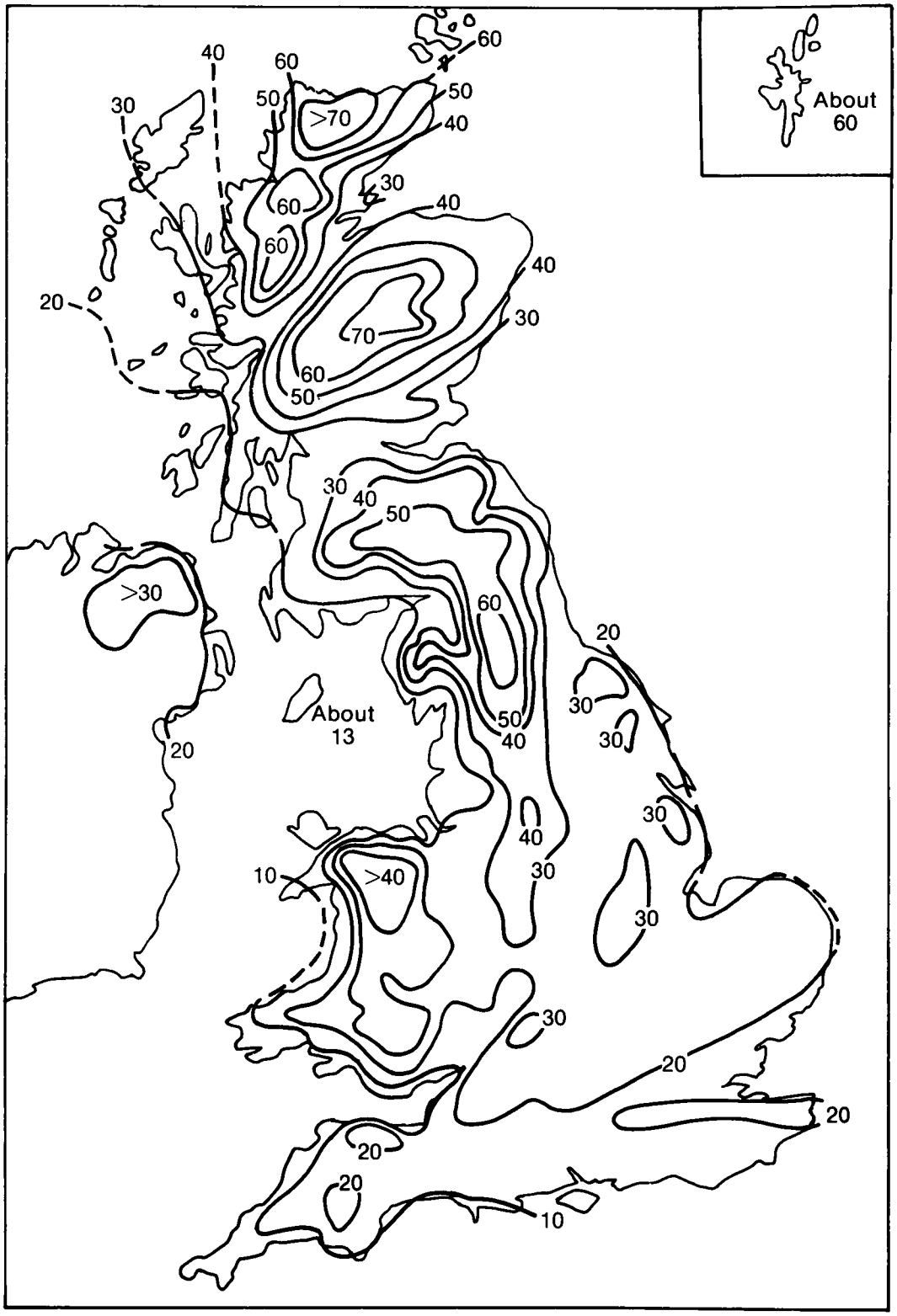

Figure 5.4 Mean number of days per year with snow falling (1941–70).

CHAPTER 6 — TURBULENCE, ICING, CONTRAILS AND SEA WAVES

6.1 Turbulence

6.1.1 *Intensity of turbulence — definitions*

The terms used for describing the intensity of turbulence are classified by aircraft operators as follows:

Description	Effect in aircraft
Light	Effects are less than those for Moderate intensity
Moderate	There may be moderate changes in aircraft attitude and/or height but the aircraft remains in control at all times. Air-speed variations are usually small. Changes in accelerometer readings of 0.5–1.0 g at the aircraft's centre of gravity. Occupants feel strain against seat belts. There is difficulty in walking. Loose objects move about.
Severe	Abrupt changes in aircraft attitude and/or height. The aircraft may be out of control for short periods. Air-speed variations are usually large. Changes in accelerometer readings greater than 1.0 g at the aircraft's centre of gravity. Occupants are forced violently against seat belts. Loose objects are tossed about.
Extreme	Effects are more pronounced than for Severe intensity

6.1.2 *Turbulence due to convection*

This occurs at the boundaries of vertical convective currents:

(a) in cloud,

(b) outside cumulonimbus clouds, especially in clear air around the anvil and just above a storm top,

(c) in dry thermals below cloud base, or in a cloudless region over any heated land mass (over deserts, dry convection may extend up to 15 000–20 000 ft), and

(d) in downdraughts associated with the onset of precipitation. These spread out at the surface, producing a line-squall close to the shower area.

Cumulonimbus clouds can extend above 40 000 ft in the United Kingdom, and above 60 000 ft in the USA and some tropical areas.

The magnitude of typical vertical currents in convective clouds, based on aircraft reports, are:

Regime	Vertical velocity ($m\ s^{-1}$)	Description of turbulence
Cumulus (humilis/mediocris)	1–3	Light
Cumulus (congestus)	3–10	Moderate
Cumulonimbus	10–25	Severe
Severe storm (USA)	20–100	Extreme
Dry thermals	1–5	Light/Moderate
Downdraughts	3–15	Moderate/Severe
Downdraughts (USA)	up to 40	Extreme

6.1.3 *Turbulence at low levels*

A rough guide to the intensity of turbulence that may be expected in the lowest few hundred feet in windy conditions is:

Surface wind	Turbulence over:		
(kn)	Sea	Flat country	Hilly country
15–35	Light/Moderate	Moderate	Severe
over 35	Moderate/Severe	Severe	Extreme

Strong sunshine added to strong wind may increase the difficulties of controlling aircraft, especially on landing and take-off.

Violent squalls create a most dangerous low-level hazard to aircraft. They may occur:

(a) during or preceding the passage of an active cold front,

(b) during or preceding the occurrence of a thunderstorm,

(c) in hilly or mountainous country, in association with 'rotor streaming', which requires:

(i) strong winds (over 25 kn) near the ground,
(ii) a sharp decrease in wind speed, accompanied by a large change in direction, at a height of 1½–2 times the height of the hills, and
(iii) a stable air mass, above the well-stirred lowest layer.

6.1.4 *Turbulence associated with mountain waves*

Mountain waves and associated turbulence may be pronounced when all the following conditions are satisfied:

(a) The wind blows with little change of direction with height, blowing within 30° of the direction normal to a prominent range of hills.

(b) The wind speed is 20 kn or more at hill-crest level, with speeds increasing with height above.

(c) There is a stable layer between the hill-crest level and a few thousand feet above.

The intensity of the turbulence is proportional to the strength of the vertical currents, and inversely proportional to the wavelength. It may be severe with short waves and strong upcurrents, but less intense if the wavelength is long. The most turbulence-prone areas are likely to be near wave crests and troughs.

Individual aircraft will experience different effects, depending on their track, speed and flight characteristics. A powered aircraft making a rapid transit of a wave system into, or down, wind will be subject to greater turbulence than when

flying in the same system across wind. At the same time, a glider may be able to gain height by flying in a fixed part of the wave system while experiencing flying conditions of extreme smoothness.

Mountain waves are probably the major reason for turbulence in the stratosphere.

A rotor zone (which is not the same as 'rotor streaming', in 6.1.3(c)) may generate violent turbulence over a limited area somewhat above and to the lee of a large mountain ridge with a well defined lee escarpment. Well developed lee waves will be present and the rotor may or may not be indicated by a long roll of ragged cumulus or stratocumulus parallel to the ridge. The 'Helm Bar' in Cumbria is a well known example.

6.1.5 *Clear Air Turbulence (CAT)*

Although this term can refer to any turbulence not associated with cloud, it is usually applied only to medium- and high-level disturbances.

Typical dimensions of CAT regions are:

Horizontally:	80-500 km along the wind direction, but only 20–100 km across the wind flow.
Vertically:	500–1000 m, but they may be as shallow as 25 m, or as deep as 4500 m near mountains.

Mean duration of CAT encounters experienced by jet transport aircraft in flight:

Light	16 minutes
Moderate	11 minutes
Severe	7 minutes

6.1.6 *Synoptic indicators of CAT*

(a) *Marked wind shear*

Both vertical and horizontal wind shears are important for the physical generation of the turbulent eddies that cause turbulence, and stability (or instability) of the air suppresses (or enhances) the effect. The Richardson Number (*Ri*), which expresses the relative magnitude of the vertical wind shear to the stability, is used in theoretical calculations. Turbulence is likely if *Ri* is less than 0.5, and certain if *Ri* is less than 0.15.

(b) *Jet streams*

About 60% of CAT reports are near jet streams. The most probable regions are:

(i) on the cold side, near and below the core,
(ii) on the warm side, above the core,
(iii) near exits with marked curvature and diffluence,
(iv) at a confluence or diffluence of two jet streams,
(v) near sharp upper troughs,
(vi) around sharp ridges on the warm side of jets,
(vii) where one jet undercuts another, and
(viii) where the tropopause height fluctuates.

(c) *Curved flow*

(i) In areas of anticyclonic curvature, where the actual wind speed approaches the critical value of twice the geostrophic wind speed.
(ii) Within 150 n mile or so of the axis of a sharp upper trough where the wind shift is over 90°.
(iii) Occasionally, across shear lines in cols where the wind direction reverses rapidly.

(d) *Topography*

CAT is reported twice as often over land as over the sea, and four times as often over mountains as over flat land.

6.1.7 *Subjective prediction of CAT*

Useful empirical rules are:

Horizontal wind shear
If shear = 20 kn/deg. of latitude, forecast moderate CAT
If shear = 30 kn/deg. of latitude, forecast severe CAT

Vertical wind shear
If shear = 6 kn/1000 ft, forecast moderate CAT
If shear = 9 kn/1000 ft, forecast severe CAT

Jet stream

If the core speed exceeds 100 kn, and vertical wind shear 4 kn/1000 ft, forecast moderate CATwithin 150 n mile.

6.2 Ice Accretion

6.2.1 *Types of icing*

Type	Source	Formation and properties
Hoar frost	Vapour	Direct deposition on surface with temperature below frost-point of ambient air. White crystalline coating.
Rime	Supercooled droplets	Impact on surface with temperature < 0 °C. Variable properties. Two extreme forms are: (a) *Opaque rime*: Drops freeze without much spreading; light porous texture with a lot of entrapped air. (b) *Clear, or glazed, ice*: Drops spread before freezing; smooth and glassy; sticks strongly to surface.
Rain ice	Supercooled	Formation similar to Clear ice. Substantial raindrops deposit may form over an extensive region. Rare in the United Kingdom.
Pack snow	Supercooled drops and snowflakes	Drops freeze on impact, embedding the snow flakes.

6.2.2 *Airframe icing*

This may form on the leading edges of wings, tailplanes and any obstructions to airflow, such as air scoops and antennae.

Potentially dangerous effects are:

(a) ice may alter the wing profile, reducing the available lift,

(b) engine intakes may be blocked, causing loss of power,

(c) weight of ice may overload the aircraft, and

(d) forward facing windows may be made opaque.

There are additional risks for helicopters:

(e) Ice on rotating blades is especially dangerous, as they are more heavily loaded than a fixed aircraft wing. Uneven ice accretion, compounding the centrifugal loads, may cause severe vibration.

(f) Cyclic pitch controls may become jammed, causing loss of control.

6.2.3 *Intensity of ice accretion*

Terms used to describe ice accretion are defined as follows:

Trace of icing	Perceptible icing; rate of accumulation slightly greater than that of sublimation. Not hazardous, even though anti-icing equipment is not used (unless encountered for more than 1 hour).
Light icing	Accumulation rate may create a problem if flight in this environment exceeds 1 hour. Occasional use of anti-icing equipment prevents accumulation.
Moderate icing	Rate of accumulation is such that even short encounters are potentially hazardous. Anti-icing equipment must be used.
Severe icing	Rate of accumulation is such that use of anti-icing equipment fails to reduce or control the hazard. Immediate diversion from the region is necessary.

6.2.4 *Icing and liquid water content*

The intensity of icing in clouds depends on their supercooled liquid water content.

Supercooled liquid water content	Icing
< 0.5 g m^{-3}	Light
0.5–1.0 g m^{-3}	Moderate
> 1.0 g m^{-3}	Severe

6.2.5 *Estimating the maximum liquid water content of a cloud*

On a tephigram:

(a) Plot the pressure and temperature at cloud base.

(b) Ascend along a saturated adiabat to the cloud-top level.

(c) The difference in HMR between the base and top of the cloud gives the maximum (adiabatic) liquid water content of the cloud, in units of g kg^{-1}.

Since at 800 hPa (a typical wet-cloud level) 1 kg of air occupies about 1 m^{-3}, the number obtained in (c) may simply be relabelled in units of g m^{-3}, which is a more useful measure of liquid water content for practical measurement.

Modifying factors:

(a) Mixing with dry air at cloud-top may reduce the actual cloud water content to around half the theoretical maximum value. Maximum values are only approached in a tiny fraction of the cloud volume.

(b) Upward motion of the cloudy air increases the water content and the risk of icing at any level. Strong upcurrents in convective clouds produce the most severe icing, but orographic and frontal upslope motions may also produce severe ice accretion at times.

6.2.6 *Icing and cloud type*

Cloud type	Probability of icing	Intensity	Water content g m^{-3}
Cu,Cb,Ns	High	May be severe	0.2–4.0
Sc,Ac,AcAs	50%	Rarely more than moderate	0.1–0.5
As	Low	Moderate or light	0.1–0.3
St	Low	Light	0.1–0.5

Liquid water content increases from zero at just below cloud base roughly linearly for the first 200–300 m above cloud base. In this region there is little or no icing, unless there is orographic uplift or embedded convective cloud.

The risk of icing increases above the lowest 300 m of the cloud. Even in layer cloud, such as anticyclonic stratocumulus forming over the sea in winter, the icing in the upper part of the cloud may be severe. This is partly due to the high liquid water content (0.5–1 g m^{-3}) and partly due to the large horizontal extent.

6.2.7 *Cloud temperature and icing risk*

Cloud temperature °C	Nature of cloud particles		Icing risk
	Supercooled water	Ice crystals	
0 to −20	many	few	High
−20 to −40	few	many	Low (but High in Cb cells)
< −40	nil	all	nil

Fig. 6.1 illustrates the icing to be expected in convective clouds under various cloud-base temperature conditions.

6.2.8 *Icing on ships*

In rough seas when the wind is strong and the air temperature below −2 °C, spray may freeze on the superstructure of a vessel. The weight of accumulated ice may eventually become a considerable hazard.

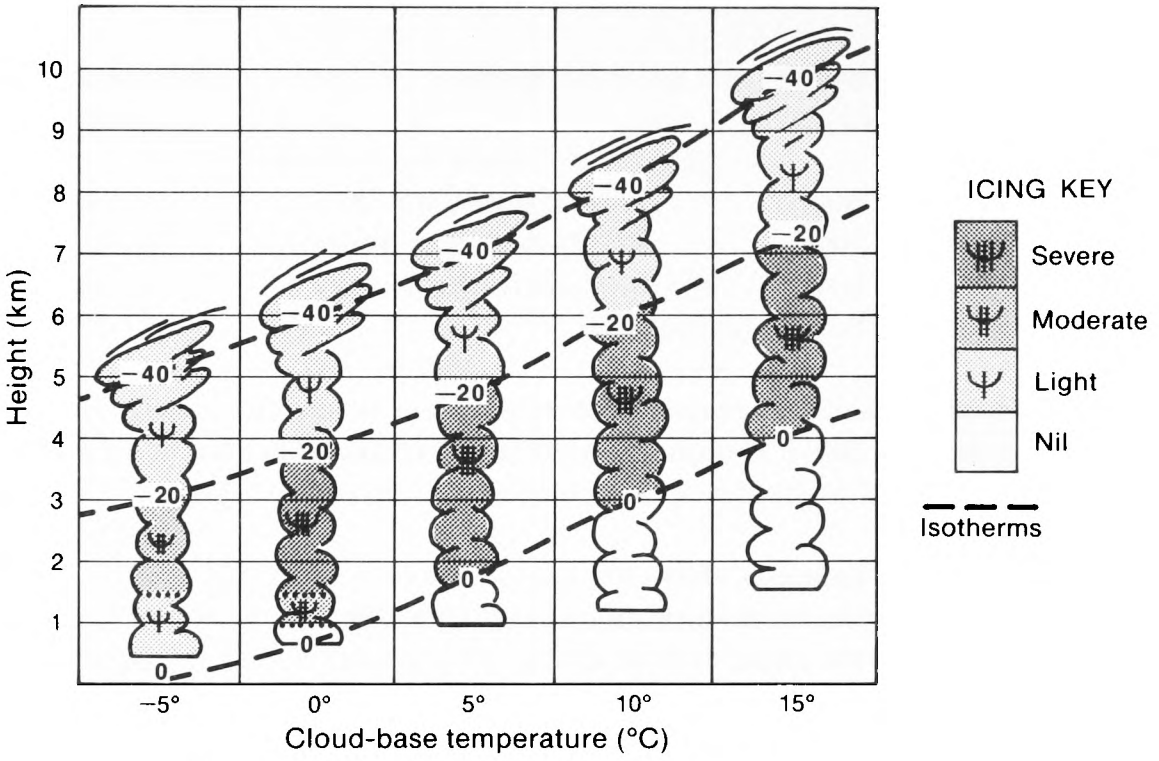

Figure 6.1 Approximate layers of icing in convective clouds.

The degree of icing depends on both temperature and wind speed, as shown in Fig. 6.2. The icing is classified in terms of thickness of accumulation per day:

Degree of icing	Accumulation (cm per 24 hours)
Light	1–3
Moderate	4–6
Severe	7–14
Very severe	15 or more

6.3 Condensation trails

6.3.1 *General*

The condensation of water vapour from the exhaust of any aircraft engine can produce long and persistent trails (contrails) if the ambient air temperature is below a critical value.

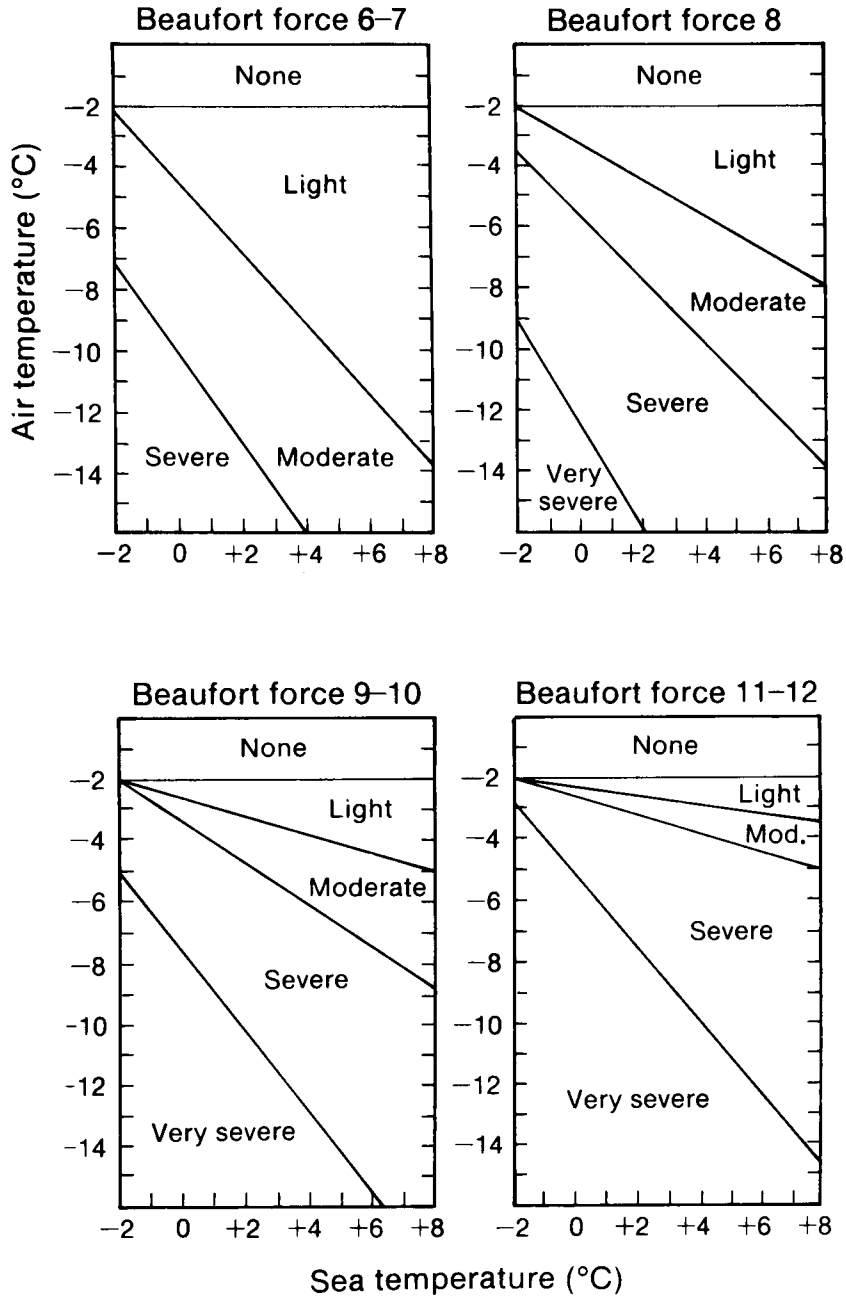

Figure 6.2 Icing on slow-moving fishing vessels in various wind conditions.

The MINTRA line printed on tephigrams gives the critical temperatures for an old piston-engined aircraft (the Spitfire), based on condensation with respect to ice. The continuing usefulness of this line lies in the fact that it represents the limiting temperature above which contrails are unlikely to be formed by any aircraft. In practice, contrails do not normally appear until the ambient temperature is several degrees lower than the printed MINTRA value.

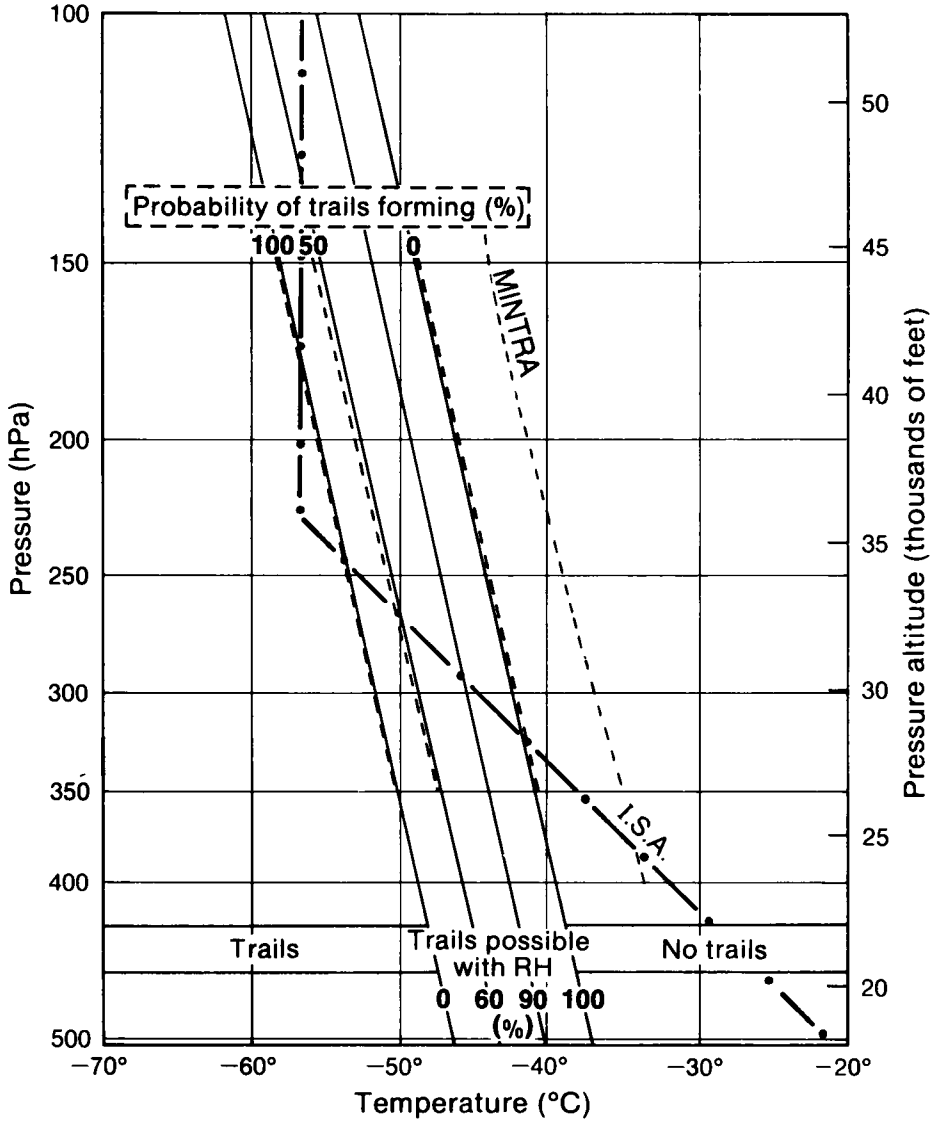

Figure 6.3 Contrail formation graph, indicating the probability of occurrence depending on the relative humidity (with respect to water) of the environment.

6.3.2 *Forecasting contrails*

(a) *Using corrections to the MINTRA value* (see Fig. 6.3)

On a tephigram, draw two lines that are, respectively, 11° and 14 °C colder than the MINTRA critical temperature (T_C) at any level. Plot a representative upper-air sounding. If the air temperature at any level is T, then :

		Forecast
If	$T > (T_C - 11)$	contrails unlikely
	$(T_C - 11) > T > (T_C - 14)$	short, non-persistent trails
	$T < (T_C - 14)$	long, persistent trails

Persistent trails are likely with high humidity and are common when aircraft fly near existing layers of cirriform cloud.

(b) *Graphical method*

Fig. 6.3 is Appleman's graph, which includes the effect of RH. Four lines are drawn to show the critical temperature for jet aircraft at different values of RH. Contrails should always form if the temperature lies to the left of the 0% RH line. No trails are to be expected if the temperature lies to the right of the 100% RH line.

6.3.3 *Probability of contrails*

In Fig. 6.3 the RH lines may be relabelled to give a practical indication of the probability that contrails will form. The 50% probability line lies just to the left of the 60% RH line.

6.4 Sea waves and swell

6.4.1 *Terminology*

Wind waves are the waves caused by the wind system being experienced at a given place and time.

Swell waves are the waves generated by a distant wind system.

Wavelength. The distance between successive wave crests (or troughs).

Period. The time between successive wave crests (or troughs).

Amplitude. The vertical distance between mean water level and wave crest.

Wave height (H). The vertical distance between a wave crest and the following trough.

Significant wave height (H_{sig}). The mean of the highest third of the waves in a wave train, over a period of 10–20 minutes. This happens to correspond to what is normally reported as the MEAN wave height.

Maximum wave height (H_{max}). The highest wave to be expected in every 100 consecutive waves. For wind waves it has been found that $H_{max} = 1.67\ H_{sig.}$

Fetch. The distance over which a given wind is blowing. Fetch limits the height which waves can attain.

Duration (D). The time during which a given wind persists. Waves take time to build but, for a given wind speed, D is not a relevant factor once a mature wave system is established.

6.4.2 *Forecasting wind-wave heights and periods*

(a) *For waves in deep water (WMO nomogram)*

Fig. 6.4 is an adaptation of a WMO nomogram which is suitable for forecasting in the Atlantic and in the northern and central parts of the North Sea.

For given values of the wind speed and the fetch, Fig. 6.4(a) may be used to forecast the Significant Wave Height and Fig. 6.4(b) the corresponding Wave Period.

The dashed lines indicate the duration in hours after which the waves will attain the computed state. If the duration is limited, the waves will not develop beyond the point given by the intersection of the wind speed and the duration on the graph.

(b) *For waves in shallow waters (Darbyshire–Draper graphs)*

Fig. 6.5 is suitable for forecasting waves in shallow coastal waters and in the southern North Sea. The layout and use of the graphs are the same as Fig. 6.4.

6.4.3 *Forecasting swell heights and periods*

The difficult task of forecasting in detail the range of wave heights and periods spreading out from a distant storm (which is both moving and developing in

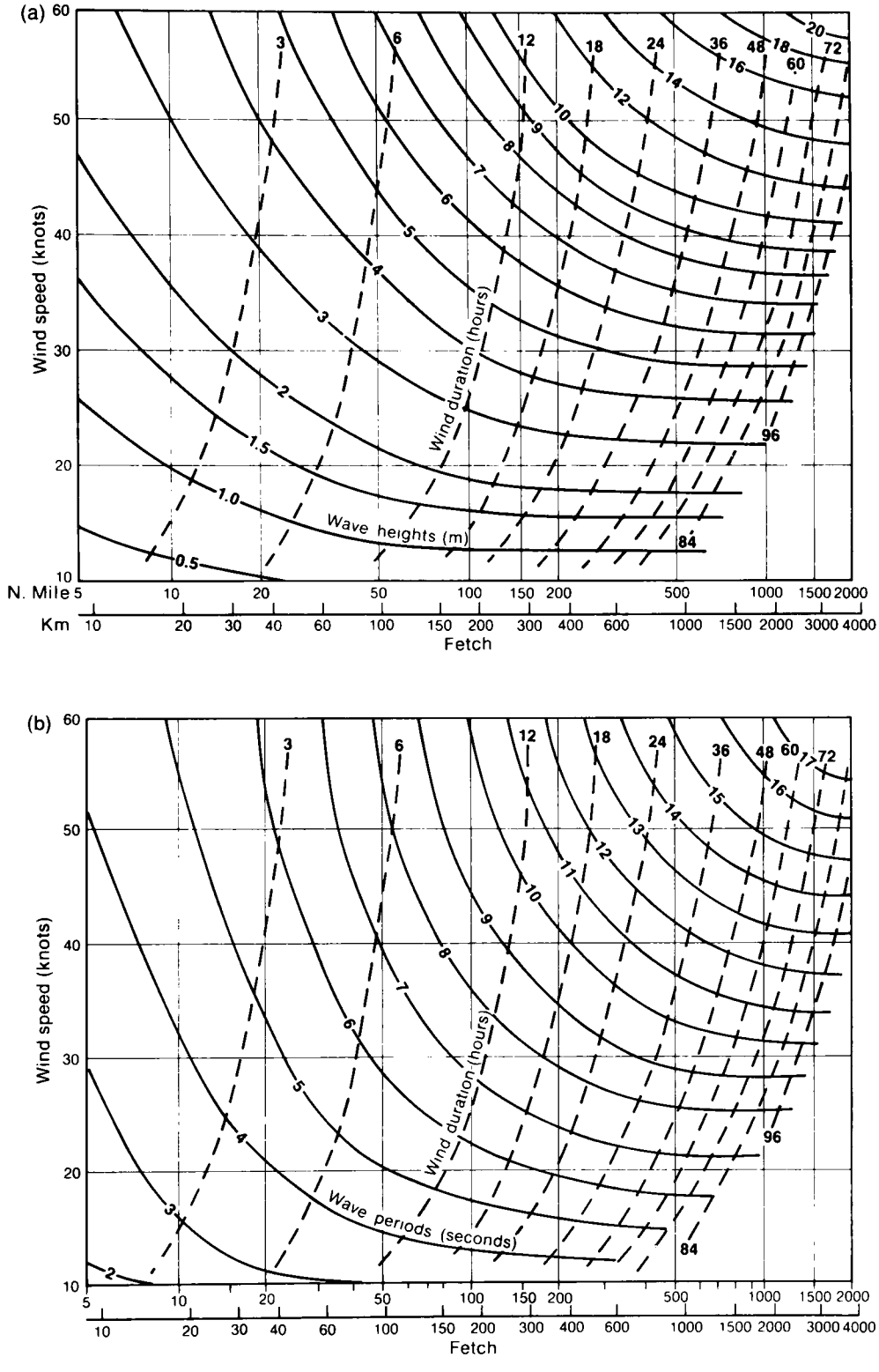

Figure 6.4 (a) Significant heights, and (b) periods, of deep-water waves (adapted from WMO nomograms).

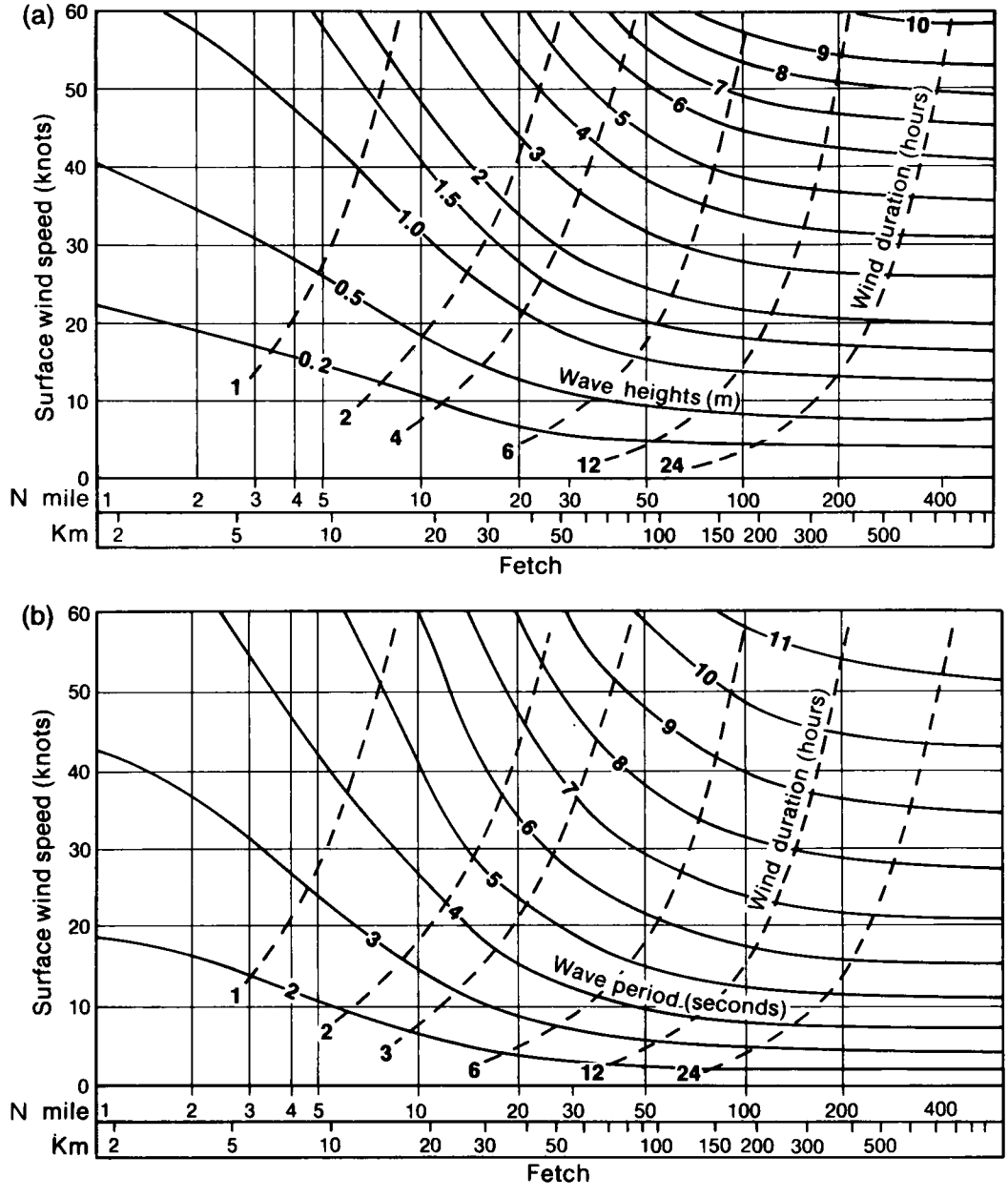

Figure 6.5 (a) Significant heights, and (b) periods, of shallow-water waves.

strength) is reduced by the practical limitations of the known data. These normally comprise little more than the distance of the storm, the maximum wave period generated in the storm area and the duration of wave generation in the direction from the storm to the forecast location.

The information that is required includes: (a) the arrival time of the first swell from the direction of the storm, (b) the height of the swell, and (c) the range of wave periods and wavelengths at any given time.

Fig. 6.6 (a graph due to Bretschneider) may be used for estimating some of the properties of the swell from a distant storm. The initial data are entered on the horizontal and vertical axes, and from their point of intersection estimates of the swell travel time, the ratio of the swell height to the initial wave-height, and the swell period can be read off.

6.4.4 *Forecasting wind waves and swell combined*

The height of the total sea generated by a combination of wind waves and swell is:

$$\sqrt{(\text{significant wave height})^2 + (\text{swell height})^2}.$$

Values may be obtained from the following Table

wind-wave height (w)

Swell heights (s)	2	4	6	8	10	12	14	16	18	20	22	24	26	28	30	32	34	36	38	40
	$\sqrt{(w^2 + s^2)}$																			
2	3	4	6	8	10	12	14	16	18	20	22	24	26	28	30	32	34	36	38	40
4	4	6	7	9	11	13	15	16	18	20	22	24	26	28	30	32	34	36	38	40
6	6	7	8	10	12	13	15	17	19	21	23	25	27	29	31	33	35	36	38	40
8	8	9	10	11	13	14	16	18	20	22	23	25	27	29	31	33	35	37	39	41
10	10	11	12	13	14	16	17	19	21	22	24	26	28	30	32	34	35	37	39	41
12	12	13	13	14	16	17	18	20	22	23	25	27	29	30	32	34	36	38	40	42
14	14	15	15	16	17	18	20	21	23	24	26	28	30	31	33	35	37	39	40	42
16	16	16	17	18	19	20	21	23	24	26	27	29	31	32	34	36	38	39	41	43
18	18	18	19	20	21	22	23	24	25	27	28	30	32	33	35	37	38	40	42	44
20	20	20	21	22	22	23	24	26	27	28	30	31	33	34	36	38	39	41	43	45
22	22	22	23	23	24	25	26	27	28	30	31	33	34	36	37	39	40	42	44	46
24	24	24	25	25	26	27	28	29	30	31	33	34	35	37	38	40	42	43	45	47
26	26	26	27	27	28	29	30	31	32	33	34	35	37	38	40	41	43	44	46	48
28	28	28	29	29	30	30	31	32	33	34	36	37	38	40	41	43	44	46	47	49
30	30	30	31	31	32	32	33	34	35	36	37	38	40	41	42	44	45	47	48	50
32	32	32	33	33	34	34	35	36	37	38	39	40	41	43	44	45	47	48	50	51
34	34	34	35	35	35	36	37	38	38	39	40	42	43	44	45	47	48	50	51	52
36	36	36	36	37	37	38	39	39	40	41	42	43	44	46	47	48	50	51	52	54
38	38	38	38	39	39	40	40	41	42	43	44	45	46	47	48	50	51	52	54	55
40	40	40	40	41	41	42	42	43	44	45	46	47	48	49	50	51	52	54	55	57

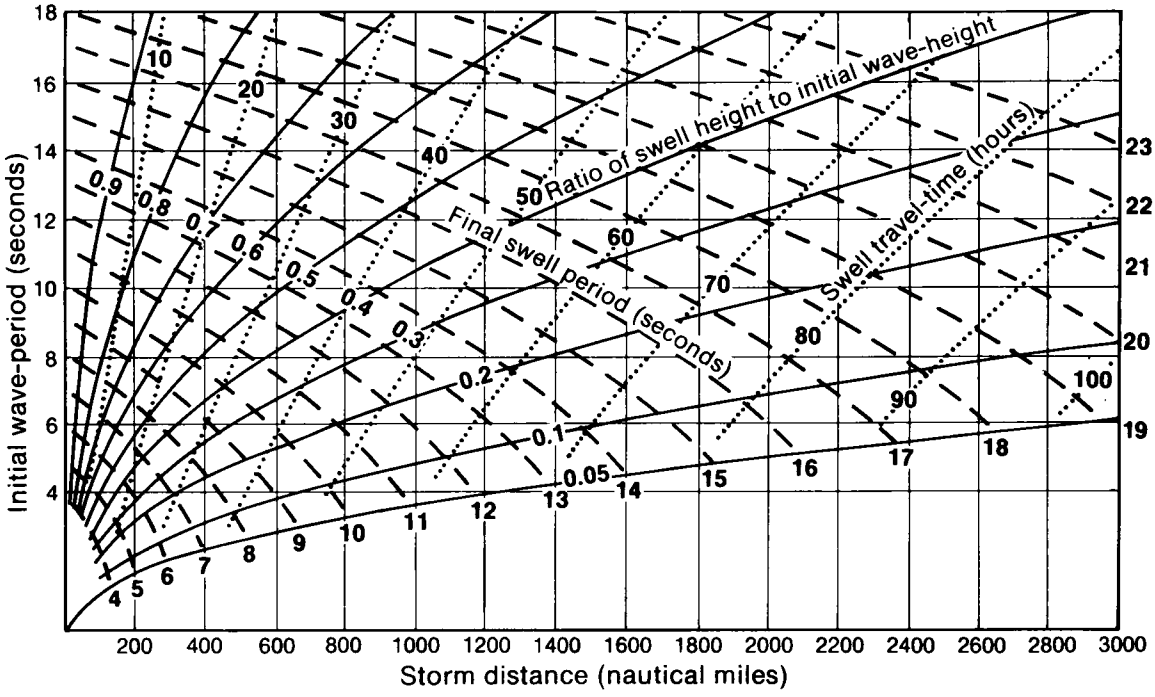

Figure 6.6 Forecasting swell height.

6.4.5 *Forecasting maximum waves*

(a) *For wind waves*

The most likely maximum wave height is 1.67 × the significant wave height. Fig. 6.7 gives the maximum wave height corresponding to a given value of the significant wave height.

(b) *For swell*

Swell height only varies a little, and for practical forecasting it may be considered as constant.

(c) *For wind waves and swell combined*

The maximum wave in a combined sea with wind waves and swell is

$$\sqrt{(\text{maximum wind wave})^2 + (\text{swell})^2}$$

The Table in section 6.4.4 can be used to evaluate the likely maximum of the combined sea, if w is taken as the maximum wind wave.

(d) *Extreme waves*

When gales persist for long periods and the fetch is long, the 'maximum' wave height may be exceeded. Fig. 6.7 gives an estimate of the 'extreme' waves which may be generated under these conditions.

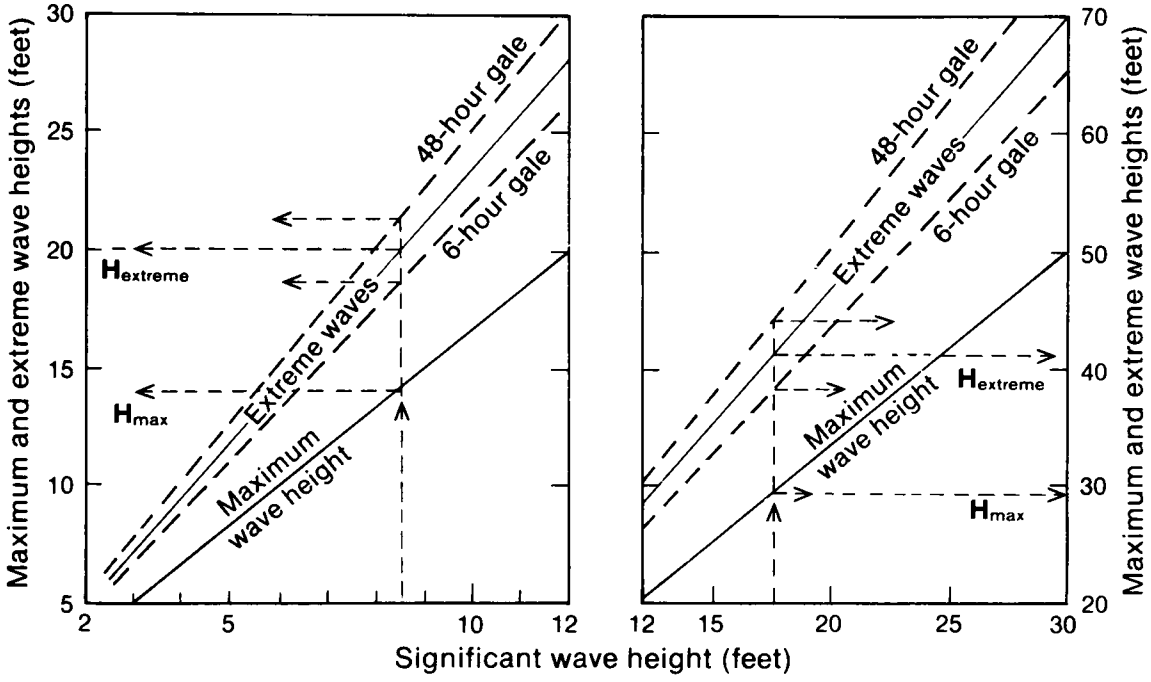

Figure 6.7 Forecasting maximum wave heights and extreme waves.

CHAPTER 7 — ANALYSIS OF METEOROLOGICAL DATA

7.1 Useful concepts

7.1.1 *Thermal winds*

The *thermal wind* in the layer between two pressure levels (see Fig. 7.1) is the vector difference between the geostrophic winds at the two levels.

$$V_{\text{thermal}} = V_A - V_B$$

or,
$$V_A = V_B + V_{\text{thermal}}.$$

A geostrophic wind is proportional to the contour height gradient at a pressure level. So a thermal wind measures the difference in the contour gradient at the two pressure levels. This is related to the horizontal temperature gradient in the layer.

A strong temperature gradient from north to south (see Fig. 7.8) implies a strong westerly thermal wind, and westerly winds increasing with height in the layer. A reversed temperature pattern gives easterly thermal winds, and westerly winds decreasing with height.

Although the thermal wind is geostrophic, practical computations use the difference between the actual winds at two levels. This is acceptably accurate.

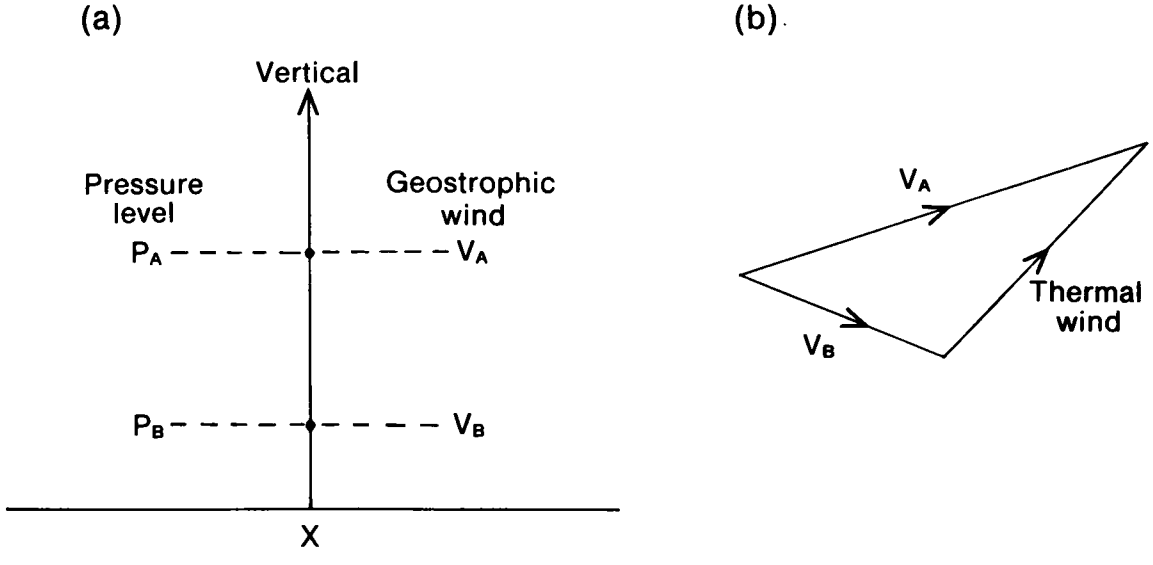

Figure 7.1 (a) Geostrophic winds at two levels above the point X, and (b) the associated vector diagram to determine the thermal wind.

7.1.2 *The vertical structure of pressure systems*

In **barotropic** regions of the atmosphere:

temperature is constant on any pressure level,
the thickness between any two pressure levels is constant, and
thermal winds are zero.

Lows and highs which remain in the same area for many days, cut off from the influences of other weather systems, may become barotropic. Wind flow patterns at all levels are identical, and are aligned vertically. Such systems are very slow moving, uniform in structure and lacking in any active development.

In **baroclinic** regions of the atmosphere, such as most of the temperate latitudes:

temperature gradients occur on surfaces of constant pressure,
thickness gradients and thermal winds may be large,
winds change with height, in speed and direction, and
wind flow patterns at different levels are not the same.

Baroclinic regions are areas of active development, and wind flow patterns at different levels are not the same. Surface lows are associated with upper-level troughs. The trough line is not vertically above the surface low but displaced increasingly with height towards the region of coldest air. Upper ridges are similarly displaced from surface anticyclones, as shown in Fig. 7.2.

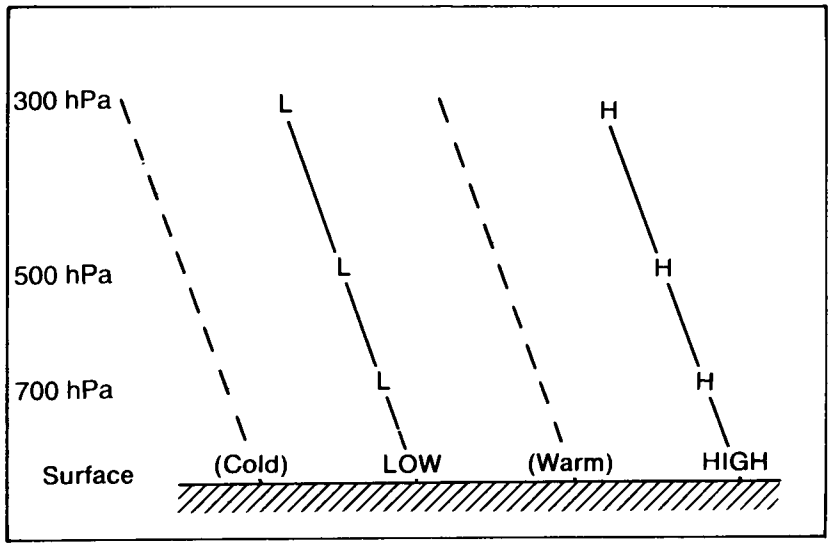

Figure 7.2 The slopes of trough (L–L) and ridge (H–H) axes with height.

7.1.3 *Ageostrophic winds*

An actual, observed wind may be considered to have two components, one of which is geostrophic and the other ageostrophic (non-geostrophic).

The direction of the geostrophic component (OG in Fig. 7.3) is parallel to the isobars (contours) but both the actual wind (OA) and the ageostrophic component (GA) generally have a cross–isobar (cross–contour) direction. (The special case of gradient wind flow is an exception to this: see section 7.1.4.)

Geostrophic winds are in exact balance with the existing pattern of isobars (contours), and cannot bring about changes in that pattern. All 'development' is the result of ageostrophic motions.

In regions where the isobars (contours) can be analysed with some confidence, the existence of ageostrophic motion is most easily recognized where the observed wind has a cross–isobar, or cross–contour, flow. The greater the magnitude of this flow, the greater the developments that follow.

7.1.4 *Trough–ridge pattern*

Contour patterns provide a convenient picture of the upper-level wind flow at a fixed time. The complexity of real situations can be simplified by considering the two basic patterns in this and the following section.

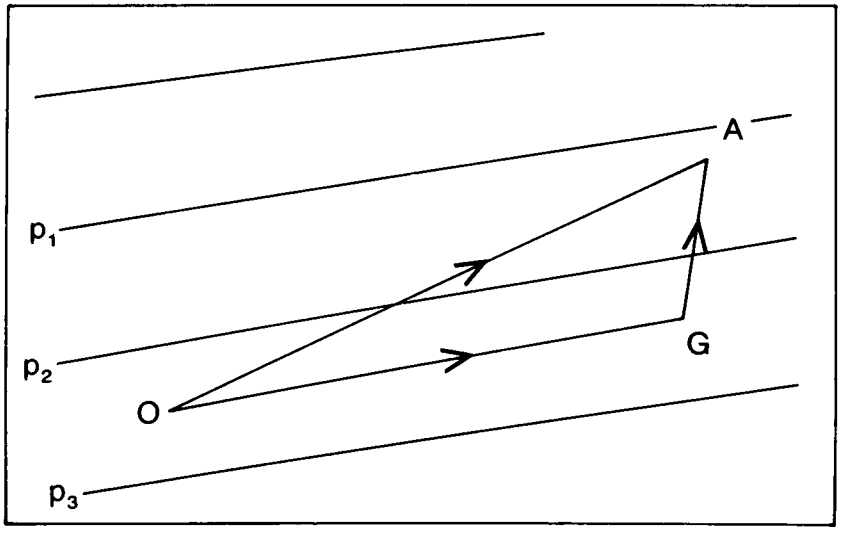

Figure 7.3 Vector diagram in which OA represents an observed wind, and OG and GA are, respectively, the geostrophic and ageostrophic components of OA.

Fig. 7.4 shows a symmetrical *trough–ridge* pattern with a uniform contour spacing. The geostrophic wind (V_g) is everywhere the same. The short-dashed contours are curved cyclonically, and in these regions the actual wind (equal to the 'gradient wind') is less than V_g, and the ageostrophic component opposes V_g. Similarly, anticyclonic curvature of the contours (shown by long dashes) gives an ageostrophic component in the same direction as V_g.

These ageostrophic motions lead to an accumulation of air as it moves through the pattern from the ridge to the trough, and a depletion of air as it moves from the trough to the ridge.

In association with the simple atmospheric model described in section 7.1.6, this upper-level pattern is associated in the lower atmosphere with 'cyclonic developments ahead of the trough' and 'anticyclonic developments ahead of the ridge'.

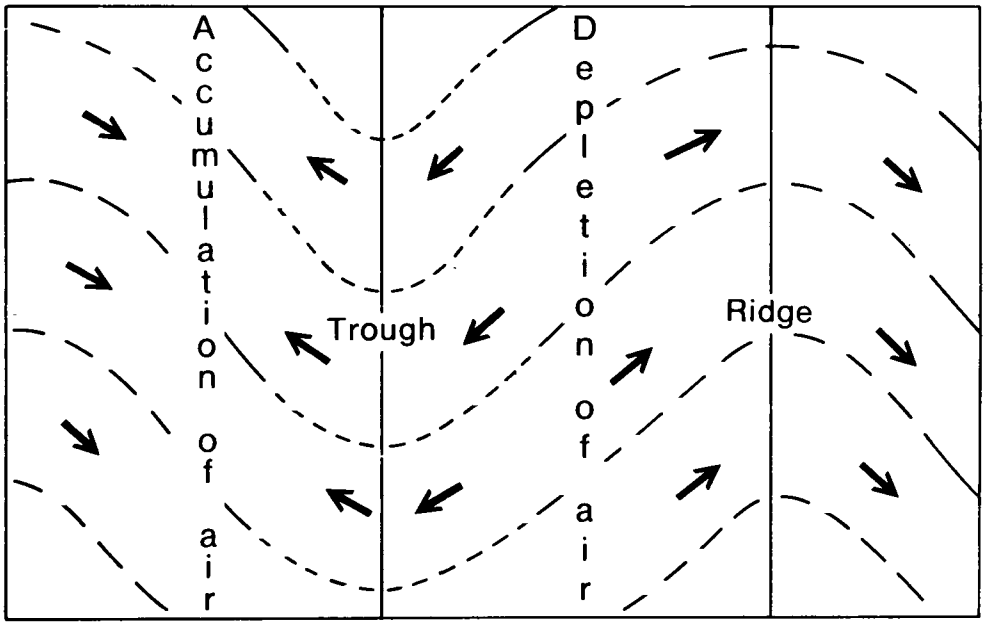

Figure 7.4 Trough-ridge pattern with uniform contour gradient and air flow from left to right. The arrows show ageostrophic wind components.

7.1.5 *Jet-stream pattern*

Fig. 7.5 shows a high-level *jet-stream* pattern with no curvature. Air flowing through this pattern accelerates into the confluent entrance and decelerates out from the diffluent exit.

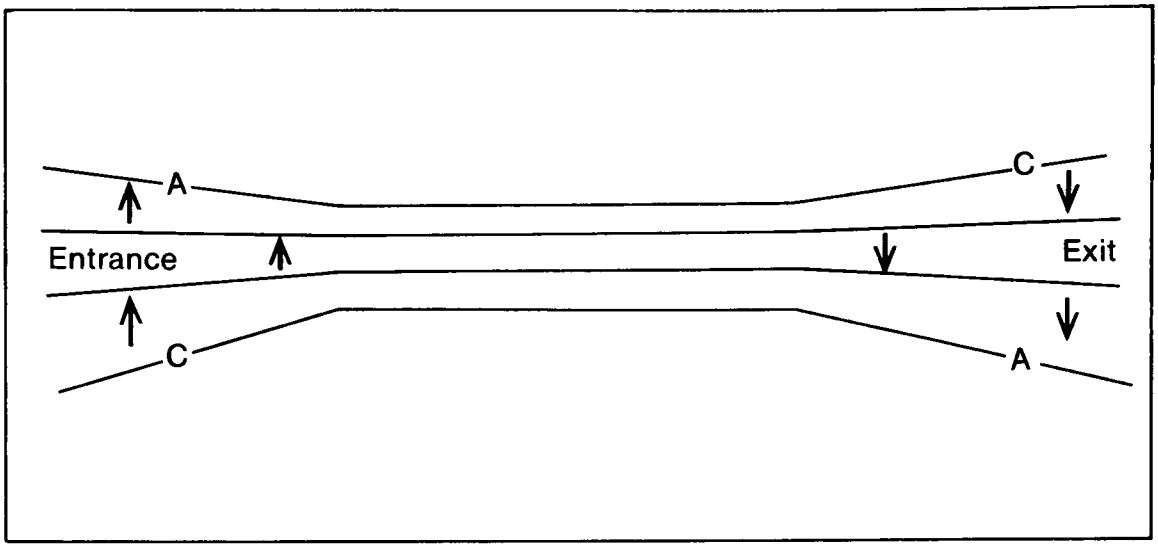

Figure 7.5 Jet-stream pattern with no curvature and air flow from left right. Arrows show ageostrophic wind components.

The accelerations produce ageostrophic flows across the contours in the entrance and exit regions. At the entrance the cross-contour flow is from high to low values, and at the exit it is from low to high. Two regions of accumulating air and two regions of depletion of air result, leading to the surface development areas shown in Fig. 7.5. See also 8.3.2.

7.1.6 *Two-layer model of atmospheric divergence and vertical motion*

Fig. 7.6 shows the concept of a two-layer structure of the temperate latitude troposphere during the active development of surface pressure systems.

The level of non-divergence separates the troposphere into two layers. The sign of the divergence is different in each, with the magnitude being greater in the upper layer. Thus, high-level divergence greater than low-level convergence leads to surface 'cyclonic development'.

Vertical motion is zero at the top and bottom of the model, and is a maximum at the level of non-divergence.

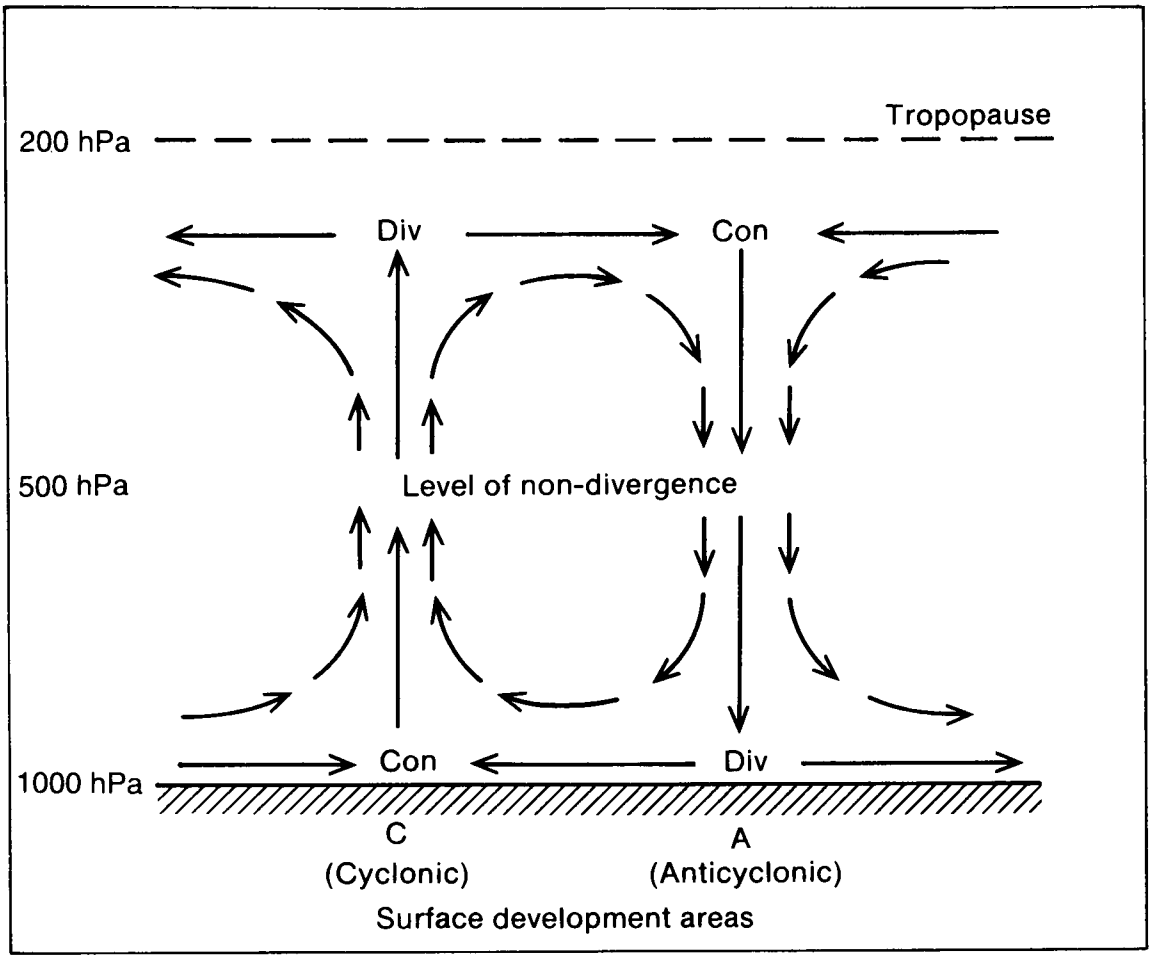

Figure 7.6 Two-layer model of the troposphere.

7.2 Broad-scale features of the troposphere

7.2.1 *Temperature distribution*

Fig. 7.7 shows winter and summer maps of the mean 1000–500 hPa thickness over part of the northern hemisphere.

Thickness gradients are stronger in winter than in summer. In both seasons the tropics are regions of more uniform thickness than the mid-latitudes, where the strong temperature contrasts are located.

Fig. 7.8 shows an example of a temperature cross-section, typical of the area near the British Isles.

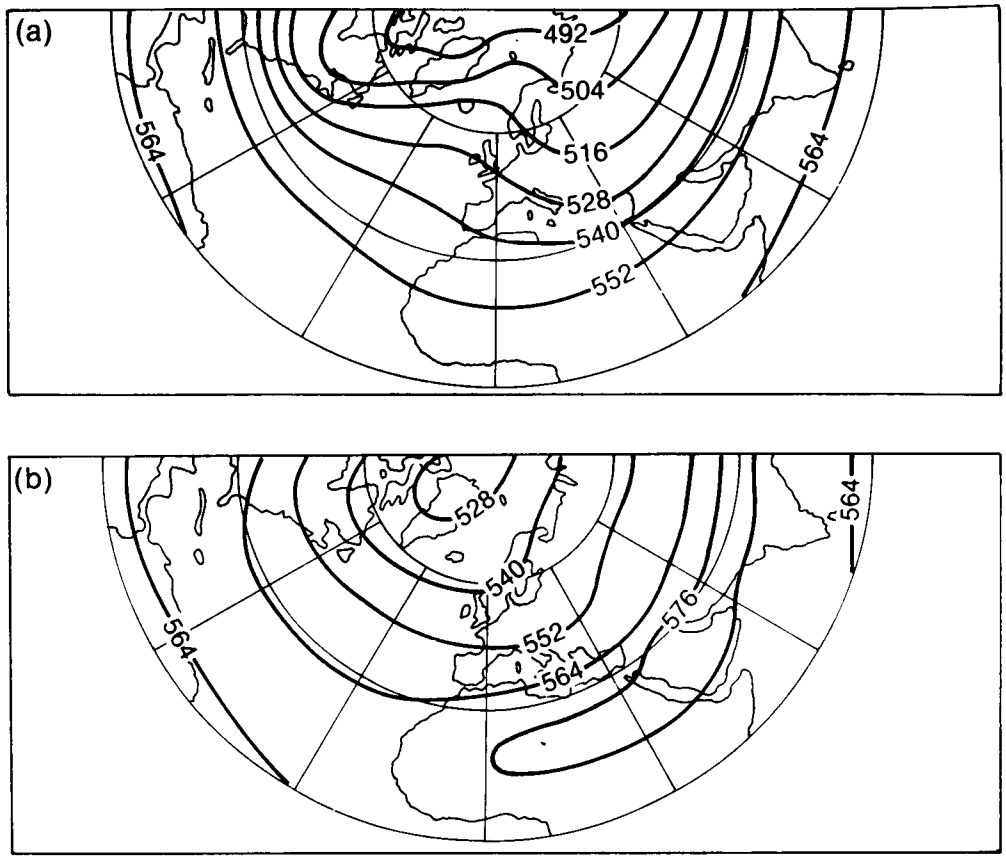

Figure 7.7 Mean 1000–500 hPa thickness values (dam) for (a) January, and (b) July.

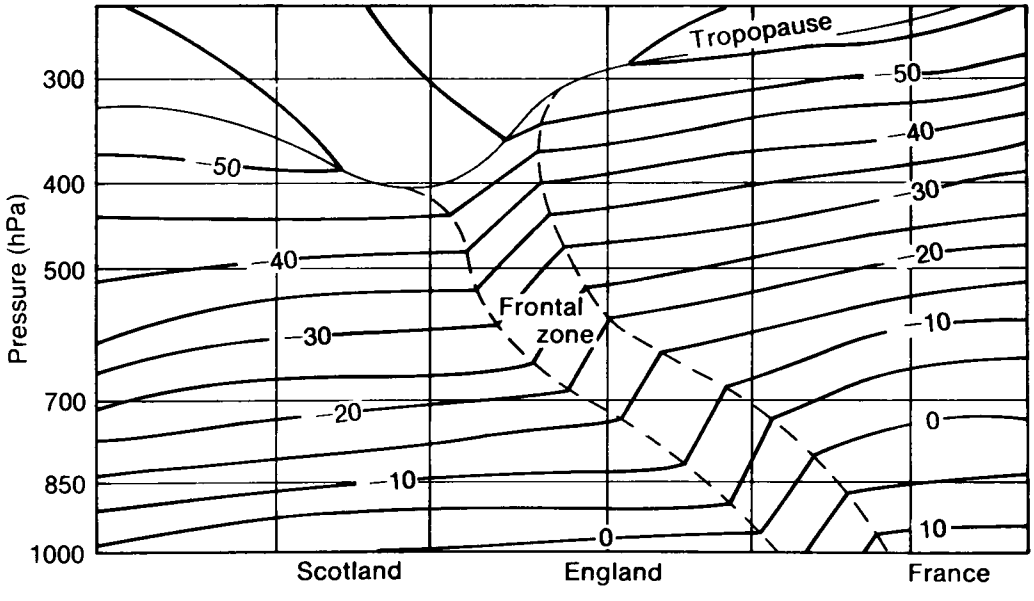

Figure 7.8 North–south cross-section of temperature (°C) through a front near the British Isles.

Temperature decreases with height in the troposphere. Isotherms slope upwards from north to south, particularly in the frontal zone. The large vertical temperature gradients in the cold and warm air masses indicate unstable air. In contrast, the more stable air in the frontal zone has only a small vertical temperature gradient, and the stratosphere has isothermal or inversion conditions.

7.2.2 *Potential temperature distribution*

Fig. 7.9 shows a cross-sections of potential temperatures for the same occasion as that of Fig. 7.8.

The isentropes of potential temperature (θ) are useful for tracking the broad-scale path of air particles. In the troposphere they slope downwards from north to south, indicating subsidence in southward moving air masses, and ascent in northward moving ones.

θ values increase with height. In the unstable, cold air the gradient of θ is small; it is rather larger in the more stable warm air, and even more pronounced in vertical sections through the frontal zone. Above the tropopause, θ increases very rapidly.

Above 700 hPa, the pattern of the isentropes of wet-bulb potential temperature (θ_w) differs little from the θ pattern, as the moisture content of the air is small.

In the lowest layers, air with high moisture content is producing:

(a) uniform θ_w with height in the warm air mass (saturated adiabatic lapse rate).

(b) decreasing θ_w with height (potential instability) at the bottom of the cold air mass,

(c) a pronounced gradient of θ_w near the surface cold front.

All of these are valuable analysis tools.

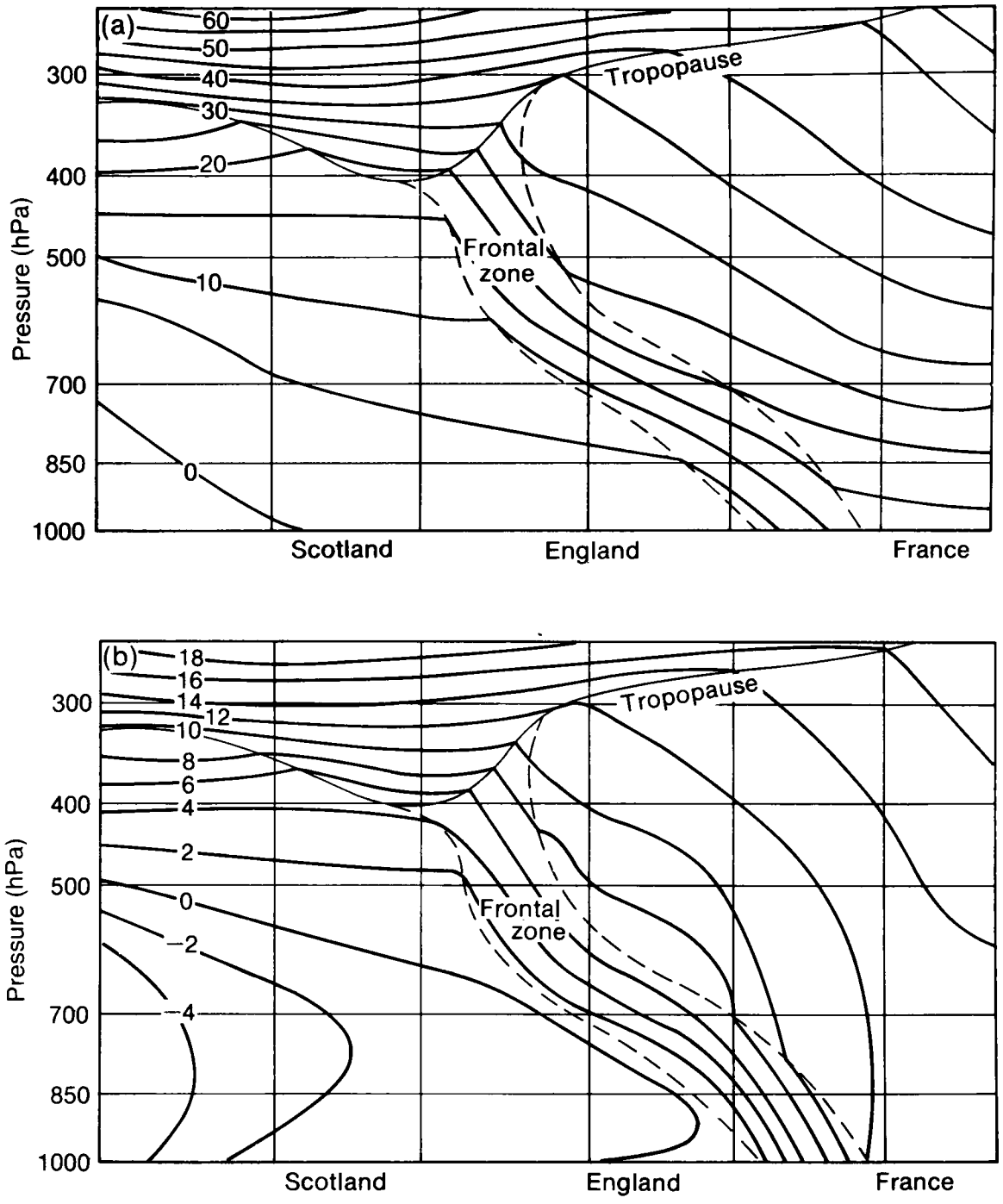

Figure 7.9 North–south cross-section through a front near the British Isles of (a) potential temperature (θ), and (b) wet-bulb potential temperature (θ_w).

7.2.3 *Airflow concepts — conveyor belts*

Synoptic charts do not represent the flow of individual air parcels.

Air parcels have a motion relative to moving pressure systems. Fast-moving air at high levels overtakes and moves through the system, while the slower-moving low-level air is overtaken by the system as it moves.

Airflow relative to a moving system (such as a front, or a storm cloud) is deduced by subtracting the system velocity from the observed winds, and assuming that the air flows along constant θ surfaces.

Fig. 7.10 is a sketch of the common airflows, relative to the fronts of a mobile depression. They are:

(a) The warm conveyor belt (WCB), shown stippled, ascending from low levels in the warm sector to medium/high levels ahead of the warm front. This is the principal airflow, and has a clearly defined polar side, marking the cold front.

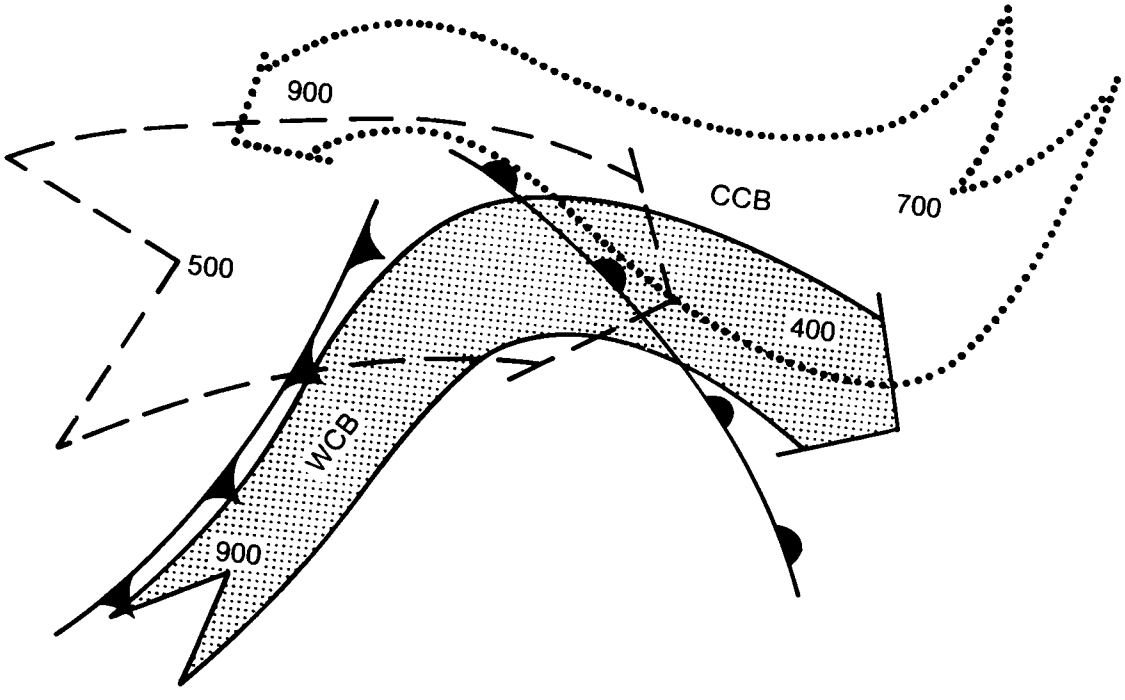

Figure 7.10 Common airflows, at heights shown (hPa), relative to the fronts of a mobile depression. Warm conveyor belt (WCB) — ascending. Cold conveyor belt (CCB) and mid-level flow — descending.

(b) The cold conveyor belt, shown dotted, drawn into the circulation of the depression and descending to low levels, beneath the warm front.

(c) A flow of mid-tropospheric air, often subsiding slowly and dry, which enters the circulation at mid levels and overtakes the cold front.

7.3 Individual synoptic-scale weather systems

7.3.1 *Frontal zones*

Fig. 7.11 shows the distribution of some useful upper-air parameters near the end of the active development stage of a frontal depression.

(a) *1000–500 hPa thickness lines*

These are almost parallel to the surface warm and cold fronts, but cross the occlusion at an angle.

The main thickness gradient (baroclinic zone) is on the cold side of the surface cold-frontal position. The thickness gradient ahead of the warm front is weaker than that behind the cold front. In the warm sector the thickness is almost uniform.

(b) *850 hPa wet-bulb potential isotherms (isentropes)*

These are concentrated along the cold side of surface frontal positions. Isentropes lie parallel to surface fronts over long distances.

(c) *Jet-stream core*

Although the core is located in the warm air mass at high levels, its position falls on the cold side of the surface fronts when it is projected onto a surface chart.

Cross-sections through fronts are illustrated in Figs 7.8, 7.9 and 7.12.

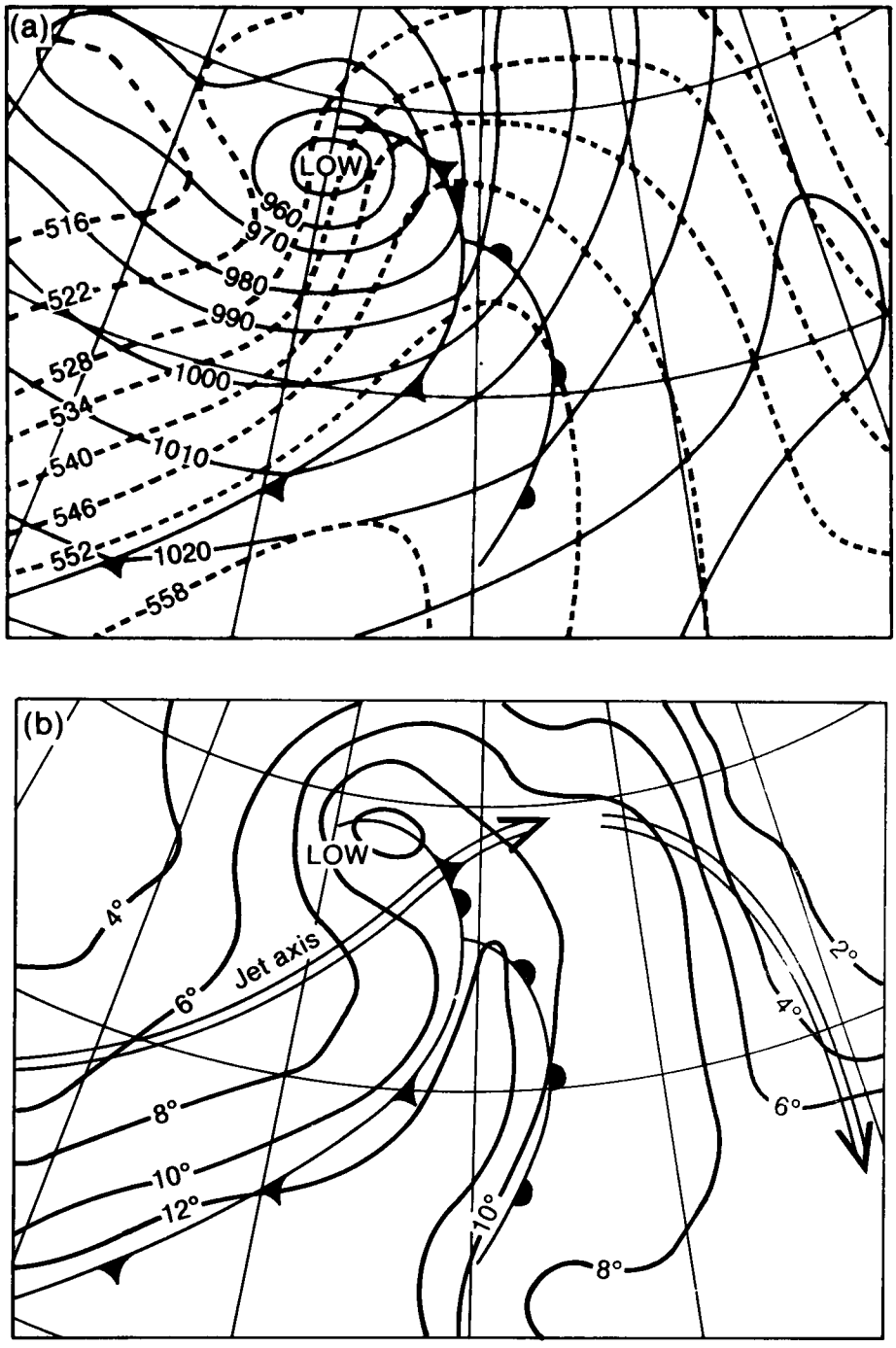

Figure 7.11 Surface fronts and associated fields on 10 January 1986, (a) mean-sea-level isobars (hPa) and 1000–500 hPa thickness lines (dam), and (b) 850 hPa wet-bulb potential temperature (°C) and 300 hPa jet axis.

7.3.2 *Jet-stream cross-section*

Fig. 7.12 is a cross-section through a typical jet-stream.

(a) Large vertical wind shears, above and below the core, generate turbulence. In this example, the vertical shear at Z is 30×10^{-3} s^{-1}, or about 20 kn/1000 ft.

(b) Horizontal wind shear is larger on the cold side than on the warm, where it is limited to the local value of f (Coriolis parameter). In this example, the local value of f is 0.1×10^{-3} s^{-1}. At X the horizontal shear is about $3f$, and at Y it is equal to f.

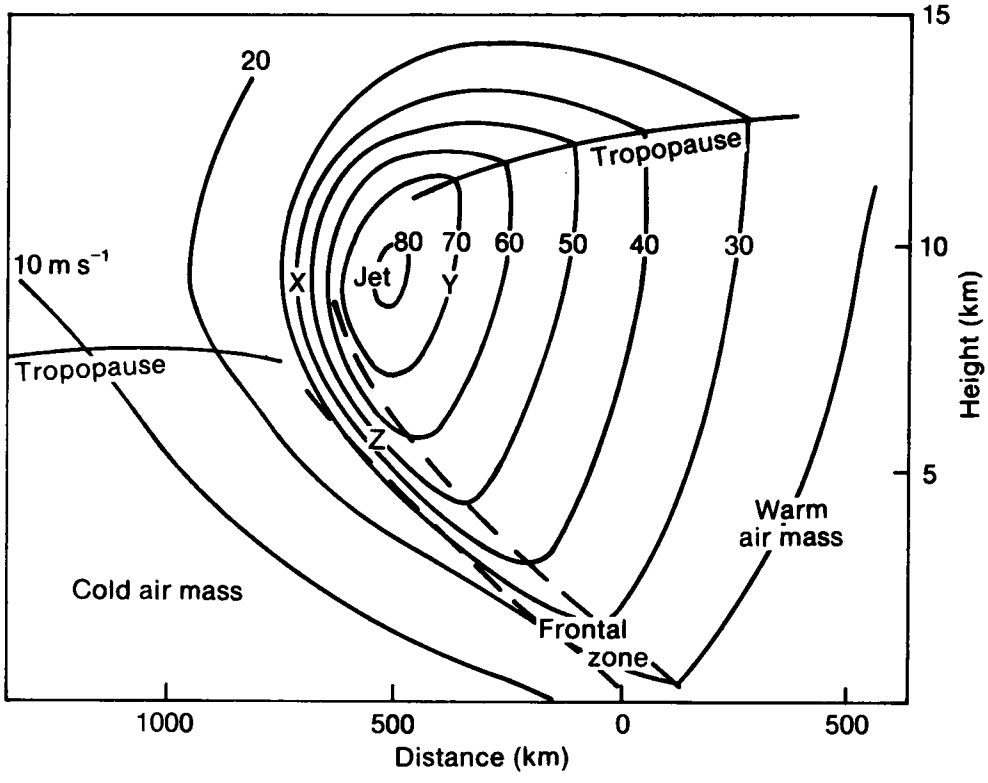

Figure 7.12 Cross-section through a typical jet stream. Winds 'blow' into the paper with speeds in metres per second. Vertical scale is 100 × horizontal.

7.3.3 *Cold-core and warm-core lows*

Fig. 7.13 shows the change of wind circulation with height in these two types.
Polar-front depressions are examples of cold-core systems.
Tropical hurricanes have warm cores.

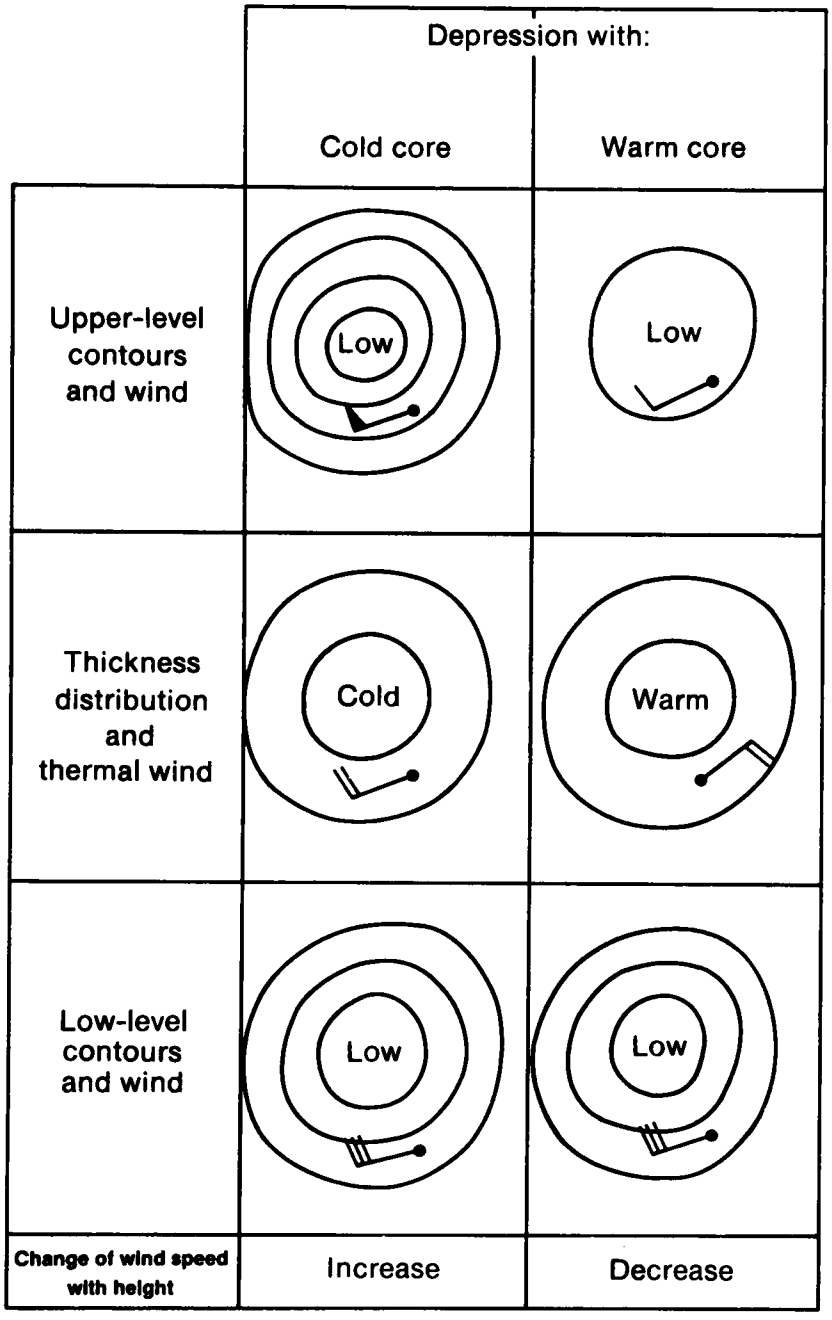

Figure 7.13 The circulation in cold-core and warm-core depressions.

7.3.4 *Anafronts and katafronts*

Warm fronts and cold fronts may have ana or kata characteristics depending on whether the warm air mass is rising up or subsiding down the frontal surface.

Anafronts are active, with deep clouds and rain. Katafronts have few upper clouds and little rain, but may be marked by low cloud and drizzle.

A front may change from ana to kata at some point along its length, or at some time during its life history.

7.3.5 *Airflow at cold fronts — rearward- and forward-sloping ascent*

Fig. 7.14 interprets an cold anafront in terms of the warm conveyor belt being undercut by the advancing cold front. Relative to the front, (a) the warm air ascends up a path which is directed towards the front. This is rearward sloping ascent. (b) Cloud and rain are formed, with line convection along the front. The axis of a low-level jet lies parallel to the surface front.

Fig. 7.15 shows the situation when (a) the warm conveyor belt is angled away from the surface cold front. Forward-sloping ascent occurs, with the main ascent and rain being carried forward over the warm sector (b), or even ahead of the warm front. This rain belt may be analysed as an upper front, and as it moves ahead of the surface cold front the system develops into a 'split front'. The surface cold front is a katafront and is slow moving, being overtaken by dry, mid-level air subsiding down the isentropes. Where θ_w decreases with height, potential instability is released.

7.4 Mesoscale organization of precipitation systems

7.4.1 *Frontal rain bands*

The term 'frontal rain band' is a convenient and simple way of describing (a) all forms of precipitation, including snow, and (b) the organization of precipitation associated **with** a front, rather than **at** a front. Sometimes a rain band may mark the position of a front, but on the mesoscale more than one, parallel, bands may occur. Not all rain bands are coincident with a front.

Fig. 7.16 sketches the usual orientation of relatively wide mesoscale bands associated with rearward-sloping ascent (anafront) and forward-sloping ascent (katafront) at a cold front. These bands are typically 50–100 km wide.

A single, very narrow band of heavy rain, known as 'line convection' may occur on a cold front with rearward-sloping ascent. The rain band is about 3 km wide, and falls from cloud of a similar depth. Line convection, which may be a

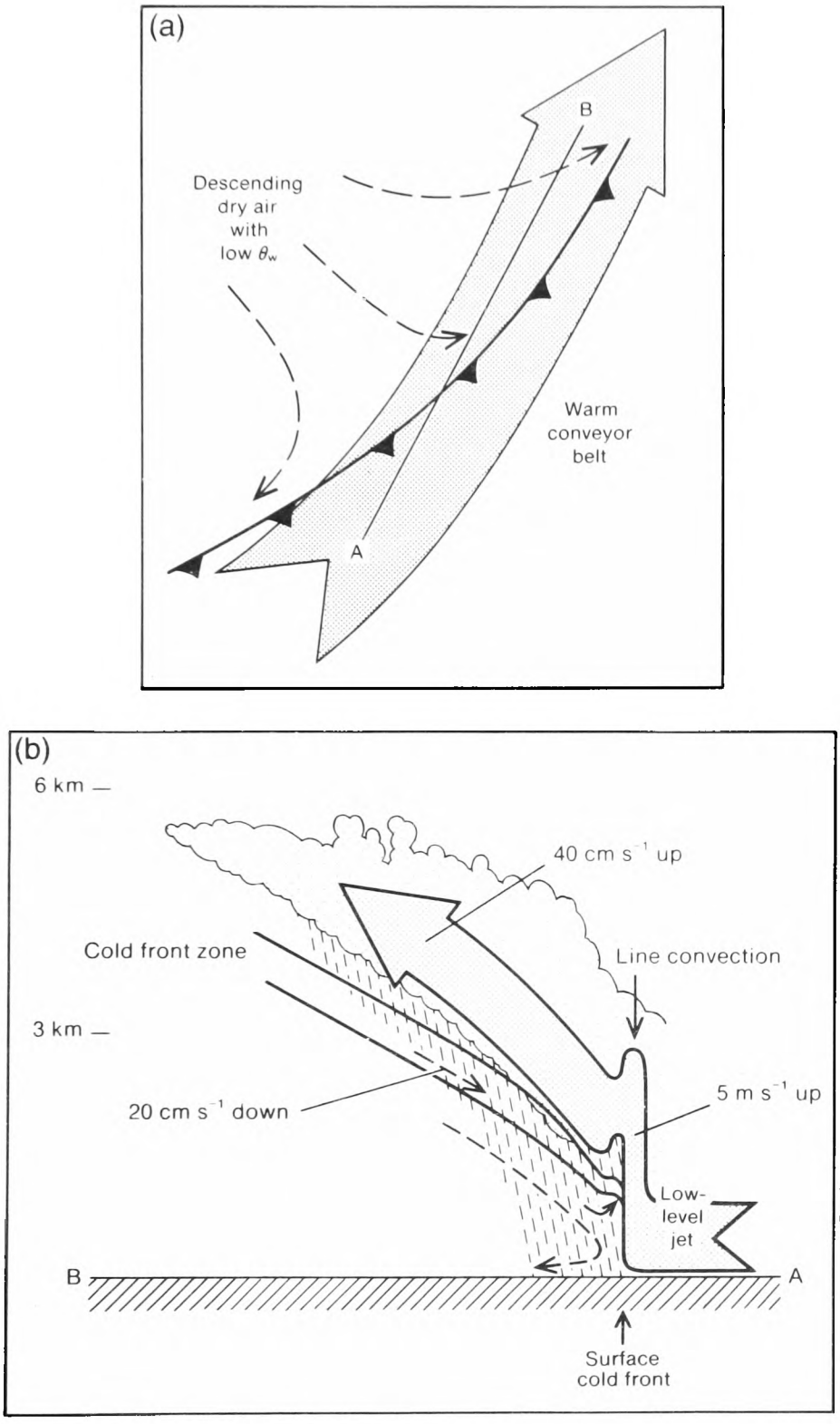

Figure 7.14 (a) Rearward-sloping ascent of the warm air relative to a cold anafront. (b) Plan view and cross-section along a line AB.

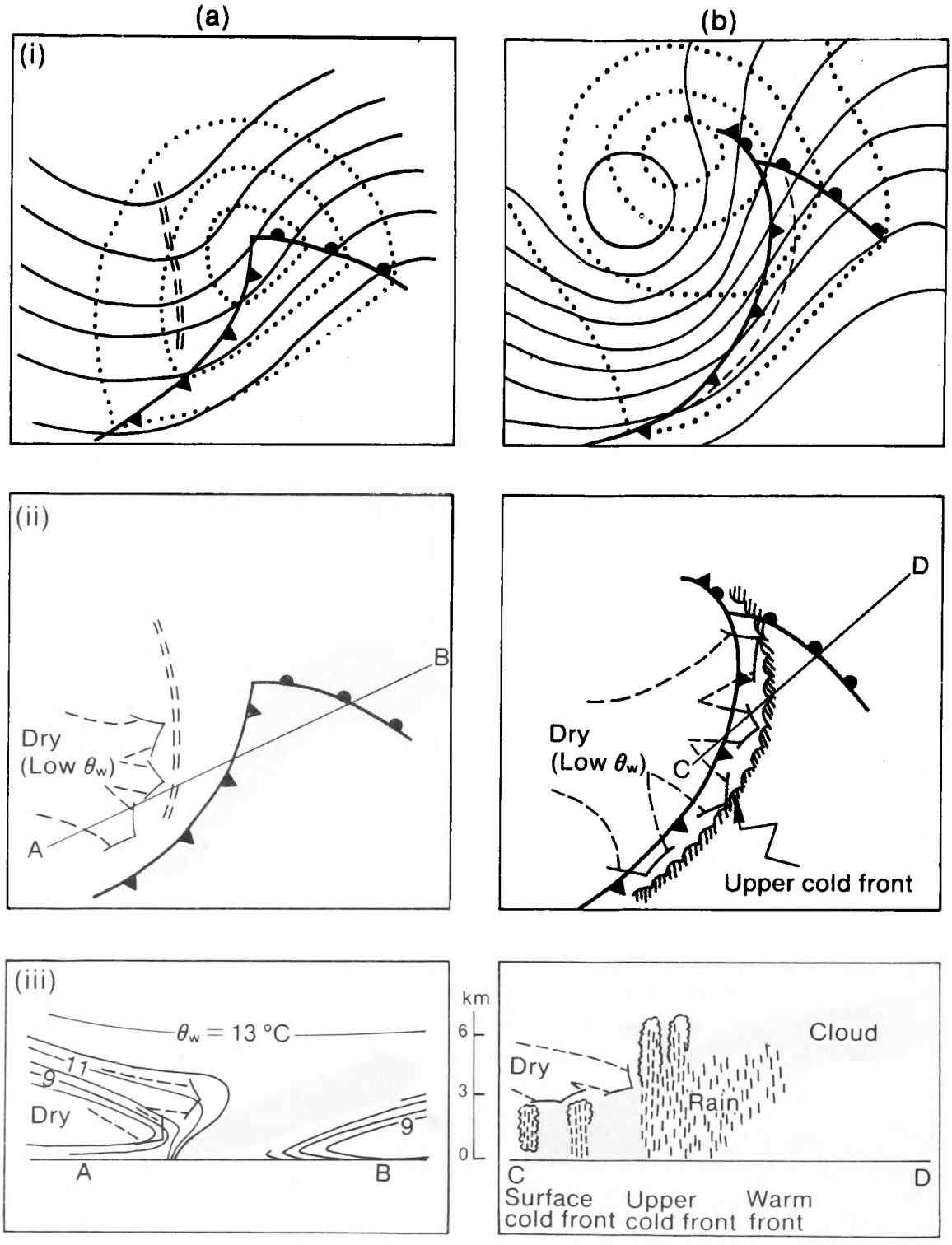

Figure 7.15 Development of a 'split' cold front from (a) developing low to (b) an occluded low. Dry subsiding air (pecked arrows) and warm moist air (shaded), with the cross-sections in (iii) along the lines shown in (ii).

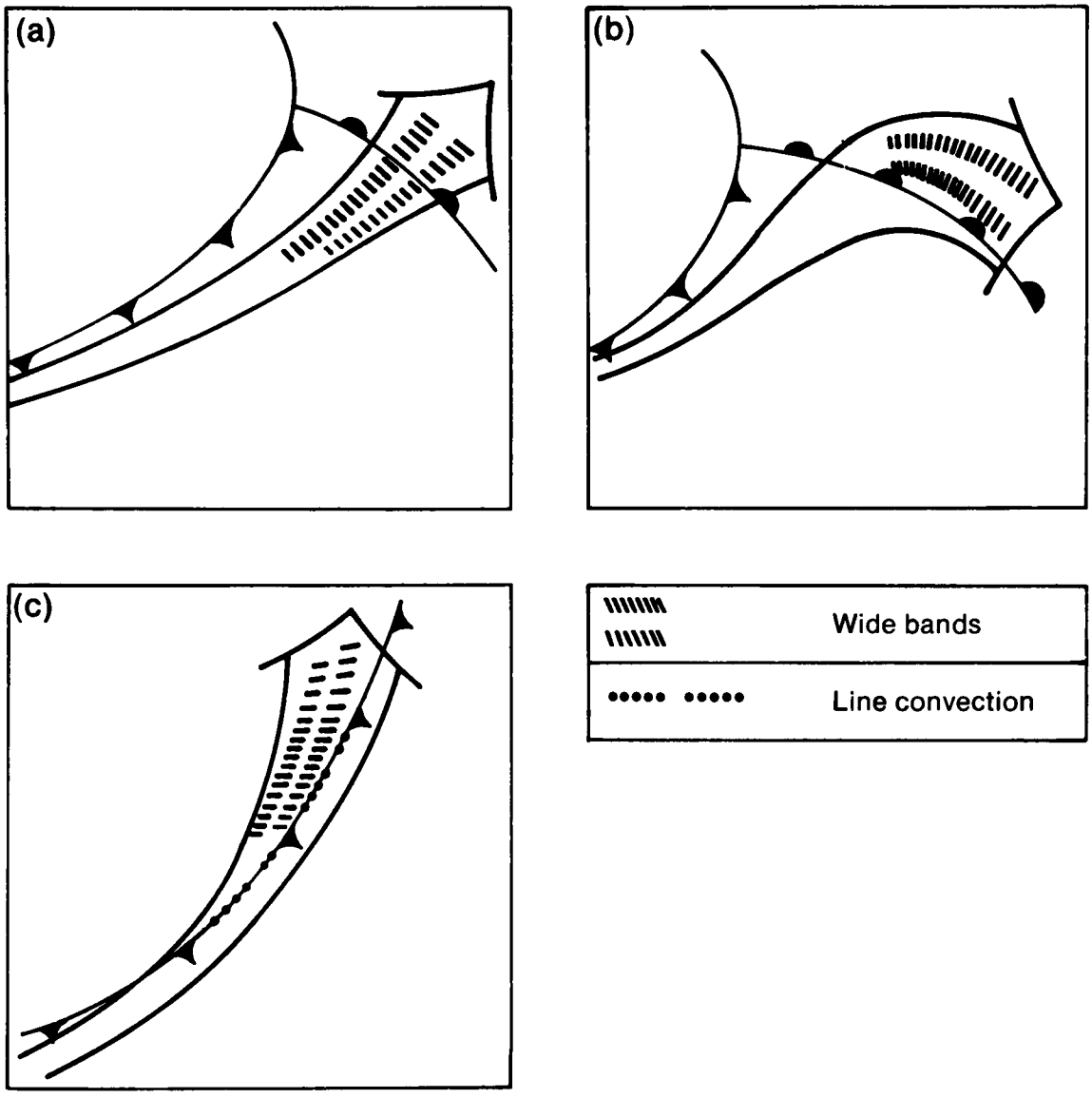

Figure 7.16 Typical orientation of mesoscale rain bands associated with warm conveyor belts ahead of cold fronts having, (a) and (b) forward-sloping ascent, and (c) rearward-sloping ascent.

discontinuous line, coincides with the surface frontal position, at the leading edge of the overall deck of frontal cloud and rain, as shown in Fig. 7.16(c).

7.4.2 *Orographic enhancement of rainfall*

Fig. 7.17 illustrates the important 'seeder-feeder' mechanism that generates enhanced rainfall over high ground. This was described in section 5.3.

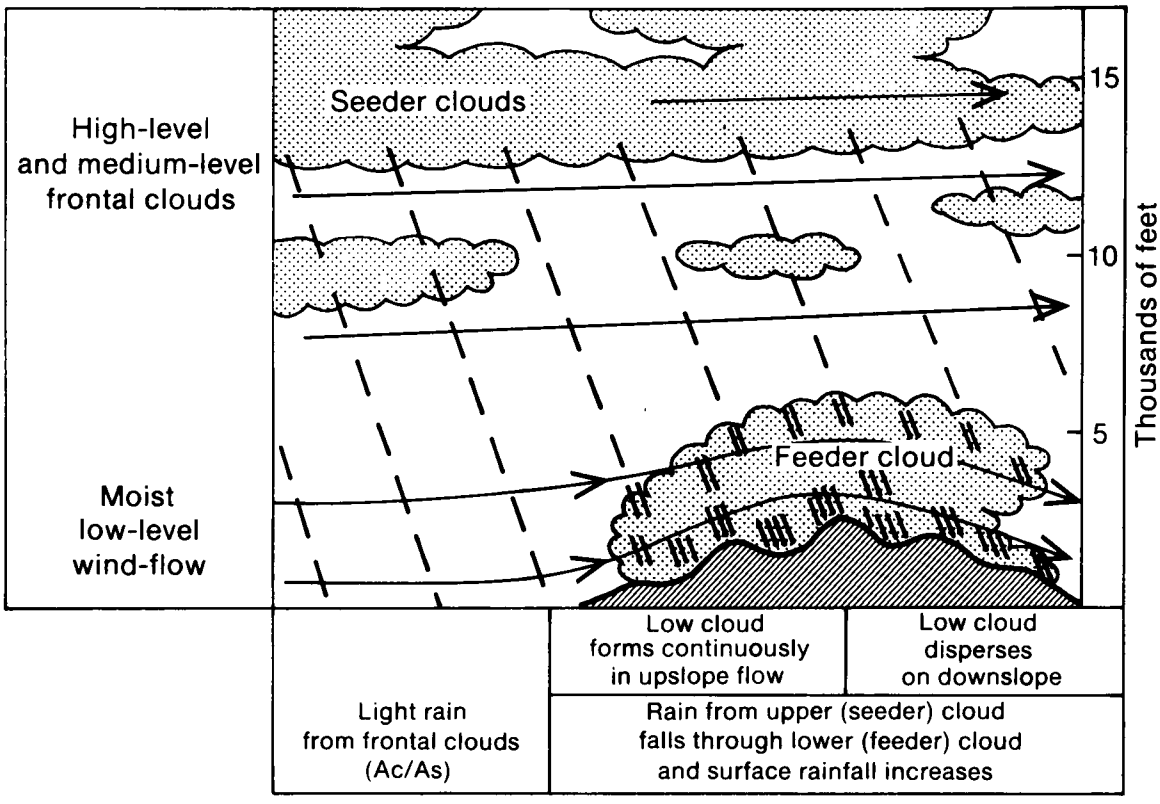

Figure 7.17 The seeder-feeder rainfall effect over hills.

Horizontal variations in the surface rainfall intensity over high ground are on the same scale as that of the hills and valleys.

7.4.3 *Organization of shallow convection*

Down-wind patterns (streets)

Cumulus cloud streets form when the depth of the surface convective layer is restricted in depth to about 2 km. The wind in the layer is usually constant in direction, with a moderate speed that increases slightly with height.

Cross-wind patterns (waves)

When the depth of the surface convective layer increases to 3–4 km, regular 'street' patterns are distorted by the circulations set up by large cumulus clouds. If conditions are suitable for the formation of lee waves (see section 1.10.2), a cross-wind pattern of cumulus rows may become established. Cumulus development will be enhanced in the ascent regions of the waves, and suppressed in the descent regions. The resulting cloud pattern is unlikely to be very clear cut.

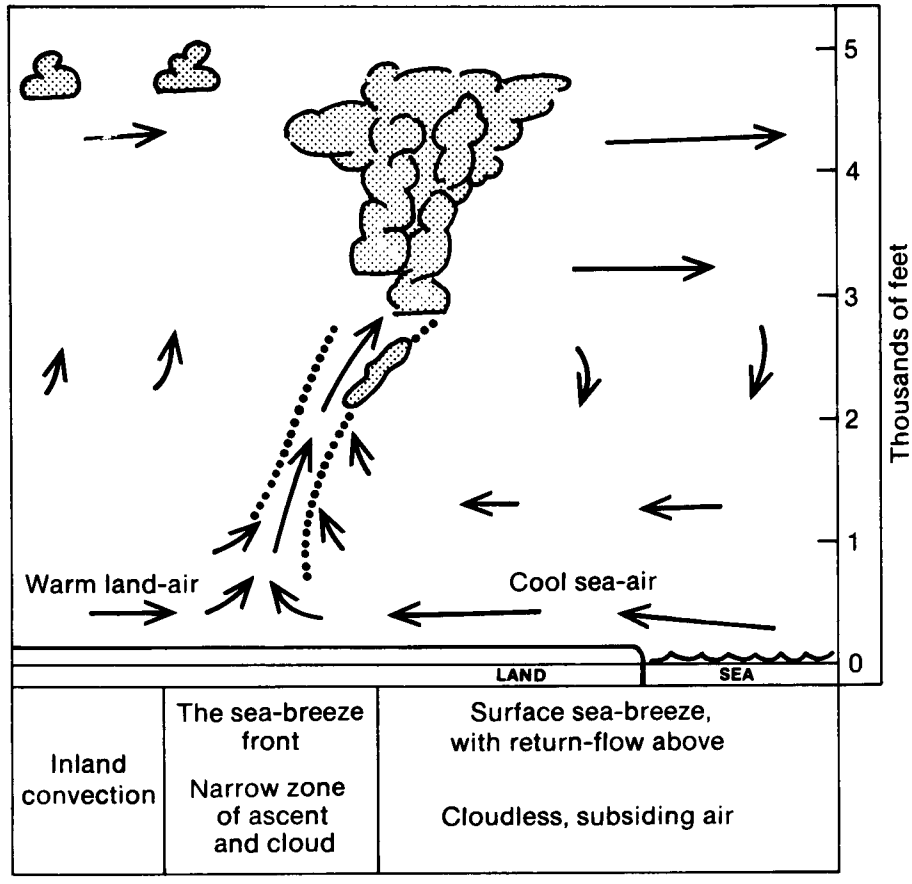

Figure 7.18 The sea-breeze.

Sea-breezes and other convergence zones

Fig. 7.18 is a typical cross-section through a sea-breeze circulation in mid-afternoon. The sea-breeze front is shown 20 km or so inland. The confluent low-level winds on either side of the front can often be identified on surface charts, and the narrow band of cloud marking the frontal convergence zone is a feature of satellite imagery.

Fig. 7.19 is a schematic ground plan of the typical cloud patterns formed along peninsulas and inlets which are subject to surface wind convergence/divergence effects, due to multiple sea- or land-breezes.

Sea-breezes and coastal convergence zones are prominent when the isobars (on the synoptic scale) run parallel to a coastline, with pressure over land higher than over the sea. Fig. 7.20 are local sketch maps, showing the association of coastal convergence/divergence zones with variations in surface friction effects over land and sea.

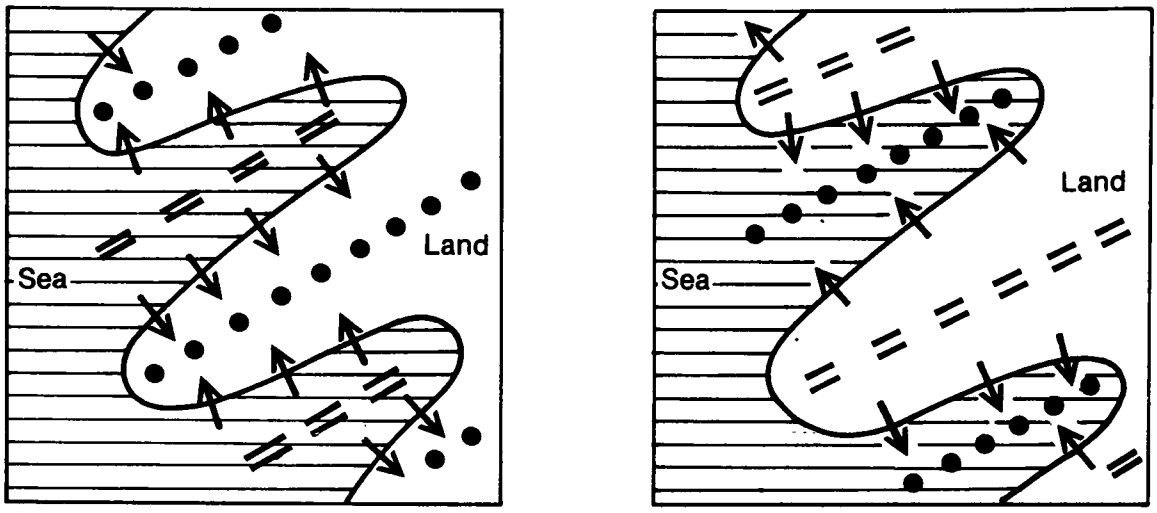

Figure 7.19 Peninsular and inlet convection patterns generated by coastal breezes, showing cloudy areas of surface convergence (....) and cloud-free area of surface divergence (====). (a) On a warm summer day, and (b) when land is relatively cold.

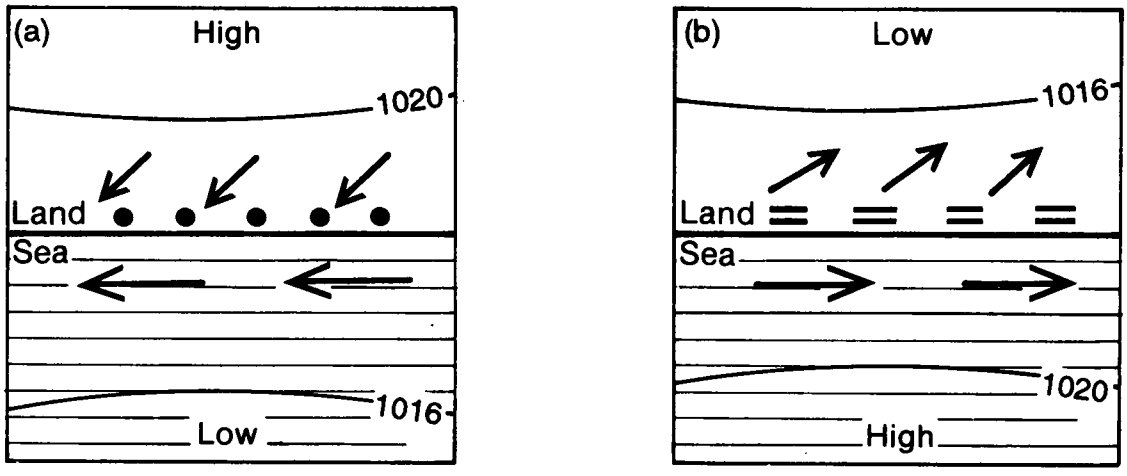

Figure 7.20 Coastal convergence divergence zones, with cloudiness indicated as in Fig. 7.19. Nominal isobars in hectopascals; arrows are surface wind vectors.

7.4.4 *Showers*

The wind shear in the cloudy convective layer is a useful key to shower distribution and persistence.

In a cumulus/cumulonimbus cloud, an updraught links the inflow at the cloud base to the outflow at the cloud top. The updraught may be vertical or sloping,

depending on the wind shear. The top of the updraught is the origin of the precipitation downdraught, which falls vertically and spreads out horizontally when it reaches the ground.

In Fig. 7.21 some basic wind-shear situations are illustrated by standard hodographs and by airflows relative to the moving storm clouds.

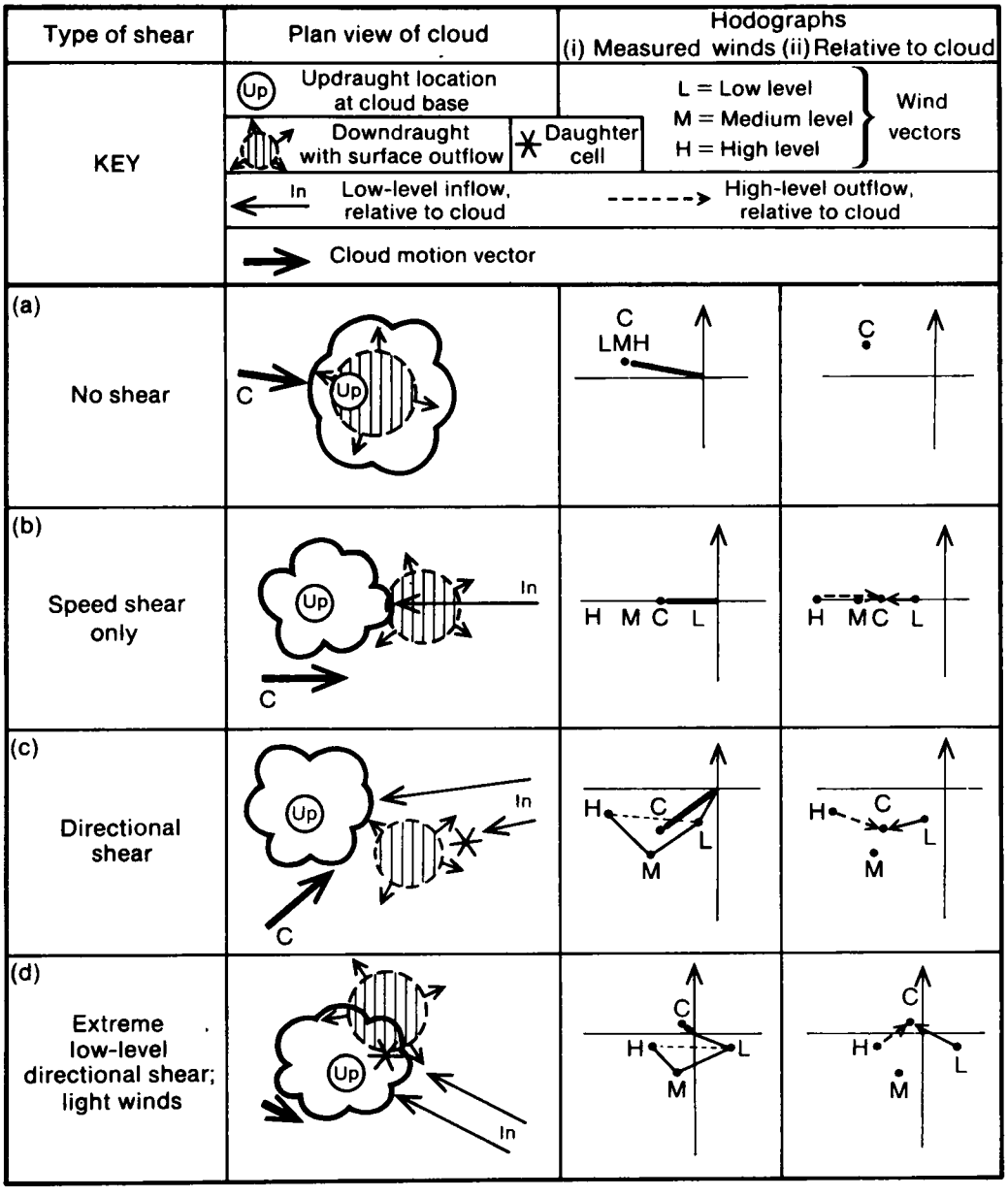

Figure 7.21 Wind shear and the character of convective precipitation for (a) insignificant showers, (b) slight showers, (c) moderate or heavy showers, and (d) severe convective storms.

(a) *No change in wind speed or direction*

There is mutual interference between coincident updraughts and downdraughts. This occurs with shallow clouds. Showers are very light and only last a few minutes.

(b) *Increasing wind speed but little change in direction with height*

The clouds slope forwards so that downdraughts fall into the inflowing surface air, cutting off the updraughts and showers do not persist.

This commonly occurs in maritime airstreams with moderately deep convection and light/moderate showers. Though each shower may have a life-span of 20–30 minutes, specific places are affected for a shorter time.

(c) *Changing wind direction and speed with height*

The storm cloud motion vector is found within the triangle formed by the wind vectors LMH. The downdraught falls to one side of low-level inflow. Successive daughter cells may be generated where the surface outflow from the downdraught meets the inflow. The storm area moves to the right of the track of individual cells.

This is typical of deep polar air masses, generating large cumulonimbus clouds with heavy, thundery showers lasting half an hour or more.

(d) *Sharp change in wind direction at about 2 km, but no strong winds*

Similar to type (c), but with slow-moving system the successive daughter cells may effectively coincide, forming a supercell system. The storm motion vector falls outside the triangle formed by the wind vectors LMH.

This may produce the most severe summertime thunderstorms with localized flooding. Southern England is a favoured location with a low-level flow of warm, continental south-easterly winds overridden by cooler, oceanic south-westerlies aloft. In extreme cases with light winds, storms may persist at a particular place for several hours with heavy rain and hail.

7.4.5 *Mesoscale convective systems*

Fig. 7.22(a) shows a classic summertime thundery situation over southern England. At low levels the warm, continental easterly is prominent on the surface chart and on the upper-air sounding from Brest (Fig. 7.22(c). A cold front is marked by strong southerly thermal winds ahead of a cold trough over Biscay (Fig. 7.22(b). Widespread thunder occurred in multicellular convection over south-west England.

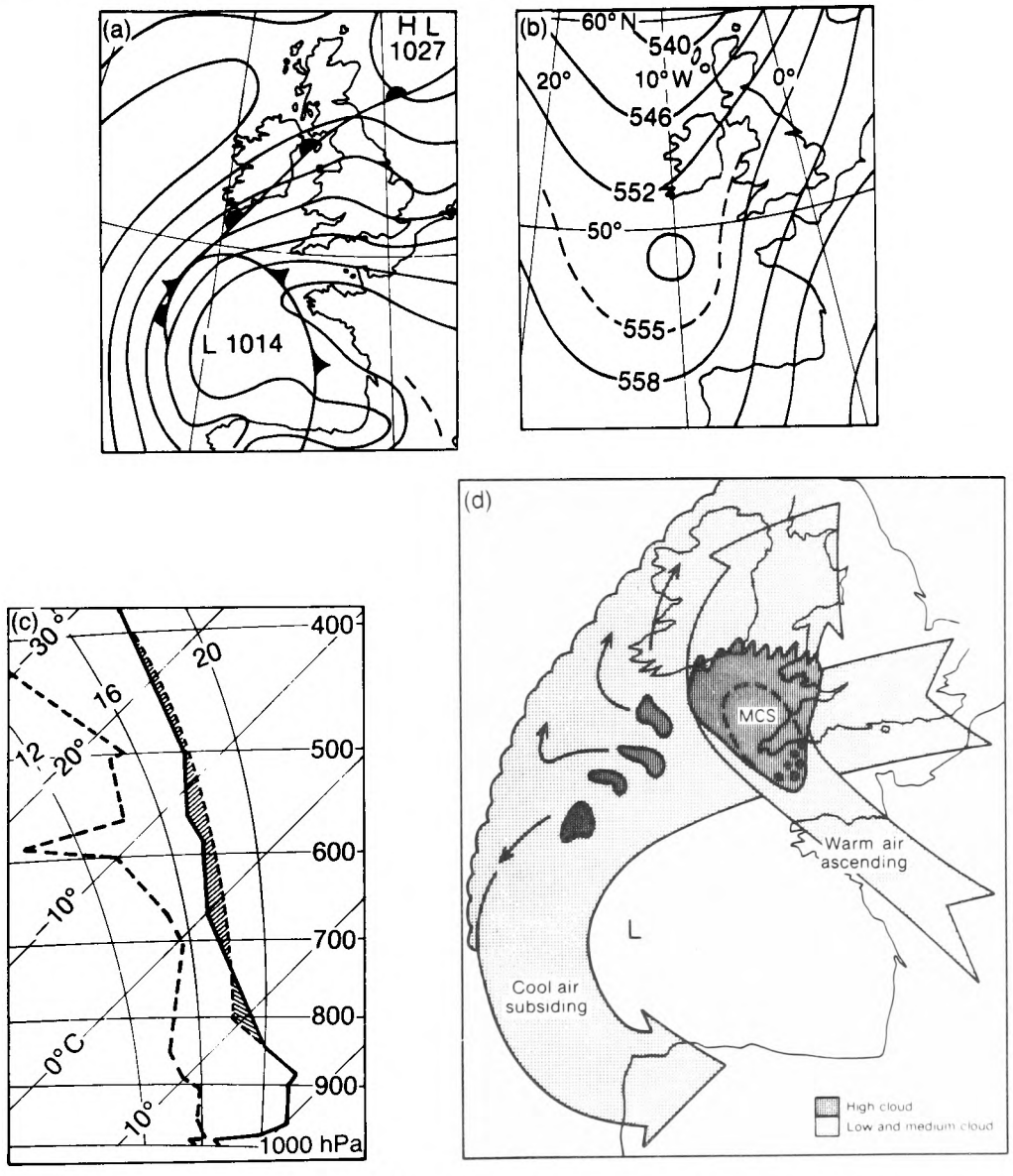

Figure 7.22 (a) Surface fronts and isobars at 2 hPa intervals, (b) 1000–500 hPa thickness lines (dam) on 11 July 1982, (c) Brest radiosonde ascent, and (d) a schematic model of the Mesoscale Convective System which generated heavy thunderstorms on that day.

Fig. 7.22(d) shows a schematic model of the principal airflows, relative to the rain area, involved in this convective system. Heavy rain falls from a cluster of cumulonimbus cells on the upwind edge of the system. From these an area of less heavy stratiform rain spreads downwind.

Characteristic properties of mesoscale convective systems near the British Isles are:

dimensions:	overall ≈300 km, with embedded cells ≈50 km
cloud-top temperature:	<−30 °C over wide area, locally <−50 °C
duration as an active system:	12 hours.

7.4.6 *Severe convective storms*

Fig. 7.23 is a schematic, two-dimensional cross-section showing the typical airflows involved in a major, self-perpetuating supercell storm. Generating thunder, hail and heavy rain, these storms may cause major local flooding, especially if they are slow moving.

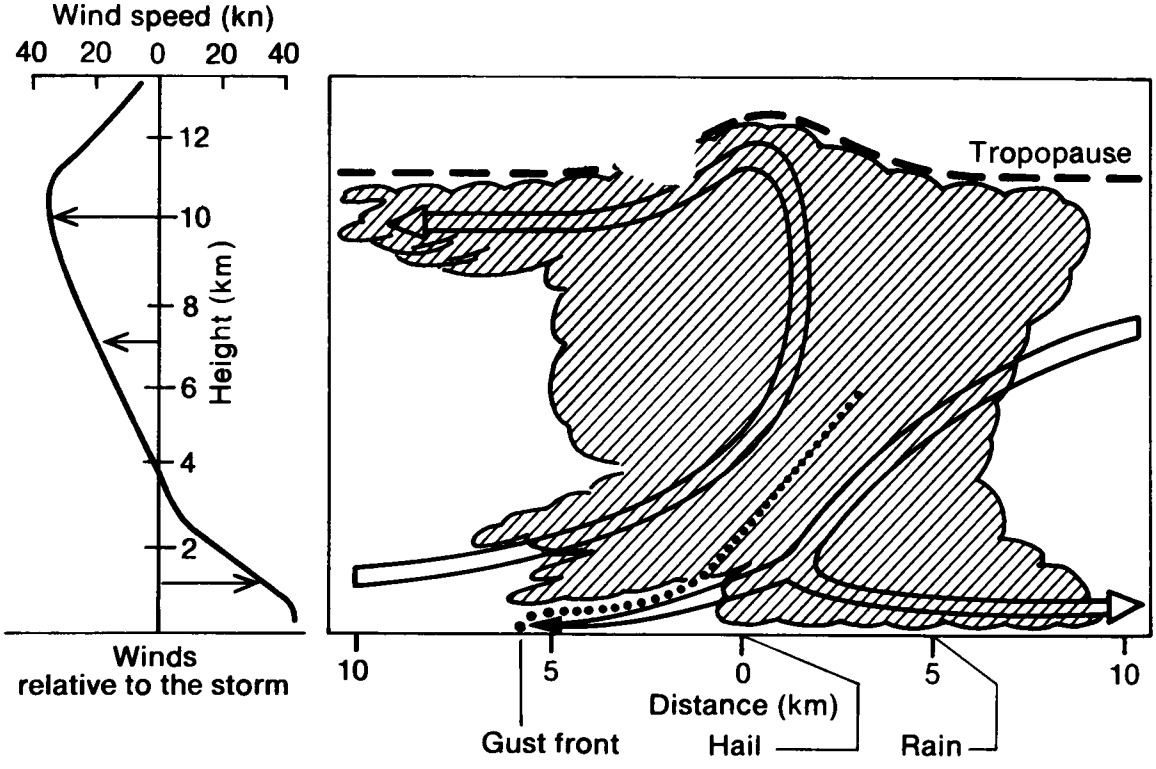

Figure 7.23 Airflow in a supercell storm, in two dimensions. Broad arrows show airflow relative to the storm.

CHAPTER 8 — SUBJECTIVE FORECASTING AIDS AND TECHNIQUES

8.1 Terminology

Absolute vorticity: The sum of the *vorticity* (ζ) relative to the earth, plus the vorticity of the earth (f).

Amplitude of a trough/ridge pattern: The latitudinal extent of a typical contour, or streamline, from the tip of a ridge to the base of a trough. In meteorology, quantitative values of amplitude are rarely used.

Anchor troughs: Long-wave troughs, persisting in the same region for several days and associated with some geographical feature such as the lee side of the Rocky Mountains.

Anticyclonic development: An increase in the extent and influence of high pressure systems, accompanied by rising pressure and intensification of existing ridges or anticyclones.

Anticyclonic disruption: Describes the nature of the changes which occur when a large amplitude upper-air trough moves eastwards, faster in the north than in the south. A slow moving cut-off low forms at the base of the trough, and to the north of this the surface pressure builds up across the neck of the disrupting trough.

Baroclinic: Describes a region of the atmosphere where constant pressure surfaces and constant density surfaces intersect. Isotherms and thickness gradients exist on constant pressure charts.

Baroclinicity: The product of the thermal wind and the *Coriolis parameter*; it is indicated in practice by the thickness gradient.

Barotropic: Describes a region of the atmosphere where surfaces of constant pressure and constant density coincide. Isobaric surfaces are isothermal and the thickness between two pressure levels is constant. Winds do not vary with height.

Blocking: Large-scale obstruction of the normal west to east progression of weather systems in mid-latitudes. It is characterized by the formation of an anticyclone (the 'blocking high') to the north of a 'cut-off low', with easterlies between. The normal westerly flow divides into two currents around this blocking

pattern. If the southern branch is relatively undistorted, the pattern is known as an 'omega block'.

Confluence: A gradual coming together of adjacent streamlines in the direction of a flow at one level.

Convergence: In meteorology it involves the *confluence* of airstreams in the horizontal, coupled with vertical (stretching) motions that preserve the air density at that level. Convergence near the ground leads to ascent of air.

Coriolis parameter: $f = 2\Omega\sin\phi$.

Cyclonic development: An increase in the activity of low-pressure systems accompanied either by falling pressure and large, deepening depressions or by the repeated formation of small, mobile lows.

Development: A term used by forecasters to describe significant changes in the surface pressure pattern. These may result from changes in intensity of existing features or from their motion, or both.

Diffluence: A gradual separation of adjacent streamlines in the direction of flow at one level.

Divergence: In mathematics, Div $\mathbf{V} = \frac{\partial u}{\partial x} + \frac{\partial v}{\partial y} + \frac{\partial w}{\partial z}$

The Divergence of a vector is a scalar quantity, which may be +ve or −ve.

In meteorology, the Divergence of velocity (of a unit mass of air) is the most used application. Divergence (the opposite of convergence) involves diffluent airstreams in the horizontal, coupled with vertical (squashing) motions that preserve the air density at that level. Near the ground, divergence leads to subsidence of air.

Gravity waves: Vertical oscillations of air moving under the action of buoyancy and gravity forces. In the atmosphere, lenticular clouds provide visible evidence of their occurrence, though the absence of such clouds does not necessarily imply the absence of waves.

Jet axis: The line of a *jet stream*'s maximum wind on a constant pressure chart.

Jet core: The line, varying with height, of the wind speed maximum of a *jet stream.*

Jet streak: A localized region on a *jet axis* where the maximum wind speed is higher than in adjacent regions. A jet streak may move through the overall *jet stream* pattern and be associated with significant weather developments.

Jet stream: A narrow belt of very strong winds at upper levels. The usual defining characteristics are the maximum wind-speed and the existence of strong wind-shears all around the wind maximum.

Long waves: Horizontally extensive wave patterns in the quasi-horizontal upper-level flow; also called *Rossby waves.* Normally restricted to patterns with *wave number* 8 or less, i.e. waves having a longitudinal separation between successive troughs of 45° or more.

Low-level jet stream: These bear some resembalance to small *jet streams* but are located in the lowest 2 km of atmosphere. Wind-speed maxima may be as low as 30–40 kn, with small but identifiable wind shears. They occur (a) at cold fronts with vigorous line convection, (b) just above low-level inversions after nocturnal radiation cooling, (c) as climatological features off the coast of Somalia.

Meridional extension: Marked elongation of upper-level troughs in a southerly direction (or less commonly used to describe the extension of ridges in a northerly direction).

Meridional flow: Air flow along a meridian of longitude, i.e. northerly or southerly flow.

Mesoscale: The scale of atmospheric systems that are detectable by an observing system with a horizontal resolution of 10–50 km.

Phase lag: The amount by which the movement of a trough axis differs between a forecast and an actual movement, or between the motions of the southern and northern parts of an elongated trough.

Progression: The movement of atmospheric systems in the normal climatological direction, i.e. from west to east in mid latitudes.

Relaxation of a trough (or ridge): A decrease in amplitude of either of these features.

Retrogression: The movement of atmospheric systems in the opposite direction to the climatological normal, i.e. from east to west in mid latitudes.

Rossby waves: Long waves in the quasi-horizontal flow at upper levels.

Synoptic scale: The scale of atmospheric systems which are detectable on weather charts having observations plotted at an average spacing of 200–500 km or more.

Trough disruption: The process whereby an upper-level trough of large meridional extent is deformed by different rates of trough movement at different latitudes. See also *anticyclonic disruption.*

Trough extension: An increase in amplitude of a trough.

Vorticity: A measure of the spin of a small element of a fluid. It is a 3-dimensional vector, but in operational meteorology only the spin about the local vertical (ζ) is important. ζ is +ve when the spin is cyclonic, and −ve when the spin is anticyclonic.

Wave number: If the longitudinal separation between successive troughs in a sinusoidal pattern is N degrees, the wave number is $360/N$. Long waves have small wave numbers; short waves have large wave numbers.

Zonal flow: Airflow along circles of latitude.

Zonal index: A measure of the strength of the zonal component of the planetary flow. It is usually measured by taking the average difference in contour height along two latitude circles.

Zonal wave number: The number of trough-ridge pairs around a selected circle of latitude on a constant pressure chart.

8.2 Typical weather sequences

8.2.1 *Life history of a Polar Front depression*

Fig. 8.1 is an idealized sequence of a temperate latitude depression developing on the Polar Front. The sequence covers a period of 2 or 3 days.

(a) *Initially*

A surface low begins to form; no circulation at upper levels. The undistorted 500 hPa contours and thickness lines steer the surface low quickly forward, parallel to the warm sector isobars.

(b) *As the surface pressure falls*

The cyclonic circulation extends upwards and thickness lines are distorted. A trough develops at 500 hPa.

In Sutcliffe's theory, the Development term gradually becomes more significant, modifying the the steering effect and the track of the depression bends to the left.

(c) *The surface low is occluded*

The tip of the warm sector is some distance from the centre of the surface low. The cyclonic circulation extends above 500 hPa and the depression

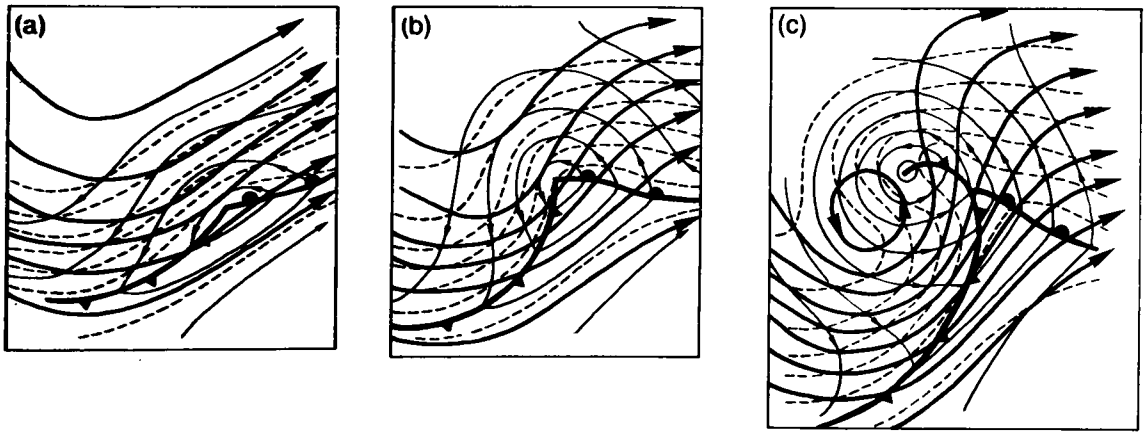

Figure 8.1 A developing depression on the polar front. A sequence of charts (left to right) at approximately 18–24 hour intervals, where thin lines are 1000 hPa contours, dashed lines are 1000–500 hPa thickness lines, and thick lines are 500 hPa contours.

becomes a slow-moving vortex. The axis of the vortex tilts towards the cold air on the south-west side of the low.

8.2.2 *Meridional extension of a trough*

Fig. 8.2 shows the development, over a period of 3 days, of an increasingly meridional upper flow over the North Atlantic leading to a plunge of cold air southwards.

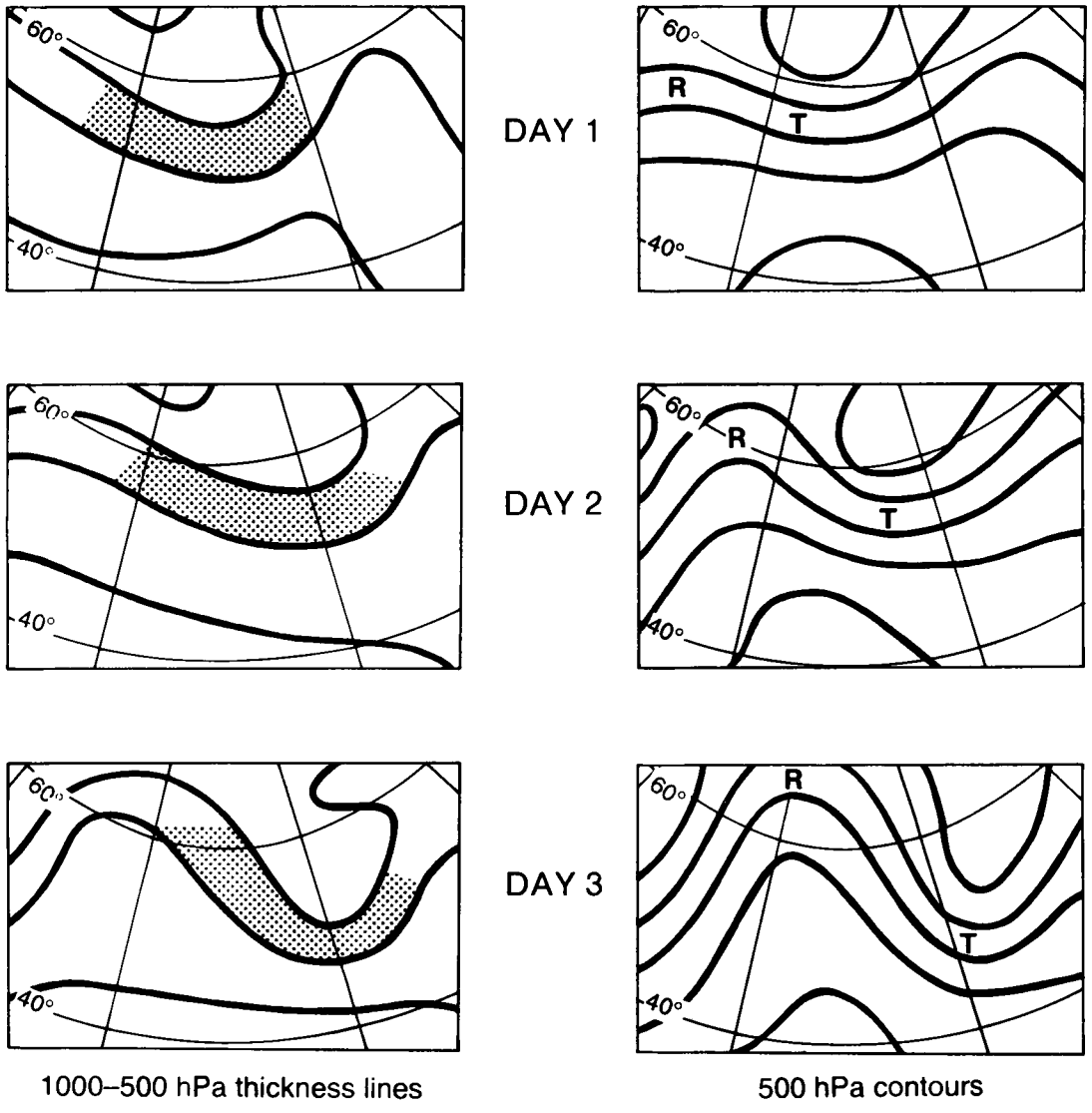

Figure 8.2 Meridional extension of an upper trough. The significant parts of the patterns are shaded between the same two isopleths on successive charts (R=ridge and T=trough). Lines of latitude shown are for 40° and 60° N, and longitudes are at 30° intervals. Isopleths are at 12 dam intervals.

The development is most likely in winter. A strong temperature contrast over the north-east coast of the USA is common, and an injection of extra cold air there from the Canadian Arctic initiates the process by sharpening the thermal gradient and backing the upper winds. For the British Isles a strengthening southerly flow at upper levels near Newfoundland is an important forecasting signal.

During Day 2 there is an increase in the amplitude of the mid-Atlantic ridge. This is followed, on Day 3, by a cold plunge (meridional trough extension).

8.2.3 *Anticyclonic disruption of a trough*

Fig. 8.3 shows a sequence of charts at daily intervals. This development may follow on from a meridional trough extension (see the previous Section).

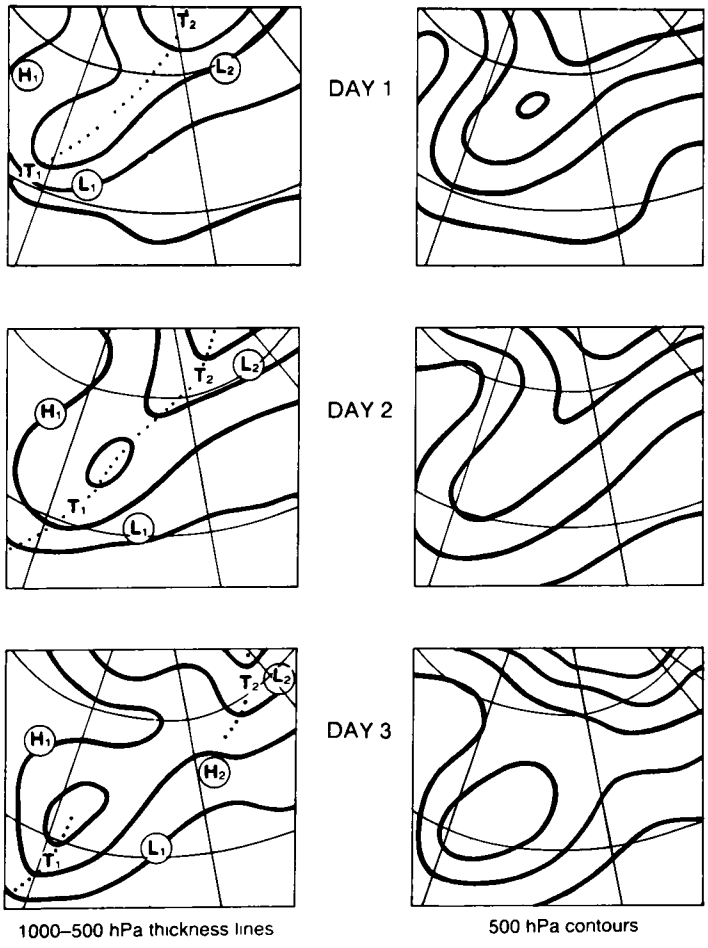

Figure 8.3 Anticyclonic disruption of an upper trough, with trough-line (T_1T_2) (dotted) and surface pressure centres (circled). For key see Fig. 8.2.

The northern part of a large amplitude trough moves quickly east. The southern part of the trough remains slow moving in low latitudes and eventually becomes a cut-off upper low.

Across the neck of the disrupting trough, surface pressure rises, giving this development its name.

8.2.4 *Short-wave systems steered through long-wave patterns*

Small, short-wave weather systems normally move more rapidly than the large, broad-scale patterns. Fig. 8.4 shows an example of a short-wave trough moving round the circulation of a large semi-permanent trough at 500 hPa. In the sequence, the charts are at daily intervals and a broad-scale trough is seen in much the same longitude at each end of the sequence. At the intervening times the broad-scale pattern is still detectable even though it is distorted by the progress of one or more short-wave troughs.

When a short-wavelength trough moves through a longer-wavelength pattern, it temporarily weakens the ridges and amplifies the troughs as it comes into phase with these slower-moving features.

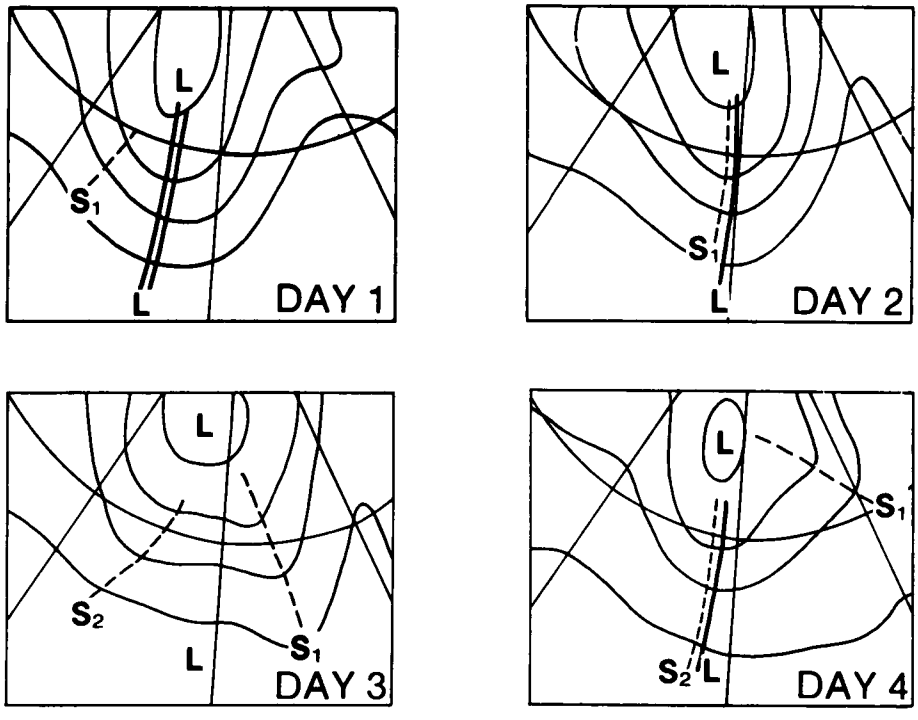

Figure 8.4 Daily sequence of short-wave troughs (S_1,S_2) moving through a long-wave 500 hPa pattern (LL).

8.2.5 *Interactions between cold troughs and fronts*

A broad-scale trough in a baroclinic westerly flow is characterized by cloudiness on the warm side of the jet core on its forward side (cloud band F in the charts of Fig. 8.5).

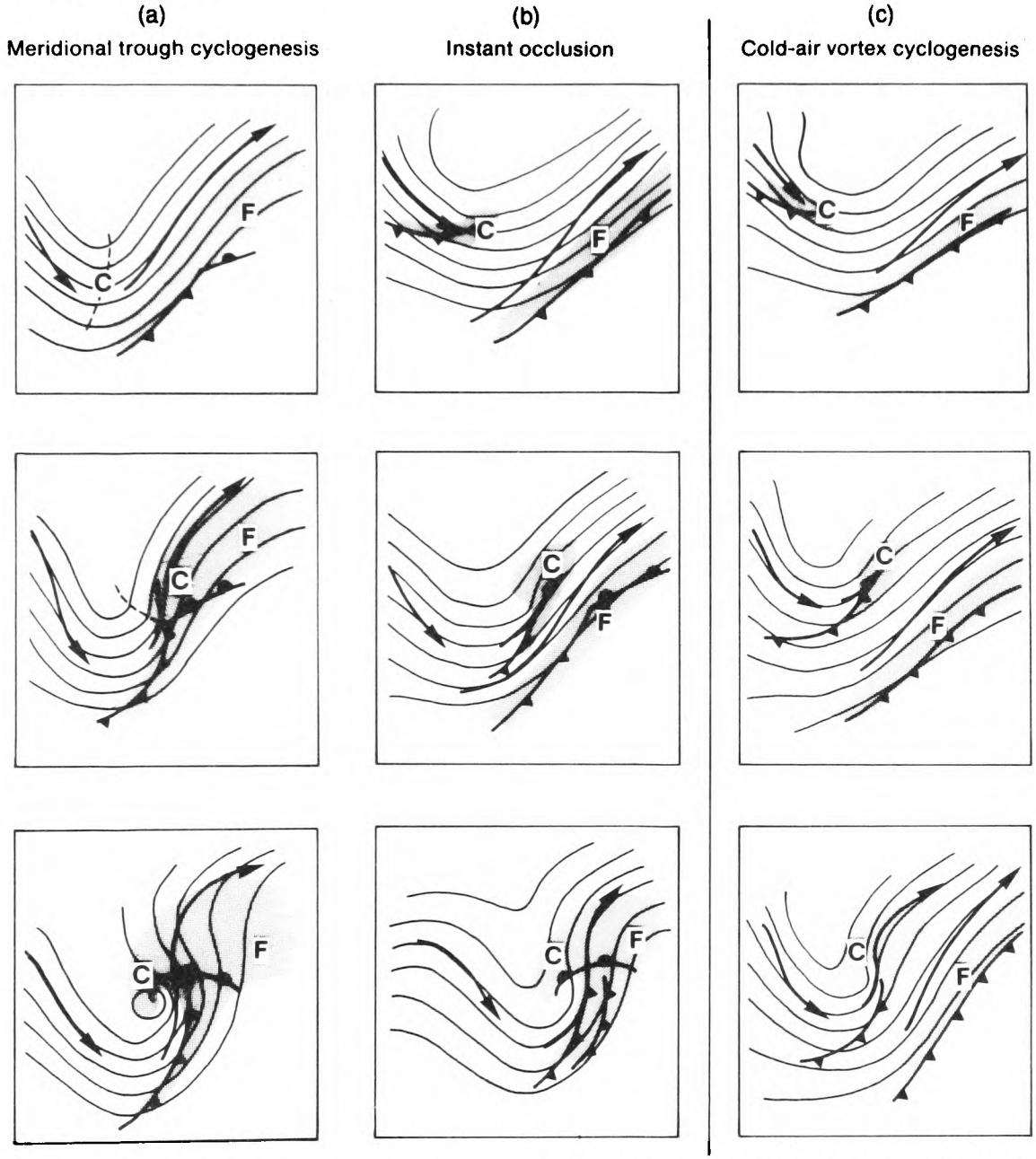

Figure 8.5 Various cyclogenetic developments which may occur when a cold trough interacts with the polar front. Surface fronts, 500 hPa contours with jet axes and main cloud cover are shown. F indicates the polar-front cloud and C indicates cloud associated with the cold trough.

Specific cyclogenetic events are likely to occur in this same region. They are triggered by short-wave disturbances moving through the pattern and coming into phase with a broad-scale 'C' area. A short-wave disturbance may be identified either by the presence of cloudiness on satellite cloud imagery, or by features of the upper-wind field such as a jet streak or a short-wave trough.

The location of the short-wave trigger in relation to the pre-existing frontal cloudiness determines the character of the subsequent cyclogenetic event. Fig. 8.5 illustrates typical alternative developments that occur in the commonly occurring cold trough and polar-front situation, namely:

(a) formation of a depression on the polar front,

(b) formation of an 'instant occlusion' next to the polar front, and

(c) formation of a cold air vortex north of the polar front.

In all three cases the short-wave disturbance forms to the rear of the broad-scale trough and moves forward through the pattern, developing on the forward side of the trough. In the case of Fig. 8.5(a) the disturbance originates so close to the frontal cloud band that its history is not readily traceable. In the other two cases, the origin and movement of the disturbance can be monitored with satellite imagery.

Fig. 8.5(a) leads to the classical development of a depression on the polar front (see section 8.2.1 above).

In Fig. 8.5(b) the short-wave disturbance develops sufficiently close to the pre-existing frontal cloud that the two cloud systems merge, forming a pattern that is superficially similar in shape to a classical occlusion. This has led to the misleading, but generally accepted, name 'instant occlusion'.

In Fig 8.5(c) the short-wave feature remains remote from the frontal zone and no interaction between the two takes place. The development is strongly dependent on positive vorticity advection (PVA) and generates a region of enhanced cloudiness within the polar air mass.

8.2.6 *Split cold fronts*

See section 7.3.5.

8.3 Assessment of development from synoptic charts

8.3.1 *Empirical rules*

(a) *Motion of surface pressure systems*

Frontal depressions move:
— in the direction of the warm sector isobars
— parallel to a line joining the isallobaric high and low.

Non-frontal depressions move:
— with the strongest winds around their periphery
— around the circulation of a larger primary depression
— as a rotating system if two (or more) equal sized lows are present.

Anticyclones move:
— towards regions of rising pressure.

(b) *Intensity of surface pressure systems*

Frontal depressions deepen:
— when pressure falls in the warm sector, or over the low centre
— when markedly cold air is drawn into the rear of their circulation.

Frontal depressions fill:
— when pressure rises in the warm sector
— some 12–24 hours after the occlusion process begins.

Non-frontal pressure systems develop:
— according to the observed pressure tendencies.

NB. Over oceans the isallobaric pattern is often difficult to define because of the scarcity of observations and the effect of ships' motions on the observed pressure tendency.

8.3.2 *Sutcliffe's development areas*

The **A** and **C** development areas associated with basic thickness patterns are in Fig. 8.6. See also section 8.4.2.

Important practical points are:

(a) The intensity of the development is proportional to the thermal wind speed. Strong thermal winds lead to strong development, weak thermal winds give negligible development.

(b) Significant developments only occur if the relevant patterns persist for at least 12–24 hours.

(c) Fig. 8.6 shows the **C** and **A** areas when the thickness lines are predominantly zonal. If there is a pronounced meridional component in their orientation, modifications may arise due to the latitude term in Sutcliffe's equation. This aids **A** development where the flow is northward and **C** development where it is towards the south.

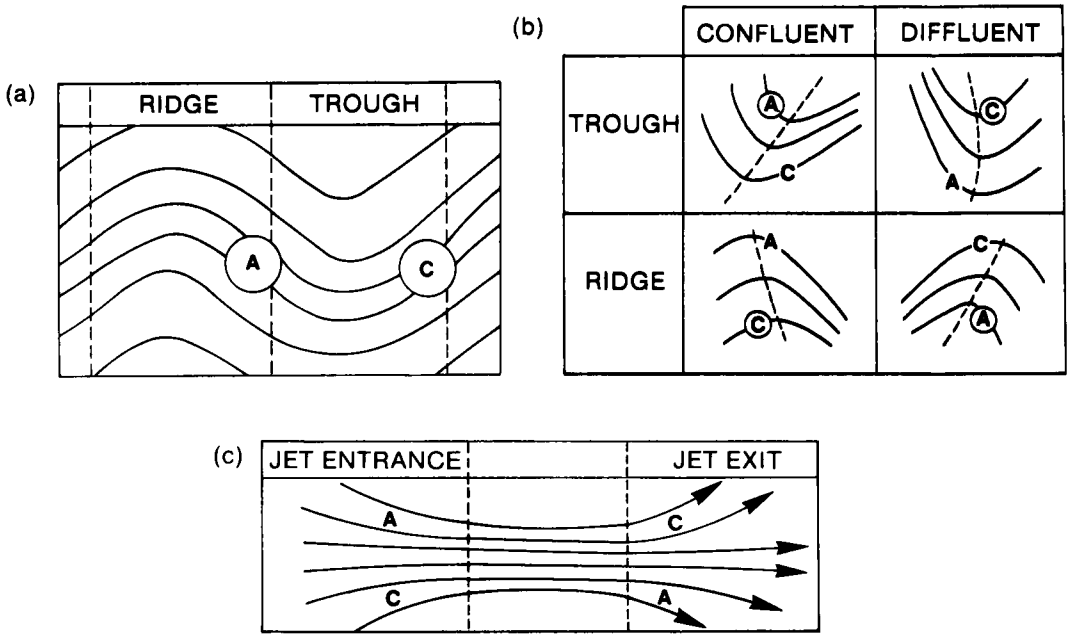

Figure 8.6 Sutcliffe development areas associated with (a) a symmetrical, sinusoidal 1000–500 hPa thickness pattern, (b) confluent and diffluent 1000–500 hPa thickness troughs and ridges, and (c) a zonal jet-stream pattern.

8.3.3 *Formation of secondary lows on fronts*

Fig. 8.7 shows typical patterns of fronts and thickness lines associated with the formation of secondary lows on fronts of various types.

In all cases the new development occurs where the front is marked by a strong thickness gradient. After it has formed, the new low moves quickly, steered by the strong thermal wind.

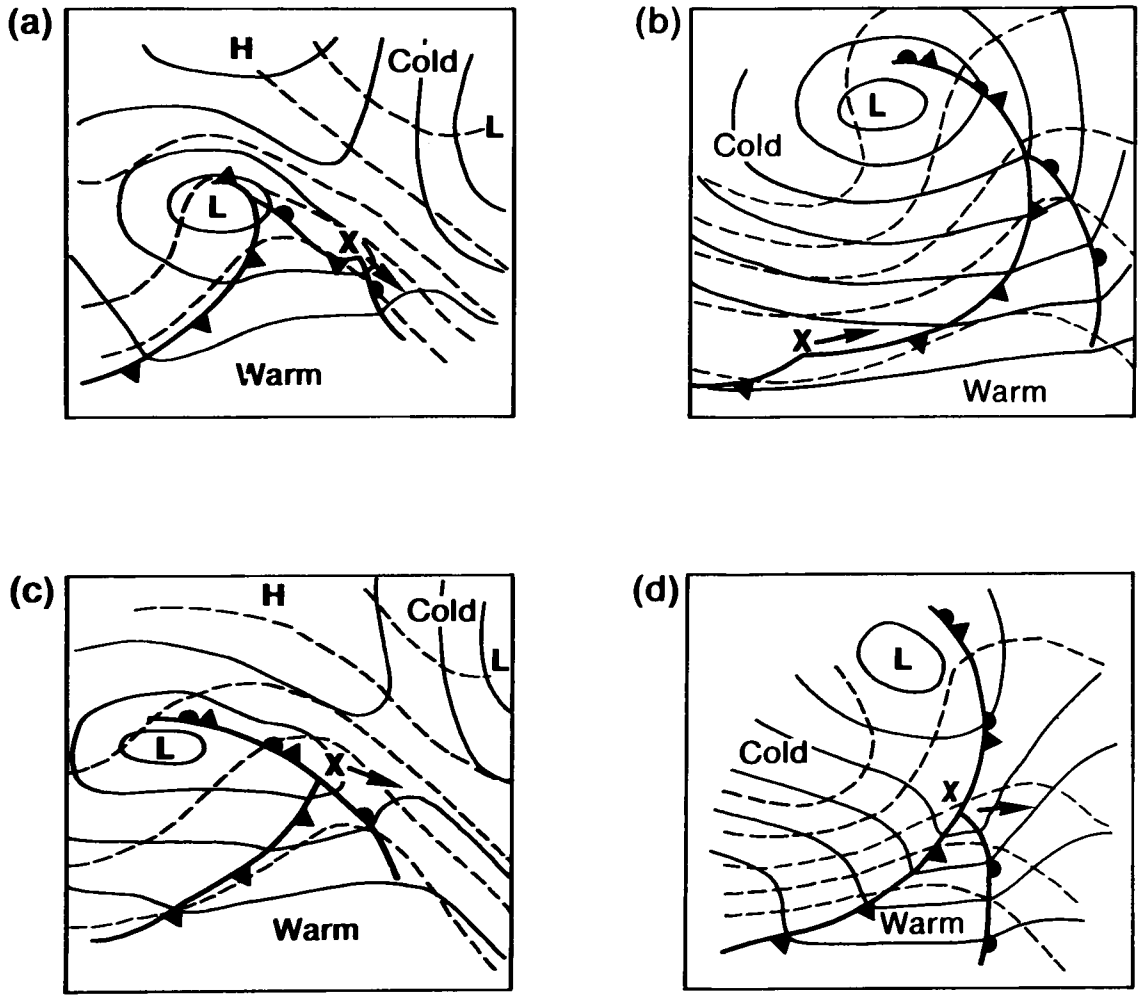

Figure 8.7 Formation of secondary lows on fronts — typical synoptic patterns associated with (a) warm front, (b) cold front, (c) warm occlusion, and (d) cold occlusion. X marks the typical location for secondary formation, while the arrow shows the direction of its likely movement. L is the pre-existing parent low. The dashed lines are 1000–500 hPa thickness lines while solid lines represent the MSL pressure pattern.

8.3.4 *Anticyclonic development*

(a) Mobile ridges form in the cold air north of the polar front, on the forward (eastern) side of upper thermal ridges, such as the **A** area in Fig. 8.8(a). These ridges, separating successive lows, move steadily eastwards in the broad, zonal pattern. The amplitude of the ridge pattern decreases with height, and is often not discernible above 700 hPa.

(b) Stationary anticyclones may develop through the anticyclonic disruption of a large-amplitude upper trough, or as an early part of the process leading to the meridional extension of the downwind trough. Fig. 8.8 shows the sequence of developments from (a) a mobile ridge-trough pattern to (b) an increasingly

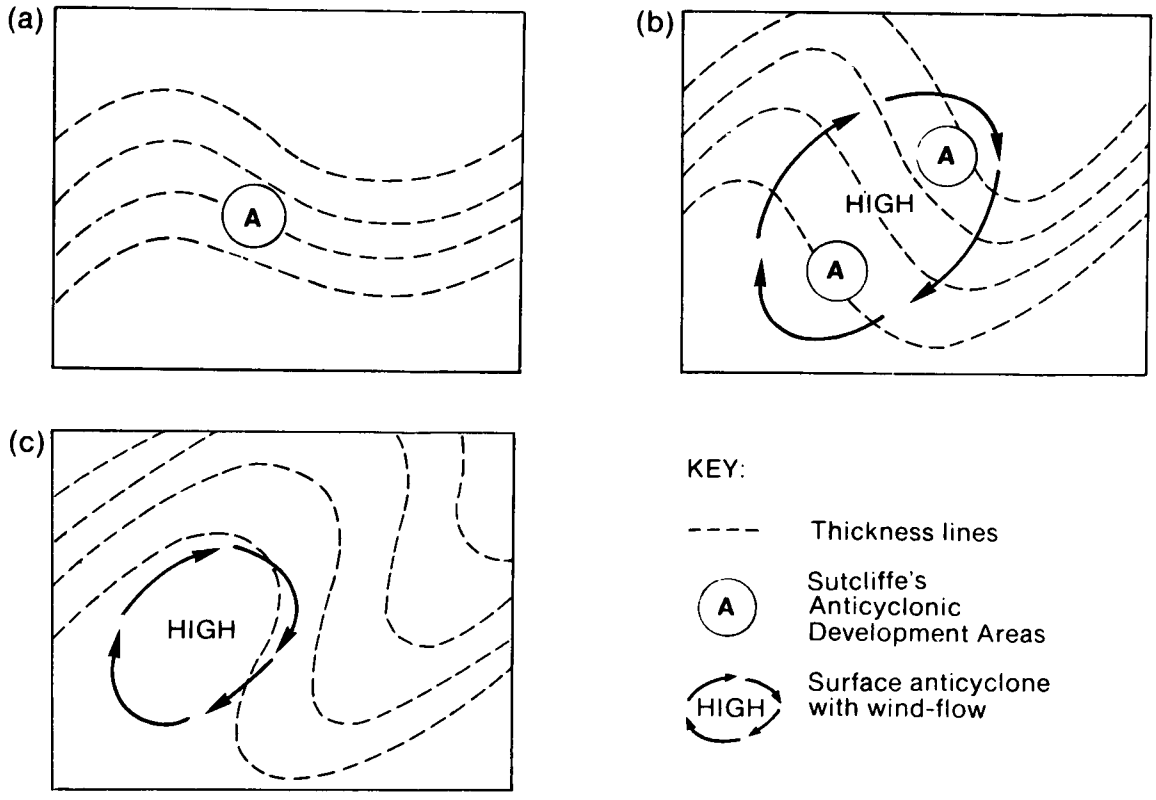

Figure 8.8 A mobile ridge transforming to a stationary high from (a) uniform ridge–trough pattern — **A** developments east of ridge, (b) more meridional flow, with a diffluent ridge-confluent trough pattern, and (c) distorted thermal pattern, with the high vortex under a uniform thermal ridge.

meridional flow, with the strongly anticyclonic 'diffluent ridge — confluent trough' development and (c) the final barotropic ridge situation. Here the high is a vortex with a deep circulation in a warm air mass and is very slow moving.

(c) Blocking patterns give rise to prolonged periods when the normal west to east airflow of mid-latitudes is 'blocked' by a persistent, opposing flow from the east. A large, stationary high is a prominent feature of such situations.

Fig. 8.9 shows typical contour patterns associated with a blocked situation. The usual gradient of thickness, with westerly thermal winds, is reversed over a considerable area. Warm air is cut off in high latitudes, and cold pools occur in lower latitudes. The normal westerly flow is either split into two equal streams as it flows round the block (Fig. 8.9(a)), or the westerly flow may be diverted to unusually low latitudes, forming what is termed an 'omega block' (Fig. 8.9(b)).

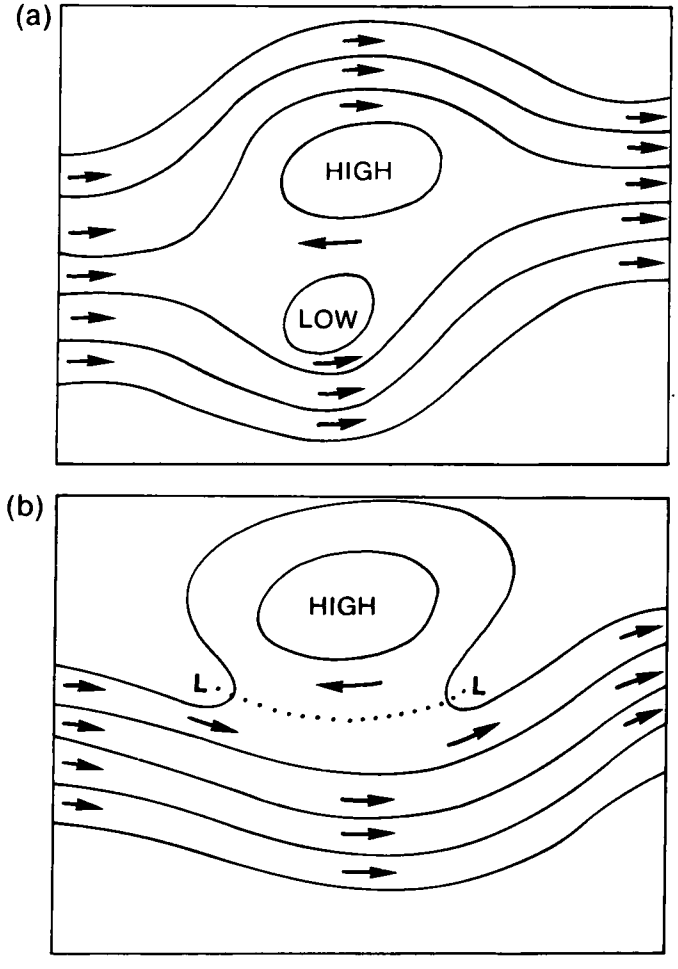

Figure 8.9 Contour patterns associated with blocks.

8.4 Dynamical concepts and applications to development

8.4.1 *Vorticity equation*

The vertical component of absolute vorticity $= \zeta + f = \zeta_a$

The Vorticity equation, in simple form, is:

$$d/dt\ \zeta_a = -\zeta_a \operatorname{div} \mathbf{V} + T - F$$

where T represents the change in ζ due to tilting of the 3-dimensional spin axis, and F represents the loss of vorticity due to frictional effects.

Above the Boundary Layer, the terms T and F are negligible. In most of the atmosphere, changes in the absolute vorticity of an air parcel are related to the divergence of velocity.

Divergence (div $\mathbf{V} > 0$) makes $d\zeta_a/dt < 0$, and ζ_a more anticyclonic.

Convergence (div $\mathbf{V} < 0$) makes $d\zeta_a/dt > 0$, and ζ_a more cyclonic.

At a level of non-divergence (often occurring around 500 hPa), all the processes which alter the absolute vorticity of an air parcel are zero or cancel each other out, and ζ_a remains constant. Air parcels then move along Constant Absolute Vorticity (CAV) trajectories.

8.4.2 *Sutcliffe's Development equation*

The basic terms in Sutcliffe's Development equation are:

$$(\zeta_{10} + f) \operatorname{div} \mathbf{V}_{10} = \mathbf{V}' \partial/\partial s\ (2\zeta_{10} + \zeta' + f)$$

$$= L + M + N.$$

The left-hand-side term represents the 1000 hPa Development. As the absolute vorticity must be +ve,

Cyclonic development (C) occurs at the surface when div $\mathbf{V}_{10}$ is −ve , and
Anticyclonic development (A) at the surface when div $\mathbf{V}_{10}$ is +ve.

The Development is generated by the three terms on the right, all of which involve advection by the thermal wind ($\mathbf{V}'$), along the thickness lines.

L is the Steering term, describing the advection of (twice) the 1000 hPa vorticity, ζ_{10}, pattern. This term predominates where the thickness lines are straight and lie nearly west–east.

M is the Development term, describing the advection of the thermal vorticity, ζ'. This is the dominant effect wherever there are changes in the gradient or curvature of the thickness lines. The development areas of section 8.3.2 are derived from this term.

N is the Latitude term, describing the advection of the earth's vorticity. It is often small in value, but does have a modifying effect on the development where the thickness lines have a significant meridional north–south trend.

8.4.3 *Omega equation*

Omega (ω) is the symbol for vertical motion in pressure coordinates.

$\omega(= dp/dt)$ is $-$ve for ascent and $+$ve for subsidence.

The Omega equation is, essentially:

$$\nabla^2\omega = \partial/\partial p\,(u\,\partial\zeta_a/\partial x + v\,\partial\zeta_a/\partial y) + \nabla^2\,(u\,\partial h'/\partial x + v\,\partial h'/\partial y).$$

This shows the distribution of vertical velocity to be dependent on the rate of change of vorticity advection with height and the horizontal distribution of thermal advection.

Since the magnitude of vorticity advection tends to increase upwards to the level of maximum winds, the following subjective interpretation may be used:

ascent (i.e. negative ω) is associated with either positive vorticity advection in the upper troposphere or a local maximum of warm advection.

descent (i.e. positive ω) is associated with either negative vorticity advection in the upper troposphere or a local maximum of cold advection.

In practice the signs of the two advection terms often differ and their magnitudes are difficult to determine subjectively. Computed values of ω are required. Theory also suggests that it is illusory to imagine ω as being generated by two separate forcing processes which act independently (see next section).

8.4.4 *Q vectors*

The Omega equation may also be written as: $\nabla^2\omega = \text{div } \mathbf{Q}$ where $\mathbf{Q}$ is a vector equal to the rate of change of the gradient of θ when moving with the geostrophic wind.

Where $\mathbf{Q}$ is convergent there is ascent; where it is divergent there is subsidence.

The Q vector combines the two forcing terms on the right-hand side of the normal Omega equation into one coherent process, and avoids having to calculate the small residual of two large but opposing effects.

Fig. 8.10 illustrates the subjective evaluation of the Q vector distribution in two standard situations of large θ gradient. At high levels the pattern of contour heights corresponds closely to that of the θ isopleths, and may be used for a qualitative estimation of the Q vectors.

From the geostrophic winds implied by the contour pattern (step 1), assess the vector **change** in the wind along the direction of a contour (step 2). Then turn the wind change vectors clockwise through 90° to obtain the Q vectors (step 3). Ascent occurs where the Q-vector field is convergent, descent where it is divergent.

8.4.5 *Potential vorticity*

Vorticity is not a conservative property which can be used to identify a particular parcel of air as it moves through the atmosphere. Vorticity is changed by convergence and divergence. But in the process, convergence stretches and divergence squashes the vortex filaments.

It turns out that the vorticity of an air parcel combined with a measure of its vertical extent is a useful dynamical property which is conservative under adiabatic conditions. It is called potential vorticity.

Potential vorticity = $(\zeta + f)/\Delta p$ = constant.

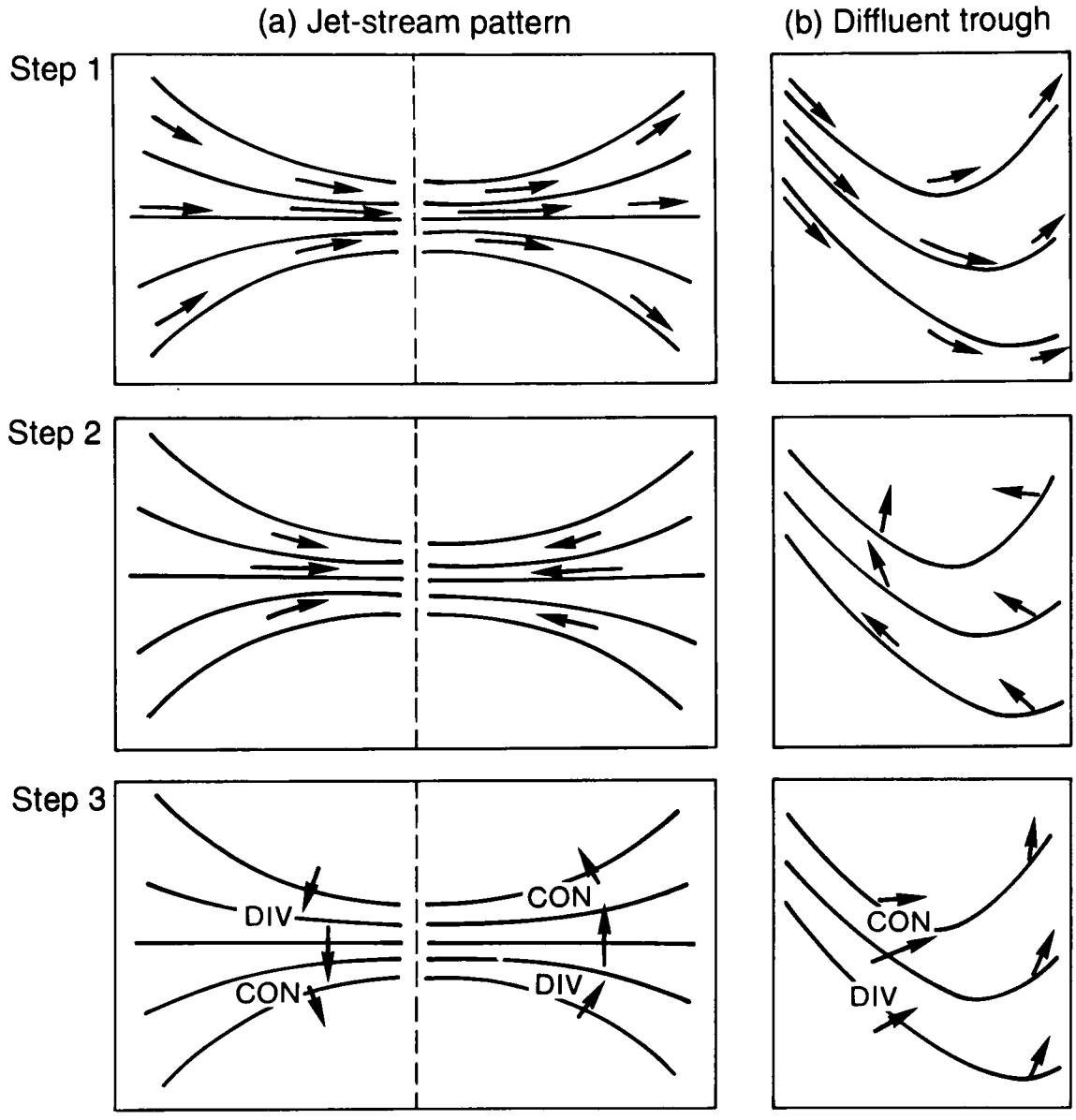

Figure 8.10 Illustrates the subjective evaluation of Q-vector fields for two situations, (a) jet-stream entrance and exit, and (b) diffluent trough. High-level contours are used as an approximation to the θ isopleth patterns.

Step 1: Arrows depict geostrophic wind vectors.

Step 2: Arrows depict the vector wind **change** in the direction of the geostrophic winds.

Step 3: Arrows are Q-vectors. They are turned clockwise through 90° from the vectors in Step 2. Regions of convergent and divergent Q vectors are marked.

Fig. 8.11 illustrates the concept for the case of air parcels bounded below by the surface, and flowing over a hill.

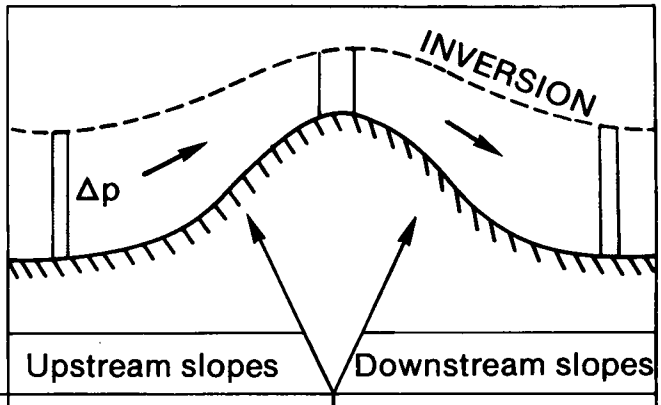

	Upstream slopes	Downstream slopes
Δp	decreases	increases
(ζ+f)	decreases	increases
ζ becomes	more anticyclonic	more cyclonic
Isobaric pattern	ridge	trough

Figure 8.11 Potential vorticity and boundary-layer airflow across a ridge.

8.4.6 *Isentropic potential vorticity*

Under dry adiabatic conditions, θ = constant and the upper and lower bounds of the air parcel in the previous section can be defined as in Fig. 8.12.

Since $(\zeta + f)/\Delta p$ = constant, then $(\zeta + f)\Delta\theta/\Delta p$ = constant ($\Delta\theta = \theta_1 - \theta_2$).

This form of the potential vorticity is called isentropic potential vorticity (IPV). It is the product of the absolute vorticity and the stability, calculated along isentropic (constant θ) surfaces.

IPV is a most conservative property of an air parcel. It is particularly useful for tracking the path of stratospheric air that enters the troposphere.

IPV is usually measured in arbitrary units, such that 1 IPV unit corresponds to $(\zeta + f) = 10^{-4}\ s^{-1}$ and $\Delta\theta/\Delta p$ = 1 K per 10 hPa. Fig. 8.12 shows that an IPV value of 1 unit is typical of tropospheric air, and a rapid increase to IPV values over 2 units occurs at the tropopause.

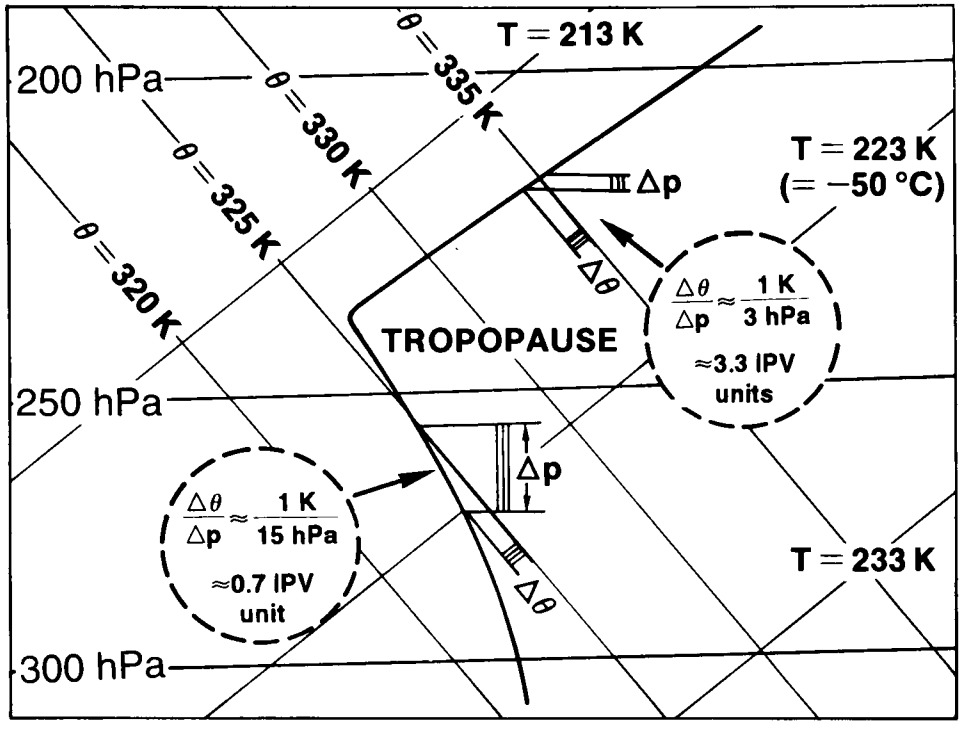

Figure 8.12 IPV values in the troposphere and stratosphere, calculated on a tephigram.

8.5 Explosive cyclogenesis

8.5.1 *Definition*

An explosively deepening depression is defined as a depression which deepens at a rate exceeding 24 hPa per day. Some such systems deepen at over twice that rate.

8.5.2 *Geographical and seasonal characteristics*

Explosive cyclogenesis (EC) is nearly always confined to oceanic regions, and predominantly occurs during the winter half of the year, with the western North Atlantic one of the world's most favoured areas. However, EC can occur even in mid-summer and forecasters must be particularly alert to this possibility owing to the increased number of weather-sensitive activities at this time of year. Explosively deepening depressions can develop from the remnants of ex-tropical storms in late summer and autumn.

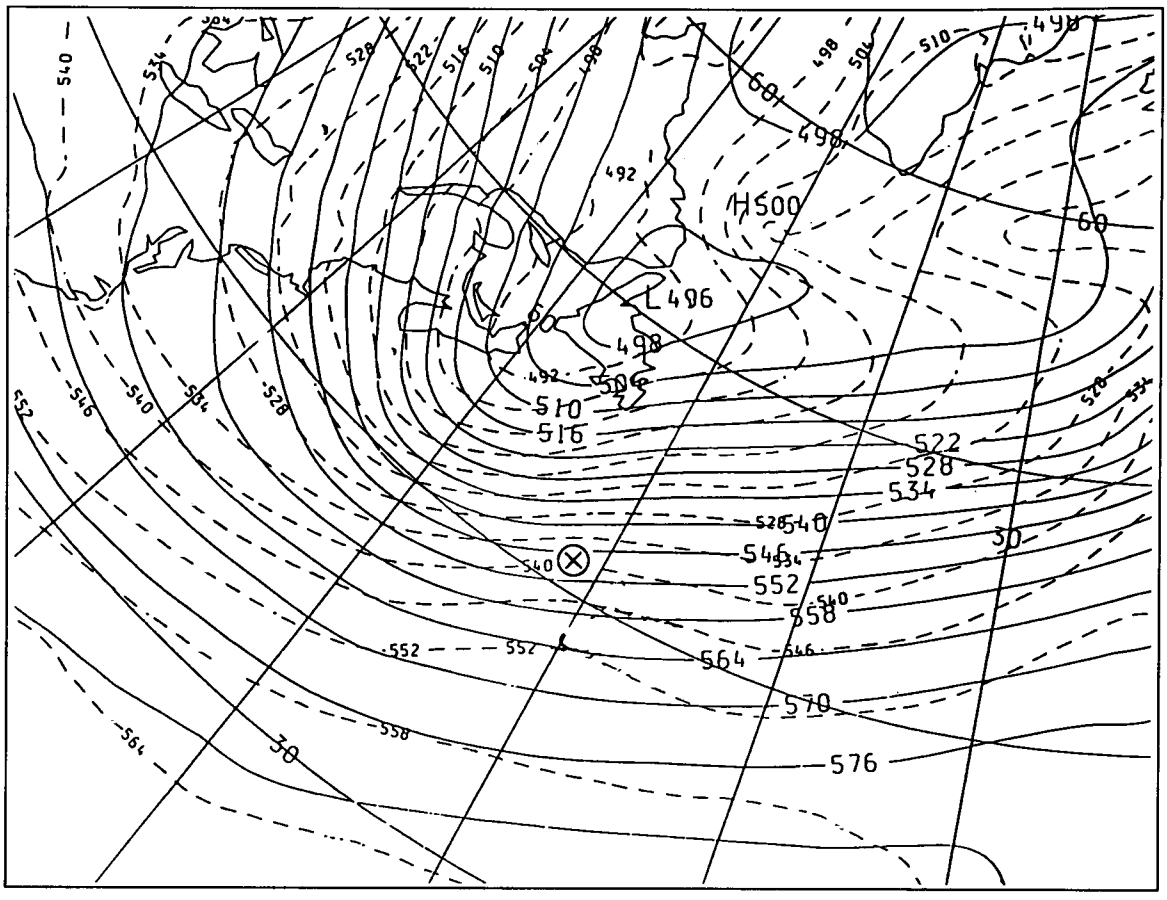

Figure 8.13 Typical 500 hPa height and 1000–500 hPa thickness pattern preceding explosive cyclogenesis. The centre of the surface low is marked by a circled cross.

8.5.3 *Characteristic upper-air patterns*

The idealized height and thermal patterns in Figs 8.5 and 8.6 normally apply. However, the thickness gradient ahead of the upper trough is always intense prior to EC — typically 20 to 30 dam per 300 nautical miles, as shown in Fig. 8.13.

A variety of upper-air patterns can lead to EC. However, by far the most favoured pattern is a short-wave trough or jet streak moving around a major mobile confluent trough. A general schematic of this type is shown in Fig. 8.14.

8.5.4 *Satellite imagery*

The onset of EC is often accompanied (or sometimes preceded) by a 'cloud head' (often referred to as a 'baroclinic leaf'), an example of which is shown in Fig. 8.15. This cloud head is characterized by:

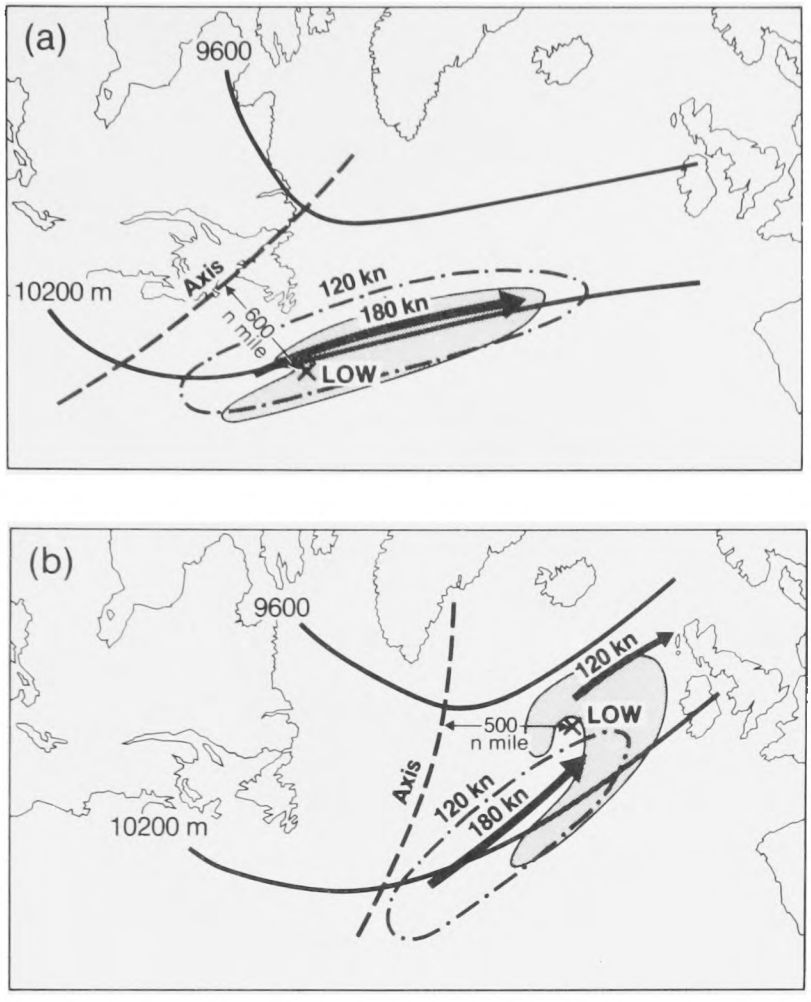

Figure 8.14 Schematic of low development ahead of a broad, mobile, confluent 250 hPa trough. Dispositions of surface centre relative to 250 hPa pattern (a) at time of onset of rapid deepening, and (b) 24 hours later. Main cloud bands are stippled. Jet axes are bold arrows.

(a) A very broad mass of dense layered cloud C, whose poleward edge often exhibits a marked and increasingly convex shape for much of its length. The cloud texture usually appears smooth on IR imagery, although VIS pictures in particular may show embedded convection arranged in transverse bands. Deep convection P in the adjacent polar air often undercuts C.

(b) A narrow region, devoid of middle and upper cloud, known as the 'dry intrusion', which separates cloud head C from the adjacent band of frontal cloud F. The 'dry intrusion' consists of recently subsided air, partially stratospheric in origin.

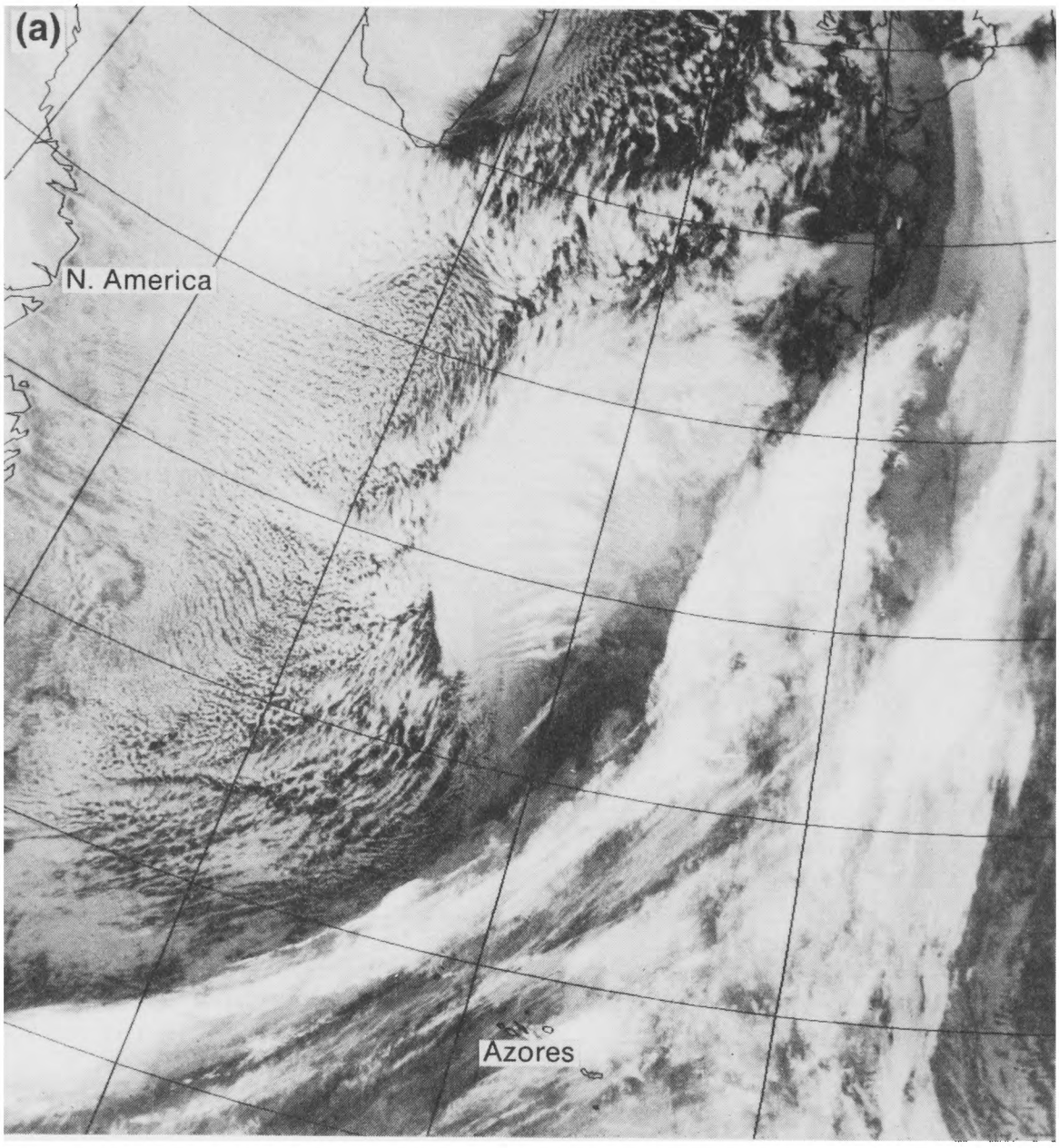

Figure 8.15 (a) Infrared image showing cloud signature associated with early stages of EC at 1550 UTC on 2 February 1991, and (b) (opposite) schematic diagram of the features described in the text.

In addition, a rope-like cloud structure (often present at RR) indicates the position of a new surface cold front, which acquires the main low-level thermal gradient at the expense of the pre-existing front beneath F.

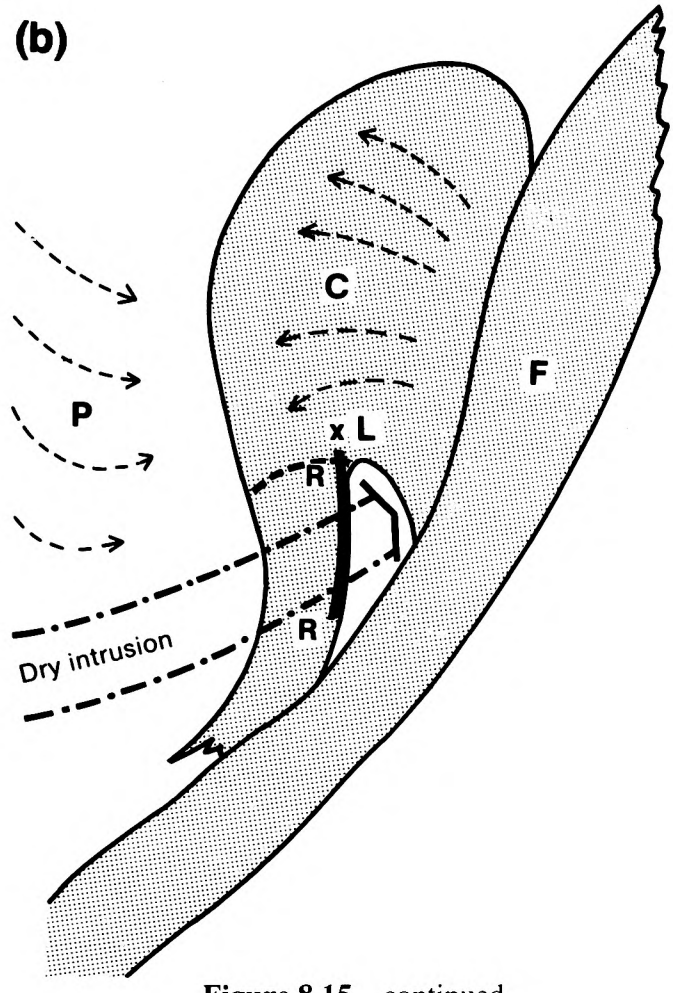

Figure 8.15 continued.

The surface depression centre is usually located within or close to the 'dry intrusion'. During deepening, the upstream tip of C evolves into a 'hook' around the surface low centre.

8.5.5 *Winds associated with explosive cyclogenesis*

Mean winds over the sea usually reach storm-force, sometimes hurricane-force, around a depression which has deepened explosively. Early in the life-cycle, strongest winds are often found in the warm sector, but following explosive deepening, they occur near the hook of cloud as seen on satellite imagery.

Rapid pressure rises to the rear of the depression centre in the cold air (sometimes exceeding 15 hPa in 3 hours) are a potent generator of damaging

winds and are characteristic of lows developing ahead of a mobile confluent upper trough (this is due to marked subsidence which typically occurs behind the confluent trough). Such a pressure surge is not a feature of lows ahead of a major diffluent trough.

8.5.6 *Precipitation*

Marked lowering of the freezing level (often by 1000 m) can occur in extensive heavy precipitation poleward of the depression centre, and rain may turn to snow over lowland areas when the 850 hPa wet-bulb potential temperature is 6 °C or lower. Thunderstorms frequently occur at the boundary between the 'dry intrusion' and the hook of cloud late in the deepening phase.

8.5.7 *Factors mitigating against EC*

(a) A rapidly relaxing upper trough.

(b) The depression centre moving from sea to land.

(c) The cloud head signature becoming ragged and ill-defined.

(d) Lack of warm air aloft.

References

McCallum, E., 1990: The Burns' Day storm, 25 January 1990. *Weather*, **45**, 166–173.

McCallum, E and Norris, W.J.T., 1990: The storms of January and February 1990. *Meteorol Mag*, **119**, 201–210.

Monk, G.A. and Bader, M.J., 1988: Satellite images showing the development of the storm of 15–16 October 1987. *Weather*, **43**, 130–135.

Norris, W.J.T. and Young, M.V., 1991: Satellite photographs — 2 February 1991 at 1533 UTC. *Meteorol Mag*, **120**, 115–116.

Young, M.V., 1990: Satellite and radar images, 0900 GMT 3 February 1990. *Weather*, **45**, 268–270.

APPENDIX I — UNITS

1. S I units

Quantity	Name (symbol)	Definition
Basic units:		
Length	metre (m)	
Mass	kilogram (kg)	
Time	second (s)	
Temperature	degree Kelvin (K)	
Derived units:		
Force	newton (N)	$kg\ m\ s^{-2}$
Pressure	pascal (Pa)	$N\ m^{-2}$
Energy	joule (J)	N m
Power	watt (W)	$J\ s^{-1}$
Frequency	hertz (Hz)	s^{-1}

2. Multiples of units

Multiple	Prefix	(symbol)	Multiple	Prefix	(symbol)
10^{-1}	deci	(d)	10	deca	(da)
10^{-2}	centi	(c)	10^{2}	hecto	(h)
10^{-3}	milli	(m)	10^{3}	kilo	(k)
10^{-6}	micro	(μ)	10^{6}	mega	(M)
10^{-9}	nano	(n)	10^{9}	giga	(G)
10^{-12}	pico	(p)	10^{12}	tera	(T)

APPENDIX II — CONVERSION TABLES

1. Temperature

Table A1. Celsius to Fahrenheit

°C	−40	−35	−30	−25	−20	−15	−10	−5	0	5	10	15	20	25	30	35	40	45	50
°F	−40	−31	−22	−13	−4	5	14	23	32	41	50	59	68	77	86	95	104	113	122

differences

°C	1	2	3	4	5
°F	2	4	5	7	9

Table A2. Fahrenheit to Celsius

°F	−40	−30	−20	−10	0	10	20	30	40	50	60	70	80	90	100	110	120	130	140
°C	−40	−34	−29	−23	−18	−12	−7	−1	4	10	15	21	27	32	38	43	49	54	60

differences

°F	1	2	3	4	5	6	7	8	9
°C	1	1	2	2	3	3	4	4	5

2. Distance

1 inch	= 25.4 mm	1 cm	= 0.39 inch
1 foot	= 30.48 cm	1 m	= 3.28 feet
1 mile	= 1.61 km	1 km	= 0.62 mile
1 n.mile	= 1.85 km	1 km	= 0.54 n mile

Table A3. Nautical miles to kilometres

n mile	10	20	30	40	50	60	70	80	90	100
km	18	37	56	74	93	111	130	148	167	185

Table A4. Kilometres to nautical miles

km	10	20	30	40	50	60	70	80	90	100
n mile	5	11	16	22	27	32	38	43	49	54

3. Area

$$1 \text{ hectare} = (100 \text{ m})^2 = 2.47 \text{ acres}$$
$$(1 \text{ km})^2 = 100 \text{ hectares} = 247 \text{ acres}$$

4. Speed

Table A5. Knots to metres/second and kilometres/hour

knots	1	2	3	4	5	10	20	30	40	50	60	70	80	90	100
$m\ s^{-1}$	0.5	1	1.5	2	2.5	5	10	15	21	26	31	36	41	46	51
$km\ h^{-1}$	1.8	3.7	5.6	7.4	9.3	19	37	56	74	93	111	130	148	167	185

$$1 \text{ knot} = 0.515 \text{ m s}^{-1} = 1.85 \text{ km h}^{-1}$$

Table A6. Metres/second to kilometres/hour and knots

$m\ s^{-1}$	1	2	3	4	5	10	20	30	40	50	60	70	80	90	100
$km\ h^{-1}$	3.6	7.2	10.8	14.4	18.0	36	72	108	144	180	216	252	288	324	360
knots	1.9	3.9	5.8	7.8	9.7	19	39	58	78	97	117	136	155	175	194

$$1 \text{ m s}^{-1} = 3.60 \text{ km h}^{-1} = 1.94 \text{ knots}$$

Table A7. Kilometres/hour to knots and metres/second

$km\ h^{-1}$	1	2	3	4	5	10	20	30	40	50	60	70	80	90	100
knots	0.5	1.1	1.6	2.2	2.7	5	11	16	22	27	32	38	43	49	54
$m\ s^{-1}$	0.3	0.6	0.8	1.1	1.4	3	5	8	11	14	17	19	22	25	28

$$1 \text{ km h}^{-1} = 0.54 \text{ knots} = 0.28 \text{ m s}^{-1}$$

Table A8. Feet/minute to knots and metres/second

$ft\ min^{-1}$	10	25	50	75	100	200	300	400	500	1000
knots	0.10	0.25	0.49	0.74	1.0	2.0	3.0	3.9	4.9	9.9
$m\ s^{-1}$	0.05	0.13	0.25	0.38	0.5	1.0	1.5	2.0	2.5	5.1

$$1000 \text{ ft min}^{-1} = 9.87 \text{ knots} = 5.08 \text{ m s}^{-1}$$

Table A9. Runway cross-wind components

		Angle between wind direction and runway heading (deg. true)								
		10	20	30	40	50	60	70	80	90
	5	1	2	2	3	4	4	4	5	5
	10	2	3	5	6	7	8	9	9	10
	15	3	5	7	9	11	13	14	14	15
	20	3	7	10	13	15	17	18	19	20
	25	4	8	12	16	19	22	23	24	25
Wind	30	5	10	15	19	23	26	28	29	30
	35	6	12	17	22	26	30	32	34	35
speed	40	7	14	20	25	30	35	37	39	40
in	45	8	15	22	29	34	39	42	44	45
	50	9	17	25	32	38	43	47	49	50
knots	55	10	19	27	35	42	48	52	54	55
	60	10	20	30	38	46	52	56		
	65	11	22	32	42	50	56			
	70	12	24	35	45	54				
	75	13	26	37	48					
	80	14	27	40						

APPENDIX III — PHYSICAL TABLES AND CONSTANTS

1. The Earth

Dimensions

Equatorial radius	6378 km	(3963 miles)
Polar radius	6357 km	(3950 miles)
Rate of rotation (Ω)	7.29×10^{-5} s^{-1}	
Total surface area	510×10^{6} km^2	
Land surface area	150×10^{6} km^2	(29.2% of total area)
Ocean surface area	360×10^{6} km^2	(70.8% of total area)

Table A10. Gravity at mean sea level

Latitude (deg)	0	50	60	90
g (m s^{-2})	9.78	9.81	9.82	9.83

Table A11. Distance of sea horizon from viewpoint at given heights

Height (ft)	6	10	20	30	50	100	200	400	600	800
Distance (n mile)	2.8	3.6	5.1	6.3	8.1	11	16	23	28	32

Table A12. Distance corresponding to 1 degree of longitude at given latitudes

Latitude (deg)	0	15	30	45	50	55	60	75	85	90
Distance (n mile)	60.4	58.3	52.2	42.6	38.7	34.5	30.1	15.5	5.2	0

Table A13. Value of Coriolis Parameter ($f = 2\Omega\sin\varphi$)

Latitude φ	degrees								
	0	15	30	45	50	55	60	75	90
f (10^{-4} s^{-1})	0.00	0.38	0.73	1.03	1.12	1.19	1.26	1.41	1.46
f (h^{-1})	0.00	0.14	0.26	0.37	0.40	0.43	0.45	0.51	0.52
$\partial f/\partial y$ (10^{-11} m^{-1} s^{-1})	2.29	2.12	1.98	1.62	1.47	1.31	1.14	0.59	0.00

2 The atmosphere

(a) Some physical properties

Mass of atmosphere = 5.27×10^{18} kg

Surface pressure:
1 'atmosphere' = 1.03 kg cm^{-2} = 14.7 lb in^{-2} = 29.9 in Hg
1 millibar = 100 dynes cm^{-2} = 100 N m^{-2} = 1 hPa

Speed of light = 2.998×10^8 m s^{-1}

Speed of sound in dry air

Temperature (°C)	−40	−20	0	20	40
Speed (m s^{-1})	306	318	331	343	354

(b) Specific heats (J deg^{-1} kg^{-1}) of atmospheric constituents:

Dry air (c_p)	1004
Dry air (c_v)	717
Water vapour (c_p)	1952
Water vapour (c_v)	1463
Liquid water (0°C)	4218
Ice (0°)	2106

(c) Latent heats (J kg^{-1}) of water substances

Vapour/Liquid	2 500 000
Liquid/Solid	334 000
Solid/Vapour	2 834 000

Table A14. ICAO Standard atmosphere (dry air)

Pressure	Temperature	Density	Height		Thickness of 1 hPa layer	
hPa	°C	g m^{-3}	m	ft	m	ft
1013.2	15.0	1225	0	0	8.3	27
1000	14.3	1212	111	364	8.4	28
950	11.5	1163	540	1773	8.8	29
900	8.6	1113	988	3243	9.2	30
850	5.5	1063	1457	4781	9.6	31
800	2.3	1012	1949	6394	10.1	33
750	−1.0	960	2466	8091	10.6	35
700	−4.6	908	3012	9882	11.2	37
650	−8.3	855	3591	11780	11.9	39
600	−12.3	802	4206	13801	12.7	42
550	−16.6	747	4865	15962	13.7	45
500	−21.2	692	5574	18289	14.7	48
450	−26.2	635	6344	20812	16.1	53
400	−31.7	577	7185	23574	17.7	58
350	−37.7	518	8117	26631	19.7	65
300	−44.5	457	9164	30065	22.3	75
250	−52.3	395	10363	33999	25.8	85
200	−56.5	322	11784	38662	31.7	104
150	−56.5	241	13608	44647	42.3	139
100	−56.5	161	16180	53083	63.4	208
90	−56.5	145	16848	55275	70.5	231
80	−56.5	128	17595	57726	79.3	260
70	−56.5	112	18442	60504	90.6	297
60	−56.5	96	19419	63711	105.7	347
50	−55.9	80	20576	67507	127.0	417
40	−54.5	64	22000	72177	160	525
30	−52.7	47	23849	78244	215	706
20	−50.0	31	26481	86881	326	1072
10	−45.4	15	31055	101885	669	2195

Table A15. The Sun

Date	Noon sun overhead (lat.)	Noon solar altitude 50° N (deg.)	Noon solar altitude 60° N (deg.)	Sunrise/sunset times (UTC) London	Manchester	Glasgow	Lerwick
Jan. 1	23 S	17	7	0805/1600	0825/1600	0850/1555	0925/1440
Jan. 16	21 S	19	9	0800/1620	0815/1620	0835/1615	0905/1500
Feb. 1	17 S	23	13	0740/1650	0755/1650	0810/1650	0830/1540
Feb. 16	13 S	27	17	0715/1715	0725/1720	0740/1720	0745/1625
Mar. 1	8 S	32	22	0645/1740	0700/1745	0710/1750	0700/1705
Mar. 16	2 S	38	28	0615/1805	0625/1815	0630/1820	0620/1745
Apr. 1	4 N	44	34	0535/1835	0545/1845	0550/1855	0535/1825
Apr. 16	10 N	50	40	0505/1855	0510/1910	0510/1925	0450/1910
May 1	15 N	55	45	0435/1925	0435/1935	0435/1955	0410/1945
May 16	19 N	59	49	0405/1945	0405/2005	0405/2025	0340/2010
June 1	22 N	62	52	0350/2005	0345/2025	0340/2050	0310/2030
June 16	23 N	63	53	0340/2020	0340/2040	0330/2105	0255/2105
July 1	23 N	63	53	0345/2020	0345/2040	0335/2105	0310/2100
July 16	21 N	61	51	0400/2010	0400/2030	0355/2050	0325/2045
Aug. 1	18 N	58	48	0420/1950	0425/2005	0420/2025	0345/2010
Aug. 16	14 N	54	44	0445/1920	0450/1935	0450/1950	0420/1930
Sept. 1	8 N	48	38	0510/1850	0515/1900	0520/1915	0500/1850
Sept. 16	3 N	43	33	0535/1815	0545/1825	0550/1835	0545/1810
Oct. 1	3 S	37	27	0600/1740	0610/1745	0620/1755	0630/1730
Oct. 16	8 S	32	22	0625/1705	0635/1710	0650/1715	0710/1645
Nov. 1	14 S	26	16	0655/1635	0705/1640	0720/1640	0755/1600
Nov. 16	18 S	22	12	0720/1610	0735/1610	0755/1610	0835/1525
Dec. 1	22 S	18	8	0745/1555	0800/1555	0820/1550	0910/1500
Dec. 16	23 S	17	7	0800/1550	0820/1550	0840/1545	0930/1440

Table A16. Rossby Long Waves — wavelength of stationary waves

Latitude (deg.)	Mean zonal wind speed (knots)									
	10	20	30	40	50	10	20	30	40	50
	wavelength									
	kilometres					degrees of longitude				
70	5100	7200	8800	10200	11400	134	190	232	268	300
60	4200	6000	7300	8400	9400	76	108	132	152	170
50	3700	5300	6400	7400	8300	52	74	90	104	116
40	3400	4800	5900	6800	7600	40	57	69	80	90
30	3200	4500	5600	6400	7200	33	47	57	66	74